

# UC San Diego

## UC San Diego Electronic Theses and Dissertations

### Title

Mechanisms that regulate the maturation and down- regulation of protein kinase C

### Permalink

<https://escholarship.org/uc/item/5rf1g476>

### Author

Gould, Christine M.

### Publication Date

2009

Peer reviewed|Thesis/dissertation

UNIVERSITY OF CALIFORNIA, SAN DIEGO

Mechanisms that Regulate the Maturation and Down-regulation  
of Protein Kinase C

A dissertation submitted in partial satisfaction of the  
requirements for the Doctor of Philosophy

in

Biomedical Sciences

by

Christine M. Gould

Committee in Charge:

Professor Alexandra C. Newton, Chair  
Professor Joseph Adams  
Professor Joan Heller Brown  
Professor Randolph Hampton  
Professor Tony Hunter  
Professor Susan S. Taylor

2009

Copyright 2009

Christine M. Gould

All Rights Reserved

The dissertation of Christine M. Gould is approved and it is acceptable in quality and form for publication on microfilm and electronically:

---

---

---

---

---

---

---

---

Chair

University of California, San Diego

2009

Dedicated to Mom and Dad

for their unconditional love and support in everything that I do. Their sacrifices have  
made everything possible for me.

Dedicated to Dr. Alexandra Newton

for her guidance, support, and optimism throughout my graduate school experience.  
She exemplifies everything that I strive and hope to be as a scientist.

Dedicated to Dr. Stephen Lynch

for his never-ending support and tolerance through the ups and downs over these years  
and for always reminding me of what I'm capable of achieving.

He has been my rock.

## TABLE OF CONTENTS

Signature Page .....	iii
Dedication .....	iii
Table of Contents .....	v
List of Figures .....	vi
Acknowledgements .....	ix
Vita and Publications .....	xi
Abstract of the Dissertation .....	xii
Chapter 1 The Life and Death of Protein Kinase C .....	1
Chapter 2 The Chaperones Hsp90 and Cdc37 Mediate the Maturation and Stabilization of Protein Kinase C through a Conserved PXXP Motif in the C-terminal Tail .....	49
Chapter 3 Elucidating the Mechanism of the Phorbol Ester-Mediated Down-regulation of PKC $\beta$ II .....	121
Chapter 4 Characterization of an <i>In Vitro</i> Autophosphorylation Site in PKC $\beta$ II .....	163
Chapter 5 Determining the Contribution of mTOR Kinase Activity to the Maturation of PKC .....	199
Chapter 6 Summary and Conclusions .....	236

## LIST OF FIGURES

Figure 1.1: Domain composition of PKC family members .....	33
Figure 1.2: Model showing the life cycle of PKC .....	34
Figure 2.1 Mutation of a PXXP motif, conserved in all AGC kinases, in the C-terminal tail of PKC $\beta$ II abolishes kinase activity .....	84
Figure 2.2: Mutation of the PXXP motif in PKC $\beta$ II prevents the maturation of the kinase, a defect that cannot be rescued by translocation to membranes .....	85
Figure 2.3: Mutation of the PXXP motif in PKC $\beta$ II does not impair phosphorylation by or binding to its upstream kinase, PDK-1 .....	86
Figure 2.4: Mutation of the PXXP motif in PKC $\beta$ II decreases binding to the chaperones Hsp90 and Cdc37 .....	87
Figure 2.5: Hsp90 activity facilitates the maturation of PKC.....	88
Figure 2.6: Mutation of the PXXP motif in conventional and novel PKC isozymes decreases the interaction with Hsp90.....	90
Figure 2.7: Inhibition of Hsp90 down-regulates PKC through a proteasome-dependent mechanism in a cell-type-dependent context .....	91
Figure 2.8: Mutation of a conserved Tyr in the $\alpha$ E-helix of the catalytic domain of PKC $\beta$ II mimics the defect of the PXXP mutant, PKC $\beta$ II-P616A/P619A .....	93
Figure 2.9: Structural representation of the residues that comprise the molecular 'clamp' between the PXXP motif and the catalytic core .....	95
Figure A2.1: Mutation of the first Pro in the PXXP motif is sufficient to abolish PKC processing .....	112
Figure A2.2: Mutation of a conserved Phe in the $\alpha$ C- $\beta$ 4 loop of the catalytic domain of PKC $\beta$ II partially impairs the processing of PKC .....	113
Figure A2.3: Mutation of a conserved basic residue in the C-terminal tail of PKC recapitulates the processing defect of the $\alpha$ C- $\beta$ 4 loop mutant, PKC $\beta$ II-F402A ...	116
Figure A2.4: Disruption of the interaction between the $\alpha$ C- $\beta$ 4 loop in the catalytic domain and the C-terminal tail of PKC $\beta$ II impairs the processing in a manner that is independent of Hsp90 .....	117

Figure A2.5: Mutation of a conserved Phe in the $\alpha$ E-helix of the catalytic domain of PKC $\beta$ II also disrupts the 'intramolecular clamp' with the PXXP motif in the C-terminal tail to abrogate processing of PKC .....	119
Figure 3.1: PKC requires its intrinsic catalytic activity in order to be down-regulated by phorbol esters .....	149
Figure 3.2: Degradation of the different species of PKC can be dissected with proteasome and PKC inhibitors.....	150
Figure 3.3: Dephosphorylation at the hydrophobic motif of PKC is a priming step in the phorbol ester-mediated down-regulation of PKC .....	151
Figure 3.4: Dephosphorylation of the priming sites in PKC is required for phorbol ester-mediated down-regulation .....	154
Figure 3.5: The phorbol ester-mediated down-regulation of PKC is insensitive to the phosphatase inhibitor, okadaic acid .....	155
Figure 3.6: Inhibition of PKC slows the phorbol ester-mediated dephosphorylation of PKC.....	156
Figure 3.7: Inhibition of PKC activity does not affect protein levels of PKC $\beta$ II-T641E/S660E, which cannot be dephosphorylated, after phorbol ester stimulation .....	157
Figure 3.8: Dephosphorylation is not a prerequisite for ubiquitination when PKC is down-regulated by phorbol esters.....	158
Figure 3.9: Model showing the proposed requirement of PKC activity-dependent dephosphorylation to promote the phorbol ester-mediated down-regulation of PKC .....	159
Figure 4.1: Location of the <i>in vitro</i> autophosphorylation sites in PKC $\beta$ II .....	187
Figure 4.2: PKC $\beta$ II autophosphorylates at Thr-17 <i>in vitro</i> .....	188
Figure 4.3: Endogenous PKC $\beta$ II autophosphorylates at Thr-17 in cells under phorbol ester stimulation, which is enhanced with inhibition of phosphatases and diminished by inhibition of PKC .....	189
Figure 4.4: PKC $\beta$ II robustly autophosphorylates at Thr-17 in the presence of phorbol esters and exogenous diacylglycerol but only weakly under natural agonist conditions .....	191

Figure 4.5: PKC $\beta$ II that is phosphorylated at Thr-17 is localized at the membrane upon phorbol ester stimulation.....	192
Figure 4.6: Mutation in the <i>in vitro</i> autophosphorylation sites, Ser-16 and Thr-17, in PKC $\beta$ II to either nonphosphorylatable or phospho-mimetic residues does not alter its catalytic activity, its ability to be processed, or its down-regulation by phorbol esters .....	193
Figure 4.7: The phosho-mimetic, PKC $\beta$ II-S16E/T17D, shows a reduced translocation to membranes upon agonist stimulation.....	195
Figure 4.8: Sequence conservation of Thr-17 in PKC $\beta$ II and a model of how Thr-17 may be sensitive to phosphatases.....	196
Figure 5.1: Inhibition of PDK-1 or PKC activity does not block the processing of PKC .....	224
Figure 5.2: Inhibition of mTOR slows the processing by affecting phosphorylation at both the turn motif (Thr-641) and the hydrophobic motif (Ser-660) of the conventional isozyme, PKC $\beta$ II .....	225
Figure 5.3: Inhibition of mTOR slows the processing of exogenous PKC $\alpha$ , a conventional PKC isozyme, and exogenous PKC $\epsilon$ , a novel PKC isozyme.....	226
Figure 5.4: The processing of endogenous PKC $\alpha$ is insensitive to the mTOR inhibitor and cannot be rescued by membrane-targeting .....	227
Figure 5.5: Exogenous PKC signals in mTORC2-deficient MEFs .....	228
Figure 5.6: Exogenous PKC $\beta$ II is processed in mTORC2-deficient MEFs. ....	229
Figure 5.7: Proposed models for the role of mTORC2 in the maturation of PKC .....	230
Figure 5.8: Identification of mTORC2-sensitive and mTORC2-insensitive PKC isozymes .....	231
Figure 6.1: A model of the life cycle of PKC .....	247

## ACKNOWLEDGEMENTS

I would like to thank the members of the Newton lab, both past and present, for their help, guidance, and support in my endeavors both inside and outside of the lab. In particular, I would like to thank Dr. Maya Kunkel for being an amazing mentor, colleague, and friend throughout my stay in the Newton Lab. I thank Dr. Charles C. King for mentoring me during my rotation. I would like to thank past and present members of Bay H, Dr. Daniel Dries, Lisa Leon Gallegos, and Dr. Ximena (Gloria) Reyes, for keeping me sane and giving me helpful advice, both scientific and personal. I thank the boys, Dr. John Brognard, Matthew Niederst, and Noel Warfel, for entertaining discussions and the endless banter. I would like to thank Dr. Natarajan Kannan and Dr. Susan S. Taylor for a very productive and fruitful collaboration. I would like to thank my friends (Dr. Alison Holzer, Dr. Chris Means, Dr. Scott Stuart) in the Biomedical Sciences Graduate Program as well as my friends in the triathlon community (Terry Martin, Dr. Shannon Werner, Dr. Dena Florczyk) who have made graduate school an amazing experience. I thank my committee members, especially Dr. Tony Hunter and Dr. Susan Taylor, for their guidance and helpful discussions. Most importantly, a HUGE thanks to my mentor, Dr. Alexandra Newton, whose constant support and mentoring, both scientifically and personally, has made graduate school an enjoyable and memorable experience for me.

The text of chapter 1 is, in full, a reprint of the material as it appears in Current Drug Targets, 2008, Gould, CM and Newton AC. I was the author of this literature review.

The text of Chapter 2 is, in full, a reprint of the material as it appears in the Journal of Biological Chemistry, February 2009, by Gould CM, Kannan N, Taylor SS, and Newton AC. I was the primary author and researcher.

## VITA

- 2002 Bachelor of Science, Truman State University
- 2009 Doctor of Philosophy, University of California, San Diego

## PUBLICATIONS

Gould CM, Kannan N, Taylor SS, Newton AC. The chaperones Hsp90 and Cdc37 mediate the maturation and stabilization of protein kinase C through a conserved PXXP motif in the C-terminal tail. *Journal of Biological Chemistry*. Volume 248, Number 8, February 20, 2009. Pgs: 4921-4935.

Abrahamsen H, Kannan N, Braughton LA, Taylor SS, Jennings PA, Newton AC. The peptidyl-prolyl isomerase Pin1 is a molecular timer in the lifetime of conventional protein kinase C isoforms. In revision.

Gould CM, Newton AC. The life and death of protein kinase C. *Current Drug Targets*. Volume 9, Number 8, August 9, 2008. Pgs: 614-625.

Facchinetti V, Ouyang W, Wei H, Soto N, Lazorchak A, Gould C, Lowry A, Newton AC, Mao Y, Miao RQ, Sessa WC, Qin J, Zhang P, Su B, Jacinto E. The mammalian target of rapamycin complex 2 controls folding and stability of Akt and protein kinase C. *Embo Journal*. Volume 27, Number 14, July 23, 2008. Pgs: 1932-1943.

Chen, D, Gould C, Garza R, Gao T, Hampton RY, Newton AC. Amplitude control of protein kinase C by RINCK, a novel E3 ubiquitin ligase. *Journal of Biological Chemistry*. Volume 282, Number 46, November 16, 2007. Pgs: 33776-33787.

Gould C and Wong AF. Designing specific protein kinase inhibitors: insight from computer simulations and sequence/structure analysis. *Pharmacology and Therapeutics*. Volume 93, Number 2-3, February-March 2002. Pgs: 169-178.

## ABSTRACT OF THE DISSERTATION

Mechanisms that Regulate the Maturation and Down-regulation of Protein Kinase C

by

Christine M. Gould

Doctor of Philosophy in Biomedical Sciences

University of California, San Diego, 2009

Professor Alexandra C. Newton, Chair

Protein kinase C (PKC) is a Ser/Thr kinase involved in a variety of cellular pathways ranging from proliferation to memory and learning. In pathological conditions where these signaling pathways have gone awry, PKC has become an important therapeutic target. In order to design specific drugs to target PKC, it is important to understand how PKC is regulated. This dissertation focuses on the life cycle of PKC, from its maturation into a catalytically, competent enzyme to its down-regulation and degradation. Specifically, we have identified novel regulators that control the maturation

of PKC and have characterized the molecular mechanisms that dictate the down-regulation of PKC. By understanding what factors influence the life cycle of PKC, we can develop more effective therapeutics to target PKC in disease.

## Chapter 1

### The Life and Death of Protein Kinase C

**Abstract**

Protein kinase C (PKC) is a family of kinases that plays diverse roles in many cellular functions, notably proliferation, differentiation, and cell survival. PKC is processed by phosphorylation and regulated by cofactor binding and subcellular localization. Extensive detail is available on the molecular mechanisms that regulate the maturation, activation, and signaling of PKC. However, less information is available on how signaling is terminated both from a global perspective and isozyme-specific differences. To target PKC therapeutically, various ATP-competitive inhibitors have been developed, but this method has problems with specificity. One possible new approach to developing novel, specific therapeutics for PKC would be to target the signaling termination pathways of the enzyme. This review focuses on the new developments in understanding how PKC signaling is terminated and how current drug therapies as well as information obtained from the recent elucidation of various PKC structures and down-regulation pathways could be used to develop novel and specific therapeutics for PKC.

## Protein kinase C structure

PKC, a member of the larger superfamily of Ser/Thr kinases, the AGC kinases, consists of 10 isozymes divided into three subclasses based on their second messenger mode of regulation (1): conventional ( $\alpha$ ,  $\beta$ I/ $\beta$ II,  $\gamma$ ), novel ( $\delta$ ,  $\epsilon$ ,  $\eta$ ,  $\theta$ ) and atypical ( $\iota$ / $\lambda$ ,  $\zeta$ ). Conventional PKCs respond to diacylglycerol and  $\text{Ca}^{2+}$ ; novel isozymes respond only to diacylglycerol; and atypical isozymes respond to neither. All PKC family members share a conserved domain architecture, consisting of a C-terminal kinase core and an N-terminal regulatory moiety (Figure 1.1A) (2). The regulatory moiety serves several functions: 1) it maintains the enzyme in an autoinhibited state in the absence of appropriate second messengers; 2) it targets the enzyme to specific cellular locations; and 3) it mediates protein-protein interactions (2). Specifically, these functions are achieved by a pseudosubstrate peptide sequence and two membrane-targeting modules, the C1 and C2 domains.

The pseudosubstrate of PKC lies N-terminal to the C1 domain. When PKC is inactive, this peptide sequence, resembling that of a substrate except for an Ala at the phospho-acceptor position, occupies the substrate-binding cavity of PKC (3). In this closed, autoinhibited conformation, PKC is relatively resistant to proteolysis (4). Upon activation of PKC, the pseudosubstrate is released from the kinase core, allowing the subsequent binding and phosphorylation of downstream substrates (5,6). The primary mechanism that drives release of the pseudosubstrate is the engagement of the membrane-targeting modules of PKC, the C1 and C2 (in the case of conventional isozymes) domains, to membranes.

The energy to release the pseudosubstrate from the substrate-binding cavity of PKC is provided by the high-affinity binding of the C1 and C2 domains to membrane lipids (7,8). The C1 domain is a small, Cys-rich globular structure that is present in all PKC isozymes (9,10). Both conventional and novel PKCs have a tandem C1 domain (C1A and C1B) that actively engage their ligands, diacylglycerol and their functional analogues, phorbol esters (11). Atypical PKCs have a defective ligand binding pocket in their C1 domain and thus are unable to respond to either diacylglycerol or phorbol esters. When the C1 domain is bound to its ligand, a hydrophobic surface is created that allows for effective retention of the domain on membranes (12,13). In addition to binding diacylglycerol and phorbol esters, the C1 domain also specifically binds the anionic phospholipid, phosphatidylserine (7). In the case of conventional PKCs, the other membrane-targeting module, the C2 domain, also binds anionic phospholipids but in a  $\text{Ca}^{2+}$ -dependent manner (7,14). Novel PKCs also contain a C2 domain but it lacks key residues required to bind  $\text{Ca}^{2+}$ ; it may play a role in protein:protein interactions (14). Atypical PKCs lack a C2 domain entirely but have an additional N-terminal domain, a PB1 domain, which has been shown to serve an important role in mediating protein:protein interactions (Figure 1.1A) (15).

The kinase core of PKCs and two AGC family members, protein kinase A (PKA) and protein kinase B (PKB)/Akt, are highly conserved with more than 40% sequence identity, primarily differing in the C-terminal tail. This tail is critical to the catalytic activity of the kinase because it contains important conserved regions that make key contacts with the kinase domain as first demonstrated in the hallmark structure of PKA (16). Recent structural work has shown that the phosphorylated C-terminal tail of PKC

(and other AGC kinases) positions a key regulatory helix, the C helix, for catalysis; it can also perform this stabilizing role in *trans* by binding the corresponding region in the upstream kinase phosphoinositide-dependent kinase 1, thus optimally positioning its C helix (PDK1) (17). Even more insight into the structural mechanism of how PKC is activated is available with the recent elucidation of crystal structures for several PKC isoforms ( $\iota$ ,  $\theta$ , &  $\beta$ II) bound to ATP-competitive inhibitors (18-20). Like its relative PKA, the kinase domain of PKC is a bilobal structure with an N-terminal lobe that is primarily  $\beta$ -sheet and a C-terminal lobe that is primarily  $\alpha$  helix; the ATP- and substrate-binding sites lie within a cleft between the two lobes (Figure 1.1B) (21). Unlike other PKC family members, PKC  $\beta$ II contains a novel  $\alpha$  helix in the turn motif that associates with the N-terminal lobe of the kinase domain and may aid in stabilizing residues in the active site (20).

### **Signal propagation**

In order for PKC to effectively transduce extracellular signals to downstream targets, PKC must be properly primed and positioned for optimal signaling. Perturbation of the phosphorylation state, conformation, or localization of PKC can disrupt these signaling events, leading to altered physiological states found in diseases such as cancer. These different levels of structural and spatial regulation of PKC allows for the design of more specific therapeutics.

## *Regulation by phosphorylation*

### 1. Processing phosphorylation

Before PKC can respond to lipid second messengers, the enzyme must first be properly processed by three ordered phosphorylations: activation loop phosphorylation, turn motif phosphorylation, and hydrophobic motif phosphorylation (22,23). The first step in the maturation process of PKC is phosphorylation of the activation loop (Thr500 in PKC  $\beta$ II) by the upstream kinase, PDK1 (Figure 1.2) (24-26). PDK1 is not only responsible for phosphorylation of PKC but also other AGC kinases such as Akt (27,28). When PKC is newly synthesized, it is loosely tethered at the membrane in a conformation in which the pseudosubstrate is out of the active site, thus adopting an open conformation with the activation loop site exposed (4). This open conformation is favorable for docking of PDK1 to the C-terminal tail of PKC and subsequent phosphorylation of the activation loop (Figure 1.2; first species of PKC on left). Phosphorylation at the activation loop is critical for the maturation of PKC in that it allows for autophosphorylation at the C-terminus, properly positions residues necessary for catalysis, and reveals access to the substrate binding site (29-31). However, once the activation loop is phosphorylated, phosphate at this site becomes dispensable for activity (23). Thus, activation loop phosphorylation is merely a primer for the subsequent C-terminal phosphorylations at the turn and hydrophobic motif. These phosphorylations serve to stabilize mature PKC; unphosphorylated or dephosphorylated species of PKC are rapidly degraded. Thus, in cells deficient in PDK1, PKC levels are grossly reduced, attesting to the instability of the non-phosphorylated form (32).

Once PDK1 phosphorylates PKC at the activation loop, the enzyme undergoes a rapid phosphorylation at the turn motif site (Thr641 in PKC  $\beta$ II, Fig. 2; 3<sup>rd</sup> species of PKC from left) (23). This site is conserved in all AGC kinases. In PKA, this phosphorylation serves to anchor the C-terminus at the upper lobe of the kinase domain by forming contacts with adjacent residues (2). In the PKC  $\beta$ II structure, this phosphorylation forms ionic contacts with basic residues (Lys374 and Arg415) on opposing  $\beta$  strands, thus differing from PKA (20). Novel isoforms do not have this Arg. Unlike phosphorylation of the activation loop site which is dispensable for activity, phosphorylation of the turn motif is absolutely required to maintain catalytic competence of the enzyme. Dephosphorylation abolishes activity (33,34). Phosphate on the turn motif locks PKC in a thermally stable conformation that, in the closed (inactive) state, is relatively resistant to phosphatases (23).

The final step in the maturation and processing of PKC is autophosphorylation at the C-terminal hydrophobic motif, a Ser/Thr flanked by hydrophobic residues. This site is also conserved among AGC kinases. For PKC  $\beta$ II, this phosphorylation occurs through an intramolecular mechanism (22). As discussed above, this phosphorylation aids in aligning the C helix for optimal catalytic activity; this site is absent in PKA (35). Functionally, phosphorylation at the hydrophobic motif is not required; however, phosphorylation of this site affects the subcellular localization and stability of PKC (36). In addition, the hydrophobic motif also provides a docking site for PDK1 (2).

Recent evidence suggests that the TORC2 complex (consisting of the mTOR kinase, rictor, mLST8, and Sin1) may be involved in regulation of the hydrophobic motif of PKC (37,38). In cells that lack components of this complex (either rictor or mLST8) PKC  $\alpha$  is

not phosphorylated at the hydrophobic motif and consequently is less stable (37).

Whether the mTORC2 complex controls events leading to the intramolecular autophosphorylation of this site remains to be established.

For conventional PKCs, phosphorylation at the C-terminal turn and hydrophobic motif sites is constitutive. Novel PKCs differ from their conventional counterparts in that their C-terminal phosphorylations are subject to modest regulation by outside stimuli; in addition, phosphorylation at this site for novel PKCs has been proposed to be catalyzed by a separate kinase (39). In this regard, addition of phorbol esters or antigen-receptor stimulation of T cells results in an increase in hydrophobic motif phosphorylation of PKC  $\theta$  that has been proposed to be independent of autophosphorylation (40). The hydrophobic motif sites of both PKC  $\delta$  and  $\epsilon$  have been shown to be sensitive to rapamycin, an inhibitor the mTOR pathway (38). Although kinase-dead mutants of novel isoforms are not phosphorylated at the hydrophobic motif, suggesting autophosphorylation, the possibility that these isoforms are controlled by a separate upstream kinase at this site remains to be unequivocally established (41).

## 2. Agonist-evoked autophosphorylation

In addition to the constitutive, processing autophosphorylations, PKC can autophosphorylate in response to agonist-evoked signaling. Novel autophosphorylation sites have been identified in PKC  $\alpha$ ,  $\beta$ ,  $\delta$ ,  $\eta$ , and  $\theta$  (42-45). These additional autophosphorylation sites are isozyme-specific and mark activated PKC; a novel autophosphorylation site in the C2 domain of PKC  $\alpha$  has been used as a dynamic marker in human cancer tissues (43). In addition to marking activated PKC, these

autophosphorylations regulate the cellular function of PKC. For example, autophosphorylation of PKC  $\theta$  is required for T cell activation, proper localization, and cross-talk between other signaling pathways, such as with Akt (45). In the invertebrate *Aplysia*, autophosphorylation of novel PKCs in the C2 domain is important for increased lipid binding and membrane translocation (46). This role of autophosphorylation in the C2 domain of novel PKCs may be conserved through vertebrates; PKC  $\eta$  also has autophosphorylation sites that are thought to be important for lipid-regulation (47). Autophosphorylation of PKC can fine-tune the differences and functional roles of each isozyme and provide an additional layer of regulation.

### 3. Tyrosine phosphorylation

Conventional, novel, and atypical PKC isozymes are phosphorylated on Tyr (48). This phosphorylation is emerging as an additional mechanism to fine tuning PKC activity and has been most studied with the novel isoform, PKC  $\delta$ . PKC  $\delta$  is phosphorylated at Tyr311 and Tyr332 in response to  $H_2O_2$  (49). The Src family of kinases can phosphorylate PKC  $\delta$  as a means to potentiate its activity and regulate activation loop phosphorylation (50-52). The EGF receptor can also phosphorylate PKC  $\delta$  in response to  $H_2O_2$  (53). Functionally, these tyrosine phosphorylations in PKC  $\delta$  aid in its ability to induce apoptosis in response to etoposide (54). Tyrosine phosphorylation may also serve an additional role in localization of PKC. Treatment of cells with tyrosine phosphatase inhibitors reverses the membrane translocation of PKC  $\beta$ II in phorbol ester-treated cells (55).

### *Regulation by lipid second messengers*

The hallmark of PKC activation in cells is translocation to cellular membranes. Once PKC has been processed by phosphorylation, it is localized to the cytosol where it is inactive with the pseudosubstrate docked in the substrate binding cavity (Fig. 2; 3<sup>rd</sup> species of PKC from left) (4). When extracellular signals cause hydrolysis of phosphatidylinositol-4,5-bisphosphate, diacylglycerol is generated and  $\text{Ca}^{2+}$  is released from intracellular stores. These second messengers,  $\text{Ca}^{2+}$  and diacylglycerol, initiate the membrane translocation and activation of PKC (Figure 1.2; 4<sup>th</sup> species of PKC from left). In the case of conventional PKCs,  $\text{Ca}^{2+}$  binds the C2 domain and pretargets PKC to the membrane (23). This initial binding to the membrane is of too low affinity to activate PKC; instead it allows the C1 domain to more effectively find its membrane-embedded ligand, diacylglycerol (56). The coordinated engagement of both the C1 and C2 domain on membranes provides the energy to release the autoinhibitory pseudosubstrate (6). Now in an open conformation, PKC can bind its substrates and initiate downstream signaling events (Figure 1.2; 4<sup>th</sup> species of PKC from left). Note that the potent analogues of diacylglycerol, phorbol esters, cause translocation and activation of PKC in the absence of  $\text{Ca}^{2+}$  because the affinity of the C1 domain for phorbol ester-containing membranes is two orders of magnitude higher than that for diacylglycerol-containing membranes; thus, the binding energy of phorbol esters to the C1 domain of PKC is sufficiently high to allow pseudosubstrate removal (23).

Novel PKCs do not have a  $\text{Ca}^{2+}$ -binding C2 domain and thus lack the membrane-pretargeting mechanism. Therefore, the novel isoforms compensate by having a C1 domain that binds diacylglycerol-containing membranes with an order of magnitude

higher affinity than the C1 domain of conventional PKCs. Thus, whereas the C2 domain of the conventional isozyme PKC  $\beta$ II is the major determinant in driving membrane binding, it is the C1B domain of the novel isozyme PKC  $\delta$  that is the major determinant for membrane binding (57). The differential affinity of conventional *versus* novel C1 domains for diacylglycerol-containing membranes is tuned by a single residue on the C1B domain: when present as Trp, as it is in novel PKCs, it confers high-affinity membrane binding and when present as a Tyr, as it is in conventional PKCs, it confers low-affinity membrane binding (58).

Atypical PKCs respond to neither diacylglycerol nor calcium. The only mode of regulation that has been well-studied is phosphorylation by PDK1 (25,26). Some studies have shown that insulin and phosphatidylinositol-3,4,5-trisphosphate (PIP<sub>3</sub>) can increase PKC  $\zeta$  activity through PDK1-dependent phosphorylation of the activation loop and autophosphorylation (59,60). Thus, unlike their other PKC counterparts, regulation of atypical PKCs depends on agonist stimulation.

#### *Regulation by scaffolding proteins*

Specificity in PKC signaling is achieved by proper spatial localization (61). Targeted kinase activity reporters have shown that PKC signals in all regions of the cell: plasma membrane, nucleus, Golgi apparatus, mitochondria, and cytosol (62). One must assume that in order for PKC to signal in these distinct cellular compartments, precise targeting mechanisms must be in place. One such mechanism is targeting by scaffolding proteins. Scaffolding proteins position PKC near its activators and substrates or at a particular cellular compartment, which allow for isozyme-specific signaling. PKC mediates protein:protein interactions through its regulatory C1 and C2 domains as well as

through the C-terminal tail. In some cases, PKC binding proteins interact with a particular conformation (unphosphorylated, phosphorylated but inactive, phosphorylated and active) of PKC, adding an additional layer of complexity to the regulation by scaffolding proteins (23). This form of regulation is unique in that therapeutics can be developed in order to disrupt or enhance PKC signaling in various regions of the cell.

When PKC is activated, it translocates from the cytosol to the plasma membrane (or other cellular membranes). This localization of activated PKC isoforms is achieved by protein:protein interactions between PKC and specific anchoring proteins. The proteins responsible for binding to activated PKC and thus regulating its activity are RACKS (receptors for activated C-kinase); this interaction is mediated by the C2 domain (reviewed in (63)). Different PKC isoforms bind to specific RACKs to target them to their proper location for cellular function. Mutation of the RACK binding site alters PKC activation in cells (63). RACKS not only bind PKC but also other signaling molecules such as PLC $\gamma$ , Src, and integrins (64). By serving as adaptors for other proteins, RACKS facilitate signaling by bringing enzymes in close proximity with their substrates or their activators. Understanding how the interaction between PKC and RACK is mediated has been informative in the design of activators and inhibitors of PKC that have therapeutic potential in cardiac disease (which will be discussed later).

Another important protein:protein interaction module is the C1 domain. A yeast two-hybrid screen using the N-terminal region of PKC  $\beta$ II as bait has identified some novel binding partners for PKC. PKC  $\beta$ II localizes to the centrosome, an organelle involved in spindle formation and cytokinesis, via the interaction of its C1A domain with pericentrin, a scaffolding protein. If this interaction is disrupted, PKC  $\beta$ II is released

from the centrosome and cell division is inhibited (65). Another protein that interacts with the C1A domain of PKC  $\beta$ II is a novel E3 ligase, RINCK (RING finger protein that interacts with C kinase). Overexpression of RINCK results in ubiquitination and degradation of PKC (66). By binding the C1 domain of PKC, these various proteins can alter the subcellular localization and activity of PKC.

One of the most promising regions for development of isozyme-specific therapeutics is the C-terminal tail of PKC. For example, PKC  $\alpha$  has been shown to play a role in synaptic plasticity by regulating the trafficking of cellular receptors that underlie the processes of memory and learning (67-69). PKC  $\alpha$  can induce cerebellar long-term synaptic depression (LTD) through protein interactions mediated by its type I PDZ (PSD-95, dishevelled, ZO1) ligand, QSAV, at its C-terminus (67). Deletion of this motif results in prevention of LTD and insertion of this motif into another conventional isoform that lacks the PDZ motif can induce LTD (67). PKC  $\alpha$  has been shown to interact with PICK1, another PDZ-containing protein, through its PDZ ligand in order to facilitate this process; thus, the PDZ ligand of PKC positions it with other signaling proteins in order to regulate important cellular functions (70).

### **Signal termination**

Extensive studies have detailed the molecular mechanisms of the maturation and activation of PKC (reviewed in (2,23)). We also now know more about where PKC signals in the cell and what are the downstream targets of PKC signaling. What is less understood are the molecular mechanisms that dictate the signal termination and “down-regulation” of PKC. It is in this part of PKC’s life cycle where there is a great

opportunity for targeting specific PKC isoforms and designing novel therapeutics to regulate specific PKC signaling pathways.

*“Reverse translocation”*

PKC's translocation to the membrane is a regulated process controlled by the generation of lipid second messengers and the subsequent allosteric activation of PKC by binding these cofactors. Just as translocation *to* the membrane initiates activation, translocation *from* the membrane initiates the termination process, and event that is also regulated. Acute activation of PKC by activation of G<sub>q</sub>-protein coupled receptors results in translocation to the membrane that is rapidly reversed; stimulation by phorbol esters prolongs interaction with the membrane (71). This reversal of PKC translocation under physiological agonist stimulation is coincident with desensitization of those receptors (71). Interestingly, PKC can still translocate to the membrane in response to phorbol esters after receptor stimulation indicating that acute activation of PKC is not enough to induce desensitization of PKC itself (71). Further studies investigating the molecular mechanism of this reverse translocation show that the C1 and C2 domains drive the membrane translocation and the catalytic activity of PKC is required for this process; it has been proposed that PKC must maintain its priming autophosphorylations at the C-terminus in order to disengage from the membrane (72,73). In phorbol ester-treated cells, tyrosine phosphorylation may also serve a role in facilitating the reverse translocation process (55). Thus, PKC is responsible for regulating its own dynamic membrane trafficking with autophosphorylation serving as a priming step to initiate the signal termination process.

### *Removal of second messengers*

Signaling pathways that activate phospholipase C (PLC) enzymes result in hydrolysis of phosphatidylinositol-4,5-bisphosphate (PIP<sub>2</sub>), giving the products diacylglycerol and inositol-1,4,5-trisphosphate (IP<sub>3</sub>). When IP<sub>3</sub> binds to receptors on the intracellular stores, Ca<sup>2+</sup> is released. PKC is activated by binding of these second messengers, diacylglycerol and Ca<sup>2+</sup>, to its regulatory modules, C1 and C2 domains, respectively.

Increasing the intracellular concentrations of Ca<sup>2+</sup> and diacylglycerol activates PKC; conversely, decreasing these ligands to basal levels inactivates PKC. PKC is acutely regulated by the presence of its activating cofactors (23). Studies using a membrane-tethered FRET-based activity reporter CKAR (C kinase activity reporter) show that PKC substrate phosphorylation oscillates with spiking levels of Ca<sup>2+</sup>, reflecting activation of conventional PKC isoforms (74). This correlation of increasing substrate phosphorylation (CKAR) with increasing Ca<sup>2+</sup> levels can be independent of diacylglycerol as seen in HeLa cells or coincident with diacylglycerol oscillations as seen in MDCK cells (74). These temporal dynamics in PKC signaling reflect a tight coupling between PKC activation and the influence of PKC and phosphatases on substrate phosphorylation. Indeed, targeting CKARs to various regions of the cell (plasma membrane, Golgi, cytosol, etc.) reveal a biphasic nature of PKC activity in response to agonist-induced signaling. Studies using these various reporters have shown that PKC has an early peak in activity followed by a late, sustained plateau (62). These differential activity profiles track with second messenger responses: Ca<sup>2+</sup> is responsible for the early peak in activity at the plasma membrane while diacylglycerol is responsible for the

second, sustained phase at Golgi (62). The levels of diacylglycerol vary at these different regions in the cell (plasma membrane, Golgi), possibly reflecting differences in activity of different PLC isoforms (75).

One way to deplete levels of diacylglycerol in the cell is through metabolism by diacylglycerol kinases (DGKs). DGK phosphorylates diacylglycerol, converting it into phosphatidic acid (76). Thus, DGKs, by removing the activating cofactor, serve an opposing role to PKCs in signaling pathways. In DGK $\delta$  knockout mice, there are increased levels of diacylglycerol and subsequently increased PKC activity that leads to aberrant phosphorylation of downstream targets (77). In cardiac remodeling pathways, DGK inhibits activation of G<sub>q</sub>-coupled signaling that leads to the activation of PKC (78). DGKs and PKCs can also physically interact, which allows for spatio-temporal control of localized diacylglycerol in the cell. PKC has been shown to catalyze an activating phosphorylation of DGK  $\gamma$  leading to a negative feedback mechanism (79). Conversely, phosphorylation of DGK  $\zeta$  by PKC is inhibitory (80). Activation of PKC can also cause translocation of DGK to where PKC is localized initiating another method of negative feedback (81). Thus, the location of PKCs and DGKs are precisely controlled in order to allow for rapid and efficient signaling by diacylglycerol. When diacylglycerol is produced, PKC is activated and that signal is terminated by the action of DGKs.

#### *Activation-induced down-regulation*

Twenty-five years ago, Nishizuka and coworkers reported that protein kinase C was the receptor for the potent tumor promoting phorbol esters; it was later shown that phorbol esters trigger the rapid redistribution of PKC from the cytosol to the membrane fraction of cells, the hallmark of PKC activation (82-84). Blumberg and coworkers

showed that phorbol esters, such as phorbol-12,13-dibutyrate (PDBu) and phorbol 12-myristate 13-acetate (PMA), elicit their actions by binding to the C1 domain, specifically competing with diacylglycerol (85-87). Conventional and novel PKCs could therefore bind to phorbol esters while atypical PKCs remain immune to their effects. Thus, PKC became known as the “receptor” for the tumor-promoting phorbol esters (88).

Chronic activation of PKC that occurs with treatment of cells with phorbol esters and bryostatins (another C1 domain binding compound) leads to the loss in activity and disappearance of PKC protein: ultimately, the down-regulation of PKC. The mechanism by which phorbol esters down-regulate PKC was first shown to be via an increased rate in proteolysis (degradation) (89). Although phorbol esters are the classical reagent used in down-regulation studies, they are not physiologically relevant agonists. The challenge in this field has been to demonstrate that natural agonists (such as hormones and growth factors) can initiate the down-regulation response. Studies have shown that the neuropeptide bombesin, platelet-derived growth factor (PDGF), or exogenous diacylglycerol can initiate the down-regulation of PKC isoforms in Swiss 3T3 fibroblasts (90). In gonadotrope cell lines, gonadotropin-releasing hormone (GnRH) can activate several PKC isozymes via a PLC-mediated pathway and initiate their down-regulation (91). Indeed, the detailed molecular mechanism of how phorbol esters and other agonists promote the down-regulation of PKC still remains elusive. However, the factors that are important for the signal propagation of PKC (activity, conformation, phosphorylation state, localization) also contribute to the regulation of the signal termination of PKC.

In order for PKC to be down-regulated, PKC must have its intrinsic catalytic activity. Mutation of the ATP binding site in PKC renders it insensitive to phorbol ester-

mediated degradation (92). However such kinase-inactive constructs of PKC still translocate to the membrane in response to phorbol ester treatment indicating that the membrane translocation of PKC is independent of its activity (92). This finding that catalytically-inactive PKC constructs are not sensitive to phorbol ester-dependent down-regulation was the first clue that autophosphorylation of PKC might be a prerequisite for the initiation of the down-regulation pathway. However, there was initial conflict over whether this was the mechanism because other studies had shown that a kinase-dead PKC could down-regulate through the activity of other endogenous PKCs (transphosphorylation) (93-95). Indeed, isozyme differences exist in down-regulation profiles. Studies performed in *Schizosaccharomyces pombe* indicated that kinase activity was required for specific isozymes (PKC  $\delta$ ) but those that could not down-regulate themselves (PKC  $\epsilon$ ) could be affected by *trans* PKC activity (96). However, later studies using PKC inhibitors confirmed the hypothesis that the catalytic activity of PKC was required for its down-regulation (91,97). What remains unclear is whether the increased proteolysis observed with phorbol ester activation of PKC is a consequence of a conformational change, a secondary effect of autophosphorylation, or whether a specific protease is activated.

When PKC is activated by its lipid cofactors, phosphatidylserine and diacylglycerol, PKC translocates to the membrane and the autoinhibitory pseudosubstrate is pulled out of the active site, leaving PKC in an open conformation (4,5). In the case of diacylglycerol, this response is transient as diacylglycerol is rapidly metabolized (98). Conversely, with the higher affinity binding of phorbol esters, translocation of PKC to the membrane is prolonged, leaving PKC in an open conformation and susceptible to the

activity of proteases. Not only does activation of PKC expose the pseudosubstrate, which can be cleaved, but also the proteolytically-labile hinge region between the regulatory and catalytic domains. The  $\text{Ca}^{2+}$ -dependent neutral proteases (m-calpain and  $\mu$ -calpain) can cleave PKC in this hinge; however, mutation of the calpain cleavage sites failed to alter the down-regulation in response to phorbol esters indicating that these proteases were not involved in the process (99). Later studies using calpain protease inhibitors failed to inhibit down-regulation confirming that they were not primarily responsible for the degradation (91). Therefore, having PKC in an open conformation is important for mediating activation-induced down-regulation but not by the action of calpain proteases.

#### *Dephosphorylation*

As mentioned earlier, activation of PKC by its lipid cofactors allosterically alters the conformation of PKC by removing the pseudosubstrate out of the substrate-binding cavity. Not only is activated PKC susceptible to cleavage by proteases but it also has a markedly increased sensitivity to dephosphorylation by phosphatases. Phosphorylation of PKC is critical for maintenance of catalytic competence. Dephosphorylation of the three processing sites (activation loop, turn motif, hydrophobic motif) of PKC inactivates the kinase. Studies show that chronic activation of PKC results in a fully dephosphorylated, inactive kinase, which precedes its degradation (97,100,101). This dephosphorylated form accumulates in a cytoskeletal, detergent-insoluble fraction of cells. This mechanism is the classical model of PKC down-regulation. Thus, discovery of the phosphatases that might control dephosphorylation of PKC under agonist-evoked activation would be important for understanding how PKC is desensitized. Upon activation, PKC translocates to the membrane compartment. The heterotrimeric type 2A

phosphatase (PP2A) is localized to the membrane and dephosphorylates PKC upon stimulation with phorbol esters (102). Addition of okadaic acid, a PP2A phosphatase inhibitor, slows this process and potentially protects PKC from down-regulation (102).

The newly-discovered protein phosphatase 2C (PP2C) family of phosphatases, the PHLPP family (for PH domain Leucine-rich repeat Protein Phosphatase), has recently been shown to regulate the phosphorylation state, and thus levels, of PKC (103,104). There are three isoforms of PHLPP: the alternatively spliced PHLPP1 $\alpha/\beta$  and PHLPP2. PHLPP was first characterized as the phosphatase responsible for dephosphorylating the hydrophobic motif of Akt (105). Since hydrophobic motif phosphorylation is primarily responsible for Akt's intrinsic catalytic activity, dephosphorylation by PHLPP ultimately inactivates the kinase (105,106). In addition, depletion of PHLPP by siRNA increases the level and duration of agonist-evoked Akt signaling, causing apoptosis and decreased cell proliferation (105,107). In contrast, phosphorylation of the hydrophobic motif in PKC primarily controls the stability of PKC. Overexpression of PHLPP leads to dephosphorylation of PKC at the hydrophobic motif which ultimately shunts it to the detergent-insoluble fraction of cells for degradation (Fig. 2; species of PKC on bottom right) (104). Conversely, depletion of PHLPP results in an up-regulation of PKC levels. Thus, PHLPP plays an important role in the regulation of PKC levels and stability.

#### *Rescue by heat shock proteins*

Once PKC has been activated by membrane binding, it is in an open conformation rendering it more sensitive to phosphatases, proteolysis, and ultimately, degradation. However, dephosphorylated PKC can be rescued with the help of heat shock proteins. When PKC is dephosphorylated at the turn motif (one of the three processing sites),

Hsp70 can bind and stabilize it, allowing it to re-phosphorylate and enter back into the pool of signaling PKC (Figure 1.2) (108). Disruption of this interaction causes PKC to accumulate in the detergent-insoluble fraction of cells, targeting it for down-regulation (108). Specifically, an invariant Leu that precedes the turn motif phosphorylation site is responsible for mediating the interaction between Hsp70 and PKC; mutation of this site subsequently increases the dephosphorylation and ubiquitination of PKC (109). Thus, Hsp70 prolongs the lifetime of PKC. Specifically, Hsp70 binds the dephosphorylated form of PKC; this differs from other binding partners such as PDK1 which binds to the C-terminus of newly synthesized PKC that has never been phosphorylated (108,110). Thus, the C-terminus of PKC serves an important role in modulating the signaling lifetime of PKC by mediating important protein:protein interactions. Through regulation of the phosphorylation state of the C-terminus, PKC can interact with specific binding partners to target it to different signaling pathways.

#### *Degradation / down-regulation pathways*

##### 1. Degradation by proteasomal pathways

A ubiquitous mechanism for protein degradation in the cell is the ubiquitin-proteasome system (UPS) (reviewed in (111)). By labeling proteins with a “tag” (ubiquitin), they are targeted to a multi-enzymatic complex, the proteasome, where they are proteolyzed and degraded (112). Ubiquitin is an 8.5 kDa polypeptide that is conjugated to proteins which serves as a molecular marker for degradation. Degradation by the proteasome involves a two successive steps: 1) priming the protein for degradation by addition of ubiquitin and 2) proteolysis of the protein via the proteasome machinery (112). In the first step, ubiquitin is activated and conjugated to the protein by the action

of the three enzymes: 1) E1, ubiquitin-activating enzyme, 2) E2, ubiquitin-conjugating enzyme and 3) E3, ubiquitin ligase (112). These enzymes work in concert to add the molecular tag that will target them to the proteasome for degradation. The second step is the actual degradation of the tagged protein by the proteasome to produce smaller peptides and free ubiquitin (112). Typically, ubiquitin is conjugated to proteins in the long chains which serve not only to target them to the proteasome, as described above, but also can also lead to other cellular functions (111). Many cellular proteins utilize the UPS for degradation.

PKC was first shown to be degraded by the ubiquitin-proteasome pathway with treatment of bryostatins; like phorbol esters, they are also strong activators of PKC and lead to the rapid dephosphorylation and down-regulation of PKC (101,113). Treatment of cells with bryostatin results in an accumulation of higher molecular weight species that are labeled with ubiquitin antibody, an accumulation that is inhibited by proteasome inhibitors (113). Later studies in human fibroblasts indicated that the UPS system is primarily responsible for degradation of PKC  $\alpha$  and PKC  $\epsilon$  isozymes upon treatment of bryostatin and PMA; addition of proteasome inhibitors inhibited down-regulation whereas inhibitors of calpain proteases, lysosomal enzymes, and vesicle trafficking had no effect (114).

What targets PKC to be degraded by the proteasome? Debate currently exists as to whether or not the phosphorylation state of PKC dictates whether it will be ubiquitinated. Several studies have suggested that dephosphorylation of the three priming sites of PKC (activation loop, turn motif, hydrophobic motif) and inactivation precedes the degradation of the enzyme (97,113,114). However, this phenomenon may

be isozyme- and cell-type specific. Although the conventional isoforms PKC  $\alpha$  and PKC  $\beta$  and the novel isoform PKC  $\epsilon$  have been shown to be dephosphorylated prior to degradation, the novel isoform PKC  $\delta$  is hyper-phosphorylated in response to PMA-induced degradation and phosphatase inhibitors such as calyculin A promote its down-regulation (97,114,115). In studies using a rat intestinal epithelial cell line, fully phosphorylated, active PKC is ubiquitinated at the plasma membrane and degraded by the proteasome in response to PMA; phosphatase inhibitors accelerate this process (116). Differences in cell-type, localization, type and duration of stimuli all could account for the differences in down-regulation mechanisms. However, fewer studies have shown ubiquitination of the fully phosphorylated enzyme (117). Additionally, other phosphorylations could play a role in targeting PKC for degradation. All PKC isozymes contain PEST sequences which are proline, glutamate, serine, and threonine residues that are thought to predispose a protein for degradation (114,118). Phosphorylation at these sequences in proteins such as I $\kappa$ B and cyclins triggers ubiquitination and degradation by the proteasome (118). Certainly phosphorylation of PEST sequences could serve as a common mechanism for targeting proteins for degradation.

In summary, activation of PKC triggers its own down-regulation. Not only does chronic activation that occurs with phorbol esters promote the ubiquitination and degradation of PKC, but also natural agonists such as diacylglycerol, bombesin, and hormones all induce ubiquitination of PKC (90,91,119). Down-regulation that occurs via the ubiquitin-proteasome pathway requires the catalytic activity of PKC; addition of kinase inhibitors inhibit this process and a kinase-dead PKC cannot be degraded (119,120). Essentially, PKC initiates its own suicide mechanism.

Since PKC is ubiquitinated and degraded, now the question arises as to what molecular machinery is responsible for this process. The prime target would be to identify the E3 ligase that tags PKC with ubiquitin. Several E3 ligases have been identified that are responsible for ubiquitination of PKC. As mentioned earlier, RINCK is an E3 ligase that ubiquitinates PKC (66). However, RINCK is not the E3 ligase responsible for the activation-induced down-regulation pathways (66). RINCK controls the amplitude of the PKC signal by regulating the basal levels of PKC in the cell; depletion of RINCK with siRNA increases PKC protein levels by mechanisms independent of the activation or phosphorylation state of PKC (66). Recently, an ubiquitin complex called LUBAC (linear ubiquitin assembly complex) comprised of HOIL-1, an E3 ligase, and a binding protein, HOIP, was shown to bind and ubiquitinate activated PKC  $\alpha$  and  $\beta$ II (121). The von Hippel-Lindau tumor suppressor protein (pVHL), another E3 ligase, targets atypical PKCs; pVHL ubiquitinates activated PKC  $\lambda$  [122]. As there are ten isozymes of PKCs with a wide range of function, it is certainly possible that there could be a specific E3 ligase for not only each PKC, but perhaps in particular cellular functions and processes. Understanding the mechanisms that recruit E3 ligases to target PKCs for degradation would provide another means of therapeutic regulation of PKC.

## 2. Down-regulation by internalization / trafficking pathways

The down-regulation of PKC is not a passive process; activation of PKC is the first step in triggering this mechanism and a catalytically-active enzyme is required. Studies have shown that the phorbol ester-induced down-regulation of PKC correlates with an

increase in endocytic, membrane transport processes (96,122,123). The desensitization of receptors occurs through internalization and targeting to endosomes (124). Active PKC is associated with membranes and thus it is highly possible that PKC is involved with this increased membrane trafficking. Here, localization and scaffolding proteins can dictate the fate of PKC. Now the question arises: how does PKC disengage from the membrane and begin the desensitization process?

Upon stimulation with PMA, PKC accumulates at a perinuclear compartment (97,123). This perinuclear accumulation is a temperature-sensitive process, suggesting that vesicular trafficking is involved (97). Decreasing the temperature also inhibits the dephosphorylation of PKC upon PMA stimulation suggesting that the dephosphorylation step coincides with membrane trafficking events (97). Indeed, the down-regulation of PKC shares similar characteristics to receptor desensitization processes. Upon stimulation with phorbol esters, PKC trafficks to an endosomal compartment as an active kinase and then is subsequently transported to a perinuclear region where it is dephosphorylated and degraded (122). This trafficking is mediated by a caveolae-dependent process (122). Interestingly, it has been shown that phorbol ester treatment disrupts caveolae; however, most likely in the time frame of treatment, the caveolae are internalized as part of this membrane trafficking event (122,125). A similar mechanism of internalization and dephosphorylation of PKC has been shown in rat intestinal epithelial cells upon bryostatin treatment (116).

Other studies have characterized PKC's activation-induced translocation to this perinuclear/juxtannuclear compartment as a subset of recycling endosomes that colocalize with the centrosome (126). Here, under long-term stimulation with phorbol esters, PKC

remains as a fully active kinase that is not degraded; PKC colocalizes with markers of recycling endosomes and not cellular compartments involved in degradation such as the proteasome and lysosome (126). Instead, PKC is actively involved in the sequestration of proteins such as transferrin, a marker for membrane recycling, to this juxtannuclear, centrosomal compartment (independent of the Golgi), deemed the “pericentriion,” and inhibitors of clathrin-dependent endocytosis can prevent this process (126,127). Interestingly, the caveolae-dependent, clathrin-*independent* trafficking of PKC as seen with other studies can occur through this clathrin-*dependent* process and thus reconcile the differences seen between these two pathways (122,127,128). However, these membrane trafficking/recycling events are observed following 60 minutes of phorbol ester treatment; it is certainly possible that the degradative events for PKC occur beyond that time frame either in that pericentriion compartment or somewhere else in the cell. The temporal and spatial dynamics of PKC down-regulation still remain to be fully elucidated.

### **PKC in disease**

PKC isozymes are involved in a wide variety of cellular processes. Since PKC isozymes are so diverse in their function, disruption of PKC signaling can have multiple cellular effects. Diseases that are affected by aberrant PKC signaling pathways include metabolic disorders such as diabetes, cardiovascular and pulmonary disorders, central nervous system dysfunction, and neuronal degeneration (129). PKC undergoes a series of processing phosphorylations that controls its stability and ultimately sets the amplitude for agonist-induced signaling in the cell. Dysregulation of PKC that alters the protein

levels in the cell affect the magnitude and duration of downstream signaling; these altered levels of PKC are associated with a variety of pathologies, most notably cancer (130-132). Indeed, identification of PKC as the receptor for the tumor-promoting phorbol esters provided the first substantial link that this enzyme may be involved in carcinogenesis (130).

The role of PKC in cancer has been reviewed quite extensively over the past few years (129-132). Almost all of the ten isozymes have been implicated in some form of cancer. The expression levels of PKCs as well as the specific cellular pathways that are affected (i.e. proliferation, apoptosis, angiogenesis) vary based on specific isozyme and tissue type. However, the genetic factors that control PKC's role in cancer are less well understood.

Advances have been made towards discovering the genes involved in carcinogenesis. With the availability of the entire human genome sequence, it is now possible to identify genes important in pathological pathways. Recently, 210 human cancer genomes were sequenced, specifically looking at the 518 kinases, in order to identify putative "passenger" and "driver" mutations that might predispose one to cancer (133). The study identified mutations predicted to be driver mutations based on the following: if a kinase possesses a higher ratio of nonsynonymous mutations compared to synonymous mutations, and this frequency is greater than the frequency expected by chance, then the given kinase is likely to possess a driver mutation, which is hypothesized to play a role in the process of tumorigenesis. Driver mutations can confer a growth advantage to the cell, inhibit apoptosis, inhibit migration, and essentially prevent the cell from being able to regulate properly; passenger mutations do not and are therefore not

selected (133). Out of the 518 kinases in the human genome, approximately 120 kinases carry at least one putative driver mutation, PKC included (133). In fact, of the 10 PKC isozyms, the conventional isozyms PKC  $\alpha$  and PKC  $\beta$  had the highest probability of carrying driver mutations; these data are consistent with proposed roles of conventional PKCs in cancer (131-133). For these two isozyms, mutations were identified in both the regulatory and kinase domains (133). Additionally, mutations have been characterized in the C1B domain and C-terminus of PKC  $\gamma$  which contribute to the development of spinocerebellar ataxia (134). Understanding how these mutations alter PKC function, stability, and localization could be key in designing therapeutics to target PKCs involved in various cancers and diseases.

### **PKC as a drug target**

Since disruption of PKC regulation has been implicated in tumorigenesis and drug resistance, PKC has become a prime candidate for the design of therapeutics, specifically as cancer therapies (131,132,135). However, the involvement of PKC isozyms in cancer is very complex due to the number of different PKC isozyms and the various roles they play in different cancer types. PKC isozyms can directly oppose each other in function: PKC  $\delta$  is typically a pro-apoptotic and anti-proliferative whereas PKC  $\epsilon$  is anti-apoptotic and proliferative (130). Within individual isozyms, differences can vary based on the cancer type: PKC  $\beta$ II is up-regulated in B-cell lymphomas and colon cancer and down-regulated in bladder cancer; similarly, PKC  $\epsilon$  is up-regulated in breast cancer and down-regulated in colon cancer (130). Thus, designing specific therapeutics for specific PKC isozyms is of great importance to prevent unwanted side effects (i.e., down-regulating

PKC  $\delta$  if trying to specifically target PKC  $\epsilon$ ). PKC drugs have been targeted against two regions of the kinase: the catalytic domain and the regulatory domain.

*Catalytic domain:* Currently there are a number of PKC inhibitors undergoing clinical trials. Two of these inhibitors, enzastaurin (LY-317615) and ruboxistaurin (Arxxant, LY-333531), which are specific for PKC  $\beta$ , are ATP-binding competitive inhibitors and are in Phase III of clinical trials for cancer drugs (131). Enzastaurin has shown promise in the treatment of colon and lung cancers, which have increased levels of PKC  $\beta$ , by inducing apoptosis, reducing proliferation, and suppressing angiogenesis, primarily mediated through the Akt/PI3K and VEGF (vascular endothelial growth factor) pathways (136,137). Ruboxistaurin has been developed as a treatment for diabetic retinopathy, which has hyperactivated PKC  $\beta$  (138,139).

With the recent elucidation of various crystal structures of the catalytic domain of PKC, optimization of PKC inhibitors targeting the catalytic domain can be achieved. For example, the PKC  $\theta$  structure has been used in structure-based design of inhibitors to target PKC  $\theta$  in the treatment of asthma and autoimmune diseases (140). The goal would be to use the structure to design specific inhibitors to test in cell-based assays and ultimately take to clinical trials. The catalytic domain of various isozymes could be compared and then tuned for selectivity for that specific isozyme (140).

*Regulatory domain:* Naturally-occurring agonists of PKC such as bryostatin have been also tested in clinical trials but have shown less success (131). These compounds bind to the C1 domain and result in the acute activation of conventional and novel PKCs, similarly to phorbol esters; however, unlike phorbol esters, bryostatins have shown anti-tumor effects such as inhibiting cell growth and promoting apoptosis by differential

regulation of PKC isozymes (131,135). As mentioned earlier, bryostatin inhibits PKC activity by down-regulating the enzyme through the ubiquitin-proteasome pathway (113,114,135,141). However, since bryostatin does target several PKC isozymes, it is hard to measure the anticancer effects.

The C2 domain is critical for determining the subcellular localization of PKC (63). Peptides have been derived from the C2 domain to serve as isozyme-specific activators and inhibitors by regulating PKC's interaction with its RACK (63). In PKC  $\epsilon$ , for example, short peptides have been developed from its C2 domain that confers cardiac protective effects against ischemic injury (142). These peptides are being investigated as potential leads to treat various cardiac conditions and have entered clinical trials (143). The benefit of this type of rational drug design is that it allows more selectivity and specificity for PKC isozymes since greater variation exists among the isozymes in their C2 domain. Indeed, targeting protein:protein interaction modules is becoming a more plausible way to target specific PKC isozymes. PKC  $\iota$ -mediated oncogenic signaling pathways can be altered by disrupting PKC  $\iota$ 's interaction with PAR6, mediated through its PB1 domain (144). Since PKC  $\iota$  mediates its oncogenic effects through its PB1 domain, disrupting that interaction has shown promise in treating lung cancer, where PKC  $\iota$  signals through its complex with PAR6 (144).

Finally, another potential region that can be used to develop specific PKC therapeutics is the C-terminal tail of PKC, which is quite variable among the isoforms. As mentioned earlier, PKC  $\alpha$  and PKC  $\zeta$  have unique PDZ ligands at their C-termini to mediate important protein:protein interactions; these can be disrupted with therapeutics to modulate PKC's activity and their downstream signaling effects. Additionally, the C-

terminal tail is important for mediating intramolecular interactions between the C2 domain and catalytic core, thus indicating that it would be a prime target for designing isozyme-specific drugs (63).

*Targeting protein regulators of PKC activity:* Another possibility for the development of therapeutics to target PKC would be to look at upstream regulators of PKC activity, i.e., phosphatases, E3 ligases. Specifically, the focus should look at the various down-regulation pathways of PKCs which seem to differ among the isozymes. The PHLPP phosphatase, which directly dephosphorylates PKC and regulates its cellular levels, is down-regulated in colon cancers which have high levels of PKCs (103). Perhaps designing drugs to target PHLPP in colon cancer would be a better way to regulate PKC's effects in this type of cancer. Additionally, the E3 ligase RINCK lies on a chromosomal position that is frequently deleted in non-small cell lung carcinoma, which also has high levels of PKCs (63,145). Since the PKC isozymes share a highly conserved catalytic core, other avenues for designing novel and specific PKC therapeutics must be considered. Targeting subcellular localization and binding partners, which vary among the isozymes, is a likely candidate.

## **Conclusion**

The PKC family represents a gold-mine for the development of novel, specific therapeutics. However, the existence of multiple highly-related isozymes with conserved catalytic and substrate-recognition mechanisms has proven a challenge for the development of specific inhibitors. Our increasing understanding of the spatio-temporal

dynamics of signaling by these family members holds promise for the design of novel therapeutics that will disrupt the localization and hence function of specific isoforms.

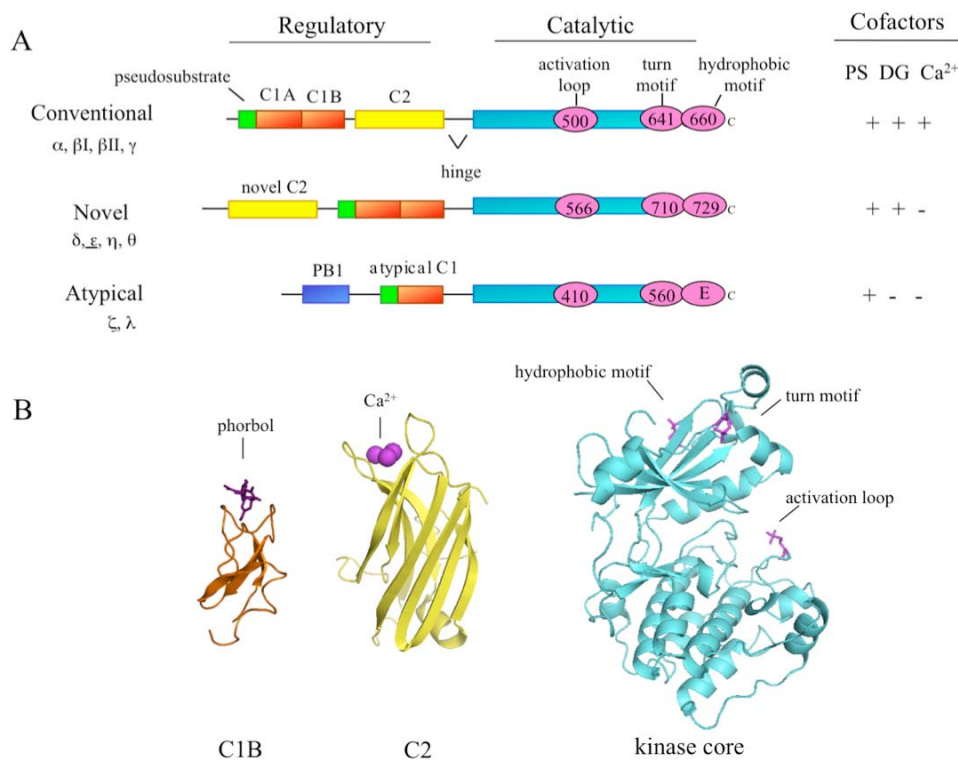


**Figure 1.1:** Domain composition of PKC family members. *A*, The primary structure of the three classes of PKC isozymes: conventional, novel, and atypical. The regulatory moiety contains the cofactor-binding modules: the pseudosubstrate (green); the C1A and C1B domains (orange) that bind phosphatidylserine for all PKCs and diacylglycerol/phorbol esters for conventional and novel PKCs; the C2 domain (yellow) that binds anionic lipids and Ca<sup>2+</sup> for conventional PKCs; and a PB1 domain (blue) that serves as a protein:protein interaction module for atypical PKCs. The requirements for cofactor binding are shown to the right: PS, phosphatidylserine; DG, diacylglycerol; and Ca<sup>2+</sup>. The catalytic moiety contains the conserved kinase domain (cyan) with the activation loop phosphorylation site (pink circle) and a C-terminal tail that contains two conserved phosphorylation sites: the turn motif and the hydrophobic motif (pink circles; note that for atypical PKCs a glutamate occupies the hydrophobic motif). The numbering of the phosphorylation sites is representative of the PKC isozyme underlined to the left. *B*, Ribbon diagrams of the C1B domain of PKC  $\delta$  (orange) with bound phorbol (purple), the C2 domain of PKC  $\beta II$  (yellow) with bound Ca<sup>2+</sup> (pink), and the kinase domain of phosphorylated PKC  $\beta II$  (blue) with phosphate at the three conserved phosphorylation sites: activation loop (pink), turn motif (orange) and hydrophobic motif (green) (12,20,146). (Adapted from (2,23))

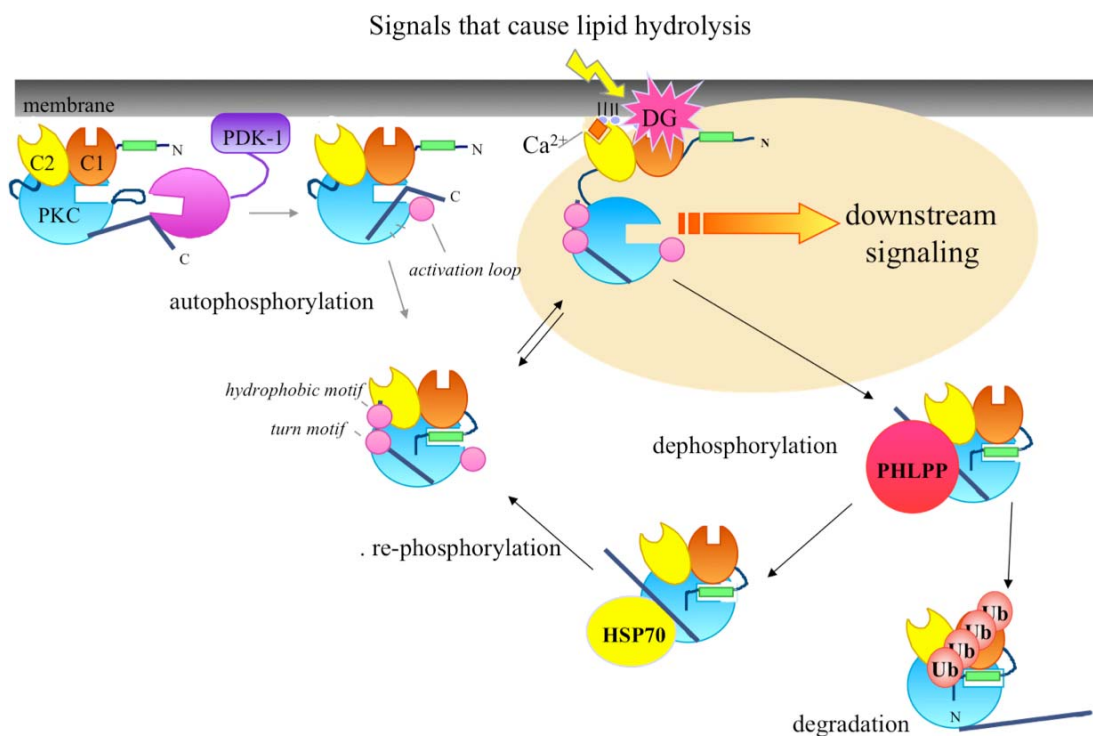


**Figure 1.2:** Model showing the life cycle of PKC. When PKC is newly synthesized, the enzyme is loosely tethered at the membrane in an open conformation with the pseudosubstrate (green) released from the substrate-binding cavity (rectangular indent in cyan circle), and the C-terminus is exposed to allow the upstream kinase, PDK-1, to bind (far left). PDK1 phosphorylates the activation loop and is released from the C-terminus. Once the C-terminus is free, PKC can autophosphorylate at the C-terminal phosphorylation sites by an intramolecular mechanism. Once PKC has been processed by phosphorylation, it is released into the cytosol and maintained in an inactive conformation with the pseudosubstrate lodged into the substrate-binding cavity (middle of the diagram). Signals that cause lipid hydrolysis and generate the second messengers,  $Ca^{2+}$  and diacylglycerol, cause the translocation of PKC from the cytosol to the membrane. Binding of  $Ca^{2+}$  and diacylglycerol to the C1 (orange) and C2 (yellow) domains, respectively, provides the energy to release the pseudosubstrate from the active site and allow downstream signaling. In this open, active conformation, PKC is susceptible to dephosphorylation by phosphatases such as PHLPP (red circle) and then targeted for ubiquitination and degradation. However, the molecular chaperone Hsp70 (yellow circle) can bind the dephosphorylated turn motif and stabilize PKC; this allows it to re-phosphorylate and re-enter the pool of competent, signaling enzyme.

## References

1. Mellor, H., and Parker, P. J. (1998) *Biochem J* **332** (Pt 2), 281-292
2. Newton, A. C. (2003) *Biochem J* **370**, 361-371
3. House, C., and Kemp, B. E. (1987) *Science* **238**, 1726-1728
4. Dutil, E. M., and Newton, A. C. (2000) *J Biol Chem* **275**, 10697-10701
5. Orr, J. W., and Newton, A. C. (1994) *J Biol Chem* **269**, 8383-8387
6. Orr, J. W., Keranen, L. M., and Newton, A. C. (1992) *J Biol Chem* **267**, 15263-15266
7. Johnson, J. E., Giorgione, J., and Newton, A. C. (2000) *Biochemistry* **39**, 11360-11369
8. Cho, W. (2001) *J Biol Chem* **276**, 32407-32410
9. Colon-Gonzalez, F., and Kazanietz, M. G. (2006) *Biochim Biophys Acta* **1761**, 827-837
10. Hurley, J. H. (2006) *Biochim Biophys Acta* **1761**, 805-811
11. Hurley, J. H., Newton, A. C., Parker, P. J., Blumberg, P. M., and Nishizuka, Y. (1997) *Protein Sci* **6**, 477-480
12. Zhang, G., Kazanietz, M. G., Blumberg, P. M., and Hurley, J. H. (1995) *Cell* **81**, 917-924
13. Dries, D. R., and Newton, A. C. (2008) *J Biol Chem*
14. Cho, W., and Stahelin, R. V. (2006) *Biochim Biophys Acta* **1761**, 838-849
15. Hirano, Y., Yoshinaga, S., Ogura, K., Yokochi, M., Noda, Y., Sumimoto, H., and Inagaki, F. (2004) *J Biol Chem* **279**, 31883-31890
16. Knighton, D. R., Zheng, J. H., Ten Eyck, L. F., Xuong, N. H., Taylor, S. S., and Sowadski, J. M. (1991) *Science* **253**, 414-420
17. Kannan, N., Haste, N., Taylor, S. S., and Neuwald, A. F. (2007) *Proc Natl Acad Sci U S A* **104**, 1272-1277

18. Messerschmidt, A., Macieira, S., Velarde, M., Badeker, M., Benda, C., Jestel, A., Brandstetter, H., Neufeind, T., and Blaesse, M. (2005) *J Mol Biol* **352**, 918-931
19. Xu, Z. B., Chaudhary, D., Olland, S., Wolfrom, S., Czerwinski, R., Malakian, K., Lin, L., Stahl, M. L., Joseph-McCarthy, D., Benander, C., Fitz, L., Greco, R., Somers, W. S., and Mosyak, L. (2004) *J Biol Chem* **279**, 50401-50409
20. Grodsky, N., Li, Y., Bouzida, D., Love, R., Jensen, J., Nodes, B., Nonomiya, J., and Grant, S. (2006) *Biochemistry* **45**, 13970-13981
21. Johnson, L. N., and Lewis, R. J. (2001) *Chem Rev* **101**, 2209-2242
22. Keranen, L. M., Dutil, E. M., and Newton, A. C. (1995) *Curr Biol* **5**, 1394-1403
23. Newton, A. C. (2001) *Chem Rev* **101**, 2353-2364
24. Dutil, E. M., Toker, A., and Newton, A. C. (1998) *Curr Biol* **8**, 1366-1375
25. Le Good, J. A., Ziegler, W. H., Parekh, D. B., Alessi, D. R., Cohen, P., and Parker, P. J. (1998) *Science* **281**, 2042-2045
26. Chou, M. M., Hou, W., Johnson, J., Graham, L. K., Lee, M. H., Chen, C. S., Newton, A. C., Schaffhausen, B. S., and Toker, A. (1998) *Curr Biol* **8**, 1069-1077
27. Alessi, D. R., James, S. R., Downes, C. P., Holmes, A. B., Gaffney, P. R., Reese, C. B., and Cohen, P. (1997) *Curr Biol* **7**, 261-269
28. Walker, K. S., Deak, M., Paterson, A., Hudson, K., Cohen, P., and Alessi, D. R. (1998) *Biochem J* **331** ( Pt 1), 299-308
29. Nolen, B., Taylor, S., and Ghosh, G. (2004) *Mol Cell* **15**, 661-675
30. Dutil, E. M., Keranen, L. M., DePaoli-Roach, A. A., and Newton, A. C. (1994) *J Biol Chem* **269**, 29359-29362
31. Orr, J. W., and Newton, A. C. (1994) *J Biol Chem* **269**, 27715-27718
32. Balendran, A., Hare, G. R., Kieloch, A., Williams, M. R., and Alessi, D. R. (2000) *FEBS Lett* **484**, 217-223
33. Edwards, A. S., Faux, M. C., Scott, J. D., and Newton, A. C. (1999) *J Biol Chem* **274**, 6461-6468
34. Bornancin, F., and Parker, P. J. (1996) *Curr Biol* **6**, 1114-1123

35. Frodin, M., Antal, T. L., Dummler, B. A., Jensen, C. J., Deak, M., Gammeltoft, S., and Biondi, R. M. (2002) *Embo J* **21**, 5396-5407
36. Edwards, A. S., and Newton, A. C. (1997) *J Biol Chem* **272**, 18382-18390
37. Guertin, D. A., Stevens, D. M., Thoreen, C. C., Burds, A. A., Kalaany, N. Y., Moffat, J., Brown, M., Fitzgerald, K. J., and Sabatini, D. M. (2006) *Dev Cell* **11**, 859-871
38. Parekh, D., Ziegler, W., Yonezawa, K., Hara, K., and Parker, P. J. (1999) *J Biol Chem* **274**, 34758-34764
39. Cameron, A. J., De Rycker, M., Calleja, V., Alcor, D., Kjaer, S., Kostecky, B., Saurin, A., Faisal, A., Laguerre, M., Hemmings, B. A., McDonald, N., Larijani, B., and Parker, P. J. (2007) *Biochem Soc Trans* **35**, 1013-1017
40. Freeley, M., Volkov, Y., Kelleher, D., and Long, A. (2005) *Biochem Biophys Res Commun* **334**, 619-630
41. Cenni, V., Doppler, H., Sonnenburg, E. D., Maraldi, N., Newton, A. C., and Toker, A. (2002) *Biochem J* **363**, 537-545
42. Durgan, J., Michael, N., Totty, N., and Parker, P. J. (2007) *FEBS Lett* **581**, 3377-3381
43. Ng, T., Squire, A., Hansra, G., Bornancin, F., Prevostel, C., Hanby, A., Harris, W., Barnes, D., Schmidt, S., Mellor, H., Bastiaens, P. I., and Parker, P. J. (1999) *Science* **283**, 2085-2089
44. Flint, A. J., Paladini, R. D., and Koshland, D. E., Jr. (1990) *Science* **249**, 408-411
45. Thuille, N., Heit, I., Fresser, F., Krumbock, N., Bauer, B., Leuthaeusser, S., Dammeier, S., Graham, C., Copeland, T. D., Shaw, S., and Baier, G. (2005) *Embo J* **24**, 3869-3880
46. Pepio, A. M., and Sossin, W. S. (2001) *J Biol Chem* **276**, 3846-3855
47. Littler, D. R., Walker, J. R., She, Y. M., Finerty, P. J., Jr., Newman, E. M., and Dhe-Paganon, S. (2006) *Biochem Biophys Res Commun* **349**, 1182-1189
48. Konishi, H., Tanaka, M., Takemura, Y., Matsuzaki, H., Ono, Y., Kikkawa, U., and Nishizuka, Y. (1997) *Proc Natl Acad Sci U S A* **94**, 11233-11237
49. Steinberg, S. F. (2004) *Biochem J* **384**, 449-459

50. Joseloff, E., Cataisson, C., Aamodt, H., Ocheni, H., Blumberg, P., Kraker, A. J., and Yuspa, S. H. (2002) *J Biol Chem* **277**, 12318-12323
51. Hall, K. J., Jones, M. L., and Poole, A. W. (2007) *Biochem J* **406**, 501-509
52. Rybin, V. O., Guo, J., Gertsberg, Z., Elouardighi, H., and Steinberg, S. F. (2007) *J Biol Chem* **282**, 23631-23638
53. Morita, M., Matsuzaki, H., Yamamoto, T., Fukami, Y., and Kikkawa, U. (2007) *J Biochem (Tokyo)*
54. Blass, M., Kronfeld, I., Kazimirsky, G., Blumberg, P. M., and Brodie, C. (2002) *Mol Cell Biol* **22**, 182-195
55. Takahashi, H., Suzuki, K., and Namiki, H. (2003) *Cell Struct Funct* **28**, 123-130
56. Nalefski, E. A., and Newton, A. C. (2001) *Biochemistry* **40**, 13216-13229
57. Giorgione, J. R., Lin, J. H., McCammon, J. A., and Newton, A. C. (2006) *J Biol Chem* **281**, 1660-1669
58. Dries, D. R., Gallegos, L. L., and Newton, A. C. (2007) *J Biol Chem* **282**, 826-830
59. Standaert, M. L., Bandyopadhyay, G., Kanoh, Y., Sajan, M. P., and Farese, R. V. (2001) *Biochemistry* **40**, 249-255
60. Standaert, M. L., Bandyopadhyay, G., Perez, L., Price, D., Galloway, L., Poklepovic, A., Sajan, M. P., Cenni, V., Sirri, A., Moscat, J., Toker, A., and Farese, R. V. (1999) *J Biol Chem* **274**, 25308-25316
61. Mochly-Rosen, D. (1995) *Science* **268**, 247-251
62. Gallegos, L. L., Kunkel, M. T., and Newton, A. C. (2006) *J Biol Chem* **281**, 30947-30956
63. Kheifets, V., and Mochly-Rosen, D. (2007) *Pharmacol Res* **55**, 467-476
64. Schechtman, D., and Mochly-Rosen, D. (2001) *Oncogene* **20**, 6339-6347
65. Chen, D., Purohit, A., Halilovic, E., Doxsey, S. J., and Newton, A. C. (2004) *J Biol Chem* **279**, 4829-4839
66. Chen, D., Gould, C., Garza, R., Gao, T., Hampton, R. Y., and Newton, A. C. (2007) *J Biol Chem*

67. Leitges, M., Kovac, J., Plomann, M., and Linden, D. J. (2004) *Neuron* **44**, 585-594
68. Perez, J. L., Khatri, L., Chang, C., Srivastava, S., Osten, P., and Ziff, E. B. (2001) *J Neurosci* **21**, 5417-5428
69. Hanley, J. G., and Henley, J. M. (2006) *Neuron* **49**, 778-780
70. Staudinger, J., Lu, J., and Olson, E. N. (1997) *J Biol Chem* **272**, 32019-32024
71. Feng, X., Zhang, J., Barak, L. S., Meyer, T., Caron, M. G., and Hannun, Y. A. (1998) *J Biol Chem* **273**, 10755-10762
72. Feng, X., and Hannun, Y. A. (1998) *J Biol Chem* **273**, 26870-26874
73. Feng, X., Becker, K. P., Stribling, S. D., Peters, K. G., and Hannun, Y. A. (2000) *J Biol Chem* **275**, 17024-17034
74. Violin, J. D., Zhang, J., Tsien, R. Y., and Newton, A. C. (2003) *J Cell Biol* **161**, 899-909
75. Kelley, G. G., Kaproth-Joslin, K. A., Reks, S. E., Smrcka, A. V., and Wojcikiewicz, R. J. (2006) *J Biol Chem* **281**, 2639-2648
76. Luo, B., Regier, D. S., Prescott, S. M., and Topham, M. K. (2004) *Cell Signal* **16**, 983-989
77. Crotty, T., Cai, J., Sakane, F., Taketomi, A., Prescott, S. M., and Topham, M. K. (2006) *Proc Natl Acad Sci U S A* **103**, 15485-15490
78. Arimoto, T., Takeishi, Y., Takahashi, H., Shishido, T., Niizeki, T., Koyama, Y., Shiga, R., Nozaki, N., Nakajima, O., Nishimaru, K., Abe, J., Endoh, M., Walsh, R. A., Goto, K., and Kubota, I. (2006) *Circulation* **113**, 60-66
79. Yamaguchi, Y., Shirai, Y., Matsubara, T., Sanse, K., Kuriyama, M., Oshiro, N., Yoshino, K., Yonezawa, K., Ono, Y., and Saito, N. (2006) *J Biol Chem* **281**, 31627-31637
80. Luo, B., Prescott, S. M., and Topham, M. K. (2003) *J Cell Biol* **160**, 929-937
81. van Baal, J., de Widt, J., Divecha, N., and van Blitterswijk, W. J. (2005) *J Biol Chem* **280**, 9870-9878
82. Castagna, M., Takai, Y., Kaibuchi, K., Sano, K., Kikkawa, U., and Nishizuka, Y. (1982) *J Biol Chem* **257**, 7847-7851

83. Kraft, A. S., and Anderson, W. B. (1983) *Nature* **301**, 621-623
84. Newton, A. C. (2004) *Trends Pharmacol Sci* **25**, 175-177
85. Konig, B., DiNitto, P. A., and Blumberg, P. M. (1985) *J Cell Biochem* **29**, 37-44
86. Blumberg, P. M., Sharkey, N. A., Konig, B., Jaken, S., Leach, K. L., and Jeng, A. Y. (1983) *Princess Takamatsu Symp* **14**, 75-87
87. Sharkey, N. A., Leach, K. L., and Blumberg, P. M. (1984) *Proc Natl Acad Sci U S A* **81**, 607-610
88. Nishizuka, Y. (1984) *Nature* **308**, 693-698
89. Young, S., Parker, P. J., Ullrich, A., and Stabel, S. (1987) *Biochem J* **244**, 775-779
90. Olivier, A. R., and Parker, P. J. (1994) *J Biol Chem* **269**, 2758-2763
91. Junoy, B., Maccario, H., Mas, J. L., Enjalbert, A., and Drouva, S. V. (2002) *Endocrinology* **143**, 1386-1403
92. Ohno, S., Konno, Y., Akita, Y., Yano, A., and Suzuki, K. (1990) *J Biol Chem* **265**, 6296-6300
93. Pears, C., and Parker, P. J. (1991) *FEBS Lett* **284**, 120-122
94. Lindner, D., Gschwendt, M., and Marks, F. (1991) *Biochem Biophys Res Commun* **176**, 1227-1231
95. Freisewinkel, I., Riethmacher, D., and Stabel, S. (1991) *FEBS Lett* **280**, 262-266
96. Goode, N. T., Hajibagheri, M. A., and Parker, P. J. (1995) *J Biol Chem* **270**, 2669-2673
97. Hansra, G., Garcia-Paramio, P., Prevostel, C., Whelan, R. D., Bornancin, F., and Parker, P. J. (1999) *Biochem J* **342** ( Pt 2), 337-344
98. Carrasco, S., and Merida, I. (2007) *Trends Biochem Sci* **32**, 27-36
99. Junco, M., Webster, C., Crawford, C., Bosca, L., and Parker, P. J. (1994) *Eur J Biochem* **223**, 259-263
100. Borner, C., Filipuzzi, I., Wartmann, M., Eppenberger, U., and Fabbro, D. (1989) *J Biol Chem* **264**, 13902-13909

101. Lee, H. W., Smith, L., Pettit, G. R., and Bingham Smith, J. (1996) *Am J Physiol* **271**, C304-311
102. Hansra, G., Bornancin, F., Whelan, R., Hemmings, B. A., and Parker, P. J. (1996) *J Biol Chem* **271**, 32785-32788
103. Brognard, J., and Newton, A. C. (in press) *Trends Endocrinol Metab*
104. Newton, A. C. (in press) *PHLPP: PH domain Leucine-rich repeat Protein Phosphatase*,
105. Gao, T., Furnari, F., and Newton, A. C. (2005) *Mol Cell* **18**, 13-24
106. Alessi, D. R., Andjelkovic, M., Caudwell, B., Cron, P., Morrice, N., Cohen, P., and Hemmings, B. A. (1996) *Embo J* **15**, 6541-6551
107. Brognard, J., Sierecki, E., Gao, T., and Newton, A. C. (2007) *Mol Cell* **25**, 917-931
108. Gao, T., and Newton, A. C. (2002) *J Biol Chem* **277**, 31585-31592
109. Gao, T., and Newton, A. C. (2006) *J Biol Chem* **281**, 32461-32468
110. Gao, T., Toker, A., and Newton, A. C. (2001) *J Biol Chem* **276**, 19588-19596
111. Herrmann, J., Lerman, L. O., and Lerman, A. (2007) *Circ Res* **100**, 1276-1291
112. Reinstein, E., and Ciechanover, A. (2006) *Ann Intern Med* **145**, 676-684
113. Lee, H. W., Smith, L., Pettit, G. R., Vinitsky, A., and Smith, J. B. (1996) *J Biol Chem* **271**, 20973-20976
114. Lee, H. W., Smith, L., Pettit, G. R., and Smith, J. B. (1997) *Mol Pharmacol* **51**, 439-447
115. Srivastava, J., Procyk, K. J., Iturrioz, X., and Parker, P. J. (2002) *Biochem J* **368**, 349-355
116. Leontieva, O. V., and Black, J. D. (2004) *J Biol Chem* **279**, 5788-5801
117. Carmena, D., and Sardini, A. (2007) *Biochem Soc Trans* **35**, 1043-1045
118. Rechsteiner, M., and Rogers, S. W. (1996) *Trends Biochem Sci* **21**, 267-271

119. Lu, Z., Liu, D., Hornia, A., Devonish, W., Pagano, M., and Foster, D. A. (1998) *Mol Cell Biol* **18**, 839-845
120. Kang, B. S., French, O. G., Sando, J. J., and Hahn, C. S. (2000) *Oncogene* **19**, 4263-4272
121. Nakamura, M., Tokunaga, F., Sakata, S., and Iwai, K. (2006) *Biochem Biophys Res Commun* **351**, 340-347
122. Prevostel, C., Alice, V., Joubert, D., and Parker, P. J. (2000) *J Cell Sci* **113** ( Pt **14**), 2575-2584
123. Becker, K. P., and Hannun, Y. A. (2004) *J Biol Chem* **279**, 28251-28256
124. von Zastrow, M. (2003) *Life Sci* **74**, 217-224
125. Smart, E. J., Ying, Y. S., and Anderson, R. G. (1995) *J Cell Biol* **131**, 929-938
126. Becker, K. P., and Hannun, Y. A. (2003) *J Biol Chem* **278**, 52747-52754
127. Idkowiak-Baldys, J., Becker, K. P., Kitatani, K., and Hannun, Y. A. (2006) *J Biol Chem* **281**, 22321-22331
128. Alvi, F., Idkowiak-Baldys, J., Baldys, A., Raymond, J. R., and Hannun, Y. A. (2007) *Cell Mol Life Sci* **64**, 263-270
129. Fields, A. P., and Gustafson, W. C. (2003) *Methods Mol Biol* **233**, 519-537
130. Griner, E. M., and Kazanietz, M. G. (2007) *Nat Rev Cancer* **7**, 281-294
131. Martiny-Baron, G., and Fabbro, D. (2007) *Pharmacol Res* **55**, 477-486
132. Koivunen, J., Aaltonen, V., and Peltonen, J. (2006) *Cancer Lett* **235**, 1-10
133. Greenman, C., Stephens, P., Smith, R., Dalgliesh, G. L., Hunter, C., Bignell, G., Davies, H., Teague, J., Butler, A., Stevens, C., Edkins, S., O'Meara, S., Vastrik, I., Schmidt, E. E., Avis, T., Barthorpe, S., Bhamra, G., Buck, G., Choudhury, B., Clements, J., Cole, J., Dicks, E., Forbes, S., Gray, K., Halliday, K., Harrison, R., Hills, K., Hinton, J., Jenkinson, A., Jones, D., Menzies, A., Mironenko, T., Perry, J., Raine, K., Richardson, D., Shepherd, R., Small, A., Tofts, C., Varian, J., Webb, T., West, S., Widaa, S., Yates, A., Cahill, D. P., Louis, D. N., Goldstraw, P., Nicholson, A. G., Brasseur, F., Looijenga, L., Weber, B. L., Chiew, Y. E., DeFazio, A., Greaves, M. F., Green, A. R., Campbell, P., Birney, E., Easton, D. F., Chenevix-Trench, G., Tan, M. H., Khoo, S. K., Teh, B. T., Yuen, S. T., Leung, S. Y., Wooster, R., Futreal, P. A., and Stratton, M. R. (2007) *Nature* **446**, 153-158

134. Seki, T., Adachi, N., Ono, Y., Mochizuki, H., Hiramoto, K., Amano, T., Matsubayashi, H., Matsumoto, M., Kawakami, H., Saito, N., and Sakai, N. (2005) *J Biol Chem* **280**, 29096-29106
135. Mackay, H. J., and Twelves, C. J. (2007) *Nat Rev Cancer* **7**, 554-562
136. Graff, J. R., McNulty, A. M., Hanna, K. R., Konicek, B. W., Lynch, R. L., Bailey, S. N., Banks, C., Capen, A., Goode, R., Lewis, J. E., Sams, L., Huss, K. L., Campbell, R. M., Iversen, P. W., Neubauer, B. L., Brown, T. J., Musib, L., Geeganage, S., and Thornton, D. (2005) *Cancer Res* **65**, 7462-7469
137. Herbst, R. S., Oh, Y., Wagle, A., and Lahn, M. (2007) *Clin Cancer Res* **13**, s4641-4646
138. Ryan, G. J. (2007) *Am J Health Syst Pharm* **64**, S15-21
139. Joy, S. V., Scates, A. C., Bearely, S., Dar, M., Taulien, C. A., Goebel, J. A., and Cooney, M. J. (2005) *Ann Pharmacother* **39**, 1693-1699
140. Mosyak, L., Xu, Z., Joseph-McCarthy, D., Brooijmans, N., Somers, W., and Chaudhary, D. (2007) *Biochem Soc Trans* **35**, 1027-1031
141. Szallasi, Z., Smith, C. B., Pettit, G. R., and Blumberg, P. M. (1994) *J Biol Chem* **269**, 2118-2124
142. Brandman, R., Disatnik, M. H., Churchill, E., and Mochly-Rosen, D. (2007) *J Biol Chem* **282**, 4113-4123
143. Churchill, E., Budas, G., Vallentin, A., Koyanagi, T., and Mochly-Rosen, D. (2007) *Annu Rev Pharmacol Toxicol*
144. Fields, A. P., Frederick, L. A., and Regala, R. P. (2007) *Biochem Soc Trans* **35**, 996-1000
145. Lahn, M., Su, C., Li, S., Chedid, M., Hanna, K. R., Graff, J. R., Sandusky, G. E., Ma, D., Niyikiza, C., Sundell, K. L., John, W. J., Giordano, T. J., Beer, D. G., Paterson, B. M., Su, E. W., and Bumol, T. F. (2004) *Clin Lung Cancer* **6**, 184-189
146. Sutton, R. B., and Sprang, S. R. (1998) *Structure* **6**, 1395-1405

This Chapter is, in full, a reprint of the material as it appears in *Current Drug Targets*, 2008, Gould C, Newton AC. I was the primary author for this literature review.

## Chapter 2

# The Chaperones Hsp90 and Cdc37 Mediate the Maturation and Stabilization of Protein Kinase C through a Conserved PXXP Motif in the C-terminal Tail

## Abstract

The life cycle of protein kinase C (PKC)<sup>\*</sup> is tightly controlled by mechanisms that mature the enzyme, sustain the activation-competent enzyme, and degrade the enzyme. Here we show that a conserved PXXP motif (Kannan, N., Haste, N., Taylor, S.S., and Neuwald, A.F., (2007) *PNAS* 104,1272-1277), in the C-terminal tail of AGC kinases, controls the processing phosphorylation of conventional and novel PKC isozymes, a required step in the maturation of the enzyme into a signaling-competent species. Mutation of both Pro616 and Pro619 to Ala in the conventional PKC  $\beta$ II abolishes the phosphorylation and activity of the kinase. Co-immunoprecipitation studies reveal that conventional and novel, but not atypical, PKC isozymes bind the chaperones Hsp90 and Cdc37 through a PXXP-dependent mechanism. Inhibitors of Hsp90 and Cdc37 significantly reduce the rate of processing phosphorylation of PKC. Of the two C-terminal sites processed by phosphorylation, the hydrophobic motif, but not the turn motif, is regulated by Hsp90. Overlay of purified Hsp90 onto a peptide array containing peptides covering the catalytic domain of PKC  $\beta$ II identified regions surrounding the PXXP segment, but not the PXXP motif itself, as major binding determinants for Hsp90. These Hsp90 binding regions, however, are tethered to the C-terminal tail via a 'molecular clamp' formed between the PXXP motif and a conserved (Y446) in the  $\alpha$ E-helix. Disruption of the clamp by mutation of the Tyr to Ala recapitulates the phosphorylation defect of mutating the PXXP motif. These data are consistent with a model in which a molecular clamp created by the PXXP motif in the C-terminal tail and determinants in the  $\alpha$ E-helix of the catalytic domain allows the chaperones Hsp90 and

Cdc37 to bind newly-synthesized PKC, a required event in the processing of PKC by phosphorylation.

## Introduction

Protein kinases, which comprise approximately 2% of the human genome, are key signal transducers that regulate a wide variety of cellular processes, such as growth, proliferation, and metabolism, through catalysis of specific phosphorylation events (1). By integrating signals from extracellular stimuli and transmitting them to targeted downstream substrates, protein kinases serve as a pivotal point of regulation within the cell. Deregulation and mutation of protein kinases play a causal role in human pathology, notably cancer, poising kinases as important targets for the design of therapeutics (2-5). Therefore, understanding the mechanisms that regulate protein kinases, such as those important for maturation and processing, would be critical for designing therapeutics that would maintain the correct functioning of signal transduction pathways.

Heat shock proteins (Hsp), such as Hsp90, are ubiquitously expressed molecular chaperones that facilitate protein folding, regulate quality control, and guide protein turnover in an effort to maintain cellular homeostasis (6-8). Unlike other chaperones such as Hsp70, which unspecifically assists in folding of nascent polypeptide chains (7), Hsp90 works with a specific and discrete set of client proteins, particularly protein kinases (9). Many of Hsp90's known client kinases, Src (10), Akt (11,12), phosphoinositide dependent kinase-1 (PDK-1) (13), and ErbB2-/HER2 (14,15), require Hsp90's activity to reach an activation-competent and mature state. Hsp90 is recruited to its kinase clients through interactions with cochaperones, such as Cdc37, which bridge the interaction between Hsp90 and the kinase client (16,17); this mechanism is revealed in a structural analysis of the Cdc37-Cdk4-Hsp90 complex (18). Cdc37, originally identified in yeast (19), is a cochaperone specific to the kinome that not only assists

Hsp90 function but can also recognize and stabilize clients independently of Hsp90 (20). By binding specific regions of the catalytic domains of these kinases, the Hsp90/Cdc37 complex utilizes ATP to promote and stabilize functional conformations of its clients (8,16,17,21). Pharmacological inhibition of Hsp90 by ansamycin antibiotics such as 17-AAG leads to the destabilization and subsequent proteasomal degradation of its clients (6,22). Recent studies have identified Hsp90 as a promising therapeutic target in cancer, as levels of chaperones and activity of client kinases are frequently up-regulated (23-25).

The protein kinase C (PKC) family of Ser/Thr kinases serves as a paradigm of how conformation and processing by phosphorylation regulates activity, localization, and inter- and intramolecular interactions (26). The mammalian PKC family consists of ten isozymes divided into three subclasses (conventional, novel, and atypical) based on their primary structure and second messenger mode of regulation. In the case of conventional PKC isozymes, newly-synthesized enzyme is loosely engaged on the membrane in a conformation that exposes the activation loop for phosphorylation by the upstream kinase, PDK-1. This phosphorylation triggers two sequential phosphorylations on the C-terminus, one on the turn motif and one on the hydrophobic motif. Phosphorylation of the turn motif is required for phosphorylation of the hydrophobic motif and has recently been shown to depend on the mammalian target of rapamycin complex 2 (mTORC2), a complex consisting of the mammalian target of rapamycin (mTOR), Rictor, Sin1, and mLST8 (29,30). Turn motif phosphorylation is rapidly followed by phosphorylation at the hydrophobic motif, a reaction that occurs by an intramolecular mechanism *in vitro* (31). Fully phosphorylated PKC is released into the cytosol in a closed conformation in which an autoinhibitory pseudosubstrate sequence occupies the substrate-binding cavity.

Upon generation of the lipid second messenger diacylglycerol (DAG) and elevation of intracellular  $\text{Ca}^{2+}$ , conventional PKC isozymes ( $\alpha$ ,  $\beta\text{I}$ ,  $\beta\text{II}$ ,  $\gamma$ ) translocate to membranes via their membrane-targeting C1 and C2 domains, where they adopt an open conformation in which the pseudosubstrate is expelled from the substrate-binding cavity, permitting phosphorylation of downstream substrates (32). Novel PKC isozymes ( $\delta$ ,  $\epsilon$ ,  $\theta$ , and  $\eta$ ) only respond to DAG, and their processing phosphorylations can occur through additional mechanisms (33,34). Atypical PKC isozymes ( $\zeta$  and  $\iota/\lambda$ ) do not respond to either  $\text{Ca}^{2+}$  or DAG but can also undergo regulation of their processing phosphorylations by external stimuli (35). In fact, atypical PKC isozymes contain a Glu at their hydrophobic motif site. Thus, even though these three sites are conserved among PKC family members, additional layers of regulation generate specificity in how these kinases become signaling-competent enzymes.

The mechanisms of regulation of PKC's activity and signaling properties by lipid second messengers and phosphorylation have been well characterized; however, mounting evidence suggests that there are many other regulatory inputs for PKC function. Recent analysis of the evolutionary constraints acting on AGC kinase sequences have underscored the importance of the C-terminal tail as a critical regulatory module (36). Deletion mutants of the C-terminal tail have been shown to abrogate PKC activity (37). In addition to containing the key regulatory phosphorylation sites and docking the upstream kinase PDK-1, the C-terminal tail contains key conserved motifs, found within all AGC kinases, that facilitate ATP binding, promote substrate binding, and structure the catalytic core (36). One such motif comprises the segment PXXP; this motif makes key contacts with the catalytic core, where it is important for modulating

movement of the catalytic domain (36). Although this PXXP motif is conserved in all the PKC isozymes, its functional role is unknown.

In this study, we address the role of the conserved Pro residues in the PXXP motif of the C-terminal tail of PKC  $\beta$ II. We show that mutation of these two Pro to Ala (P616A and P619A) results in a kinase that is not processed by phosphorylation in cells and is thus inactive. Further analysis reveals that this mutant is not able to bind the chaperones Hsp90 and Cdc37, an event that is required for the processing of PKC by phosphorylation. Our peptide array data indicate that Hsp90 binds to regions of the catalytic core such as the  $\alpha$ C- $\beta$ 4 loop and the  $\alpha$ D-helix that serve as hinge points for C-helix movement (36). Structural analysis delineates that these hinge points are tethered to the C-terminal tail through a molecular clamp formed between the PXXP segment and AGC conserved residues in the  $\alpha$ E-helix. Mutation of one of the 'clamping' residues, a conserved Tyr (Y446), recapitulates the defect resulting from mutation of the PXXP motif. Our data support a model in which the PXXP motif participates in an intramolecular clamp with determinants in the  $\alpha$ E helix of the kinase core, by providing a recognition surface for Hsp90 to bind and facilitate the maturation of PKC, a required step in the processing of the enzyme.

## Materials and Methods

*Plasmids.* The cloning of rat PKC  $\beta$ II into the mammalian expression vector pCDNA3 and subsequent generation of the phosphorylation site mutants (T641E and S660E) has been previously described (38,39). The construction of the NH<sub>2</sub>-terminal Myc-tagged PDK-1 in pCDNA3 has been previously described (40). Expression constructs for wildtype bovine PKC  $\alpha$  and rat PKC  $\zeta$  were generous gifts from Dr. Alex Toker (Harvard Medical School). Mouse PKC  $\delta$  was a generous gift from Dr. Peter Blumberg (National Institutes of Health). PKC  $\beta$ II-YFP was cloned as described previously (41). PKC  $\beta$ II-RFP was constructed by PCR amplification and subsequent cloning into a pCDNA3 vector with mRFP as a C-terminal tag (42). The other PKC mutants, PKC  $\beta$ II-K371R, PKC  $\beta$ II-P616A/P619A, PKC  $\beta$ II-P616A/P619A-YFP, PKC  $\beta$ II-Y446A, PKC  $\alpha$ -P613A/P616A, PKC  $\delta$ -P617A/P620A, and PKC  $\zeta$ -P534A/P537A were all generated using the QuikChange site-directed mutagenesis kit (Stratagene).

*Materials.* Human Hsp90 $\alpha$  recombinant protein was purchased from Genway. Purified His-PDK-1 was a generous gift from Charles C. King. PKC substrate peptide (Ac-FKKSFKL-NH<sub>2</sub>) was obtained from Anaspec. Oligonucleotides were purchased from Integrated DNA Technologies. Easy Tag [<sup>35</sup>S]Methionine/Cysteine (Met/Cys, 1175 Ci mmol<sup>-1</sup>) and [ $\gamma$ -<sup>32</sup>P]ATP (3000 Ci mmol<sup>-1</sup>) were purchased from PerkinElmer Life Sciences. Met/Cys-deficient DMEM was purchased from Invitrogen. 17-(Allylamino)-17-demethoxygeldanamycin (17-AAG) was purchased from A.G. Scientific, Inc. Carbobenzoyl-L-leucyl-L-leucyl-leucinal (MG-132), phorbol 12-myristate 13-acetate (PMA), and phorbol-12,13-dibutyrate (PDBu) were purchased from Calbiochem.

Celastrol was purchased from Cayman Chemical. Polyclonal antibodies to PKC  $\alpha$ , PKC  $\beta$ II, PKC  $\delta$ , PKC  $\zeta$ , and Cdc37 were obtained from Santa Cruz Biotechnology.

Monoclonal antibodies to PKC  $\alpha$ , PKC  $\beta$ , and Hsp90 were obtained from BD Transduction Laboratories. A phospho-specific antibody (pT500) that specifically recognizes the phosphorylated activation loop of PKC isozymes was characterized previously (43). A phospho-specific PKC antibody to the hydrophobic motif phosphorylation site (PKC  $\beta$ II Ser660) and one to the turn motif phosphorylation site (PKC  $\alpha$ / $\beta$ II Thr638/641) were purchased from Cell Signaling Technology. An anti-Myc monoclonal (9E10) antibody was purchased from Covance. A monoclonal anti- $\beta$ -actin antibody was purchased from Sigma-Aldrich. Ultra-Link protein A/G beads were obtained from ThermoScientific. Electrophoresis reagents were obtained from Bio-Rad. All other materials and chemicals were reagent-grade.

*Cell Culture and Transfection.* tsA201, COS7, HeLa, and MCF7 cells were maintained in DMEM (Cellgro) containing 10% fetal bovine serum (Hyclone) and 1% penicillin/streptomycin at 37°C in 5% CO<sub>2</sub>. MCF-10A cells were maintained in Mammary Epithelium Growth Medium (Clonetics) at 37°C and 5% CO<sub>2</sub>. Transient transfection of tsA201 cells was carried out using Effectene transfection reagents (Qiagen) and transient transfection of COS7 cells was carried out using the FuGENE transfection reagent (Roche Applied Science).

*Immunofluorescence.* COS7 cells were transiently co-transfected with PKC  $\beta$ II-RFP and PKC  $\beta$ II-P616A/P619A-YFP for 24 h. Cells were washed once and imaged in Hanks' balanced salt solution with 1 mM Ca<sup>2+</sup>. Epifluorescent images were acquired on a Zeiss Axiovert microscope (Carl Zeiss MicroImaging, Inc.) using a Micro-Max digital camera

(Roper-Princeton Instruments) controlled by Metafluor Software (Universal Imaging, Corp). Optical filters were obtained from Chromas Technologies and Semrock, Inc. Cells were treated with 200 nM PDBu, and the same cells were used to acquire YFP and RFP images through a 10% neutral density filter. YFP images were obtained using a 495/10-nm excitation filter, a 505-nm dichroic mirror, and a 535/25-nm emission filter. RFP images were obtained using a 560/25-nm excitation filter, a 593-nm dichroic mirror, and a 629/53-nm emission filter.

*Kinase assays.* For the PKC activity assay, detergent-solubilized lysates (20 mM HEPES pH 7.5, 0.1% TritonX-100, 2 mM DTT, 1 mM PMSF) from untransfected tsA201 cells and tsA201 cells transfected with empty vector, WT PKC  $\beta$ II, or PKC  $\beta$ II-P616A/P619A were assayed for PKC activity for 8 min by monitoring  $^{32}\text{P}$  incorporation from [ $\gamma$ - $^{32}\text{P}$ ]ATP into a synthetic PKC-selective peptide (Ac-FKKSFKL-NH<sub>2</sub>) in a paper assay as described previously (38). The standard reaction mix contained 20 mM HEPES pH 7.5, 2 mM DTT, 5 mM MgCl<sub>2</sub>, 100  $\mu\text{M}$  ATP, 50  $\mu\text{M}$  peptide substrate and 100  $\mu\text{Ci}$  [ $\gamma$ - $^{32}\text{P}$ ]ATP. Non-activating conditions included 2 mM EGTA. Activating conditions included 140  $\mu\text{M}$  phosphatidylserine / 3.8  $\mu\text{M}$  diacylglycerol membranes and 2 mM CaCl<sub>2</sub>. The activity of the transfected kinase was determined by first subtracting  $^{32}\text{P}$ -incorporation in control (vector-transfected) lysate samples and then normalizing the Ca<sup>2+</sup>/lipid-stimulated peptide phosphorylation to PKC expression (determined by Western blot analysis); activity is expressed in relative units. For the PDK-1 activity assay, COS7 cells expressing either empty vector, WT PKC  $\beta$ II, or PKC  $\beta$ II-P616A/P619A were lysed in Buffer A (50 mM Tris pH 7.4, 1% TritonX-100, 50 mM NaF, 10 mM Na<sub>4</sub>P<sub>2</sub>O<sub>7</sub>, 100 mM NaCl, 5 mM EDTA, 1 mM Na<sub>3</sub>VO<sub>4</sub>, and 1 mM PMSF),

and detergent-solubilized lysates were incubated with a monoclonal anti-PKC  $\alpha$  antibody (cross-reactive with PKC  $\beta$ ) overnight at 4°C to allow immune complex formation. The immune complexes were collected with Ultra-Link Protein A/G beads. After washing the immune complexes with Buffer A, they were resuspended in the kinase buffer (20 mM HEPES, pH 7.4, 2 mM DTT). The standard reaction mix contained the immune complexes, 20 mM HEPES, 500  $\mu$ M ATP, and 2 mM MgCl<sub>2</sub>. The reaction was performed in the absence or presence of purified His-PDK-1 (0.5 nM) and in non-activating or activating PKC conditions. Non-activating conditions included 2 mM EGTA. Activating conditions included 140  $\mu$ M phosphatidylserine / 3.8  $\mu$ M diacylglycerol membranes and 2 mM CaCl<sub>2</sub>. The reaction was allowed to proceed for 30 min at 30°C and stopped by addition of Laemmli sample buffer. The samples were separated by SDS-PAGE, transferred to PVDF membrane, and analyzed for pT500 phosphorylation by Western blotting.

*PMA time course.* COS7 cells were transiently transfected with WT PKC  $\beta$ II or PKC  $\beta$ II-P616A/P619A. Approximately 24 h post-transfection, cells were treated with 200 nM PMA for 0, 15, 30, and 90 min. The cells were lysed in buffer A, and whole cell lysates were analyzed by SDS-PAGE and Western blotting.

*Pulse-chase analysis.* COS7 cells were transfected with WT PKC  $\beta$ II, PKC  $\beta$ II-P616A/P619A, PKC  $\beta$ II T641E, or PKC  $\beta$ II S660E. At 24-30 hr post-transfection, cells were incubated with Met/Cys-deficient DMEM for 30 min at 37 °C. The cells were then pulse-labeled with 0.5 mCi ml<sup>-1</sup> [<sup>35</sup>S]Met/Cys in Met/Cys-deficient DMEM for 7 min at 37 °C, media was removed, and cells were chased with DMEM containing 5 mM unlabeled methionine and 5 mM unlabeled cysteine (44). At the indicated times, cells

were lysed in buffer A, centrifuged at 16,000 x g for 5 min at 22°C, and PKC  $\beta$ II in the supernatant was immunoprecipitated with an anti-PKC  $\alpha$  monoclonal antibody (cross-reactive with PKC  $\beta$ II) overnight at 4°C. The immune complexes were collected with Ultra-Link protein A/G beads, washed with Buffer A, separated by SDS-PAGE, transferred to PVDF membrane, and analyzed by autoradiography. For the inhibitor experiments, cells were pretreated for 3 hr with 1  $\mu$ M 17-AAG, 30 min with 10  $\mu$ M celastrol, or both prior to the pulse-chase. Pulse-chase experiments of endogenous PKC  $\alpha$  followed the same protocol as described above. Densitometric analysis was performed using NIH Image J analysis software, and the kinetic analysis was performed using Kaleidograph software (version 4.0).

*Immunoprecipitation.* To examine the interaction of PKC with endogenous Hsp90, COS7 cells were transfected with either WT PKC ( $\alpha$ ,  $\beta$ II,  $\delta$ ,  $\zeta$ ) or the respective construct with a mutated PXXP motif. For PKC  $\beta$ II, the interaction of Hsp90 with the kinase-dead mutant PKC  $\beta$ II-K371R and PKC  $\beta$ II-Y446A was also assessed. Approximately 24 h post-transfection, the cells were lysed in buffer A, centrifuged at 16,000 x g for 5 min at 22°C, and the detergent-solubilized supernatants were incubated with the appropriate PKC antibody overnight at 4°C. The immune complexes were collected with Ultra-Link protein A/G beads, washed with Buffer A, and analyzed by SDS-PAGE and Western blotting. This method was also used to assess the interaction of PKC with endogenous Cdc37. For the PDK-1 co-immunoprecipitation experiments, COS7 cells were co-transfected with WT PKC  $\beta$ II, PKC  $\beta$ II-K371R, or PKC  $\beta$ -P616A/P619A and either empty vector or Myc-PDK-1. Cells were lysed as described above and incubated with a

monoclonal anti-Myc antibody overnight at 4°C to form immune complexes with Myc-PDK-1. The immune complexes were collected, washed, and analyzed as described above for the Hsp90 experiments. Densitometric analysis was performed using NIH Image J analysis software (version 1.40).

*Analysis of 17-AAG-induced down-regulation of PKC.* COS7 cells were transiently transfected with WT PKC  $\beta$ II or PKC  $\beta$ II P616A/P619A. Approximately 24 hr post-transfection, the cells were treated with 1  $\mu$ M 17-AAG for 0, 1, 4, 12, and 24 hr. For MG-132 experiments, the cells were first pretreated with 10  $\mu$ M MG-132 for approximately 3 h. The cells were lysed in Buffer A, and whole cell lysates were analyzed by SDS-PAGE and Western blotting. Similar experiments were performed in HeLa, MCF-10A, and MCF7 cells lines to assess endogenous PKC levels.

*Hsp90 overlay of the catalytic domain of PKC  $\beta$ II.* The catalytic domain of PKC  $\beta$ II (a.a. 342-673) was divided into 18 amino acid peptides, with a two amino acid shift, and synthesized using the Intavis Multiprep Peptide Synthesizer (Intavis Bioanalytical Instruments AG), which spotted the peptides onto an AC-S01 type amino-PEGylated membrane (Intavis AG). After activation of the membrane with ethanol, the membrane was blocked, washed, and then incubated overnight with 100 nM human Hsp90 $\alpha$  recombinant protein. After incubation with the Hsp90 protein, the peptide array was analyzed by Western blot analysis with a monoclonal anti-Hsp90 antibody.

## Results

*A conserved PXXP motif in the C-terminal tail of PKC  $\beta$ II is necessary for catalytic activity* - A conserved PXXP motif in the C-terminal tail of AGC kinases has been proposed to be an important site for allosteric regulation of the catalytic domain (Figure 2.1A & B) (36). To examine the biochemical role of this conserved PXXP motif in PKC  $\beta$ II, we mutated both Pro-616 and Pro-619 to Ala (P616A/P619A) and first assessed the catalytic activity of the construct in an *in vitro* kinase assay. Lysates from tsA201 cells expressing either WT PKC  $\beta$ II or PKC  $\beta$ II-P616A/P619A were assayed for activity towards a PKC peptide substrate in the presence or absence of activating cofactors; activity attributed to the transfected PKC was obtained by subtracting the endogenous activity determined from control lysates. Mutation of the PXXP motif in PKC  $\beta$ II abolished kinase activity; in fact, this construct behaved as a modest dominant-negative of endogenous activity (Figure 2.1C). Curiously, Western blot analysis of lysates revealed that the PKC  $\beta$ II-P616A/P619A construct migrated faster than wild-type enzyme (Figure 2.1D, *dash*). Previous studies have established that WT PKC  $\beta$ II migrates primarily as an upper band (*asterisk*) that represents a species quantitatively phosphorylated at the two C-terminus sites, with a minor fraction migrating as a faster-mobility species (*dash*) that represents kinase that is unphosphorylated (44). Consistent with PKC  $\beta$ II-P616A/P619A migrating as the unphosphorylated species, it was not labeled by phospho-specific antibodies to the activation loop T500 (Figure 2.1D, *middle panel*), nor was it labeled by phospho-specific antibodies to the two C-terminal sites, the turn motif T641 or the hydrophobic motif S660 (data not shown). Thus, mutation of both Pro residues in the PXXP motif resulted in an inactive, unphosphorylated kinase.

*Mutation of the PXXP motif in PKC  $\beta$ II prevents the maturation of PKC -*

Accumulation of unphosphorylated PKC could reflect the inability of the P616A/P619A construct to be processed by phosphorylation, or it could reflect an increased phosphatase sensitivity resulting in accumulation of matured, phosphorylated PKC that has been dephosphorylated (45). To discriminate between these two possibilities, we asked whether newly-synthesized PKC matured into the phosphorylated species by pulse-chase analysis (Figure 2.2A). COS7 cells transfected with WT PKC  $\beta$ II or PKC  $\beta$ II-P616A/P619A were pulse-labeled with [<sup>35</sup>S]Met/Cys and chased for up to 4 hours with unlabeled media. Immunoprecipitated PKC was analyzed by autoradiography, and the processing of the pulsed pool was determined by the mobility of the radiolabeled band on SDS-PAGE. The autoradiogram in Figure 2.2A shows that newly-synthesized PKC  $\beta$ II appeared as a faster-migrating species (*lane 1, dash*) that shifted to a slower-mobility species over the course of the chase (*lanes 2-6, asterisk*). The mobility shift reflects the two tightly-coupled processing phosphorylations at the C-terminus, the turn motif (T641) and hydrophobic motif (S660) (Figure 2.1A). Importantly, mutation of the PXXP motif in PKC  $\beta$ II prevented maturation of PKC, as assessed by its co-migration with the faster-migrating, unphosphorylated species even after 4 hours of chase (*lanes 7-12, dash*). These data reveal that mutation of both Pro residues in the PXXP motif prevents the processing of PKC  $\beta$ II by phosphorylation.

Newly-synthesized PKC is loosely tethered at the membrane by its regulatory modules in an open conformation (pseudosubstrate exposed), which allows PDK-1 to phosphorylate the activation loop and initiate the maturation process (27). To test whether the lack of processing of PKC  $\beta$ II-P616A/P619A resulted from improper

localization of the mutant to the membrane, we forced membrane association by taking advantage of the ability of phorbol esters to recruit PKC to the membrane, independently of the phosphorylation-state of the enzyme. To this end, we transfected COS7 cells with either WT PKC  $\beta$ II or PKC  $\beta$ II-P616A/P619A and treated the cells with the phorbol ester PMA. The Western blot in Figure 2.2B shows that the PXXP mutant continued to migrate as a faster-mobility species following PMA treatment (*lanes 5-8, dash*). Note that PMA treatment caused a characteristic increase in the amount of unphosphorylated PKC (*lanes 1-4, dash*), consistent with the ability of phorbol esters to promote the dephosphorylation and eventual down-regulation of the enzyme (46). To ensure that the PXXP mutant PKC  $\beta$ II-P616A/P619A was properly recruited to the membrane upon phorbol ester treatment, we co-transfected COS7 cells with fluorescently-tagged constructs, WT PKC  $\beta$ II-RFP and PKC  $\beta$ II-P616A/P619A-YFP, and simultaneously co-imaged them in the absence and presence of the phorbol ester PDBu. Although modest differences in localization were observed, the fluorescent images in Figure 2.2C reveal that both WT PKC  $\beta$ II-YFP and PKC  $\beta$ II-P616A/P619A-YFP translocated to the membrane upon treatment with PDBu (Figure 2.2C, *right panels*). Similar results were obtained when WT PKC  $\beta$ II-RFP or PKC  $\beta$ II-P616A/P619A-YFP were transfected separately into cells (data not shown). Therefore, these data demonstrate that the inability of PKC  $\beta$ II-P616A/P619A to mature is not a consequence of improper subcellular localization.

*The upstream kinase PDK-1 can bind and phosphorylate the PXXP mutant PKC  $\beta$ II-P616A/P619A* - The first step in the maturation process of PKC is phosphorylation of the activation loop by PDK-1. Because the PXXP mutant PKC  $\beta$ II-P616A/P619A has a

defect in maturation (Figure 2.2A), we tested if the mutant was a suitable substrate for PDK-1. Immunoprecipitated WT PKC  $\beta$ II or PKC  $\beta$ II-P616A/P619A from detergent-solubilized lysates was incubated with purified His-PDK-1 in the absence or presence of  $\text{Ca}^{2+}$  and phosphatidylserine/DAG membranes (to induce the membrane-bound open conformation in which the PDK-1 site is unmasked) in an *in vitro* kinase assay (Figure 2.3A). Activation loop phosphorylation was detected using a phospho-specific antibody to the T500 activation loop site (cross-reactive with all PKC isozymes); indeed, this antibody detected endogenous PKC  $\alpha$  in the vector lanes (Figure 2.3A, lanes 1-3, arrow). WT PKC  $\beta$ II was robustly labeled with the pT500 antibody regardless of the addition of PDK-1 (Figure 2.3A, lanes 4-6, asterisk), as expected for the normally matured, fully phosphorylated enzyme (43). In contrast, PKC  $\beta$ II-P616A/P619A was not labeled by the pT500 antibody in the absence of His-PDK-1 (Figure 2.3A, lane 7, dash). However, addition of His-PDK-1 resulted in the activation loop phosphorylation of the PKC  $\beta$ II-P616A/P619A mutant (Figure 2.3A, lane 8, dash), although to a much lesser extent than WT. Additionally, PDK-1-catalyzed phosphorylation did not depend on PKC being bound to membranes (lane 9), indicating that the PKC  $\beta$ II-P616A/P619A mutant was in the open conformation in which the pseudosubstrate does not occupy the substrate-binding pocket, reflecting the conformation of newly-synthesized PKC (27). These data reveal that the activation loop of the PKC  $\beta$ II-P616A/P619A is accessible and can be phosphorylated by PDK-1.

Having established that PDK-1 can phosphorylate the activation loop of the PKC  $\beta$ II-P616A/P619A *in vitro*, we next addressed if the phosphorylation defect observed in cells resulted from impaired binding of PDK-1 to this mutant in cells. COS7 cells were

co-transfected with WT PKC  $\beta$ II, PKC  $\beta$ II-K371R (a catalytically-inactive mutant that also cannot be processed by phosphorylation), or PKC  $\beta$ II-P616A/P619A with empty vector or Myc-PDK-1. Figure 2.3B reveals that both mutants migrated as the faster mobility, unphosphorylated species (*dash*) whereas WT PKC  $\beta$ II migrated as the slower mobility, phosphorylated species (*asterisk*). Myc-PDK-1 was immunoprecipitated from detergent-solubilized lysates (Figure 2.3B, *left panel, IP*), and the interaction with PKC  $\beta$ II was assessed by Western blot. Both WT  $\beta$ II and the unphosphorylated mutants, PKC  $\beta$ II-K371R and PKC $\beta$ II-P616A/P619A, immunoprecipitated with Myc-PDK-1 (Figure 2.3B, *lanes 2, 4, and 6, upper panel, IP*). Normalizing the amount of PKC  $\beta$ II bound to Myc-PDK-1 (*upper panel, IP*) to the amount of PKC  $\beta$ II in the lysate (*upper panel, Lysate*) indicated no significant preference of PDK-1 for the PXXP mutant compared to WT PKC  $\beta$ II (Figure 2.3C,  $n = 13$ ,  $p = 0.20$ ). Importantly, the C-terminal tail was still fully functional for binding PDK-1. Similarly, additional co-immunoprecipitation studies revealed that the binding of another C-terminal partner of PKC, Hsp70 (45,47), was maintained with the PKC  $\beta$ II-P616A/P619A mutant (data not shown). Taken together with the *in vitro* phosphorylation experiments, these data exhibit that the defect in processing of the PKC  $\beta$ II-P616A/P619A mutant does not arise from defective binding of PDK-1 or inaccessibility of the activation loop site to phosphorylation by PDK-1.

*Mutation of the PXXP motif in PKC  $\beta$ II disrupts the interaction with Hsp90 and its cochaperone, Cdc37* – Recent studies with other AGC kinase family members, Akt and PDK-1, have described the role of heat shock proteins, particularly Hsp90, in the maturation and stabilization of these kinases (11-13). Because the PKC  $\beta$ II-

P616A/P619A mutant has a clear defect in maturation (Figure 2.2A), we explored if Hsp90 might play a role in this process. WT PKC  $\beta$ II, PKC  $\beta$ II-K371R, or PKC  $\beta$ II-P616A/P619A was expressed in COS7 cells and immunoprecipitated from detergent-solubilized lysates. The amount of endogenous Hsp90 bound was detected on Western blots (Figure 2.4A). As in previous experiments, the phospho-defective mutants migrated as the faster-mobility, unphosphorylated species (*middle panel, dash*) whereas WT PKC  $\beta$ II migrated primarily as the mature, phosphorylated species (*middle panel, asterisk*). Hsp90 bound to WT PKC  $\beta$ II, an interaction that was markedly enhanced with the unphosphorylated kinase-dead construct PKC  $\beta$ II-K371R. In prominent contrast, there was no detectable binding of Hsp90 to the PXXP mutant PKC  $\beta$ II-P616A/P619A (Figure 2.4A, *upper panel, lane 4*). Quantitative analysis of the ratio of bound Hsp90 to PKC in the immunoprecipitate demonstrated that mutation of the PXXP motif in PKC  $\beta$ II decreased the interaction with Hsp90 a striking 5-fold relative WT PKC  $\beta$ II (Figure 2.4B,  $p < 0.05$ ,  $n = 4$ ). Conversely, 5-fold more Hsp90 bound the PKC  $\beta$ II-K371R construct compared to WT PKC  $\beta$ II (Figure 2.4B,  $p < 0.01$ ,  $n = 4$ ). Thus, although both constructs are completely unphosphorylated and inactive, Hsp90 discriminated between an intact PXXP motif (in the PKC  $\beta$ II-K371R mutant) and a mutated PXXP motif. Consistent with this result, another mutant PKC that cannot be processed by phosphorylation, PKC  $\beta$ II-T641AAA (44), bound Hsp90 significantly better than WT PKC  $\beta$ II (data not shown). These data show that Hsp90 preferentially recognizes the unphosphorylated form of PKC via a mechanism that is driven by the PXXP motif.

Hsp90 functions as a complex in cells with other cochaperones such as Cdc37 (16,17). To test whether the PXXP motif mediates the interaction with other cochaperones in the Hsp90 complex, we checked if Cdc37 was present in immune complexes of PKC (Figure 2.4C). WT PKC  $\beta$ II or PKC  $\beta$ II-P616A/P619A was immunoprecipitated from detergent-solubilized lysates (Figure 2.4C, *middle panel, IP*), and bound endogenous Cdc37 was assessed by Western blot analysis (*upper panel, IP*). This cochaperone was readily detected in immunoprecipitates of WT PKC  $\beta$ II (*IP, lane 2*) but was not detectable in immunoprecipitates of the PKC  $\beta$ II-P616A/P619A mutant (*lane 3*). Thus, the PXXP motif mediates the interaction of PKC with both Hsp90 and its cochaperone Cdc37.

*Inhibition of Hsp90 slows the maturation of PKC* – Since the PXXP mutant PKC  $\beta$ II-P616A/P619A cannot be processed by phosphorylation and, furthermore, has reduced interaction with the Hsp90/Cdc37 chaperones, we next addressed whether Hsp90 activity is required for the maturation of PKC. Specifically, we tested how the Hsp90 inhibitor 17-AAG affected the rate of maturation of PKC as assessed by pulse-chase analysis (Figure 2.5A). This potent inhibitor is a derivative of geldanamycin, an antibiotic of the ansamycin class produced by *Streptomyces hygroscopicus*, which binds to the N-terminal ATP binding pocket of Hsp90 and prevents ATP binding and hydrolysis that is essential for protein folding processes (6). COS7 cells transfected with WT PKC  $\beta$ II were pretreated with 17-AAG prior to pulse-chase analysis (Figure 2.5A). The autoradiogram in Figure 2.5A shows that newly-synthesized PKC migrated as a single, faster mobility band (*dash*) and then shifted to a slower mobility band (*asterisk*) over the course of the chase. Addition of 17-AAG slowed the maturation of PKC (compare *lane 2* and *lane 7*).

Quantitative analysis revealed that in the absence of the inhibitor, PKC was processed with a half-time of  $13.2 \pm 0.8$  min (Figure 2.5B, *circles*); however, in the presence of the inhibitor, the rate of processing of PKC was slowed 2-fold, with the half-time of processing increasing to  $25 \pm 4$  min (*squares*). These data reveal that inhibition of endogenous Hsp90 activity decreases the rate of processing of PKC.

We next examined the effect of inhibiting Hsp90 on the processing of endogenous PKC  $\alpha$ , another conventional PKC isozyme by pulse- chase analysis (Figure 2.5C). The autoradiogram in Figure 2.55C shows that newly-synthesized PKC  $\alpha$  migrated as a faster-mobility band (*dash*) and shifted to a slower-mobility band (*asterisk*) over the course of the chase with a half-time of  $\sim 10$  min (*lane 3*) in the absence of the Hsp90 inhibitor. However, in the presence of the Hsp90 inhibitor, the half-time to shift to the fully-phosphorylated, slower-mobility species (*asterisk*) was approximately 4-fold slower (half time  $\sim 45$  min). Interestingly, a band of intermediate mobility (*double dash*) was detected at 10 min of chase (Figure 2.5C, *lane 8*) in the sample treated with the Hsp90 inhibitor. This band represents a species of PKC that is phosphorylated at only one of the two C-terminal sites (44). The half-time for phosphorylation at this site was similar to that for full phosphorylation in the absence of inhibitor (the ratio of upper (*asterisk* or *double dash*) and lower bands (*dash*) at the 10 min chase time points are similar with and without inhibitor (Figure 2.5C, *lanes 3* and *8*)). These data suggest that Hsp90 inhibition impairs the processing of one of the two C-terminal sites.

To explore which of the two C-terminal sites Hsp90 regulates, we investigated the rate of processing of phosphorylation site constructs of PKC  $\beta$ II in which carboxyl-terminal phosphorylation site residues were individually replaced with Glu, the phospho-

mimetics PKC  $\beta$ II-T641E (turn motif mutant) and PKC  $\beta$ II S660E (hydrophobic motif mutant) (Figure 2.5D). Both mutants were processed by phosphorylation with half-times only slightly slower from those of WT PKC  $\beta$ II: analysis of the ratio of upper to lower mobility species indicated approximately 70% of WT PKC, 50% of T641E, and 40% of S660E was processed following 30 min chase (Figure 2.5D, *lane 3*). Note that the mobility shift for the T641E mutant reflects phosphorylation of Ser660, which causes a readily detectable shift, and that the mobility shift for the S660E mutant reflects phosphorylation of Thr641, a modification that causes a smaller mobility shift.

Importantly, 17-AAG treatment slowed the processing of WT PKC  $\beta$ II and PKC  $\beta$ II-T641E approximately 2-fold (compare ratios of upper and lower mobility species at the 30 min time point, *lanes 3* and *7*), but did not affect the rate of processing of the PKC  $\beta$ II-S660E mutant (the ratio of upper to lower mobility species was approximately 1 at the 90 min time point both in the absence or presence of 17-AAG (*lanes 4* and *8*)). The lack of sensitivity of PKC  $\beta$ II-S660E phosphorylation at Thr641 to Hsp90 inhibition suggests that Hsp90 controls the final phosphorylation step of PKC, that of Ser660.

The Hsp90 inhibitor, 17-AAG, used in the preceding pulse-chase experiments specifically targets the ATPase activity of Hsp90 and would not affect potential regulation of PKC by Cdc37. To investigate the effect of disrupting the interaction of Hsp90 with its cochaperones on PKC maturation, we took advantage of a recently described Hsp90 inhibitor, celastrol, that not only inhibits ATP binding to Hsp90, but also inhibits the interaction of Hsp90 with Cdc37 (21,48). COS7 cells transfected with WT PKC  $\beta$ II were pretreated with 17-AAG, celastrol, or both prior to pulse-labeling with [<sup>35</sup>S]Met/Cys (Figure 2.5E). The autoradiogram in Figure 2.5E shows that the processing

of PKC was slowed approximately 2-fold by 17-AAG, as observed previously in Figure 2.5A: the amount of unphosphorylated lower band (*dash*) and phosphorylated upper band (*asterisk*) was approximately equal at the 15 min (*lane 2*) and 30 min (*lane 7*) time points in the absence or presence of 17-AAG, respectively. Celastrol had a much more striking effect on the maturation of PKC, with PKC migrating primarily as the unphosphorylated species even after 90 min chase. In the presence of both 17-AAG and celastrol, processing of PKC was completely inhibited. These data underscore the importance of both Hsp90 activity and the Hsp90/Cdc37 interaction for the proper maturation of PKC.

*The PXXP motif also mediates the interaction of other conventional and novel PKC isozymes with Hsp90* - Given the conservation of the hydrophobic motif amongst PKC isozymes, we addressed if other isozymes of PKC are controlled by Hsp90. We mutated the PXXP motif to AXXA for another conventional PKC, PKC  $\alpha$  (PKC  $\alpha$ -P613A/P616A), a novel PKC, PKC  $\delta$  (PKC  $\delta$ -P617A/P620A), and an atypical PKC, PKC  $\zeta$  (PKC  $\zeta$ -P534A/P537A), and tested the interaction of each mutant with Hsp90 (Figure 2.6). COS7 cells were transfected with empty vector (*lanes 1 and 4*), WT PKC isozymes (*lanes 2 and 5*), or the corresponding PXXP mutant (*lanes 3 and 6*). Specific PKC isozymes were immunoprecipitated from detergent-solubilized lysates and bound endogenous Hsp90 was assessed by Western blot analysis. Hsp90 was detected in the immune complexes of all three wild-type isozymes as well as the corresponding AXXA mutants (Figure 2.6A/C/E, *lanes 2 and 3*). However, quantitative analysis of the amount of Hsp90 bound to PKC (*IP, upper panel*), normalized to the amount of Hsp90 in the lysate (*Lysate, upper panel*), indicated striking isozyme-specific effects of perturbing the PXXP motif. Notably, mutation of the PXXP motif in the conventional PKC  $\alpha$

dramatically reduced the interaction with Hsp90 to ~10% of the level bound to WT PKC  $\alpha$  (Figure 2.6B, \*\*\* $p < 0.001$ ,  $n = 3$ ). This protein migrated with a faster mobility than wild-type PKC  $\alpha$  on SDS-PAGE (*lane 6, dash*), indicating that it, like its counterpart in PKC  $\beta$ II, was not processed by phosphorylation. This result is consistent with Hsp90 inhibition slowing the maturation of endogenous PKC  $\alpha$  in COS7 cells (Figure 2.5C). Similarly, mutation of the PXXP motif in the novel PKC  $\delta$  reduced the interaction with Hsp90: ~70% less Hsp90 was observed in the immune complex of the mutant compared to that of WT PKC  $\delta$  (Figure 2.6D, \* $p < 0.05$ ,  $n = 3$ ). Indeed, similar to that of the conventional PKCs, the maturation of PKC  $\delta$ -P617A/P620A is impaired, and it has reduced phosphorylation at both the turn and hydrophobic motif sites (data not shown); although the mobility of the mutant is not detectably different from that of WT PKC  $\delta$  (Figure 2.6C, *middle panel*). Pulse-chase analysis of another novel PKC isozyme, PKC  $\epsilon$ , revealed that the rate of processing was also slowed 2-fold by 17-AAG (data not shown). In contrast to mutation of the conventional and novel isozymes, mutation of the PXXP motif in the atypical PKC  $\zeta$  did not affect the interaction with Hsp90 (Figure 2.6F,  $n = 3$ ). It is noteworthy that PKC  $\zeta$  differs from the conventional and novel isozymes in that it has a Glu at the hydrophobic motif phosphorylation site. These data are consistent with Hsp90 binding and facilitating the phosphorylation of conventional and novel PKC isozymes via the conserved PXXP motif.

*Inhibition of Hsp90 activity results in the down-regulation of PKC via a proteasome-mediated pathway* - Chaperones, such as Hsp90, not only facilitate the proper folding and maturation of kinases but also stabilize vulnerable structural

conformations that are susceptible to degradation mechanisms (6,8). Therefore, we next addressed whether Hsp90 serves an additional stabilizing role for PKC. COS7 cells were transfected with either WT PKC  $\beta$ II or PKC  $\beta$ II P616A/P619A and treated with 17-AAG for increasing amounts of time; protein levels in whole cell lysates were analyzed by Western blot (Figure 2.7A). The top panel in Figure 2.7A shows that WT PKC  $\beta$ II was significantly depleted by 12 hr (*lane 4*) and absent by 24 hr (*lane 5*) with inhibitor treatment. 17-AAG also down-regulated PKC  $\beta$ II-P616A/P619A (*lanes 6-10*; darker exposure). Quantitative analysis of the PKC levels normalized to actin (*bottom panel*) revealed that PKC  $\beta$ II-P616A/P619A was ~10-fold more sensitive to Hsp90 inhibition than WT PKC  $\beta$ II (Figure 2.7B, half-time for depletion of PKC  $\beta$ II-P616A/P619A was approximately 1 hr, compared to 10 hrs for WT PKC  $\beta$ II). These data indicate that Hsp90 activity not only controls the processing of PKC, but also the degradation of PKC.

Studies have shown that Hsp90 inhibition leads to down-regulation via ubiquitination and degradation by the proteasome (29,49). To determine if the down-regulation we observed with 17-AAG occurred via a proteasome-mediated pathway, COS7 cells were transfected with WT PKC  $\beta$ II or PKC  $\beta$ II-P616A/P619A, pretreated with the proteasome inhibitor MG-132, and then treated with 17-AAG for 12 or 24 hr (Figure 2.7C). The Western blot in Figure 2.7C reveals that the steady-levels of both WT PKC  $\beta$ II and PKC  $\beta$ II-P616A/P619A were reduced following 17-AAG treatment, as reported above (Figure 2.7C, *lanes 2-3* and *lanes 11-12*). Pre-treatment with MG-132 completely protected the PKC  $\beta$ II-P616A/P619A construct from degradation both in the absence (*lanes 14-15*) as well as in the presence 17-AAG (*lanes 17-18*): in fact, inhibition of the proteasome dramatically increased the steady-state levels of this

construct. The proteasome inhibitor also prevented the 17-AAG-triggered depletion of WT PKC  $\beta$ II (*lanes 8-9*). Note that the proteasome inhibitor resulted in the accumulation of dephosphorylated PKC (*dash*): this is consistent with the dephosphorylated species of PKC being degraded by proteasomal pathways. These data demonstrate that Hsp90 protects PKC from proteasomal degradation, as previously reported for other client proteins.

To determine if long-term Hsp90 inhibition down-regulated other PKC isozymes, we examined the levels of endogenous PKC  $\alpha$ , PKC  $\delta$ , and PKC  $\zeta$  in COS7 cells upon treatment with 17-AAG (Figure 2.7D). Hsp90 inhibition resulted in a significant loss of each of these isozymes (*lane 5*). Although Hsp90 regulation of the processing of PKC is an isozyme-specific process, these data illustrate that Hsp90 control of the degradation of PKC is not isozyme-specific. However, because a previous study reported that PKC is insensitive to 17-AAG-induced down-regulation in MCF7 cells (11), we investigated if the 17-AAG-induced degradation depended on cell type. To this end, we treated HeLa cells (Figure 2.7E, *lanes 1-3*), MCF-10A cells (*lanes 4-6*), or MCF7 cells (*lanes 7-9*) with 17-AAG for 0 hr, 12 hr, and 24 hr and monitored endogenous PKC levels. PKC  $\alpha$ , PKC  $\delta$ , and PKC  $\zeta$  levels were dramatically reduced in both HeLa and MCF-10A (a normal breast cell line) cells (Figure 2.7E, *lanes 1-6, top 3 panels*). In marked contrast, 17-AAG caused only a very modest degradation of PKC isozymes in MCF7 cells (a breast cancer cell line), even after 24 hours treatment (Figure 2.7E, *lanes 7-9, top 3 panels*). Therefore, the efficiency of Hsp90-mediated stabilization of PKC isozymes depends on cell type.

*Mutation of a conserved Tyr that interacts with the PXXP motif recapitulates the defect of mutating the PXXP motif* – To determine whether the interaction of Hsp90 with

PKC was mediated directly by the PXXP motif, or if, instead, the PXXP motif indirectly controls the binding of Hsp90, we performed a peptide walk of PKC sequence and asked which segments bind Hsp90. Specifically, 18-mer peptides derived from the catalytic domain of PKC  $\beta$ II (a.a 342-673), moving down the sequence 2 residues at a time, were spotted onto a membrane, which was then incubated with purified Hsp90 protein. Hsp90 specifically bound clusters of sequences; these are shown in Figure 8A, with the sequence of the spotted peptide shown to the right of the peptide spot. Four interacting regions were detected in the array: the Gly-rich loop, the  $\alpha$ C- $\beta$ 4 loop, the  $\alpha$ D-helix, and the novel  $\alpha$  helix and turn motif (*highlighted in red*) sequences of PKC  $\beta$ II (Figure 2.8A) (50). Interestingly, Hsp90 did not significantly bind the peptide sequences that contained the PXXP motif (*highlighted in blue in the novel  $\alpha$  helix and turn motif segment*). These data show that Hsp90 directly binds peptide segments that are proximal to the PXXP motif, but not the PXXP motif itself. These binding surfaces are mapped onto the structure of PKC  $\beta$ II (Figure 2.8B, *dark blue*). Note that the  $\alpha$ C- $\beta$ 4 loop and the  $\alpha$ D-helix, two of the strongest Hsp90 binding regions, flank the N and C-terminal ends of the PXXP motif, respectively.

Previous analysis of AGC kinase sequences and structure had identified key residues in the  $\alpha$ E-helix of the catalytic domain that serve as a docking site for the PXXP motif (36). In particular, a conserved tyrosine (Y446) in the  $\alpha$ E-helix maximally packs up against P616 in the PXXP motif to simulate a ‘molecular clamp’ (see Figure 2.9). Sequence alignment portrays that this Tyr is conserved in several AGC family members, including all PKC isozymes, Akt, and PKA (Figure 2.8C, *red*). To test if mutation of this conserved Tyr in PKC  $\beta$ II (Y446) to an Ala would recapitulate the processing defect of

the PKC  $\beta$ II-P616A/P619A mutant, COS7 cells were transfected with empty vector, WT PKC  $\beta$ II, or PKC  $\beta$ II-Y446A, and whole cell lysates were analyzed by Western blot. The Western blot in Figure 2.8D indicates that the Y446A construct migrated as the faster-mobility, unphosphorylated form (*dash*). Consistent with this result, a phospho-specific antibody to the hydrophobic motif site (pS660) did not detect any phosphorylation of this mutant (*middle panel, asterisk; note that the upper band labeled with the pS660 antibody in the vector and Y446A lanes represents endogenous PKC  $\alpha$* ). Furthermore, the Y446A mutant was not labeled by phospho-specific antibodies to the other two sites, T500 and T641 (data not shown). Thus, perturbation of the intramolecular clamp between the  $\alpha$ E helix and the PXXP segment by mutation of Y446 recapitulated the processing defect observed upon mutation of the PXXP motif.

Lastly, we wanted to determine if mutation of Y446, similar to mutation of the PXXP motif that abrogated maturation, abolished Hsp90 binding. COS7 cells were transfected with vector, WT PKC  $\beta$ II, PKC  $\beta$ II-K371R, PKC  $\beta$ II-P616A/P619A, or PKC  $\beta$ II-Y446A, the PKC was immunoprecipitated, and bound endogenous Hsp90 was detected by Western blot (Figure 2.8E, *upper panel, IP*). As reported above, Hsp90 bound both WT PKC  $\beta$ II and PKC  $\beta$ II-K371R (*upper panel, IP, lanes 2-3*). However, Hsp90 failed to bind either the PKC  $\beta$ II-P616A/P619A mutant or the PKC  $\beta$ II-Y446A mutant (*upper panel, IP, lanes 4-5, n = 3*). These data are consistent with Hsp90 binding a surface that is structured by the PXXP motif and  $\alpha$ E helix.

## Discussion

The foregoing data demonstrate that the molecular chaperones, Hsp90 and Cdc37, control the processing by phosphorylation of conventional and novel PKC isozymes. Binding of these chaperones is dependent upon a “molecular clamp” that is formed between a conserved PXXP motif in the C-terminal tail of PKC and determinants in the  $\alpha$ E helix of the catalytic domain. Perturbation of this structural motif by mutation or pharmacological inhibition of the chaperones results in an abrogation of the maturation process. Of the two C-terminal phosphorylation sites on PKC, only that of the hydrophobic motif is sensitive to Hsp90 inhibition. In addition, we show that Hsp90 has a second role in stabilizing conventional, novel, and atypical PKC isozymes. Thus, the Hsp90/Cdc37 complex plays an essential role in allowing the maturation of isozymes that require hydrophobic motif phosphorylation and, additionally, in stabilizing all subclasses of this family of kinases.

*The PXXP motif forms an intramolecular clamp* – Our findings show that the PXXP motif is critical for the maturation and proper catalytic function of PKC. Specifically, the PXXP motif anchors the flexible C-terminal tail to the catalytic core by forming a molecular clamp with residues in the  $\alpha$ E-helix. A number of residues in this clamp, including the sequence FYAAE, are conserved across all AGC kinases. Mutation of the conserved Tyr (Y446 in PKC  $\beta$ II) in this sequence mimics the processing defect of mutating the PXXP motif in PKC  $\beta$ II. Thus, mutation of either portion of this clamp, i.e. the PXXP motif or the conserved Tyr of the  $\alpha$ E-helix, perturbs the structure of the catalytic domain, preventing Hsp90/Cdc37 from binding, and thus inhibiting the maturation of PKC by phosphorylation. In support of this model, mutation of the

adjacent conserved Phe, F445 in PKC  $\beta$ II, also mimics the processing defect of mutating the PXXP motif (data not shown). Thus, the PXXP motif serves as a folding nucleus to modulate events necessary for proper catalytic function by promoting interaction with the Hsp90/Cdc37 complex.

The PXXP motif is conserved across all AGC kinases and may also serve a common function. Our data indicate that Hsp90 facilitates maturation for both conventional and novel PKC isozymes. Studies with Akt have shown that this PXXP motif is necessary for proper localization in T-cells as well as activation (51,52). Indeed, the Akt1 PXXP mutant P424A/P427A is unphosphorylated, catalytically inactive, and migrates as a faster mobility species (52). Inhibition of Hsp90 blocks the activation and maturation of Akt (12). Whether the PXXP motif controls Akt maturation in the same manner as it does for PKC remains to be established.

*PKC is a client kinase of the Hsp90/Cdc37 chaperone complex* – The Hsp90/Cdc37 complex has over 100 known client kinases involved in a wide array of signaling pathways (53). PDK-1 and Akt, both members of the AGC kinase superfamily, have been previously established as clients of these chaperones (11-13). The identification of PKC as another client of the Hsp90/Cdc37 chaperone complex underscores the importance of this chaperone in kinase regulation. In the case of PKC, the chaperoning activity of Hsp90/Cdc37 serves two purposes: 1) facilitating the maturation of PKC by processing phosphorylations and 2) regulating the stability of PKC.

An intact PXXP motif is required for the selective binding of Hsp90 to unphosphorylated, unprocessed forms of PKC compared to phosphorylated PKC. The

tight binding of Hsp90 to mutants of PKC that cannot be phosphorylated (e.g. kinase-inactive mutant PKC  $\beta$ II-K371R, or the turn motif mutant PKC  $\beta$ II-T641AAA (data not shown (38)) is abolished upon mutation of the PXXP motif. Thus, the PXXP motif critically regulates the binding of Hsp90 to unphosphorylated PKC.

In order for PKC to mature into a catalytically-competent enzyme, it must first undergo three processing phosphorylations on the activation loop, the turn motif, and the hydrophobic motif. The activation loop step is dependent upon the upstream kinase PDK-1 while the latter two phosphorylation steps rely on accessory protein complexes and autophosphorylation. Hsp90 does not appear to be necessary for the first phosphorylation step by PDK-1 because the PKC  $\beta$ II-P616A/P619A mutant was phosphorylated by PDK-1 *in vitro* and bound PDK-1 in cells; although it was unable to complete the maturation process in cells. Recent studies have shown that Hsp90 is necessary to stabilize mutants in Akt and PKC that lack turn motif phosphorylation, which is promoted by the mTORC2 complex (29,30). However, our data reveal that phosphorylation at the turn motif site is not sensitive to Hsp90 inhibition: the rate of processing of a mutant with a constitutive negative charge at the hydrophobic motif (PKC  $\beta$ II S660E) is not slowed by Hsp90 inhibition, whereas the rate of processing of a mutant with a constitutive negative charge at the turn motif (PKC  $\beta$ II T641E) is slowed. These data suggest that Hsp90/Cdc37 facilitates the hydrophobic motif phosphorylation step. Consistent with this model, the processing of atypical PKC isozymes, which have a Glu at the phospho-acceptor position of the hydrophobic motif, is not impaired by mutation of the PXXP motif.

How Hsp90 facilitates the phosphorylation of the hydrophobic motif is not clear. Enzymological studies with pure protein have demonstrated that, in the case of PKC  $\beta$ II, this site is autophosphorylated by an intramolecular mechanism (54). This result would suggest that this segment of the C-terminal tail must access the active site during the maturation of PKC. Thus, one possibility is that Hsp90 facilitates conformational transitions that allow this to occur. It is noteworthy that mutation of the hydrophobic motif site to Ala in either PKC  $\alpha$  or PKC  $\beta$ II does not prevent the maturation of PKC: although constructs with Ala at this position are less stable than phosphorylated wild-type enzyme, they are nonetheless phosphorylated at the PDK-1 site and turn motif and retain catalytic activity (38,55). Thus, Hsp90 not only facilitates the phosphorylation of the hydrophobic motif, but it likely plays an additional role in the maturation of PKC.

Once phosphorylated, the hydrophobic motif phosphorylation site serves as an important site of regulation in AGC kinases. Phosphorylation at the hydrophobic motif promotes a stable, active, and phosphatase-resistant kinase; dephosphorylation of this site in PKC promotes its ubiquitination and down-regulation (56). Structural studies have shown that hydrophobic motif phosphorylation in AGC kinases stabilizes the N-lobe of the kinase domain by docking into a hydrophobic groove; this interaction leads to an ordering of the  $\alpha$ C helix that allows optimal binding to ATP and also stabilizes a closed, active conformation by interacting with the activation loop phosphate (57,58). Studies have shown that Hsp90/Cdc37 can bind to the N-lobe and  $\alpha$ C helix of the catalytic domain of various client kinases, which are important regions involved in kinase dynamics (8,59). Because hydrophobic motif phosphorylation is necessary for generation

of a stable, active kinase for PKC, it is plausible that the role of Hsp90/Cdc37 in the maturation process is to stabilize these regions as PKC completes its maturation.

In addition to its role in facilitating maturation, the Hsp90/Cdc37 complex also stabilizes PKC. Long-term treatment with Hsp90 inhibitors promotes the down-regulation of PKC isozymes by a proteasomal-dependent mechanism. Interestingly, we also observed rapid down-regulation of PKC  $\beta$ II-P616A/P619A suggesting that any residual interaction occurring with Hsp90 was sensitized to Hsp90 inhibition. This 17-AAG-induced down-regulation was observed in all PKC isozyme families. Indeed, Hsp90 inhibition leads to the degradation of other client kinases (8,53). However, this effect is cell-type dependent. A previous study claimed that PKC was not a client of Hsp90 by assessing 17-AAG-induced down-regulation in MCF7 cells (11). However, we see decreased PKC levels in not only COS7 cells but also HeLa and MCF-10A cells. Interestingly, we did not observe as striking a decrease in MCF7 cells. These findings indicate that Hsp90 regulation of PKC is cell-type dependent and may reflect abnormalities within signaling pathways of different cell environments.

*PKC, Hsp90, and Cdc37 in cancer* – Altered expression levels of both PKC  $\beta$ II and the molecular chaperones Hsp90 and Cdc37 have been observed in various cancers (21,24,25,60). These chaperones are unique as oncogenes because they promote tumorigenicity by stabilizing over-expressed or mutated oncogenic proteins (6). Whether PKC levels are elevated in cancer because of defective interaction with Hsp90/Cdc37 remains to be established. However, it is noteworthy that a recent study of the genes mutated in glioblastoma multiforme identified a mutation in PKC  $\alpha$ , P613S, as a cancer-driving mutation (5). This residue in PKC  $\alpha$  corresponds to the first Pro of the PXXP

motif (Figure 2.1B). Based on our data, it is tempting to speculate that the tumorigenic phenotype could arise from the lack of processing of PKC  $\alpha$  due to mutation of the PXXP motif. Interestingly, a recent study has shown that PKC  $\alpha$  protein expression is necessary for glioma cell proliferation and not necessarily its kinase activity (61).

Hsp90 has become an appealing drug target in cancer therapeutics. A recent study showed that the Hsp90 inhibitor 17-AAG potentiated the activity of the PKC  $\beta$ II-specific inhibitor, enzastaurin, in malignant glioma (62). Although Akt activity is up-regulated in this cancer pathway (62), the efficacy of these two inhibitors could also be explained by Hsp90 regulation of PKC. The identification of PKC as a client of the Hsp90/Cdc37 chaperone complex suggests that Hsp90 and PKC inhibitors could serve as potential therapeutics in treating pathologies that have associated PKC mutations or elevated levels of PKC.

*Summary* – Our data reveal that PKC is a client kinase of the Hsp90/Cdc37 chaperone complex. Interaction with these chaperones depends on a “molecular clamp” created by a conserved PXXP motif in the C-terminal tail and determinants in the  $\alpha$ E helix of the catalytic domain (Figure 2.9). Hsp90/Cdc37 serves two functions for PKC: 1) it facilitates maturation into a signaling-competent enzyme and 2) it stabilizes the mature enzyme. These data identify new molecular mechanisms that regulate the function and stability of PKC. Knowledge of these mechanisms could be helpful in the design of therapies to target pathologies that have aberrant PKC signaling.

**Acknowledgments**

We thank Charles C. King for purifying His-PDK-1, C.J. Allison for synthesizing the peptide array, Robert Romano for technical advice, and Newton lab members for helpful discussions.

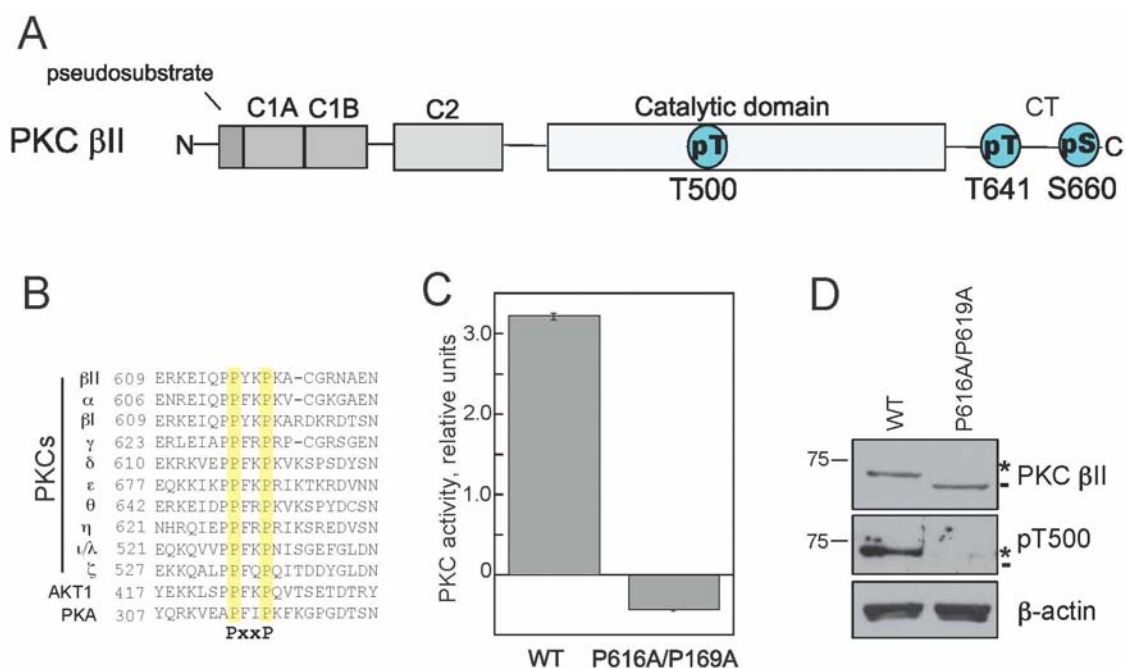


**Figure 2.1:** Mutation of a PXXP motif, conserved in all AGC kinases, in the C-terminal tail of PKC  $\beta$ II abolishes kinase activity. **A**, Schematic representation of the domain composition of PKC  $\beta$ II showing pseudosubstrate, C1A and C1B domains, and C2 domain in the N-terminal regulatory moiety, followed by the catalytic domain and C-terminal tail in the kinase moiety. The three processing phosphorylation sites, activation loop (T500), turn motif (T641), and hydrophobic motif (S660), in PKC  $\beta$ II are indicated by cyan circles. **B**, Partial sequence alignment of AGC family members, PKA, Akt1, and the ten PKC isozymes. A conserved PXXP motif in the C-terminal tail is highlighted in yellow. **C**, Lysates from tsA201 cells expressing either WT PKC  $\beta$ II or PKC  $\beta$ II-P616A/P619A were assayed for PKC activity in the absence or presence of lipid and  $\text{Ca}^{2+}$ ; cofactor-dependent activity attributed to transfected PKC  $\beta$ II (i.e. after subtraction of endogenous activity obtained from control lysates) was normalized to PKC  $\beta$ II expression in the lysate determined by Western blot. Data represent the mean  $\pm$  S.E.M. from four independent experiments. **D**, Western blot showing the expression and phosphorylation of WT PKC  $\beta$ II and PKC  $\beta$ II-P616A/P619A used in the kinase assay with the indicated antibodies. Unphosphorylated PKC  $\beta$ II is labeled with a *dash* and fully-phosphorylated PKC  $\beta$ II is labeled with an *asterisk*. Lysates were probed for  $\beta$ -actin as a loading control (*lower panel*).

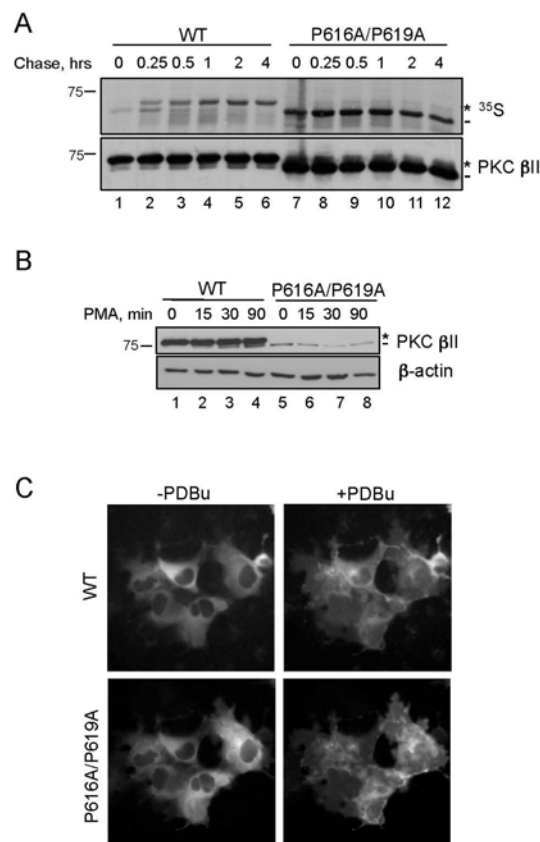


**Figure 2.2:** Mutation of the PXXP motif in PKC  $\beta$ II prevents the maturation of the kinase, a defect that cannot be rescued by translocation to membranes. *A*, Autoradiogram from a pulse-chase analysis of COS7 cells transfected with WT PKC  $\beta$ II (*lanes 1-6*) or PKC  $\beta$ II-P616A/P619A (*lanes 7-12*). Transfected cells were labeled with [ $^{35}$ S]Met/Cys and chased for the indicated times. The *asterisk* denotes the position of the mature, fully-phosphorylated species of PKC, and the *dash* represents the newly-synthesized, unphosphorylated species of PKC. Total PKC in the immunoprecipitate is labeled by an anti-PKC  $\beta$ II antibody. *B*, COS7 cells were transfected with WT PKC  $\beta$ II (*lanes 1-4*) or PKC  $\beta$ II-P616A/P619A (*lanes 5-8*) and then treated with PMA for the indicated times. Whole cell lysates were separated by SDS-PAGE and then analyzed for total PKC (PKC  $\beta$ II) or total protein content ( $\beta$ -actin). The *asterisk* denotes the position of fully-phosphorylated PKC, and the *dash* denotes the position of unphosphorylated PKC. *C*, Representative images of COS7 cells transfected with WT PKC $\beta$ II-RFP (*upper panels*) and PKC  $\beta$ II-P616A/P619A-YFP (*lower panels*) before (*left panels*) and after (*right panels*) PDBu (200 nM) treatment for 15 min.

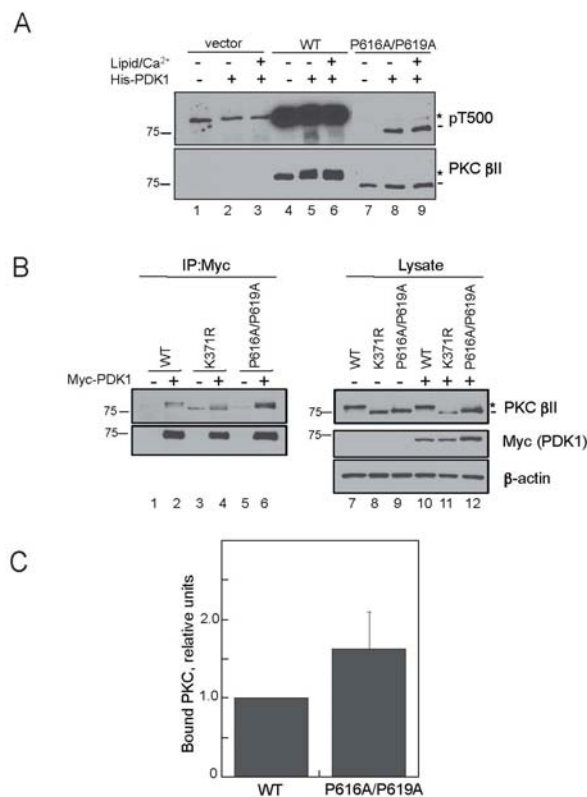


**Figure 2.3:** Mutation of the PXXP motif in PKC  $\beta$ II does not impair phosphorylation by or binding to its upstream kinase, PDK-1. *A*, COS7 cells were transfected with vector (*lanes 1-3*), WT PKC  $\beta$ II (*lanes 4-6*), or PKC  $\beta$ II-P616A/P619A (*lanes 7-9*), and immunoprecipitated PKC  $\beta$ II was incubated with purified His-PDK-1 (0.5 nM) alone or together with, Ca<sup>2+</sup> and lipid in an *in vitro* kinase assay. The immunoprecipitates were analyzed by Western blot for pT500 and total PKC  $\beta$ II. The *asterisk* indicates the position of the fully-phosphorylated PKC, the *dash* indicates the position of the unphosphorylated PKC, and the *arrow* indicates the position of endogenous PKC  $\alpha$ . Note that phosphorylation of T500 does not cause a mobility shift in WT PKC. *B*, COS7 cells were co-transfected with WT PKC  $\beta$ II (*lanes 1-2*), PKC  $\beta$ II-K371R, a catalytically inactive PKC, (*lanes 3-4*), or PKC  $\beta$ II-P616A/P619A (*lanes 5-6*) and either empty vector (*lanes 1, 3, and 5*) or Myc-PDK-1 (*lanes 2, 4, and 6*). Myc-PDK-1 was immunoprecipitated from detergent-solubilized lysates, and PKC interaction was assessed by Western blotting. Five percent of the detergent-solubilized lysates was analyzed by Western blotting to show the amount of Myc-PDK-1 and PKC  $\beta$ II present in the lysates. The *asterisk* denotes the position of fully-phosphorylated PKC, and the *dash* denotes the position of unphosphorylated PKC. An anti- $\beta$ -actin antibody indicates total protein loading in the lysate. *C*, Graph showing densitometric analysis of Western blots in *B*. Data represent the mean  $\pm$  S.E.M. of 13 independent experiments.

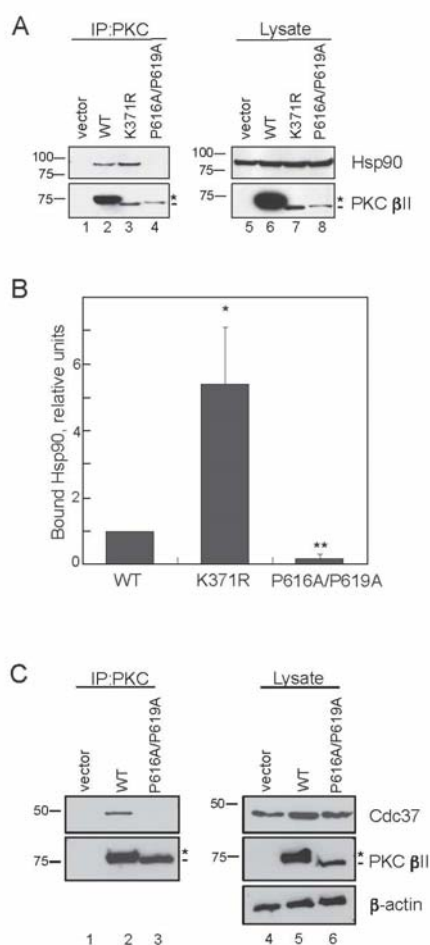


**Figure 2.4:** Mutation of the PXXP motif in PKC  $\beta$ II decreases binding to the chaperones Hsp90 and Cdc37. *A*, COS7 cells were transfected with empty vector (*lanes 1 and 5*), WT PKC  $\beta$ II (*lanes 2 and 6*), PKC  $\beta$ II-K371R (*lanes 3 and 7*), or PKC  $\beta$ II-P616A/P619A (*lanes 4 and 8*). PKC was immunoprecipitated from detergent-solubilized lysates, and endogenous Hsp90 interaction was assessed by Western blot. Five percent of the detergent-solubilized lysates was analyzed to show the amount of Hsp90 and PKC  $\beta$ II present in the lysate. The *asterisk* denotes the position of fully-phosphorylated PKC, and the *dash* denotes the position of unphosphorylated PKC. *B*, Graph representing densitometric analysis of the Western blots shown in *A*. Data represent the mean  $\pm$  S.E.M. of six independent experiments. \* $p < 0.05$  versus WT and \*\* $p < 0.01$  versus WT by Student's t-test. *C*, COS7 cells were transfected with vector (*lanes 1 and 4*), WT PKC  $\beta$ II (*lanes 2 and 5*), or PKC  $\beta$ II-P616A/P619A (*lanes 3 and 6*). Endogenous Cdc37 interaction was assessed as described in *A*. The *asterisk* denotes the position of fully-phosphorylated PKC, and the *dash* denotes the position of unphosphorylated PKC.

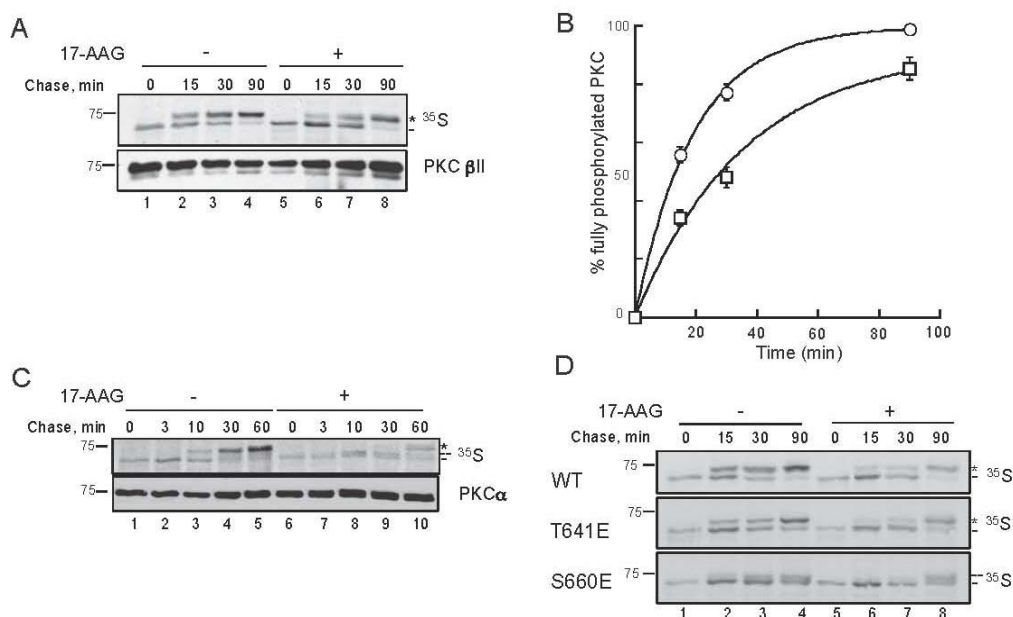


**Figure 2.5:** Hsp90 activity facilitates the maturation of PKC. *A*, Autoradiogram from a pulse-chase analysis of COS7 cells transfected with WT PKC  $\beta$ II in the absence (*lanes 1-4*) or presence (*lanes 5-8*) of 17-AAG (1  $\mu$ M). Transfected cells were labeled with [<sup>35</sup>S]Met/Cys and then chased for the indicated times. PKC was immunoprecipitated from detergent-solubilized lysates and analyzed by autoradiography. The *asterisk* denotes the position of mature, fully-phosphorylated PKC, and the *dash* denotes the position of newly-synthesized, unphosphorylated PKC. An anti-PKC  $\beta$ II antibody indicates the amount of PKC in the immunoprecipitates. *B*, Graph representing the data shown in the autoradiogram in *A*. This graph shows the relative amount of fully-phosphorylated PKC (*asterisk*) as a percentage of the total PKC protein in the absence (*circles*) or presence (*squares*) of 17-AAG (1  $\mu$ M). Data are representative of three independent experiments. *C*, Autoradiogram from a pulse-chase analysis of endogenous PKC  $\alpha$  in COS7 cells in the absence (*lanes 1-5*) or presence (*lanes 6-10*) of 17-AAG (1  $\mu$ M). Cells were labeled with [<sup>35</sup>S]Met/Cys and then chased for the indicated times. PKC was immunoprecipitated from detergent-solubilized lysates and analyzed by autoradiography. The *asterisk* denotes the position of mature, fully-phosphorylated PKC (phosphorylated at both C-terminal sites); the *double dash* denotes the position of PKC phosphorylated at only one C-terminal site; and the *single dash* denotes the position of newly-synthesized, unphosphorylated PKC. An anti-PKC  $\alpha$  antibody indicates the amount of PKC present in the immunoprecipitates. *D*, Autoradiogram from a pulse-chase analysis of COS7 cells transfected with WT PKC  $\beta$ II, PKC  $\beta$ II-T641E, or PKC  $\beta$ II S660E in the absence (*lanes 1-4*) and presence (*lanes 5-8*) of 17-AAG (1  $\mu$ M). Transfected cells were pulse-labeled and analyzed as shown in *A*. The *asterisk* denotes the fully-phosphorylated, mature PKC; the *double dash* denotes the position of phosphorylation at T641; and the *dash* denotes the newly-synthesized, unphosphorylated PKC.

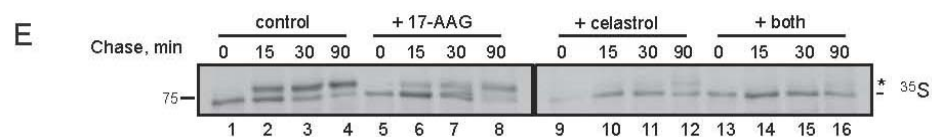


**Figure 2.5:** (continued) *E*, Autoradiogram from a pulse-chase analysis of COS7 cells transfected with WT PKC  $\beta$ II and treated with DMSO (*lanes 1-4*), 17-AAG (1  $\mu$ M, *lanes 5-8*), celastrol (10  $\mu$ M, *lanes 9-12*), or both 17-AAG and celastrol (*lanes 13-16*). Transfected cells were pulse-labeled and analyzed as shown in *A*. The *asterisk* denotes the fully-phosphorylated, mature PKC, and the *dash* denotes the newly-synthesized, unphosphorylated PKC.

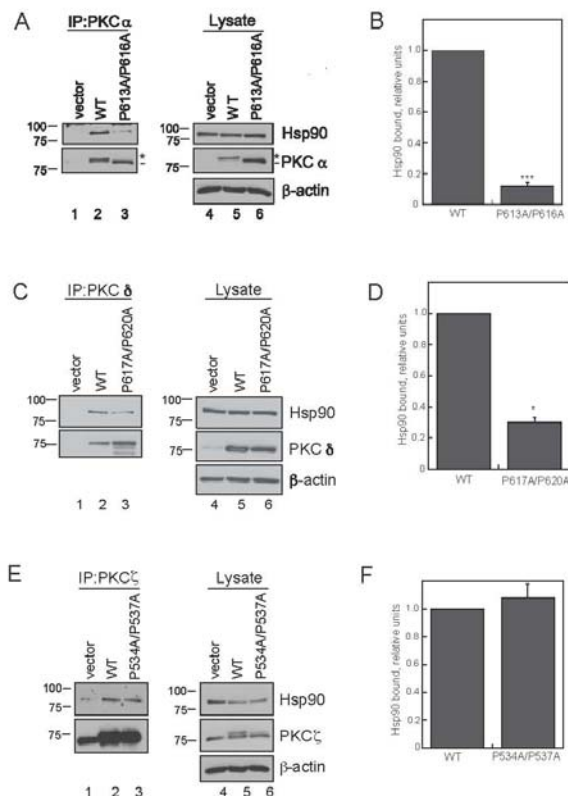


**Figure 2.6:** Mutation of the PXXP motif in conventional and novel PKC isozymes decreases the interaction with Hsp90. *A*, COS7 cells were transiently transfected with empty vector (*lanes 1 and 4*), WT PKC  $\alpha$  (*lanes 2 and 5*), or PKC  $\alpha$ -P613A/P616A (*lanes 3 and 6*). PKC was immunoprecipitated from detergent-solubilized lysates, and endogenous Hsp90 interaction was assessed by Western blot. Five percent of the detergent-solubilized lysate was analyzed by Western blot to show the amount of PKC and Hsp90 present in the lysate. The *asterisk* denotes the position of fully-phosphorylated PKC, and the *dash* denotes the position of unphosphorylated PKC. Total protein loading is indicated by an anti- $\beta$ -actin antibody. *B*, Graph representing densitometric analysis of the Western blots shown in *A*. Data represent the mean  $\pm$  S.E.M. of three independent experiments. \*\*\* $p < 0.001$  versus WT by Student's t-test. *C*, COS7 cells were transiently transfected with empty vector (*lanes 1 and 4*), WT PKC  $\delta$  (*lanes 2 and 5*), or PKC  $\delta$ -P617A/P620A (*lanes 3 and 6*). PKC was immunoprecipitated, and endogenous Hsp90 interaction was analyzed as described in *A*. *D*, Graph representing densitometric analysis of the Western blots shown in *C*. Data represent the mean  $\pm$  S.E.M. of three independent experiments. \* $p < 0.05$  versus WT by Student's t-test. *E*, COS7 cells were transiently transfected with empty vector (*lanes 1 and 4*), WT PKC  $\zeta$  (*lanes 2 and 5*), or PKC  $\zeta$ -P534A/P537A (*lanes 3 and 6*). PKC was immunoprecipitated, and endogenous Hsp90 interaction was analyzed as described in *A*. *F*, Graph representing densitometric analysis of Western blots shown in *E*. Data represent the mean  $\pm$  S.E.M. of three independent experiments.

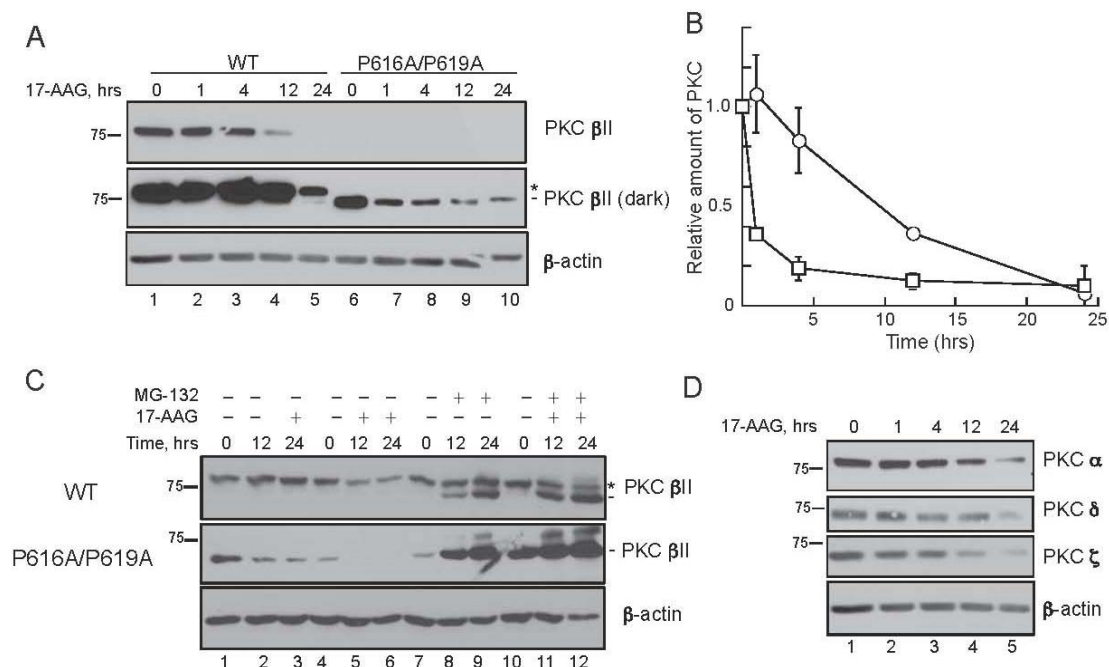


**Figure 2.7:** Inhibition of Hsp90 down-regulates PKC through a proteasome-dependent mechanism in a cell-type-dependent context. *A*, COS7 cells were transiently transfected with WT PKC  $\beta$ II (lanes 1-5) or PKC  $\beta$ II-616A/P619A (lanes 6-10). Cells were treated with 17-AAG (1  $\mu$ M) for the indicated times. Whole cell lysates were analyzed by Western blotting for total PKC (PKC  $\beta$ II) and total protein content ( $\beta$ -actin). The *asterisk* denotes the position of fully-phosphorylated PKC, and the *dash* denotes the position of unphosphorylated PKC. *B*, Graph representing densitometric analysis of Western blots shown in *A*. The relative amounts of WT PKC  $\beta$ II (white circles) and PKC  $\beta$ II-P616A/P619A (white squares) are indicated. Data are representative of three independent experiments. *C*, COS7 cells were transiently transfected with WT PKC  $\beta$ II (left) or PKC  $\beta$ II-P616A/P619A (right). Cells were then treated with 17-AAG (1  $\mu$ M, lanes 2-3, 11-12), MG-132 (10  $\mu$ M, lanes 5-6, 14-15), or both (lanes 8-9, 17-18) for the times indicated. Whole cell lysates were separated by SDS-PAGE and analyzed by Western blotting. PKC  $\beta$ II and  $\beta$ -actin were detected with the indicated antibodies. The *asterisk* denotes the position of fully-phosphorylated PKC, and the *dash* denotes the position of unphosphorylated PKC. Data are representative of three independent experiments. *D*, COS7 cells were treated with 17-AAG (1  $\mu$ M) for the indicated times. Whole cell lysates were analyzed by Western blotting for endogenous PKC  $\alpha$ , PKC  $\delta$ , PKC  $\zeta$ , and  $\beta$ -actin for total protein loading. Data are representative of three independent experiments.

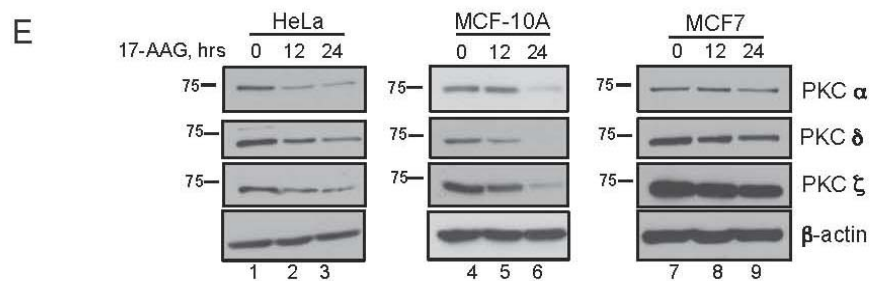


**Figure 2.7:** (continued) *E*, HeLa cells (*lanes 1-3*), MCF-10A cells (*lanes 4-6*), and MCF7 cells (*lanes 7-9*) were treated with 17-AAG (1  $\mu$ M) for the indicated times. Whole cell lysates were analyzed by Western blotting for endogenous PKC  $\alpha$ , PKC  $\delta$ , PKC  $\zeta$ , and  $\beta$ -actin for total protein loading. Data are representative of three independent experiments.

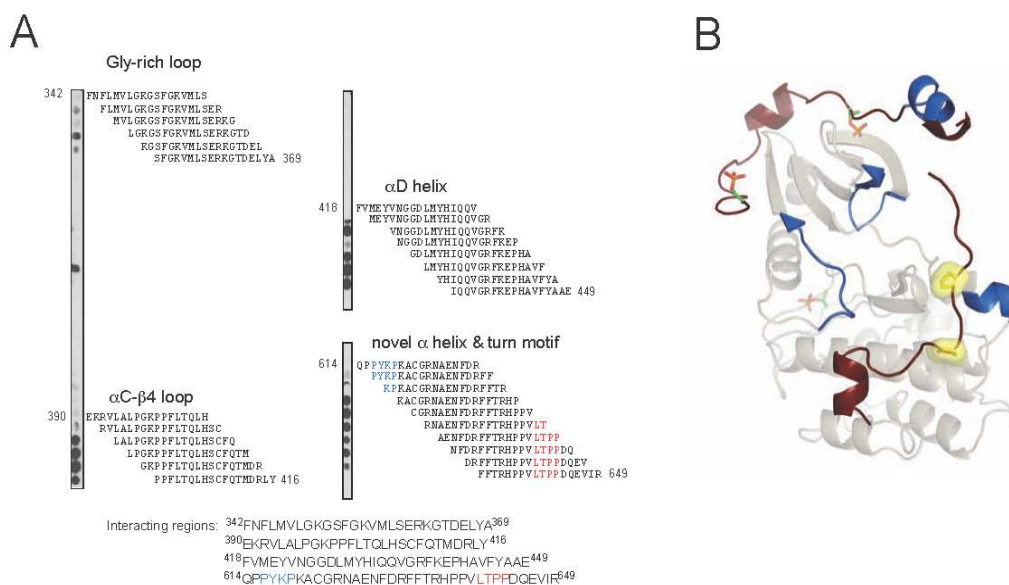


**Figure 2.8:** Mutation of a conserved Tyr in the  $\alpha$ E-helix of the catalytic domain of PKC  $\beta$ II mimics the defect of the PXXP mutant, PKC  $\beta$ II-P616A/P619A. **A**, Peptide overlay of the catalytic domain of PKC  $\beta$ II with purified Hsp90 $\alpha$ . 18-residue peptides covering the catalytic domain (a.a. 342-673) of PKC  $\beta$ II and staggered by two amino acids were spotted onto a membrane, and overlaid with 100 nM Hsp90 $\alpha$ , and Hsp90 binding detected with an anti-Hsp90 antibody. The residues highlighted in *blue* are the PXXP motif, and the residues highlighted in *red* are the residues delineating the turn motif phosphorylation site. **B**, Ribbon diagram representation of the catalytic domain of PKC  $\beta$ II. A homology model of the PKC  $\beta$ II was built using the crystal structure of PKC  $\theta$  (PDB:1XJD) as the template. The C-terminal tail is highlighted in *dark red* with the Pro of the PXXP motif as *yellow* surface representations. The processing phosphorylation sites (activation loop (T500), turn motif (T641), and hydrophobic motif (S660)) are shown as stick representations (*orange and green*). The regions identified in the peptide overlay are mapped onto the catalytic domain and are highlighted in *dark blue*.

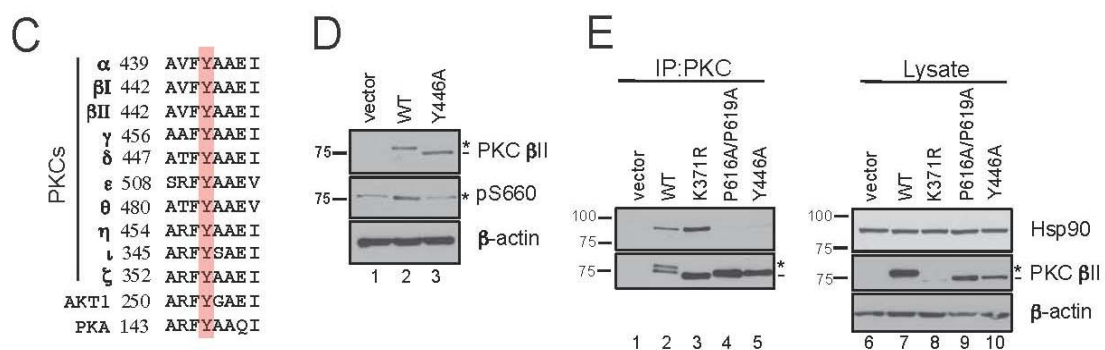


**Figure 2.8:** (continued) *C*, Partial sequence alignment of part of the conserved  $\alpha$ E-helix in the AGC kinases, the PKCs, Akt1, and PKA. A conserved Tyr is highlighted in red. *D*, COS7 cells were transiently transfected with empty vector (*lane 1*), WT PKC  $\beta$ II (*lane 2*), or PKC  $\beta$ II-Y446A (*lane 3*). Whole cell lysates were analyzed for total PKC (PKC  $\beta$ II), phosphorylated PKC (pS660), and total protein content ( $\beta$ -actin) by Western blotting. The asterisk denotes the position of phosphorylated PKC, and the dash denotes the position of unphosphorylated PKC. *E*, COS7 cells were transfected with empty vector (*lanes 1 and 6*), WT PKC  $\beta$ II (*lanes 2 and 7*), PKC  $\beta$ II-K371R (*lanes 3 and 8*), PKC  $\beta$ II-P616A/P619A (*lanes 4 and 9*), or PKC  $\beta$ II-Y446A (*lanes 5 and 10*). PKC was immunoprecipitated from detergent-solubilized lysates, and endogenous Hsp90 interaction was assessed by Western blot. Five percent of the detergent-solubilized lysates was analyzed to show the amount of Hsp90 and PKC  $\beta$ II present in the lysate. The asterisk denotes the position of fully-phosphorylated PKC, and the dash denotes the position of unphosphorylated PKC. Data are representative of three independent experiments.

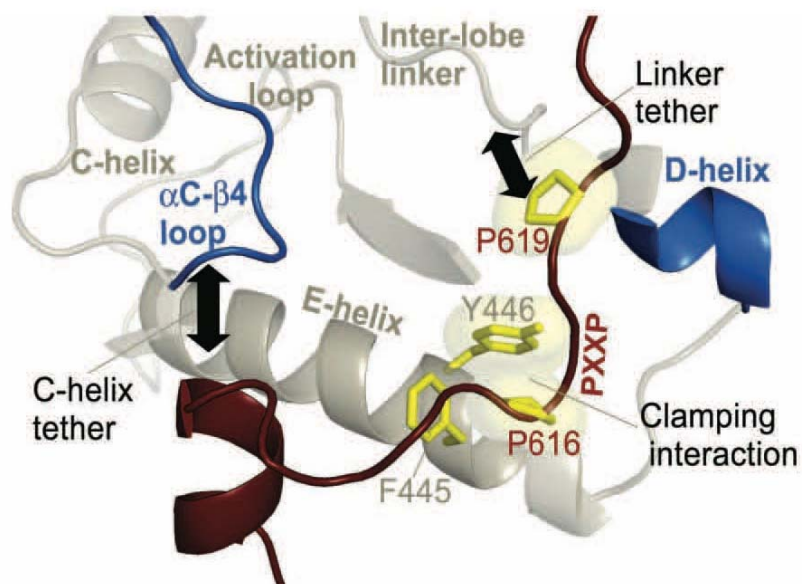


**Figure 2.9:** Structural representation of the residues that comprise the molecular 'clamp' between the PXXP motif and the catalytic core. Structural representation of the residues that comprise the molecular "clamp" between the PXXP motif and catalytic core. The PXXP motif in the C-terminal tail (highlighted in *dark red*) and the determinants in the  $\alpha$ E-helix of the catalytic domain are highlighted in *yellow*. Other key regions, such as the  $\alpha$ C- $\beta$ 4 loop, C-helix, D-helix, inter-lobe linker and the activation loop, of the catalytic domain are also represented. The tethering of the  $\alpha$ C- $\beta$ 4 loop and the inter-lobe linker by the C-terminal tail is highlighted by *black arrows*.

## References

1. Manning, G., Whyte, D. B., Martinez, R., Hunter, T., and Sudarsanam, S. (2002) *Science* **298**, 1912-1934
2. Torkamani, A., and Schork, N. J. (2008) *Cancer Res* **68**, 1675-1682
3. Majumder, P. K., and Sellers, W. R. (2005) *Oncogene* **24**, 7465-7474
4. Greenman, C., Stephens, P., Smith, R., Dalgliesh, G. L., Hunter, C., Bignone II, G., Davies, H., Teague, J., Butler, A., Stevens, C., Edkins, S., O'Meara, S., Vastrik, I., Schmidt, E. E., Avis, T., Barthorpe, S., Bhamra, G., Buck, G., Choudhury, B., Clements, J., Cole, J., Dicks, E., Forbes, S., Gray, K., Halliday, K., Harrison, R., Hills, K., Hinton, J., Jenkinson, A., Jones, D., Menzies, A., Mironenko, T., Perry, J., Raine, K., Richardson, D., Shepherd, R., Small, A., Tofts, C., Varian, J., Webb, T., West, S., Widada, S., Yates, A., Cahill, D. P., Louis, D. N., Goldstraw, P., Nicholson, A. G., Brasseur, F., Looijenga, L., Weber, B. L., Chiew, Y. E., DeFazio, A., Greaves, M. F., Green, A. R., Campbell, P., Birney, E., Easton, D. F., Chenevix-Trench, G., Tan, M. H., Khoo, S. K., Teh, B. T., Yuen, S. T., Leung, S. Y., Wooster, R., Futreal, P. A., and Stratton, M. R. (2007) *Nature* **446**, 153-158
5. McLendon, R., Friedman, A., Bigner, D., Van Meir, E. G., Brat, D. J., Mastrogiannakis, M., Olson, J. J., Mikkelsen, T., Lehman, N., Aldape, K., Alfred Yung, W. K., Bogler, O., Vandenberg, S., Berger, M., Prados, M., Muzny, D., Morgan, M., Scherer, S., Sabo, A., Nazareth, L., Lewis, L., Hall, O., Zhu, Y., Ren, Y., Alvi, O., Yao, J., Hawes, A., Jhangiani, S., Fowler, G., San Lucas, A., Kovar, C., Cree, A., Dinh, H., Santibanez, J., Joshi, V., Gonzalez-Garay, M. L., Miller, C. A., Milosavljevic, A., Donehower, L., Wheeler, D. A., Gibbs, R. A., Cibulskis, K., Sougnez, C., Fennell, T., Mahan, S., Wilkinson, J., Ziaugra, L., Onofrio, R., Bloom, T., Nicol, R., Ardlie, K., Baldwin, J., Gabriel, S., Lander, E. S., Ding, L., Fulton, R. S., McLellan, M. D., Wallis, J., Larson, D. E., Shi, X., Abbott, R., Fulton, L., Chen, K., Koboldt, D. C., Wendl, M. C., Meyer, R., Tang, Y., Lin, L., Osborne, J. R., Dunford-Shore, B. H., Miner, T. L., Delehaunty, K., Markovic, C., Swift, G., Courtney, W., Pohl, C., Abbott, S., Hawkins, A., Leong, S., Haipek, C., Schmidt, H., Wiechert, M., Vickery, T., Scott, S., Dooling, D. J., Chinwalla, A., Weinstock, G. M., Mardis, E. R., Wilson, R. K., Getz, G., Winckler, W., Verhaak, R. G., Lawrence, M. S., O'Kelly, M., Robinson, J., Alexe, G., Beroukhi, R., Carter, S., Chiang, D., Gould, J., Gupta, S., Korn, J., Mermel, C., Mesirov, J., Monti, S., Nguyen, H., Parkin, M., Reich, M., Stransky, N., Weir, B. A., Garraway, L., Golub, T., Meyerson, M., Chin, L., Protopopov, A., Zhang, J., Perna, I., Aronson, S., Sathiamoorthy, N., Ren, G., Wiedemeyer, W. R., Kim, H., Won Kong, S., Xiao, Y., Kohane, I. S., Seidman, J., Park, P. J., Kucherlapati, R., Laird, P. W., Cope, L., Herman, J. G., Weisenberger, D. J., Pan, F., Van Den Berg, D., Van Neste, L., Mi Yi, J., Schuebel, K. E., Baylin, S. B., Absher, D. M.,

- Li, J. Z., Southwick, A., Brady, S., Aggarwal, A., Chung, T., Sherlock, G., Brooks, J. D., Myers, R. M., Spellman, P. T., Purdom, E., Jakkula, L. R., Lapuk, A. V., Marr, H., Dorton, S., Gi Choi, Y., Han, J., Ray, A., Wang, V., Durinck, S., Robinson, M., Wang, N. J., Vranizan, K., Peng, V., Van Name, E., Fontenay, G. V., Ngai, J., Conboy, J. G., Parvin, B., Feiler, H. S., Speed, T. P., Gray, J. W., Brennan, C., Socci, N. D., Olshen, A., Taylor, B. S., Lash, A., Schultz, N., Reva, B., Antipin, Y., Stukalov, A., Gross, B., Cerami, E., Qing Wang, W., Qin, L. X., Seshan, V. E., Villafania, L., Cavatore, M., Borsu, L., Viale, A., Gerald, W., Sander, C., Ladanyi, M., Perou, C. M., Neil Hayes, D., Topal, M. D., Hoadley, K. A., Qi, Y., Balu, S., Shi, Y., Wu, J., Penny, R., Bittner, M., Shelton, T., Lenkiewicz, E., Morris, S., Beasley, D., Sanders, S., Kahn, A., Sfeir, R., Chen, J., Nassau, D., Feng, L., Hickey, E., Weinstein, J. N., Barker, A., Gerhard, D. S., Vockley, J., Compton, C., Vaught, J., Fielding, P., Ferguson, M. L., Schaefer, C., Madhavan, S., Buetow, K. H., Collins, F., Good, P., Guyer, M., Ozenberger, B., Peterson, J., and Thomson, E. (2008) *Nature* **455**, 1061-1068
6. Whitesell, L., and Lindquist, S. L. (2005) *Nat Rev Cancer* **5**, 761-772
  7. Hartl, F. U., and Hayer-Hartl, M. (2002) *Science* **295**, 1852-1858
  8. Caplan, A. J., Mandal, A. K., and Theodoraki, M. A. (2007) *Trends Cell Biol* **17**, 87-92
  9. Pearl, L. H., and Prodromou, C. (2006) *Annu Rev Biochem* **75**, 271-294
  10. Xu, Y., Singer, M. A., and Lindquist, S. (1999) *Proc Natl Acad Sci U S A* **96**, 109-114
  11. Basso, A. D., Solit, D. B., Chiosis, G., Giri, B., Tsihchlis, P., and Rosen, N. (2002) *J Biol Chem* **277**, 39858-39866
  12. Sato, S., Fujita, N., and Tsuruo, T. (2000) *Proc Natl Acad Sci U S A* **97**, 10832-10837
  13. Fujita, N., Sato, S., Ishida, A., and Tsuruo, T. (2002) *J Biol Chem* **277**, 10346-10353
  14. Xu, W., Mimnaugh, E., Rosser, M. F., Nicchitta, C., Marcu, M., Yarden, Y., and Neckers, L. (2001) *J Biol Chem* **276**, 3702-3708
  15. Xu, W., Mimnaugh, E. G., Kim, J. S., Trepel, J. B., and Neckers, L. M. (2002) *Cell Stress Chaperones* **7**, 91-96
  16. Pearl, L. H. (2005) *Curr Opin Genet Dev* **15**, 55-61

17. Karnitz, L. M., and Felts, S. J. (2007) *Sci STKE* **2007**, pe22
18. Vaughan, C. K., Gohlke, U., Sobott, F., Good, V. M., Ali, M. M., Prodromou, C., Robinson, C. V., Saibil, H. R., and Pearl, L. H. (2006) *Mol Cell* **23**, 697-707
19. Reed, S. I. (1980) *Genetics* **95**, 561-577
20. MacLean, M., and Picard, D. (2003) *Cell Stress Chaperones* **8**, 114-119
21. Gray, P. J., Jr., Prince, T., Cheng, J., Stevenson, M. A., and Calderwood, S. K. (2008) *Nat Rev Cancer* **8**, 491-495
22. Kamal, A., Boehm, M. F., and Burrows, F. J. (2004) *Trends Mol Med* **10**, 283-290
23. Gray, P. J., Jr., Stevenson, M. A., and Calderwood, S. K. (2007) *Cancer Res* **67**, 11942-11950
24. Pick, E., Kluger, Y., Giltane, J. M., Moeder, C., Camp, R. L., Rimm, D. L., and Kluger, H. M. (2007) *Cancer Res* **67**, 2932-2937
25. McCarthy, M. M., Pick, E., Kluger, Y., Gould-Rothberg, B., Lazova, R., Camp, R. L., Rimm, D. L., and Kluger, H. M. (2008) *Ann Oncol* **19**, 590-594
26. Newton, A. C. (2003) *Biochem J* **370**, 361-371
27. Dutil, E. M., and Newton, A. C. (2000) *J Biol Chem* **275**, 10697-10701
28. Gao, T., Toker, A., and Newton, A. C. (2001) *J Biol Chem* **276**, 19588-19596
29. Facchinetti, V., Ouyang, W., Wei, H., Soto, N., Lazorchak, A., Gould, C., Lowry, C., Newton, A. C., Mao, Y., Miao, R. Q., Sessa, W. C., Qin, J., Zhang, P., Su, B., and Jacinto, E. (2008) *EMBO J* **27**, 1932-1943
30. Ikenoue, T., Inoki, K., Yang, Q., Zhou, X., and Guan, K. L. (2008) *EMBO J* **27**, 1919-1931
31. Keranen, L. M., Dutil, E. M., and Newton, A. C. (1995) *Curr Biol* **5**, 1394-1403
32. Orr, J. W., Keranen, L. M., and Newton, A. C. (1992) *J Biol Chem* **267**, 15263-15266
33. Ziegler, W. H., Parekh, D. B., Le Good, J. A., Whelan, R. D., Kelly, J. J., Frech, M., Hemmings, B. A., and Parker, P. J. (1999) *Curr Biol* **9**, 522-529

34. Freeley, M., Volkov, Y., Kelleher, D., and Long, A. (2005) *Biochem Biophys Res Commun* **334**, 619-630
35. Standaert, M. L., Bandyopadhyay, G., Kanoh, Y., Sajan, M. P., and Farese, R. V. (2001) *Biochemistry* **40**, 249-255
36. Kannan, N., Haste, N., Taylor, S. S., and Neuwald, A. F. (2007) *Proc Natl Acad Sci U S A* **104**, 1272-1277
37. Yeong, S. S., Zhu, Y., Smith, D., Verma, C., Lim, W. G., Tan, B. J., Li, Q. T., Cheung, N. S., Cai, M., Zhu, Y. Z., Zhou, S. F., Tan, S. L., and Duan, W. (2006) *J Biol Chem* **281**, 30768-30781
38. Edwards, A. S., Faux, M. C., Scott, J. D., and Newton, A. C. (1999) *J Biol Chem* **274**, 6461-6468
39. Edwards, A. S., and Newton, A. C. (1997) *J Biol Chem* **272**, 18382-18390
40. Chou, M. M., Hou, W., Johnson, J., Graham, L. K., Lee, M. H., Chen, C. S., Newton, A. C., Schaffhausen, B. S., and Toker, A. (1998) *Curr Biol* **8**, 1069-1077
41. Dries, D. R., Gallegos, L. L., and Newton, A. C. (2007) *J Biol Chem* **282**, 826-830
42. Campbell, R. E., Tour, O., Palmer, A. E., Steinbach, P. A., Baird, G. S., Zacharias, D. A., and Tsien, R. Y. (2002) *Proc Natl Acad Sci U S A* **99**, 7877-7882
43. Dutil, E. M., Toker, A., and Newton, A. C. (1998) *Curr Biol* **8**, 1366-1375
44. Sonnenburg, E. D., Gao, T., and Newton, A. C. (2001) *J Biol Chem* **276**, 45289-45297
45. Gao, T., and Newton, A. C. (2006) *J Biol Chem* **281**, 32461-32468
46. Gould, C. M., and Newton, A. C. (2008) *Curr Drug Targets* **9**, 614-625
47. Gao, T., and Newton, A. C. (2002) *J Biol Chem* **277**, 31585-31592
48. Zhang, T., Hamza, A., Cao, X., Wang, B., Yu, S., Zhan, C. G., and Sun, D. (2008) *Mol Cancer Ther* **7**, 162-170
49. Moriwaki, Y., Kim, Y. J., Ido, Y., Misawa, H., Kawashima, K., Endo, S., and Takahashi, R. (2008) *Neurosci Res* **61**, 43-48

50. Grodsky, N., Li, Y., Bouzida, D., Love, R., Jensen, J., Nodes, B., Nonomiya, J., and Grant, S. (2006) *Biochemistry* **45**, 13970-13981
51. Kane, L. P., Mollenauer, M. N., and Weiss, A. (2004) *J Immunol* **172**, 5441-5449
52. Jiang, T., and Qiu, Y. (2003) *J Biol Chem* **278**, 15789-15793
53. Citri, A., Harari, D., Shohat, G., Ramakrishnan, P., Gan, J., Lavi, S., Eisenstein, M., Kimchi, A., Wallach, D., Pietrokovski, S., and Yarden, Y. (2006) *J Biol Chem* **281**, 14361-14369
54. Behn-Krappa, A., and Newton, A. C. (1999) *Curr Biol* **9**, 728-737
55. Bornancin, F., and Parker, P. J. (1997) *J Biol Chem* **272**, 3544-3549
56. Gao, T., Brognard, J., and Newton, A. C. (2008) *J Biol Chem* **283**, 6300-6311
57. Yang, J., Cron, P., Thompson, V., Good, V. M., Hess, D., Hemmings, B. A., and Barford, D. (2002) *Mol Cell* **9**, 1227-1240
58. Frodin, M., Antal, T. L., Dummler, B. A., Jensen, C. J., Deak, M., Gammeltoft, S., and Biondi, R. M. (2002) *EMBO J* **21**, 5396-5407
59. Huse, M., and Kuriyan, J. (2002) *Cell* **109**, 275-282
60. Fields, A. P., and Gustafson, W. C. (2003) *Methods Mol Biol* **233**, 519-537
61. Cameron, A. J., Procyk, K. J., Leitges, M., and Parker, P. J. (2008) *Int J Cancer* **123**, 769-779
62. Jane, E. P., and Pollack, I. F. (2008) *Cancer Lett* **268**, 46-55

**Footnotes**

§This work was supported by 2T32 GM-07752 (CG) and NIH GM-43154 and NIH P01 DK54441.

\*The abbreviations used are as follows: PKC, protein kinase C; AGC, c-AMP-dependent protein kinase/protein kinase G/protein kinase C; DAG, diacylglycerol; PDK-1, phosphoinositide-dependent kinase 1; Hsp, heat shock protein; Cdc37, cell division cycle 37; mTOR, mammalian target of rapamycin; mTORC2, mammalian target of rapamycin complex 2; RFP, red fluorescent protein; YFP, yellow fluorescent protein; Met/Cys, methionine/cysteine; PDBu, phorbol-12,13-dibutyrate; PMA, phorbol 12-myristate 13-acetate; 17-AAG, 17-(allylamino)-17-demethoxygeldanamycin; MG-132, carbobenzoxy-L-leucyl-L-leucyl-leucinal; PP2A, protein phosphatase 2A

This Chapter is, in full, a reprint of the material as it appears in The Journal of Biological Chemistry, 2009, Gould C, Kannan N, Taylor SS, Newton AC. I was the primary researcher and author; coauthors provided technical assistance and helped direct and supervise the research included in this chapter.

## APPENDIX

### Introduction

This Appendix presents additional data addressing the role of the PXXP motif in the maturation of PKC as well discusses other key structural interactions that affect PKC maturation. These data coincide with the significance of the findings presented in this chapter. However, in order to maintain the restrictions set by publication, some of these data were referred to as “data not shown”. The rest of the data are unpublished but relevant to the study. Herein are these data and a brief discussion of their importance.

### Contribution of the individual Pro in the PXXP motif

As the work in this chapter described, mutation of the PXXP motif in PKC disrupted a molecular clamp in the catalytic domain of PKC to prevent interaction with the chaperones Hsp90 and Cdc37, resulting in an unphosphorylated, immature kinase. However, we were curious if both Pro contributed equally to this effect or if one Pro was more significant than the other. To this end, we singly mutated P616 or P619 in PKC  $\beta$ II to Ala and then expressed the constructs in COS7 cells (Figure A2.1). Whole cell lysates were analyzed by SDS-PAGE and Western blotting for total PKC. As shown previously, WT PKC  $\beta$ II primarily migrates as a slower mobility species that is fully phosphorylated at the C-terminal processing sites (*lane 2, asterisk*) with a minor fraction that is unphosphorylated at a faster mobility (*dash*). Mutation of both Pro to Ala in the PXXP motif results in an unphosphorylated species that migrates solely as the faster mobility

form (*lane 3, dash*). Interestingly, mutation of P616 results in species that co-migrates with the double mutant (*lane 4, dash*), while mutation of P619 results in species that is partially processed and migrates as doublet (*lane 5, asterisk and dash*). These data show that mutation of the first Pro in the PXXP motif, Pro 616, is sufficient to prevent PKC maturation. This Pro in PKC  $\beta$ II, Pro 616, aligns with the same Pro in the PXXP motif of its conventional counterpart, PKC  $\alpha$ , which has recently been shown to be a potential cancer-driving mutation in glioblastoma multiforme, as discussed earlier in the Chapter. Studies with PKC  $\alpha$  knockout mice have shown that they spontaneously develop intestinal tumors in comparison to their wildtype littermates, indicating a protective role for PKC  $\alpha$  (1). Therefore, it would be interesting to investigate the link between inactivating PKC (by mutation of its PXXP which prevents its maturation) and the progression of glioblastoma.

#### Identification of other mutations that affect the processing of PKC

One of the key regions identified in the peptide walk of the catalytic domain of PKC  $\beta$ II that is important for mediating the interaction with Hsp90 is the  $\alpha$ C- $\beta$ 4 loop. Functionally, this loop interacts with the C-terminal tail of AGC kinases to facilitate C-helix movement; the C-helix contains key conserved residues that are necessary for the coordination of ATP and subsequent activation of the kinase (2,3). The  $\alpha$ C- $\beta$ 4 loop is one of the primary determinants for Hsp90 interaction with its client kinases; this region creates a specific surface to facilitate Hsp90 binding (4). In order to delineate specific residues in this region required for the Hsp90 interaction, we performed an alanine scan through two different peptides encompassing the  $\alpha$ C- $\beta$ 4 loop of PKC  $\beta$ II

(<sup>388</sup>MVEKRVLALPGKPPFLTQLHSCFQT<sup>412</sup> and <sup>398</sup>ALPGKPPFLTQLHSCFQTMDRLYFV<sup>419</sup>). An alanine was substituted for each consecutive residue in the peptide. The subsequent 25-mer peptides were then spotted onto nitrocellulose membranes, incubated with purified Hsp90, and probed with an anti-Hsp90 antibody to detect Hsp90 binding to the peptides (Figure A2.2). For each peptide set, positive and negative control peptides were included, which reproduces the previous results seen with Hsp90 in the original array (+ and -). The interaction with the wildtype peptide (*3<sup>rd</sup> peptide listed*) was abolished upon replacement of alanine for a few specific residues (*red asterisks*) while alanine replacement of other residues only slightly reduced the interaction (*grey asterisks*).

In both array sets, the peptides containing an alanine at F402, L403, and F410 did not bind Hsp90 (Figure A2.2 A,B, *red asterisk*). These residues are highly conserved in the  $\alpha$ C- $\beta$ 4 loop sequence of AGC kinases (Figure A2.2 C, *yellow*). PKC  $\beta$ II-F402 corresponds with F102 in PKA, which lies in close proximity to the  $\alpha$ E-helix, the other half of the PXXP intramolecular clamp (Figure A2.2 D). This residue is extremely important for AGC kinases because it directly interacts with the C-terminal tail; these conserved interactions between the catalytic domain and the C-terminal tail allow for proper activation and functioning of these kinases (2). Additionally, an alanine at R392 also abrogated Hsp90 interaction and is conserved in the  $\alpha$ C- $\beta$ 4 loop sequence (Figure A2.2 A, C).

Because F402 and R392 were identified in the alanine scan array as possible key residues to affect Hsp90 binding, we wanted to test whether mutation of these critically conserved residues disrupted the processing of PKC. We generated three mutants, PKC

$\beta$ II-F402A, PKC  $\beta$ II-R392A, and PKC  $\beta$ II-R392M (to conserve residue size), and expressed them in COS7 cells (Figure A2.2 E). WT PKC  $\beta$ II primarily migrated as a slower mobility species (*lane 2, asterisk*) that is fully phosphorylated at the activation loop (*pT500 panel*) and C-terminal processing sites (*pS660* and *pT641 panels*). Conversely, the PXXP mutant, PKC  $\beta$ II-P616A/P619A, migrated as a faster mobility species (*lane 3, dash*) that was not phosphorylated at either the activation loop or processing phosphorylation sites (*middle panels; note this mutant migrates as a slower mobility species (asterisk) which represents endogenous PKC  $\alpha$  in these cells (compare to vector lane)*). Both PKC  $\beta$ II-R392 mutants migrated similarly to WT PKC  $\beta$ II (*lanes 4 and 5*) and were fully phosphorylated. Interestingly, PKC  $\beta$ II-F402A migrated as a doublet (*lane 6, asterisk and dash*); approximately 50% of this mutant was fully phosphorylated. These data reveal that mutation of this critical Phe in PKC  $\beta$ II, F402, partially impairs maturation.

PKC  $\beta$ II-F402 interacts with a key basic residue in the C-terminal tail, K611. This basic residue is conserved in AGC kinases and corresponds to R308 in PKA (Figure A2.3 A). This interaction has been characterized for PKA as it facilitates movement of key regulatory elements within the catalytic domain, such as the C-helix and C-terminal tail, and it links the two lobes of the catalytic domain together (2). Since PKC  $\beta$ II-F402 lies in close proximity to K611 in the structure (Figure A2.3 B), we asked if mutation of the Lys also disrupted PKC maturation, similar to mutation of F402 (Figure A2.2 E). Figure A2.3 C shows that PKC  $\beta$ II-K612A exhibits a similar processing defect as PKC  $\beta$ II-F402A (*compare lanes 4 and 5*); both mutants migrated as a doublet (*asterisk and*

*dash*) equally as compared to WT PKC  $\beta$ II (*lane 2*). The slower mobility species for both mutants were phosphorylated at both C-terminal processing sites (*pS660* and *pT641 panels, asterisk*). Thus, mutation of K611, which forms a strong interaction with F402, also impairs PKC maturation.

Since these two mutants, PKC  $\beta$ II-F402A and PKC  $\beta$ II-K611A, exhibited a defect in processing by phosphorylation (although not as extreme as the PXXP mutant PKC  $\beta$ II-P616A/P619A), we next asked if these mutants also showed an impaired interaction with Hsp90. COS7 cells were transfected with WT PKC  $\beta$ II, PKC  $\beta$ II-K371R, PKC  $\beta$ II-P616A/P619A, PKC  $\beta$ II-F402A, or PKC  $\beta$ II-K611A, and PKC was immunoprecipitated from detergent-solubilized lysates. The amount of endogenous Hsp90 bound to PKC was detected by Western blot (Figure A2.4 A). As shown in previous experiments, the phospho-defective mutants PKC  $\beta$ II-K371R and PKC  $\beta$ II-P616A/P619A migrated primarily as the faster mobility, unphosphorylated species (*middle panel, dash*), whereas WT PKC  $\beta$ II migrated as the slower mobility, fully phosphorylated species (*asterisk*). The partially-impaired processing mutants, PKC  $\beta$ II-F402A and PKC  $\beta$ II-K611A, migrated as a doublet with approximately 50% migrating as the slower mobility, fully phosphorylated species and 50% migrating as the faster mobility, unphosphorylated species (*asterisk and dash*). WT PKC  $\beta$ II bound Hsp90 (*IP, lane 2*), an interaction that was enhanced with the unphosphorylated, kinase-dead construct PKC  $\beta$ II-K371R (*IP, lane 3*) and abolished with the unphosphorylated, PXXP mutant PKC  $\beta$ II-P616A/P619A (*IP, lane 4*). These mutants served as positive and negative controls, respectively. For both partially-impaired processing mutants, PKC  $\beta$ II-F402A and PKC  $\beta$ II-K611A, an

interaction with Hsp90 was detected (*IP, lanes 5 and 6*). However, quantitative analysis of the ratio of Hsp90 bound to PKC in the immunoprecipitate indicated that these mutations did not significantly alter the interaction with Hsp90 as compared to WT PKC  $\beta$ II (Figure A2.4 *B*,  $n = 3$ ).

Inhibition of Hsp90 activity slows the maturation of WT PKC. Therefore, we explored whether Hsp90 inhibitors would also affect the maturation of the impaired processing mutant PKC  $\beta$ II-F402A. As described earlier in Chapter 2, the processing of a pool of newly-synthesized PKC can be monitored by a pulse-chase analysis. COS7 cells were transfected with either WT PKC  $\beta$ II or PKC  $\beta$ II-F402A and pretreated with radicicol, an ATP-competitive Hsp90 inhibitor, prior to pulse-chase analysis. Radicicol acts in a similar manner to the antibiotic geldanamycin and its derivative 17-AAG by binding to the ATP-binding pocket and depleting cells of Hsp90-dependent signaling proteins (5). The autoradiogram in Figure A2.4 *C* shows that WT PKC  $\beta$ II processes with a half-time of approximately 15 min (*top panel, lane 2*) in the absence of inhibitor (similar to 17-AAG) but is slowed approximately 2-fold to 30 min (*top panel, lane 7*) in the presence of inhibitor. The impaired processing mutant PKC  $\beta$ II-F402A is processed more slowly than WT PKC  $\beta$ II with a half-time of approximately 30 min (*bottom panel, lane 3*) in the absence of inhibitor. However, similarly to WT PKC, the processing of the mutant is slowed in the presence of radicicol with a half-time between 30 and 90 min (*bottom panel, lanes 7 and 8*). Thus, even though PKC  $\beta$ II-F402A is impaired in its ability to become fully phosphorylated, that partial processing is dependent upon the activity of Hsp90. Therefore, mutation of F402 in PKC  $\beta$ II must eliminate an Hsp90-independent component that is required for proper maturation of PKC.

Figure A2.3 C shows that both PKC  $\beta$ II-F402A and PKC  $\beta$ II-K611A have impaired processing with approximately 50% of the mutant being fully phosphorylated. As mentioned earlier, these residues are highly conserved in AGC kinases as they form a tight interaction within the catalytic domain; PKC  $\beta$ II-F402 in the  $\alpha$ C- $\beta$ 4 loop lies in close proximity to PKC  $\beta$ II-K611 in the C-terminal tail (Figure A2.3 B). These conserved interactions between the C-terminal tail and catalytic domain demonstrate how the C-terminal tail serves as an important regulatory module for AGC kinase function. Therefore, we were curious if mutation of both of these residues would completely abolish PKC maturation. COS7 cells were transfected with WT PKC  $\beta$ II, PKC  $\beta$ II-P616A/P619A, PKC  $\beta$ II-F402A, PKC  $\beta$ II-K611A, or PKC  $\beta$ II-F402A/K611A, and whole cell lysates were analyzed by SDS-PAGE and Western blotting for total and phosphorylated PKC. Figure A2.4 D shows that WT PKC  $\beta$ II primarily migrates as the slower mobility, fully phosphorylated species (*lane 2, asterisk*) while PKC  $\beta$ II-P616A/P619A primarily migrates as the faster mobility, unphosphorylated species (*lane 3, dash*). The faint signal observed for pS660 and pT641 phosphorylation for this mutant represents labeling of endogenous PKC  $\alpha$  in COS7 cells, which migrates with the same mobility as WT PKC  $\beta$ II (*lane 3, pS660 and pT641 panels, asterisk*). As shown earlier in Figure A2.4 B, PKC  $\beta$ II-F402A and PKC  $\beta$ II-K611A migrate as a doublet (*lanes 4 and 5, asterisk and dash*) that is indicative of partial processing. Indeed, these mutants have phosphorylation at the C-terminal processing sites as detected by phospho-specific antibodies (*lanes 4 and 5, middle panels, asterisk*). However, the double mutant PKC  $\beta$ II-F402A/K611A migrates solely as the faster mobility, unphosphorylated species (*lane*

6, *dash*) and is not labeled with phospho-specific antibodies, similar to the PXXP mutant PKC  $\beta$ II-P616A/P619A. These data indicate that disruption of the interaction between F402 in the catalytic domain and K611 in the C-terminal tail abolishes PKC maturation.

Other residues that contribute to the ‘intramolecular clamp’ between the PXXP motif and the  $\alpha$ E-helix of PKC

The PXXP motif in the C-terminal tail of PKC forms an ‘intramolecular clamp’ with a conserved Tyr in the  $\alpha$ E-helix of the catalytic domain to facilitate interaction with the molecular chaperone Hsp90 and promote the proper processing of the enzyme. Specifically, this Tyr (Y446) interacts with the first Pro of the PXXP motif (P616); as mentioned earlier, this Pro was identified in PKC  $\alpha$  to be mutated in glioblastoma. Another conserved residue in the proximity of P616 and is also highly conserved in the  $\alpha$ E-helix of AGC kinases (Figure 2.8 C) is F445 (Figure A2.5 A). We were curious if mutation of this conserved Phe would recapitulate the same processing defect of the PKC mutants, PKC  $\beta$ II-P616A/P619A (PXXP) and PKC  $\beta$ II-Y446A ( $\alpha$ E-helix). COS7 cells were transfected with WT PKC  $\beta$ II, PKC  $\beta$ II-P616A/P619A, PKC  $\beta$ II-Y446A, PKC  $\beta$ II-F402A/K611A, or PKC  $\beta$ II-F445A, and whole cell lysates were analyzed by SDS-PAGE and Western blotting for phospho- and total PKC (Figure A2.5 B). WT PKC  $\beta$ II primarily migrated as a slower mobility species that is fully phosphorylated (*lane 2, asterisk*). The processing-defective mutants PKC  $\beta$ II-P616A/P619A, PKC  $\beta$ II-Y446A, and PKC  $\beta$ II-F402A/K611A all migrated as a faster mobility species that is unphosphorylated (*lanes 3-5, dash*). Phosphorylation at the Ser660 processing

phosphorylation site was only detected for WT PKC  $\beta$ II (*lane 2, asterisk, middle panel*). The phospho-signal detected in the processing-defective mutants is labeling endogenous PKC  $\alpha$  (*compare asterisk in lanes 3-5 to vector (lane 1)*). Interestingly, the other  $\alpha$ E-helix mutant, PKC  $\beta$ II-F445A, also exhibited a defect in processing and migrated as the faster mobility, unphosphorylated species (*lane 6, dash*), similarly to the other processing-defective mutants. These data indicate that F445 in the  $\alpha$ E-helix of the catalytic domain is another important component of the ‘intramolecular clamp’ with the PXXP motif in the C-terminal tail.

### Summary

These data illustrate how conserved, structural interactions between the C-terminal tail and the catalytic domain control the processing of PKC. The C-terminal tail serves as a critical point in the regulation of PKC.

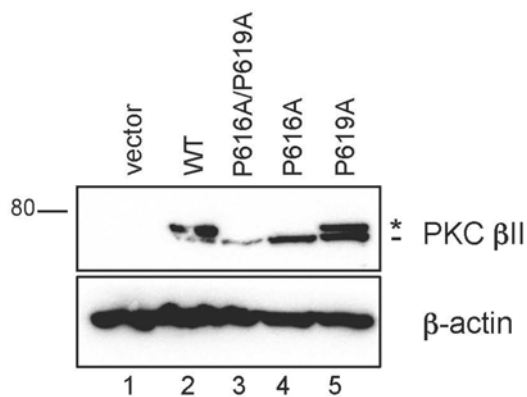


**Figure A2.1:** Mutation of the first Pro in the PXXP motif is sufficient to abolish PKC processing. COS7 cells were transiently transfected with empty vector (*lane 1*), WT PKC  $\beta$ II (*lane 2*), PKC  $\beta$ II-P616A/P619A (*lane 3*), PKC  $\beta$ II-P616A (*lane 4*), or PKC  $\beta$ II-P619A (*lane 5*). Whole cell lysates were analyzed for total PKC (PKC  $\beta$ II) and total protein content ( $\beta$ -actin) by Western blotting. The *asterisk* denotes the position of fully phosphorylated PKC, and the *dash* denotes the position of unphosphorylated PKC.



C

PKA	90	NEKRILQAVN-----FPFLV
AKT1	197	TENRVLQNSR-----HPFLT
PKCa	386	VEKRVLALLDK-----PPFLT
PKCb	389	VEKRVLALPGK-----PPFLT
PKCg	398	VEKRVLALGGRGPGGRPHFLT
PKCd	396	VEKRVLTAAE-----NPFLT
PKCe	455	TEKRILALARK-----HPYLT
PKCt	427	VEKRVLSLAW-----HPFLT
PKCh	401	TEKRILSLARN-----HPFLT
PKCi	292	TEKHFVEQASN-----HPFLV
PKCz	299	TEKHFVEQASS-----NPFLV

D

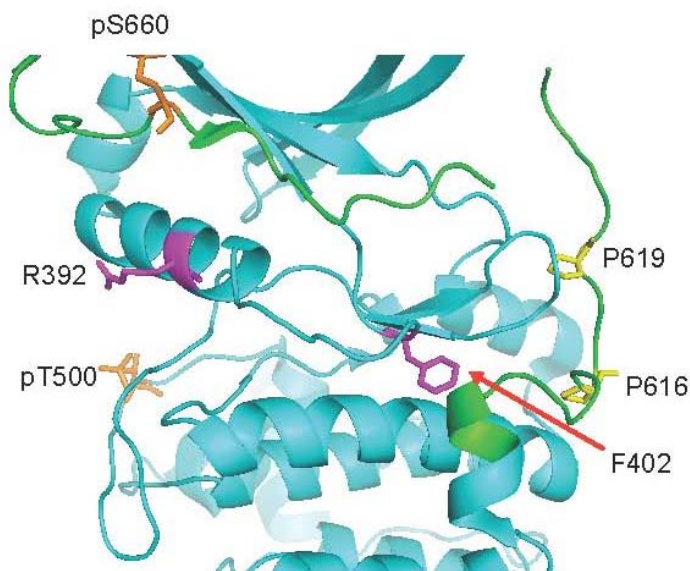


**Figure A2.2:** (continued) *C*, partial sequence alignment of the AGC kinase family members PKA, Akt1, and the 10 PKC isozymes. A conserved Arg and Phe in the  $\alpha$ C- $\beta$ 4 loop region of the catalytic domain are highlighted in *yellow*. *D*, ribbon diagram cartoon representation of the catalytic domain (*cyan*) of PKC  $\beta$ II (Protein Data Bank Number: 2I0E). Residues are shown in sticks representation. The activation loop phosphorylation (pT500) and the hydrophobic motif phosphorylation (pS660) are indicated in *orange*. The C-terminal tail is shown in *green*, and the Pro of the PXXP motif (P616, P619) are indicated in *yellow*. The two residues (R392, F402) identified in the alanine scan array are shown in *magenta*.

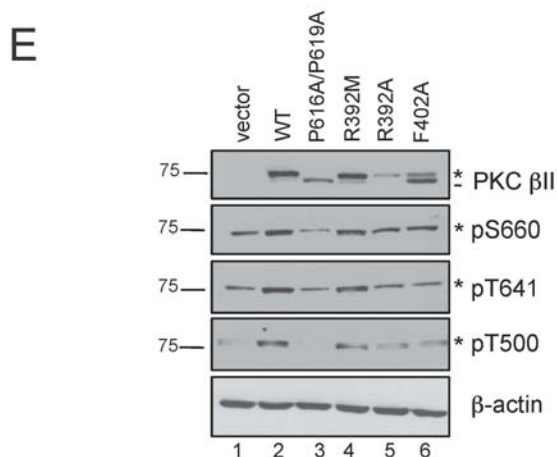


**Figure A2.2:** (continued) *E*, COS7 cells were transiently transfected with either vector (*lane 1*), WT PKC  $\beta$ II (*lane 2*), PKC  $\beta$ II-P616A/P619A (*lane 3*), PKC  $\beta$ II-R392M (*lane 4*), PKC  $\beta$ II-R392A (*lane 5*), or PKC  $\beta$ II-F402A (*lane 6*). Whole cell lysates were analyzed for total PKC (PKC  $\beta$ II), phospho-PKC (pS660, pT641, pT500), and total protein content ( $\beta$ -actin) by Western blotting. The *asterisk* denotes the position of fully phosphorylated PKC, and the *dash* denotes the position of unphosphorylated PKC.

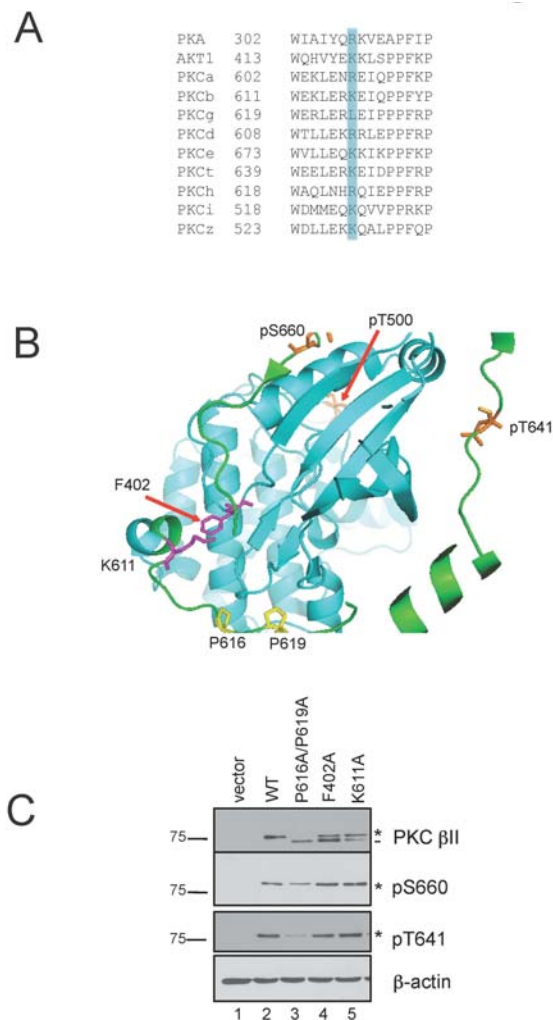


**Figure A2.3:** Mutation of a conserved basic residue in the C-terminal tail of PKC recapitulates the processing defect of the  $\alpha$ C- $\beta$ 4 loop mutant, PKC  $\beta$ II-F402A. *A*, partial sequence alignment of the AGC kinase family members PKA, Akt1, and the 10 PKC isozymes. A conserved basic residue in the C-terminal tail is highlighted in *blue*. *B*, ribbon diagram cartoon representation of the catalytic domain (*cyan*) of PKC  $\beta$ II (Protein Data Bank Number: 2I0E). Residues are shown in sticks representation. The activation loop phosphorylation (pT500) and the C-terminal processing phosphorylations (pT641 and pS660) are indicated in *orange*. The C-terminal tail is shown in *green*, and the Pro of the PXXP motif (P616, P619) are indicated in *yellow*. The two residues (K611, F402) that interact are shown in *magenta*. *C*, COS7 cells were transiently transfected with either vector (*lane 1*), WT PKC  $\beta$ II (*lane 2*), PKC  $\beta$ II-P616A/P619A (*lane 3*), PKC  $\beta$ II-F402A (*lane 4*), or PKC  $\beta$ II-K611A (*lane 5*). Whole cell lysates were analyzed for total PKC (PKC  $\beta$ II), phospho-PKC (pS660 and pT641), and total protein content ( $\beta$ -actin) by Western blotting. The *asterisk* denotes the position of fully phosphorylated PKC, and the *dash* denotes the position of unphosphorylated PKC.

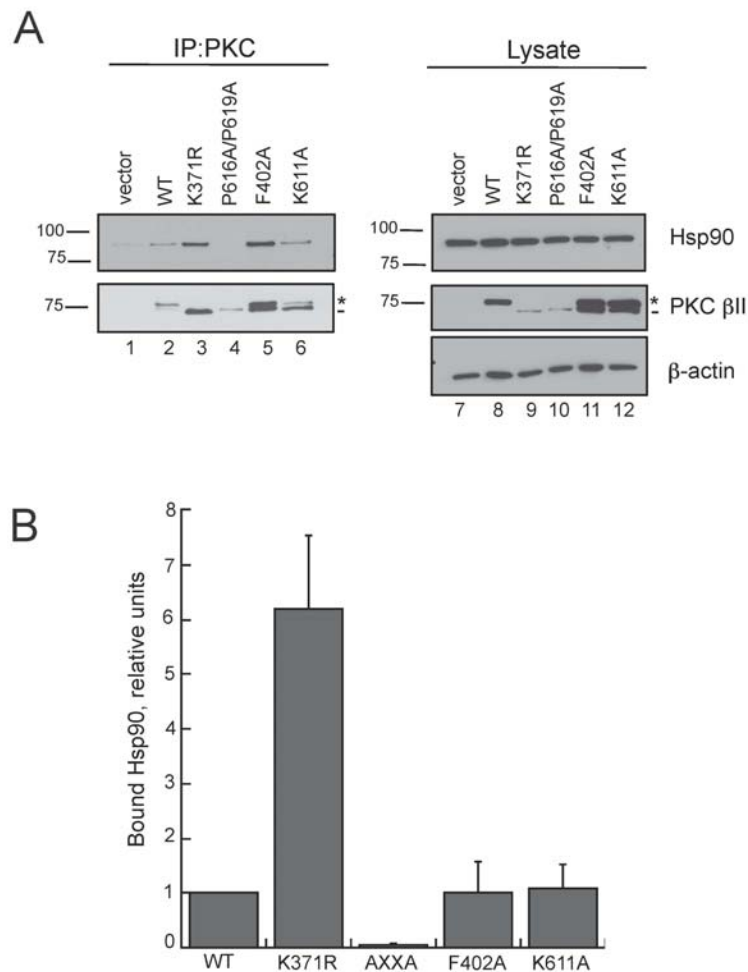
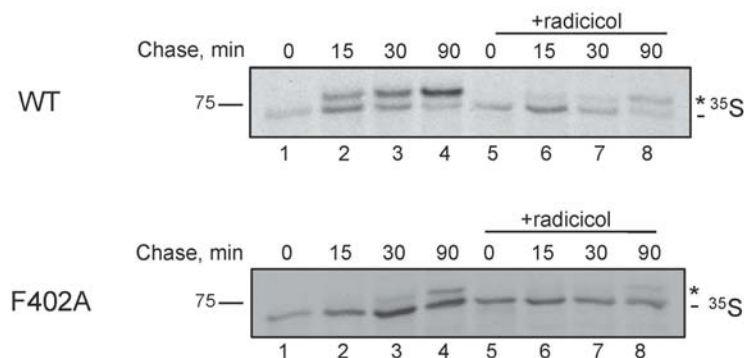


**Figure A2.4:** Disruption of the interaction between the  $\alpha$ C- $\beta$ 4 loop in the catalytic domain and the C-terminal tail of PKC  $\beta$ II impairs the processing in a manner that is independent of Hsp90. *A*, COS7 cells were transiently transfected with vector (*lanes 1 and 7*), WT PKC  $\beta$ II (*lanes 2 and 8*), PKC  $\beta$ II-K371R (*lanes 3 and 9*), PKC  $\beta$ II-P616A/P619A (*lanes 4 and 10*), PKC  $\beta$ II-F402A (*lanes 5 and 11*), or PKC  $\beta$ II-K611A (*lanes 6 and 12*). PKC was immunoprecipitated (*IP*) from detergent-solubilized lysates, and endogenous Hsp90 interaction was assessed by Western blot. Five percent of the detergent-solubilized lysates was analyzed to show the amount of Hsp90 and PKC  $\beta$ II present in the lysate. The *asterisk* denotes the position of fully phosphorylated PKC, and the *dash* denotes the position of unphosphorylated PKC. *B*, a graph representing densitometric analysis of the Western blots shown in *A*. Data represent the mean  $\pm$  S.E. of three independent experiments.

C



D

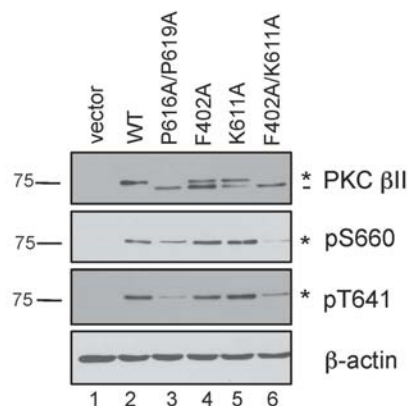


**Figure A2.4:** (continued) C, Autoradiogram from a pulse-chase analysis of COS7 cells transfected with WT PKC  $\beta$ II (*top panel*) or PKC  $\beta$ II-F402A (*bottom panel*) in the absence (*lanes 1-4*) or in the presence (*lanes 5-8*) of radicicol (1  $\mu$ M). Transfected cells were labeled with [ $^{35}$ S]Met/Cys and then chased for the indicated times. PKC was immunoprecipitated from detergent-solubilized lysates and analyzed by autoradiography. The *asterisk* denotes the position of mature, fully phosphorylated PKC, and the *dash* denotes the position of newly-synthesized, unphosphorylated PKC. D, COS7 cells were transiently transfected with either vector (*lane 1*), WT PKC  $\beta$ II (*lane 2*), PKC  $\beta$ II-P616A/P619A (*lane 3*), PKC  $\beta$ II-F402A (*lane 4*), PKC  $\beta$ II-K611A (*lane 5*), or PKC  $\beta$ II-F402A/K611A (*lane 6*). Whole cell lysates were analyzed for total PKC (PKC  $\beta$ II), phospho-PKC (pS660 and pT641), and total protein content ( $\beta$ -actin) by Western blotting. The *asterisk* denotes the position of fully phosphorylated PKC, and the *dash* denotes the position of unphosphorylated PKC.

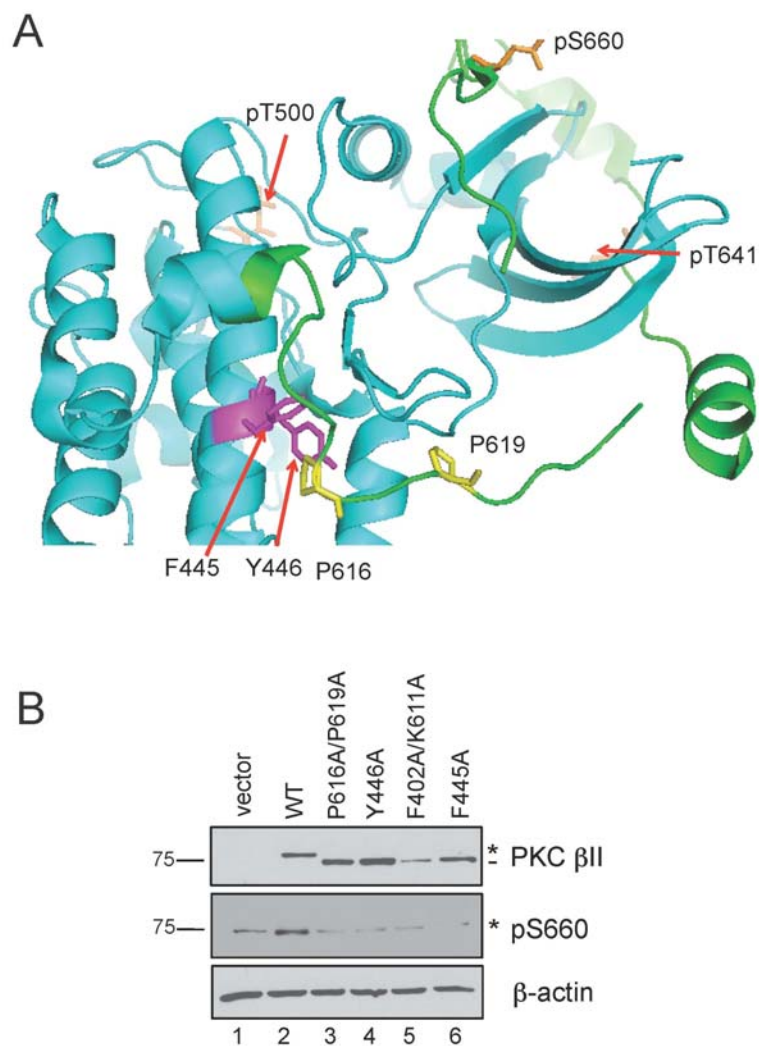


**Figure A2.5:** Mutation of a conserved Phe in the  $\alpha$ E-helix of the catalytic domain of PKC  $\beta$ II also disrupts the 'intramolecular clamp' with the PXXP motif in the C-terminal tail to abrogate processing of PKC. *A*, ribbon diagram cartoon representation of the catalytic domain (*cyan*) of PKC  $\beta$ II (Protein Data Bank Number: 2I0E). Residues are shown in sticks representation. The activation loop phosphorylation (T500) and the C-terminal processing phosphorylations (T641 and S660) are indicated in *orange*. The C-terminal tail is shown in *green*, and the Pro of the PXXP motif (P616, P619) are indicated in *yellow*. The two residues (F445, Y446) in the  $\alpha$ E-helix are shown in *magenta*. *B*, COS7 cells were transiently transfected with either vector (*lane 1*), WT PKC  $\beta$ II (*lane 2*), PKC  $\beta$ II-P616A/P619A (*lane 3*), PKC  $\beta$ II-Y446A (*lane 4*), PKC  $\beta$ II-F402A/K611A (*lane 5*), or PKC  $\beta$ II-F445A (*lane 6*). Whole cell lysates were analyzed for total PKC (PKC  $\beta$ II), phospho-PKC (pS660), and total protein content ( $\beta$ -actin) by Western blotting. The *asterisk* denotes the position of fully phosphorylated PKC, and the *dash* denotes the position of unphosphorylated PKC.

**References**

1. Oster, H., and Leitges, M. (2006) *Cancer Res* 66, 6955-6963
2. Kannan, N., Haste, N., Taylor, S. S., and Neuwald, A. F. (2007) *Proc Natl Acad Sci U S A* 104, 1272-1277
3. Kannan, N., Neuwald, A. F., and Taylor, S. S. (2008) *Biochim Biophys Acta* 1784, 27-32
4. Citri, A., Harari, D., Shohat, G., Ramakrishnan, P., Gan, J., Lavi, S., Eisenstein, M., Kimchi, A., Wallach, D., Pietrokovski, S., and Yarden, Y. (2006) *J Biol Chem* 281, 14361-14369
5. Marcu, M. G., Schulte, T. W., and Neckers, L. (2000) *J Natl Cancer Inst* 92, 242-248

## Chapter 3

# Elucidating the Mechanism of the Phorbol Ester-Mediated Down-Regulation of PKC $\beta$ II

**Abstract**

One of the key regulatory mechanisms that control the life cycle of PKC is phosphorylation. Phosphorylation at the priming C-terminal sites facilitates activation whereas dephosphorylation at these sites promotes degradation. Chronic activation of PKC that occurs with phorbol esters, potent, tumor-promoting analogues of diacylglycerol, leads to the dephosphorylation and subsequent degradation of PKC, a process termed 'down-regulation.' Previous studies have characterized that dephosphorylation of the activated, mature enzyme is one of the molecular mechanisms involved in this process, and several phosphatases that act on PKC have been identified. However, HOW this dephosphorylation is regulated remains unclear. This chapter focuses on the mechanisms underlying the phorbol ester-mediated down-regulation of PKC. Specifically, this research utilizes pharmacological inhibitors and phospho-mimetic PKC mutants to dissect the contribution of PKC activity and dephosphorylation to the down-regulation process. Here, we show that inhibition of PKC prevents down-regulation by causing selective accumulation of the fully phosphorylated species following PMA stimulation. A phospho-mimetic mutant that cannot be dephosphorylated, PKC  $\beta$ II-T641E/S660E, is relatively resistant to the phorbol ester-mediated down-regulation compared to WT PKC  $\beta$ II or the single phospho-mimetic mutants, PKC  $\beta$ II-T641E and PKC  $\beta$ II-S660E; however, this mutant is robustly ubiquitinated after PMA stimulation. These single phospho-mimetic mutants are dephosphorylated and down-regulated more rapidly than WT PKC  $\beta$ II; this effect can be blocked with a PKC inhibitor. Additionally, we show that the phorbol ester-mediated down-regulation is okadaic acid-insensitive, consistent with the role of the phosphatase

PHLPP in facilitating this process. These data demonstrate that dephosphorylation is the driving mechanism of the phorbol ester-mediated down-regulation, a step dependent upon the activity of PKC; however, additional pathways can regulate the fully phosphorylated form of the enzyme.

## Introduction

The catalytic competence and stability of PKC is dictated by the phosphorylation state of the enzyme. Extensive studies have characterized how phosphorylation at three conserved sites (the activation loop, turn motif, and hydrophobic motif) facilitates the maturation, activation, and stability of PKC (1). This fully phosphorylated species of PKC is the catalytically-competent form of the enzyme, capable of transducing signals mediated by its activating second messengers,  $\text{Ca}^{2+}$  and lipid (phosphatidylserine and diacylglycerol). The concerted effort of both phosphorylation and binding to second messengers leads to the allosteric activation of PKC, resulting in substrate phosphorylation. Termination of PKC signaling occurs through either removal of the second messengers or by dephosphorylation at the priming sites (2).

PKC was initially characterized as the 'receptor' for the potent, tumor-promoting, phorbol esters (3). These compounds are functional analogues of diacylglycerol that bind with high affinity to the C1 domain and cause PKC to redistribute to the membrane fraction of cells (4,5). Phorbol esters retain activated PKC at the membrane, where PKC exhibits an enhanced sensitivity to the action of cellular phosphatases (6). This enhanced membrane localization results in chronic activation of PKC, ultimately leading to a loss of activity through dephosphorylation at the priming sites and disappearance of PKC protein, a process known as 'down-regulation.' Studies have shown that PKC requires its intrinsic catalytic activity in order to be down-regulated; mutation of the ATP binding site renders PKC insensitive to phorbol ester-mediated degradation (7). This finding uncoupled the effects of phorbol esters on membrane translocation and down-regulation, suggesting that PKC's ability to autophosphorylate may initiate its own desensitization.

Additionally, the phorbol ester-mediated down-regulation of PKC is thought to be an 'active' process, where PKC activity drives its recycling to endosomal/perinuclear compartments (8-11).

Although the molecular events leading to the maturation and activation of PKC have been well-defined, the mechanisms governing the phorbol ester-mediated down-regulation of PKC, such as the link between PKC activity and dephosphorylation, are unclear. The classic model of PKC down-regulation involves dephosphorylation at the C-terminal priming sites and accumulation in the cytoskeletal, detergent-insoluble fraction of cells, where it is eventually degraded by the proteasome; PKC inhibitors can block this process (2). Indeed, both PP2A-type phosphatases and the recently discovered PP2C-type phosphatase, PHLPP, have been shown to dephosphorylate PKC and promote this process; however, whether PKC activity can regulate these phosphatases remains unknown (6,12). In support of the hypothesis that it is the dephosphorylated form of PKC that is degraded, heat shock proteins such as Hsp70 can rescue and stabilize this species of PKC to protect it from down-regulation (13,14). However, recent studies have suggested that it is the fully phosphorylated species of PKC that is ubiquitinated and down-regulated (15). Thus, we wondered if two different pathways could exist for phorbol ester-induced PKC down-regulation?

Ubiquitin is a small 8.5 kDa polypeptide that is conjugated to proteins in order to serve as molecular 'tag' for degradation by the large, multi-subunit, ATPase complex, the proteasome (16). Ubiquitin is activated and conjugated to targeted proteins by the consecutive action of three classes of enzymes: 1) E1, ubiquitin-activating enzyme, 2) E2, ubiquitin-conjugating enzyme, and 3) E3, ubiquitin ligase. Typically, ubiquitin is

conjugated to proteins in long chains, where the nature of the lysine linkage between ubiquitin molecules (K48, K63) dictate the fate of the protein (17). Polyubiquitinated K48-linkages target proteins for degradation by the proteasome whereas polyubiquitinated K63-linkages are involved in other cellular functions. PKC is polyubiquitinated after phorbol ester stimulation and recent studies have characterized that linkage is K48, a proteasomal-targeting signal (15,18,19).

Here, we show that the down-regulation of PKC requires dephosphorylation of the priming sites, and event that, in turn depends on the intrinsic catalytic activity of PKC. First, pharmacological inhibition of PKC prevents the dephosphorylation of PKC following phorbol ester stimulation, resulting in accumulation of fully-phosphorylated PKC. Second, a phospho-mimetic mutant at the two C-terminal priming sites, T641E/S660E, is relatively resistant to phorbol ester-mediated down-regulation; however this mutant is robustly ubiquitinated after PMA stimulation. Consistent with the finding that the catalytic activity of PKC is required to initiate dephosphorylation at the priming sites, we show that inhibition of PKC protects both C-terminal sites from dephosphorylation: each of the single-site phospho-mimetics (S660E or T641E) is relatively protected from phorbol ester-mediated dephosphorylation. In summary, these data reveal that the phorbol ester-mediated degradation of PKC occurs by a two-step process: 1. Dephosphorylation of the C-terminal priming sites by a mechanism that depends on the intrinsic catalytic activity of PKC and 2. Degradation of the dephosphorylated enzyme by a mechanism that depends on the proteasome.

## Materials and Methods

*Materials* – Oligonucleotides were purchased from Integrated DNA Technologies. Easy Tag [<sup>35</sup>S]Met/Cys (1175 Ci mmol<sup>-1</sup>) was purchased from PerkinElmer Life Sciences. Met/Cys-deficient DMEM was purchased from Invitrogen. Phorbol 12-myristate 13-acetate (PMA), Calyculin A, carbobenzoxy-L-leucyl-L-leucyl-leucinal (MG-132), okadaic acid, and Gö6983 were purchased from Calbiochem. Polyclonal antibodies to PKC  $\beta$ II and PKC  $\alpha$  were purchased from Santa Cruz Biotechnology. Monoclonal antibodies to PKC  $\alpha$ , PKC  $\beta$ , and Hsp90 were purchased from B.D. Transduction Laboratories. A polyclonal antibody to the hydrophobic motif phosphorylation site (PKC  $\beta$ II Ser-660) was purchased from Cell Signaling Technology. A monoclonal antibody to  $\beta$ -actin and N-ethyl maleimide (NEM) were purchased from Sigma Aldrich. A monoclonal antibody to ubiquitin was purchased from Covance. Ultra-Link protein A/G beads were purchased from Thermo Scientific. Electrophoresis reagents were obtained from Biorad. All other chemicals and materials were reagent-grade.

*Plasmids* - The PKC  $\beta$  mutants, PKC  $\beta$ II-K371R, PKC  $\beta$ II-T641E, PKC  $\beta$ II-S660E, and PKC  $\beta$ II-T641E/S660E, were generated using the QuikChange site-directed mutagenesis kit (Stratagene). An NH<sub>2</sub>-terminal HA tagged PKC  $\alpha$  was generated by PCR amplification and subsequent cloning into EcoRI (5') and XbaI (3') sites in pCDNA3.

The corresponding HA-PKC  $\alpha$  mutants, HA-PKC  $\alpha$ -T638E, HA-PKC  $\alpha$ -S657E, and HA-PKC  $\alpha$ -T638E/S657E, were generated using QuikChange site-directed mutagenesis.

*Cell culture and transfection* - tsA201 and COS7 cells were maintained in DMEM (Cellgro) containing 10% fetal bovine serum (Hyclone) and 1% penicillin/streptomycin at 37°C in 5% CO<sub>2</sub>. Transient transfection of tsA201 cells was carried out using Effectene

transfection reagent (Qiagen), and transient transfections of COS7 cells were carried out using FuGENE transfection reagent (Roche Applied Science).

*PMA time courses* – For endogenous PKC experiments, COS7 cells were treated with 200 nM PMA for the indicated times in the absence or presence of either 50 nM Calyculin A or 1  $\mu$ M Gö6983. Cells were lysed in Buffer A (50 mM Tris, 50 mM NaF, 10 mM  $\text{Na}_4\text{P}_2\text{O}_7$ , 100 mM NaCl, 5 mM EDTA, 1% Triton X-100, 1 mM  $\text{Na}_3\text{VO}_4$ , and 1 mM PMSF). Whole cell lysates were analyzed by SDS-PAGE and Western blotting. For the PKC mutant experiments, COS7 cells were transiently transfected with WT PKC  $\beta$ II, PKC  $\beta$ II-K371R, PKC  $\beta$ II-T641E, PKC  $\beta$ II-S660E, PKC  $\beta$ II-T641E/S660E, HA-PKC  $\alpha$ , HA-PKC  $\alpha$ -T638E, HA-PKC  $\alpha$ -S657E, or HA-PKC  $\alpha$ -T638E/S657E and treated with 200 nM PMA for the indicated times. For inhibitor experiments, cells were pretreated with 10  $\mu$ M MG-132, 1  $\mu$ M Gö6983, or 50 nM okadaic acid prior to PMA stimulation. Cells were lysed in Buffer A, and whole cell lysates were analyzed by SDS-PAGE and Western blotting. Chemiluminescent images were obtained using the FluorChem Q (Alpha Innotech), and densitometric analysis was performed using the AlphaView Q software.

*Pulse-chase analysis* – COS7 cells were transfected with WT PKC  $\beta$ II. At 24–30 h after transfection, cells were incubated with Met/Cys-deficient DMEM for 30 min at 37 °C. The cells were then pulse-labeled with 0.5 mCi  $\text{ml}^{-1}$  [ $^{35}\text{S}$ ]Met/Cys in Met/Cys-deficient DMEM for 7 min at 37 °C, media were removed, and cells were chased with DMEM containing 5 mM unlabeled methionine and 5 mM unlabeled cysteine (20). At the indicated times, cells were lysed in Buffer A and centrifuged at 16,000 x g for 5 min at 22°C, and PKC  $\beta$ II in the supernatant was immunoprecipitated with an anti-PKC  $\alpha$

monoclonal antibody (cross-reactive with PKC  $\beta$ II) overnight at 4 °C. The immune complexes were collected with Ultra-Link protein A/G beads, washed with Buffer A, separated by SDS-PAGE, transferred to polyvinylidene difluoride (PVDF) membrane, and analyzed by autoradiography.

*Ubiquitination assay* – tsA201 cells were transiently transfected with either WT PKC  $\beta$ II or PKC  $\beta$ II-T641E/S660E and treated with 200 nM PMA and 10  $\mu$ M MG-132 for the indicated times. Cells were lysed in Buffer A supplemented with 10 mM NEM and 10  $\mu$ M MG-132 and centrifuged at 16,000 x *g* for 5 min at 22°C. PKC was immunoprecipitated from detergent-solubilized lysates with a monoclonal anti-PKC  $\alpha$  antibody overnight at 4°C. The immune complexes were collected with Ultra-Link protein A/G beads, washed with Buffer A plus 10 mM NEM, separated by SDS-PAGE, and analyzed by Western blotting.

## Results

*The phorbol ester-mediated down-regulation of PKC requires PKC's intrinsic catalytic activity* – In order for PKC to be down-regulated by phorbol esters, it has been previously reported that PKC must be catalytically active (7). We wanted to confirm the requirement of PKC activity for this process through two approaches: pharmacological inhibition of PKC and mutation of PKC to render it catalytically-inactive (PKC  $\beta$ II-K371R). First, COS7 cells were treated with PMA for increasing time in the absence or presence of the PKC inhibitor Gö6983; total PKC was assessed by Western blot (Figure 3.1 A). In the absence of inhibitor (*lanes 1-6*), endogenous PKC  $\alpha$  (a phorbol ester-responsive PKC) levels decreased dramatically by 4 h (*lane 6, PKC  $\alpha$  panel*). PKC  $\alpha$  was also rapidly dephosphorylated as detected by a phospho-specific antibody to the hydrophobic motif (*data not shown*). However, in the presence of the PKC inhibitor Gö6983, the decrease in total PKC levels was blocked, and dephosphorylation was slowed (*lanes 7-12, PKC  $\alpha$  panel and data not shown*). Since dephosphorylation of the priming sites is a primary mechanism for the down-regulation of PKC (8,21), we tested if the phosphatase inhibitor, Calyculin A, would inhibit down-regulation. To our surprise, PMA stimulation in the presence of Calyculin A (*lanes 13-18*) trapped a faster mobility species of PKC  $\alpha$ , which represents PKC that has been dephosphorylated (*lane 17, dash*). However, the rate of disappearance of the slower mobility, fully phosphorylated form with PMA stimulation was similar for both untreated and Calyculin A-treated cells (*compare lanes 4-6 with 16-18, asterisk*). Thus, inhibition of PKC prevents dephosphorylation and degradation, and inhibition of phosphatases by Calyculin A accelerates dephosphorylation and degradation. These data suggest that a PKC-

dependent phosphorylation event triggers dephosphorylation at the priming sites.

As another way to assess the requirement for PKC activity in the phorbol ester-mediated down-regulation, we utilized a 'kinase-dead' PKC, PKC  $\beta$ II-K371R, which has a mutation at a conserved Lys in the catalytic domain that prevents binding to ATP ((22). COS7 cells were transfected with WT PKC  $\beta$ II or PKC  $\beta$ II-K371R and treated with PMA for up to 24 h (Figure 3.1 B). WT PKC  $\beta$ II initially migrates as a slower mobility, fully phosphorylated form that is characteristic of the mature, active kinase (*lane 1, asterisk*). With increasing time of PMA treatment, a faster mobility species accumulates for WT PKC  $\beta$ II (*lanes 2-6, dash*); this species represents PKC that has become dephosphorylated (23). By 24 h, WT PKC  $\beta$ II levels have depleted ~80%, and no phosphorylated PKC is present (*lane 6*). In contrast, PKC  $\beta$ II-K371R migrates primarily as the faster mobility, unphosphorylated species (*lanes 7-12, dash*); this mutant is unable to be processed by phosphorylation (24). With PMA stimulation, the levels of the kinase-dead PKC are unaffected. These data with the pharmacological inhibitor and kinase-dead mutant reveal that PKC activity is required for the phorbol ester-mediated down-regulation, consistent with previous studies.

*Pharmacological inhibitors uncouple the degradation of the phosphorylated and unphosphorylated forms of PKC* – Since the phorbol ester-mediated down-regulation of PKC requires PKC activity and occurs through a proteasome-dependent mechanism, we explored the effects of PKC and proteasome inhibitors on this process. COS7 cells were transfected with WT PKC  $\beta$ II and treated with PMA for 0 h (*lanes 1-4*), 3 h (*lanes 5-8*) and 6 h (*lanes 9-12*) in the absence or presence of the PKC inhibitor Gö6983 and the proteasome inhibitor MG-132 (Figure 3.2 A). In the absence of PMA, WT PKC  $\beta$ II

primarily migrates as the slower mobility, fully phosphorylated species (*lane 1, asterisk*), which is unaffected by Gö6983 (*lane 2*). Interestingly, MG-132 treatment alone or with Gö6983 (in the absence of PMA) results in the accumulation of the faster mobility, unphosphorylated species of PKC (*lane 3-4, dash*); this result is consistent with previous results showing that the unphosphorylated form of PKC is inherently unstable and rapidly degraded in the cell (25). Upon PMA stimulation in the absence of inhibitors (*lanes 5 and 9*), the faster mobility form of PKC is detected at 3 h (*lane 5, dash*), and there was a loss in the slower mobility form (*asterisk*); this mobility shift is indicative of dephosphorylation that occurs with phorbol ester treatment and is confirmed by probing with phospho-specific antibodies (*data not shown*). At 6 h PMA treatment, PKC levels have diminished ~70% as PKC was dephosphorylated and subsequently degraded (*lane 9*). Inhibition of the proteasome with MG-132 in the presence of PMA selectively accumulated the faster mobility, unphosphorylated form of PKC (*lanes 7-8 and 11-12, dash*). Conversely, inhibition of PKC with Gö6983 selectively accumulated the slower mobility, fully phosphorylated form of PKC (*lanes 6, 8, 10, and 12, asterisk*) after PMA stimulation, which we also observed using phospho-specific antibodies (*data not shown*). These data indicate that the faster mobility form of PKC is primarily degraded through the proteasome and that PKC activity is required for either the dephosphorylation or degradation of the slower mobility form.

In order to determine whether the nonphosphorylated species of PKC that accumulated in the presence of PMA and MG-132 was produced by dephosphorylation of the activated, mature PKC enzyme and not through the accumulation of newly-synthesized PKC, we performed a pulse-chase analysis to monitor a radiolabeled pool of

PKC in the presence of PMA and the inhibitors (Figure 3.2 B). COS7 cells were transfected with WT PKC  $\beta$ II, pulse-labeled with [ $^{35}$ S]Met/Cys, and chased for 90 min with unlabeled media (*lanes 2-7*). After a 90 min chase, cells were treated with MG-132 alone (*lane 3*), Gö6983 alone (*lane 4*), PMA alone (*lane 5*), and PMA with the inhibitors (*lanes 6-7*) for 4 h. PKC was immunoprecipitated from detergent-solubilized lysates and analyzed by autoradiography. The autoradiogram in Figure 3.2 B shows that the newly-synthesized PKC appears as the faster mobility species (*lane 1, dash*) that shifts to a slower mobility species after the 90 min chase (*lane 2, asterisk*). This mobility shift is indicative of the two tightly-coupled, C-terminal processing phosphorylations, the turn motif (Thr-641) and the hydrophobic motif (Ser-660). Treatment with either MG-132 or Gö6983 alone (*lanes 3-4*) did not alter the mobility of PKC; it primarily migrated as the slower mobility species (*asterisk*). However, after treatment with PMA for 4 h, PKC migrated as a doublet of equal intensity, indicative of dephosphorylation of the mature enzyme (*compare lanes 2 and 5*). In the presence of MG-132 and PMA, the faster mobility form selectively accumulated (*lane 6, dash*) while the slower mobility form selectively accumulated in the presence of Gö6983 and PMA (*lane 7, asterisk*). These data demonstrate that inhibition of the proteasome after PKC activation prevents degradation of the dephosphorylated PKC, and inhibition of PKC after PKC activation prevents either dephosphorylation or degradation of the mature enzyme.

*Dephosphorylation facilitates the short-term phorbol ester-mediated down-regulation of PKC* - Phorbol esters promote the dephosphorylation of activated PKC, which can lead to its degradation by the proteasome. Indeed, our data show that treatment with proteasome inhibitors results in selective accumulation of

dephosphorylated PKC in phorbol ester-treated cells (Figure 3.2). However, it still remains unclear if dephosphorylation followed by proteasomal degradation is the primary molecular mechanism for this phorbol ester-mediated down-regulation. To determine whether dephosphorylation is a prerequisite for this down-regulation process, we utilized a phospho-mimetic mutant, PKC  $\beta$ II-T641E/S660E, which cannot be dephosphorylated at its C-terminus. COS7 cells were transfected with WT PKC  $\beta$ II (*lanes 1-6*), PKC  $\beta$ II-T641E (*lanes 7-12*), PKC  $\beta$ II-S660E (*lanes 13-18*), or PKC  $\beta$ II-T641E/S660E (*lanes 19-24*) and treated with PMA for increasing time up to 6 h; protein levels in whole cell lysates were analyzed by Western blot (Figure 3.3 A). For WT PKC  $\beta$ II, PMA treatment increased the amount of the faster mobility, dephosphorylated species (as indicated by phospho-specific antibodies, *data not shown*) prior to degradation of protein levels (*lanes 4-6, dash*). Quantitative analysis revealed that PMA down-regulated WT PKC  $\beta$ II with a half-time of  $1.75 \pm 0.04$  h (Figure 3.3 B, *circles*). Strikingly, the phospho-mimetic turn motif mutant, PKC  $\beta$ II-T641E, was down-regulated rapidly with PKC migrating primarily as the faster mobility, unphosphorylated species at 0.25 h (*lane 14, dash*). However, total protein levels for this mutant plateaued at 3 h (*lane 17*); the half-time for down-regulation was  $\sim 3$ -fold faster than WT PKC  $\beta$ II at  $0.7 \pm 0.1$  h (Figure 3.3 B, *squares*). Similarly, the phospho-mimetic hydrophobic motif mutant, PKC  $\beta$ II-S660E, also down-regulated rapidly with PKC migrating as the faster mobility, unphosphorylated species by 0.5 h (*lane 21, dash*), and total protein levels plateaued also by 3 h (*lane 23*). For this mutant, the half-time for down-regulation was similar to WT at  $2.2 \pm 0.8$  h (Figure 3.3 B, *diamonds*). Importantly, when the double phospho-mimetic mutant, PKC  $\beta$ II-T641E/S660E, which cannot be dephosphorylated at the priming C-terminal sites and

migrates solely as the slower mobility species (*lanes 7-12, asterisk*), was treated with PMA, an ~40% decrease in total protein level occurred but plateaued at 1 h (Figure 3.3 B, *triangles*).

We observed differences in the rate of dephosphorylation between WT PKC  $\beta$ II and the two phospho-mimetic mutants, PKC  $\beta$ II-T641E and PKC  $\beta$ II-S660E, after PMA stimulation. The large (~ 4 kD) mobility shift that occurs upon PMA treatment of PKC  $\beta$ II-T641E represents dephosphorylation at the hydrophobic motif (Ser-660), while the smaller (~ 2 kD) mobility shift that occurs upon PMA treatment of PKC  $\beta$ II-S660E represents dephosphorylation at the turn motif (Thr-641) (23). Figure 3.3 C depicts the rate of dephosphorylation for the two C-terminal mutants and WT PKC  $\beta$ II after PMA treatment. Dephosphorylation was monitored as an increase in the faster mobility species of PKC (*dash*) and confirmed with phospho-specific antibodies (*data not shown*). The half-times of dephosphorylation for each construct were measured as a percentage of the slower mobility species (*asterisk*) compared to the total amount of PKC (Figure 3.3 A). As shown in Figure 3.3 A, PKC  $\beta$ II-T641E is rapidly dephosphorylated after PMA treatment; the half-time is  $0.3 \pm 0.1$  h (Figure 3.3 A, *lane 14* and Figure 3.3 C, *squares*). PKC  $\beta$ II-S660E is dephosphorylated ~2-fold slower than PKC  $\beta$ II-T641E with half-time of  $1.5 \pm 0.3$  h (*diamonds*). WT PKC  $\beta$ II is dephosphorylated at the slowest rate with a half-time of  $4.0 \pm 0.8$  h, ~13-fold slower than PKC  $\beta$ II-T641E and ~3-fold slower than PKC  $\beta$ II-S660E. These data suggest that dephosphorylation at the priming sites is a prerequisite for phorbol ester-mediated down-regulation of PKC.

PKC  $\alpha$ , another conventional PKC family member like PKC  $\beta$ II, is also a phorbol

ester-responsive PKC that is down-regulated. We were curious if mutation of the C-terminal sites to phospho-mimetics followed a similar trend as its counterpart, PKC  $\beta$ II. COS7 cells were transfected with WT HA-PKC  $\alpha$  (*lanes 1-6*), HA-PKC  $\alpha$ -T638E/S657E (*lanes 7-12*), HA-PKC  $\alpha$ -T638E (turn motif mutant, *lanes 13-18*) or HA-PKC  $\alpha$ -S657E (hydrophobic motif mutant, *lanes 19-24*) and treated with PMA for increasing time; total protein levels from whole cell lysates were analyzed by Western blot (Figure 3.3 D). Similarly to PKC  $\beta$ II, the turn motif and hydrophobic motif phospho-mimetic mutants were rapidly dephosphorylated and degraded compared to WT HA-PKC  $\alpha$  while the double phospho-mimetic that cannot be dephosphorylated, HA-PKC  $\alpha$ -T638E/S657E, remained resistant. These data are consistent with the role of dephosphorylation for conventional PKC isozymes at the priming sites to facilitate PKC down-regulation.

*Dephosphorylation at the C-terminal priming phosphorylation sites is critical for the long-term phorbol ester-mediated down-regulation of PKC* – The phospho-mimetic mutant, PKC  $\beta$ II-T641E/S660E, which cannot be dephosphorylated, exhibited only a modest decrease in total PKC levels for PMA treatment up to 6 h (Figure 3.3 B, *triangles*). However, we were interested in knowing if this mutant would eventually be degraded upon long-term PMA treatment (up to 24 h). COS7 cells were transfected with WT PKC  $\beta$ II (*lane 1-4*), PKC  $\beta$ II-T641E (*lanes 5-8*), PKC  $\beta$ II-S660E (*lanes 9-12*), or PKC  $\beta$ II-T641E/S660E (*lanes 13-16*) for up to 24 h with PMA (Figure 3.4 A). Total PKC protein levels in whole cell lysates were analyzed by Western blot. For WT PKC  $\beta$ II and the single phospho-mimetic mutants, PKC levels were significantly depleted by 12 h (~60%,  $p < 0.5$ ) and 24 h (~ 80%,  $p < 0.01$ ) after PMA treatment (Figure 3.4 B).

However, PKC  $\beta$ II-T641E/S660E only showed a modest decrease, ~40%, in protein level by 24 h PMA similar to the 6 h time point (Figure 3.3 A). These data indicate that dephosphorylation at both Thr-641 and Ser-660 is essential for the PMA-induced down-regulation of PKC  $\beta$ II.

*The phorbol ester-mediated down-regulation of PKC is okadaic acid-insensitive –*

The first step in the phorbol ester-induced down-regulation of PKC is dephosphorylation at the hydrophobic motif by the PHLPP phosphatase, a PP2C-type phosphatase that is insensitive to common pharmacological phosphatase inhibitors such as okadaic acid (12). As shown previously, PKC  $\beta$ II-T641E is rapidly dephosphorylated and down-regulated upon PMA stimulation; this dephosphorylation step occurs at the hydrophobic motif and is regulated by PHLPP. To confirm that this dephosphorylation step is indeed okadaic acid-insensitive, we transfected COS7 cells with WT PKC  $\beta$ II (A), PKC  $\beta$ II-T641E (B) or PKC  $\beta$ II-S660E (C) and treated with PMA in the absence (*lanes 1-6*) or presence (*lanes 7-12*) of okadaic acid (Figure 3.5). WT PKC  $\beta$ II is dephosphorylated after PMA treatment with a half-time at ~4 h (*lane 4*), which remains unaffected in the presence of okadaic acid (*lane 8*). Similarly, PKC  $\beta$ II-T641E and PKC  $\beta$ II-S660E are dephosphorylated and rapidly down-regulated after PMA treatment with half-times of ~0.25 h and ~1 h, respectively (Figure 3.5 B *lane 2* and C *lane 3*), which also remains unaffected in the presence of okadaic acid (Figure 3.5 B *lane 10* and Figure 3.5 C *lane 11*). These data demonstrate that the PMA-induced dephosphorylation and degradation of PKC levels are insensitive to okadaic acid, consistent with the role of the PHLPP phosphatase regulating this process.

*PKC activity is required for the phorbol ester-induced dephosphorylation -*

Inhibition of PKC activity selectively protected the slower mobility, phosphorylated form of PKC (Figure 3.2). By locking a negative charge at the C-terminal phosphorylation sites, PKC  $\beta$ II was unable to be down-regulated by phorbol esters, suggesting that dephosphorylation at those sites was a prerequisite for this process (Figure 3.4). Therefore, we wanted to determine if PKC activity was required for the PMA-induced dephosphorylation. COS7 cells were transfected with WT PKC  $\beta$ II (A), PKC  $\beta$ II-T641E (C), or PKC  $\beta$ II-S660E (E) and treated with PMA in the absence (*lanes 1-6*) or presence (*lanes 7-12*) of the PKC inhibitor Gö6983 (Figure 3.6). Dephosphorylation was monitored as an increase in the faster mobility species of PKC (*dash*) and confirmed with phospho-specific antibodies (*data not shown*). The half-times of dephosphorylation for each construct in the absence or presence of Gö6983 were measured as a percentage of the slower mobility species (*asterisk*) compared to the total amount of PKC (Figure 3.6 B, D, and F). In the absence of inhibitor, the half-time for dephosphorylation of WT PKC  $\beta$ II after PMA treatment was  $6 \pm 1$  h (Figure 3.6 B, *white circles*). In the presence of Gö6983, the half-time was dramatically slowed (*black circles*). As shown earlier, PKC  $\beta$ II-T641E was rapidly dephosphorylated upon PMA treatment with a half-time of  $0.3 \pm 0.1$  h, which was slowed  $\sim 6$ -fold in presence of the inhibitor with a half-time of  $1.8 \pm 0.5$  h. (Figure 3.6 D, *white versus black squares*). Similarly, PKC  $\beta$ II-S660E was dephosphorylated with a half-time of  $2.4 \pm 0.9$  h in the absence of inhibitor (Figure 3.6 F, *white diamonds*), which was slowed  $\sim 3$ -fold in the presence of the inhibitor ( $6 \pm 3$  h, *black diamonds*). Thus, PKC activity is necessary for its dephosphorylation upon activation by phorbol esters.

*PKC activity is not required for degradation of the fully phosphorylated form*

*after phorbol ester stimulation* - We observed that the phospho-mimetic, PKC  $\beta$ II-T641E/S660E, which cannot be dephosphorylated at the priming phosphorylation sites, was slightly down-regulated (~40% decrease in protein levels) after PMA stimulation (Figure 3.3). Therefore, we explored whether PKC activity may be involved in this process. COS7 cells were transfected with PKC  $\beta$ II-T641E/S660E and treated with PMA for in the indicated times in the absence and presence of Gö6983 (Figure 3.7 A). As shown earlier, this PKC mutant migrates as the slower mobility, fully phosphorylated species (*asterisk*). Quantification of these data revealed that neither PMA nor Gö6983 treatment had a significant effect on protein levels for this mutant (Figure 3.7 B). These data indicate that dephosphorylation is necessary for phorbol ester-induced down-regulation and that PKC activity regulates that process.

*Dephosphorylation is not required for ubiquitination after phorbol ester stimulation* –Previous studies have shown that the fully phosphorylated species of PKC can be ubiquitinated and degraded after activation by phorbol esters (15,19,26,27). Therefore, we asked if PKC  $\beta$ II-T641E/S660E, which mimics the fully phosphorylated form, could be ubiquitinated after phorbol ester stimulation. tsA201 cells were transfected with WT PKC  $\beta$ II (*lanes 1-3*) or PKC  $\beta$ II-T641E/S660E (*lanes 4-6*) and treated with PMA for 15 and 30 min (Figure 3.8 A). PKC was immunoprecipitated from detergent-solubilized lysates and assayed for ubiquitination by Western blot. Figure 3.8 A shows that both constructs were ubiquitinated after PMA treatment (*lanes 2-3* and *lanes 5-6*). Quantitative analysis revealed that PKC  $\beta$ II-T641E/S660E was ~ 7-fold and ~ 3-fold more ubiquitinated than WT PKC  $\beta$ II at 15 and 30 min, respectively (Figure 3.8 B). Therefore, the fully “phosphorylated” species of PKC can be ubiquitinated and

targeted for degradation without dephosphorylation.

## Discussion

Signaling molecules, such as protein kinases, are under strict, regulatory mechanisms that dictate the level of activation. For PKC, the phosphorylation state of the enzyme determines its catalytic competence; dephosphorylated PKC is inactive and subject to degradation mechanisms. When PKC is chronically activated by phorbol esters, these desensitization pathways are initiated. These foregoing studies demonstrate that PKC activity-dependent dephosphorylation is required for the phorbol ester-mediated down-regulation of PKC. Through pharmacological inhibitors, we show that 1) PKC activity is necessary for dephosphorylation of the fully matured enzyme and 2) proteasomal activity is necessary for degrading dephosphorylated PKC. Single phospho-mimetics at the turn and hydrophobic motif, PKC  $\beta$ II-T641E and PKC  $\beta$ II-S660E, respectively, are rapidly dephosphorylated and degraded in response to phorbol esters compared to the wildtype enzyme, events that are slowed by pharmacological inhibition of PKC. A phospho-mimetic mutant that cannot be dephosphorylated, PKC  $\beta$ II-T641E/S660E, is unable to be down-regulated by phorbol esters but is ubiquitinated, thus uncoupling dephosphorylation and ubiquitination.

*Pharmacological inhibitors can dissect the different mechanisms involved in the phorbol ester-mediated down-regulation of PKC* – Our findings show that we can selectively accumulate different species (unphosphorylated *versus* phosphorylated) through the use of pharmacological inhibitors. First, inhibition of PKC trapped the slower mobility, fully phosphorylated species of PKC; this effect was PMA-dependent (Figure 3.2). This result suggests that PKC activity is either required for the PMA-induced dephosphorylation of PKC or that PKC activity is required for degradation of the

fully phosphorylated species of PKC after PMA stimulation. Inhibition of PKC did not fully block PKC dephosphorylation, indicating a PKC-independent component to the PMA-induced dephosphorylation.

Secondly, inhibition of the proteasome trapped the faster mobility, unphosphorylated species of PKC; this effect was PMA-independent as dephosphorylated PKC accumulated in the absence of PMA stimulation when the proteasome was inhibited (Figure 3.2 A). In the absence of PMA, inhibition of the proteasome is most likely accumulating newly-synthesized PKC that has yet to undergo processing by phosphorylation. However, in the presence of PMA, inhibition of the proteasome is most likely accumulating dephosphorylated as well as newly-synthesized forms of PKC. We used a pulse-chase analysis to distinguish between these two different species of PKC by radiolabeling and monitoring a specific pool of PKC in the cell and found that proteasome inhibition blocks degradation of the dephosphorylated form. Use of protein translation inhibitors such as cycloheximide would also differentiate between these two unphosphorylated species of PKC. The unphosphorylated form of PKC is unstable and is rapidly degraded in the cell; PKC mutants that are defective in phosphorylation at the priming sites are sensitive to proteasome inhibitors as well as to the inhibition or disruption of the interaction with heat shock proteins, such as Hsp70 and Hsp90, which facilitate stabilization of these constructs (13,25).

This is the first study that has dissected the contributions of the different mechanisms involved in the phorbol ester-mediated down-regulation of PKC. The classical model of PKC down-regulation is dephosphorylation of the priming sites, which precedes degradation of the enzyme. Since the phosphorylation state of PKC  $\beta$ II can be

easily monitored by distinct, electrophoretic mobility shifts, we can determine why PKC activity is required for this down-regulation process and what form of PKC is being degraded by the proteasome.

*PKC activity is required for its dephosphorylation after phorbol ester stimulation*

– To determine if PKC activity was required for the PMA-induced dephosphorylation or for the degradation of the fully phosphorylated enzyme, we utilized a double phospho-mimetic mutant that cannot be dephosphorylated at the priming sites, PKC  $\beta$ II-T641E/S660E. This mutant migrates at the mobility of the mature, fully phosphorylated enzyme. The levels of this mutant were largely unaffected by phorbol esters, which was independent of PKC activity, suggesting that PKC activity facilitates its own dephosphorylation after activation. This hypothesis is not unprecedented; a constitutively active PKC can stimulate the dephosphorylation of other PKCs in the cell, suggesting that PKC activity may somehow regulate a phosphatase (8). Certainly PKC has been linked to phosphatases, such as PP2A and PHLPP, and is often scaffolded in the vicinity of phosphatases to facilitate temporal and spatial control of localized signaling events (28-30). PKC activity is necessary for the membrane trafficking events that occur after phorbol ester stimulation; it is plausible that the phosphatase(s) responsible for PMA-induced dephosphorylation resides in these endosomal/perinuclear compartments (11).

*Dephosphorylation is an ordered process that drives the phorbol ester-mediated down-regulation of PKC* – After long-term stimulation with phorbol esters, PKC  $\beta$ II-T641E/S660E does not significantly down-regulate as compared to wildtype PKC and the single phospho-mimetic mutants. Recent studies have suggested that the fully phosphorylated, mature enzyme can be ubiquitinated and degraded through a

proteasome-dependent mechanism (15). However, treatment with proteasome inhibitors does not recover the modest decrease seen in protein levels after PMA stimulation, indicating that particular species of PKC is resistant to phorbol ester-mediated down-regulation (*data not shown*). One explanation for this discrepancy can be explained by the fact that this study did not account for the rapid degradation of the dephosphorylated form of PKC after PMA treatment; their use of phospho-specific antibodies to the processing sites of PKC indicated dephosphorylation after PMA treatment even though they did not see the faster mobility species. It is plausible that variations in these mechanisms differ in a cell-type dependent context; however, our studies and previous work clearly indicate that dephosphorylation precedes degradation after phorbol ester stimulation (8).

The maturation of PKC occurs through a series of ordered phosphorylations that have been extensively characterized. Presumably, PKC would also be dephosphorylated in a similar order. The use of phosphatase inhibitors as well as mutants has demonstrated that loss at Ser-660 (the hydrophobic motif) does not abrogate PKC activity whereas loss at Thr-641 (the turn motif) does (31,32). The activation loop site, Thr-500, is dispensable for activity once PKC has matured into a fully phosphorylated enzyme (23).

Dephosphorylation at Ser-660 triggers the subsequent dephosphorylation of the other sites; studies with the PHLPP phosphatase, which dephosphorylates the hydrophobic motifs of Akt and PKC, have shown that it promotes the phorbol ester-mediated down-regulation of PKC.

Interestingly, the use of single phospho-mimetic mutants, PKC  $\beta$ II-T641E and PKC  $\beta$ II-S660E, has not been demonstrated in studies of phorbol ester-mediated down-

regulation. These mutants allow the monitoring of dephosphorylation at one of the C-terminal phosphorylation sites by locking negative charge at the other. Our data reveal that the single phospho-mimetic mutants dephosphorylate and down-regulate at different rates, indicating a role for dephosphorylation of these sites in the phorbol ester-mediated down-regulation of PKC. PKC  $\beta$ II-T641E, which is dephosphorylated at the hydrophobic motif, is dephosphorylated and down-regulated  $\sim$  18-fold and  $\sim$ 3-fold faster than WT PKC  $\beta$ II, respectively. This result is consistent with the PHLPP studies that demonstrated rapid degradation of PKC upon dephosphorylation of the hydrophobic motif (12). The heightened sensitivity of this mutant to phorbol esters suggests that Glu at the Thr-641 is not a good phospho-mimetic, since negative charge at that position is sufficient for catalytic activity (32-34). Indeed, structural studies have described the synergizing roles of these C-terminal phosphorylations to promote the stability and activation at the enzyme, with the major force being hydrophobic motif phosphorylation (35). In support of this hypothesis, other studies have indicated that a phospho-mimetic at the turn motif shows an increased sensitivity to phosphatases (33).

PKC  $\beta$ II-S660E, which is dephosphorylated at the turn motif, is dephosphorylated  $\sim$ 2-fold faster than WT  $\beta$ II, but protein levels are down-regulated slightly slower than WT PKC  $\beta$ II. Negative charge at the hydrophobic motif may hinder phosphatase access to the turn motif. Indeed, the phosphate of the hydrophobic motif interacts with conserved basic residues to promote stability of the enzyme; atypical PKCs utilize a Glu to perform the same function (35). At 6 h PMA, PKC  $\beta$ II-S660E levels plateaued at  $\sim$ 50% of the initial amount whereas WT PKC  $\beta$ II and PKC  $\beta$ II-T641E levels plateaued at  $\sim$ 20% of the initial amount. These data indicate the driving dephosphorylation step that

facilitates phorbol ester-mediated down-regulation occurs at the hydrophobic motif because locking negative charge at the hydrophobic motif interferes with the PKC's ability to fully down-regulate after phorbol ester stimulation.

*Dephosphorylation and ubiquitination events after phorbol ester stimulation can be uncoupled* – The phorbol ester-mediated down-regulation of PKC occurs through a proteasome-dependent mechanism; inhibitors of the proteasome block degradation of PKC. What remains unclear is if the proteasome down-regulates both the dephosphorylated and fully phosphorylated forms of PKC; studies have indicated that both mechanisms can occur. Our data show that proteasome inhibitors selectively accumulate both the newly-synthesized and dephosphorylated forms of PKC. Another question is the ordering of events – does ubiquitination promote dephosphorylation of PKC or is the dephosphorylated form of PKC ubiquitinated? Ubiquitination serves not only to target proteins to the proteasome but also as a 'signal' to recruit binding partners and alter subcellular localization, depending on the nature of the ubiquitin linkage (17). One study reports that the fully phosphorylated form of PKC is degraded by the proteasome; perhaps this ubiquitination event recruits the appropriate phosphatase. A recent study, as well as submitted work from our lab, has shown that both K48 and K63-linked ubiquitin chains can be conjugated to PKC after phorbol ester treatment (18). Thus, ubiquitination of PKC may not only target PKC for degradation but also serve a secondary non-proteasomal function that has yet to be determined. Indeed, PKC  $\beta$ II-T641E/S660E, which cannot be dephosphorylated at the priming sites, is robustly ubiquitinated in cells after PMA stimulation but is modestly down-regulated in protein levels. This finding demonstrates that dephosphorylation and ubiquitination can be

uncoupled after phorbol ester stimulation.

*The involvement of phosphatases in the phorbol ester-mediated down-regulation of PKC* - Our lab recently established that the PHLPP phosphatase dephosphorylates the hydrophobic motif of PKC; depletion of PHLPP levels in the cell attenuates the phorbol ester-mediated down-regulation of PKC (12). Consistent with the role of PHLPP promoting the phorbol ester-mediated down-regulation of PKC, treatment with the phosphatase inhibitor, okadaic acid, had no effect on the dephosphorylation or down-regulation of PKC protein. The hydrophobic motif phospho-mimetic mutant, PKC  $\beta$ II-S660E, also was insensitive to okadaic acid, which is not consistent with previous studies. Gao *et al.* showed that okadaic acid slowed the dephosphorylation at Thr-641 of PKC  $\beta$ II-S660E by ~ 2-fold; this effect was not within experimental error (12). Future work with this mutant is required in order to determine if dephosphorylation at the turn motif is also mediated by an okadaic acid-insensitive phosphatase.

In addition to PHLPP, both PP2A and PP1 can dephosphorylate PKC (23). Treatment with Calyculin A in the presence of PMA trapped a faster mobility, unphosphorylated species of PKC. This result is surprising because the unphosphorylated form of PKC is highly susceptible to degradation by the proteasome. However, the rate of disappearance of the fully phosphorylated species was similar in untreated and Calyculin A-treated cells in the presence of phorbol esters, suggesting that a Calyculin A-sensitive phosphatase may mediate the degradation of the unphosphorylated form of PKC and that dephosphorylation of the priming sites, Thr-641 and Ser-660, are not Calyculin-sensitive.

*Model* – Our data support a model in which dephosphorylation of PKC, initiated

by PHLPP at the hydrophobic motif, drives the phorbol ester-mediated down-regulation Figure 3.9 A. This rapidly dephosphorylated species is most likely ubiquitinated and degraded through the proteasome. Proteasome inhibitors, in fact, accumulate this dephosphorylated species. This process is dependent upon PKC activity; inhibition of PKC results in a dramatic slowing in the rate of dephosphorylation and the subsequent down-regulation. When PKC is unable to be dephosphorylated, it can still be robustly ubiquitinated after phorbol esters but is unable to be effectively down-regulated (Figure 3.9 B).

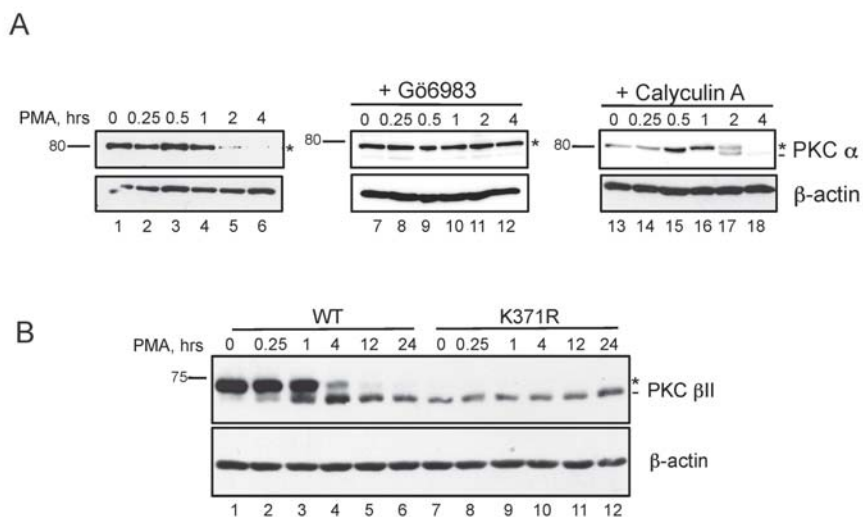


**Figure 3.1:** PKC requires its intrinsic catalytic activity in order to be down-regulated by phorbol esters. *A*, COS7 cells were treated with PMA alone (200 nM, lanes 1-6) or in the presence of the PKC inhibitor Gö6983 (1  $\mu$ M, lanes 7-12) or phosphatase inhibitor Calyculin A (50 nM, lanes 13-18) for the indicated times. Whole cell lysates were analyzed by SDS-PAGE and Western blotting for total PKC (PKC  $\alpha$ ) and total protein ( $\beta$ -actin). The *asterisk* denotes the position of the fully phosphorylated species, and the *dash* denotes the position of the unphosphorylated species. *B*, COS7 cells were transiently transfected with either WT PKC  $\beta$ II (lanes 1-6) or catalytically-inactive PKC, PKC  $\beta$ II-K371R (lanes 7-12) and treated with 200 nM PMA for the indicated times. Whole cell lysates were analyzed by SDS-PAGE and Western blotting for total PKC (PKC  $\beta$ II) and total protein ( $\beta$ -actin). The *asterisk* denotes the position of fully phosphorylated PKC, and the *dash* denotes the position of unphosphorylated PKC.

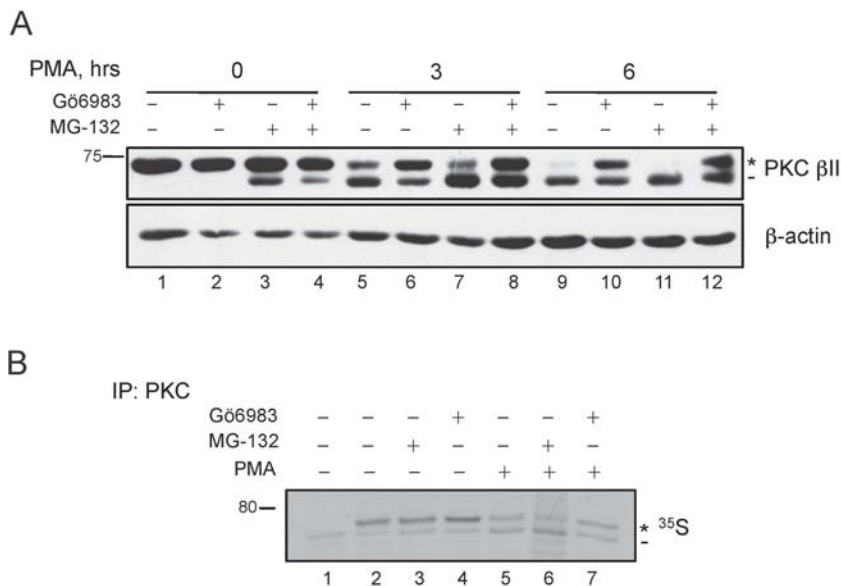


**Figure 3.2:** Degradation of the different species of PKC can be dissected with proteasome and PKC inhibitors. *A*, COS7 cells were transiently transfected with WT PKC  $\beta$ II and treated with either 200 nM PMA alone (*lanes 1, 5, and 9*) or pretreated with 10  $\mu$ M MG-132 (*lanes 2, 6, and 10*) or 1  $\mu$ M Gö6983 (*lanes 3, 7, and 11*) or both (*lanes 4, 8, and 12*) prior to PMA stimulation for the indicated times. Whole cell lysates were analyzed by SDS-PAGE and Western blotting for total PKC (PKC  $\beta$ II) and total protein ( $\beta$ -actin). The *asterisk* denotes the position of phosphorylated PKC, and the *dash* denotes the position of unphosphorylated PKC. *B*, Autoradiogram from a pulse-chase analysis of COS7 cells transfected with WT PKC  $\beta$ II. Transfected cells were labeled with [ $^{35}$ S]Met/Cys, chased for 90 min, and then treated with 10  $\mu$ M MG-132 (*lanes 3 and 6*) or 1  $\mu$ M Gö6983 (*lanes 4 and 7*) in the absence (*lanes 2-4*) and presence of 200 nM PMA (*lanes 5-7*) for 4 h. PKC was immunoprecipitated from detergent-solubilized lysates and analyzed by autoradiography. The *asterisk* denotes the position of mature, fully phosphorylated PKC, and the *dash* denotes the position of unphosphorylated PKC (either newly-synthesized as in *lane 1* or dephosphorylated as in *lane 5*).

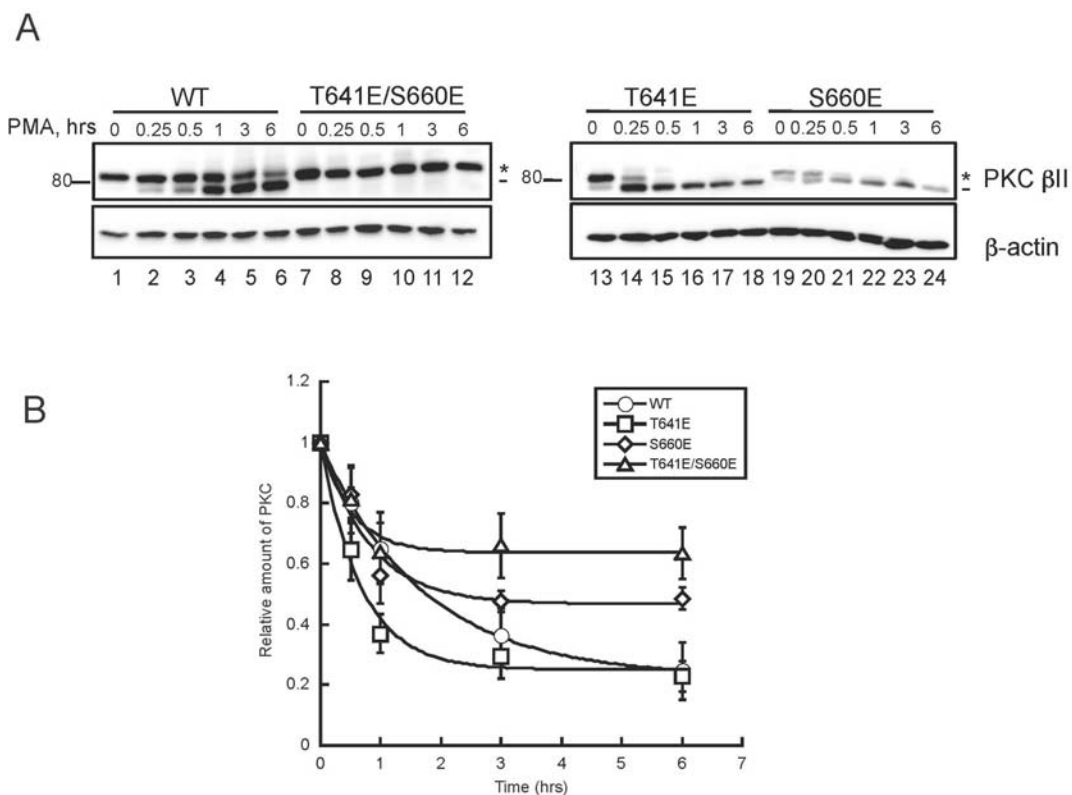


**Figure 3.3:** Dephosphorylation at the hydrophobic motif of PKC is a priming step in the phorbol ester-mediated down-regulation of PKC. *A*, COS7 cells were transiently transfected with WT PKC  $\beta$ II (*lanes 1-6*), PKC  $\beta$ II-T641E/S660E (*lanes 7-12*), PKC  $\beta$ II-T641E (*lanes 13-18*), or PKC  $\beta$ II-S660E (*lanes 19-24*) and treated with 200 nM PMA for the indicated times. Whole cell lysates were analyzed by SDS-PAGE and Western blotting for total PKC (PKC  $\beta$ II) and total protein ( $\beta$ -actin). The *asterisk* denotes the position of fully phosphorylated PKC, and the *dash* denotes the position of unphosphorylated PKC. *B*, Graph representing densitometric analysis of the data quantified in *A*. The relative amounts of WT PKC  $\beta$ II (*circles*), PKC  $\beta$ II-T641E (*squares*), PKC  $\beta$ II-S660E (*diamonds*), and PKC  $\beta$ II-T641E/S660E (*triangles*) are indicated. Data are representative of at least three independent experiments.

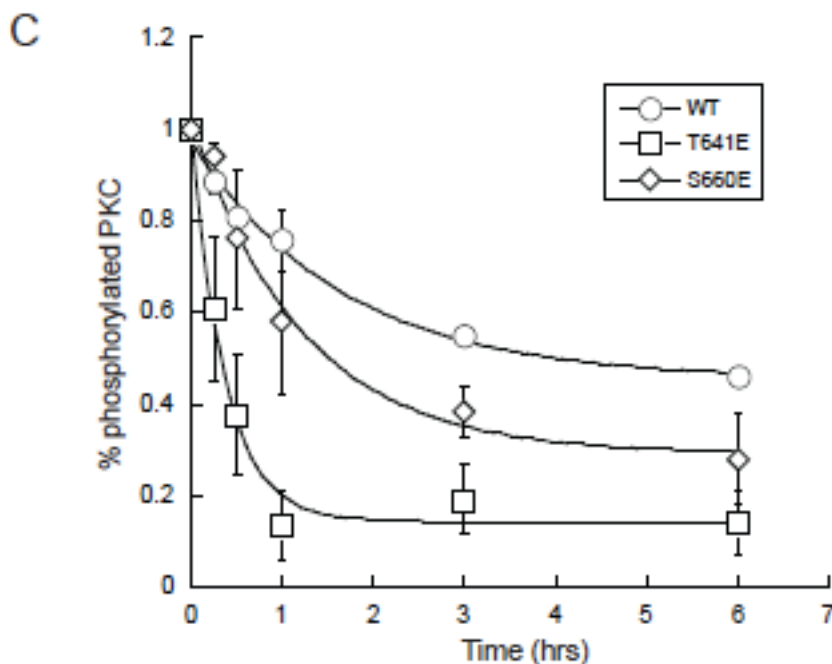


**Figure 3.3:** (continued) C, Graph representing densitometric analysis of the rate of dephosphorylation for WT PKC  $\beta$ II (circles), PKC  $\beta$ II-T641E (squares), and PKC  $\beta$ II-S660E (diamonds) of the data shown in A. The amount of the upper band (asterisk) was normalized to the total amount of PKC detected by the PKC  $\beta$ II antibody. The initial time point was set to 1, and the relative amount of phosphorylation (% of total) was obtained by normalizing to time zero (no PMA treatment). Data represent the mean  $\pm$  S.E. of three independent experiments.

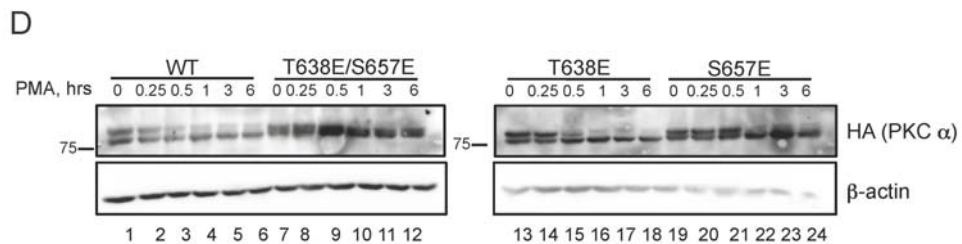


**Figure 3.3:** (continued) *D*, COS7 cells were transiently transfected with WT HA-PKC  $\alpha$  (lanes 1-6), HA-PKC  $\alpha$ -T638E/S657E (lanes 7-12), HA-PKC  $\alpha$ -T638E (lanes 13-18), or HA-PKC  $\alpha$ -S657E (lanes 19-24) and treated with 200 nM PMA for the indicated times. Whole cell lysates were analyzed by SDS-PAGE and Western blotting for total PKC (HA) and total protein ( $\beta$ -actin).

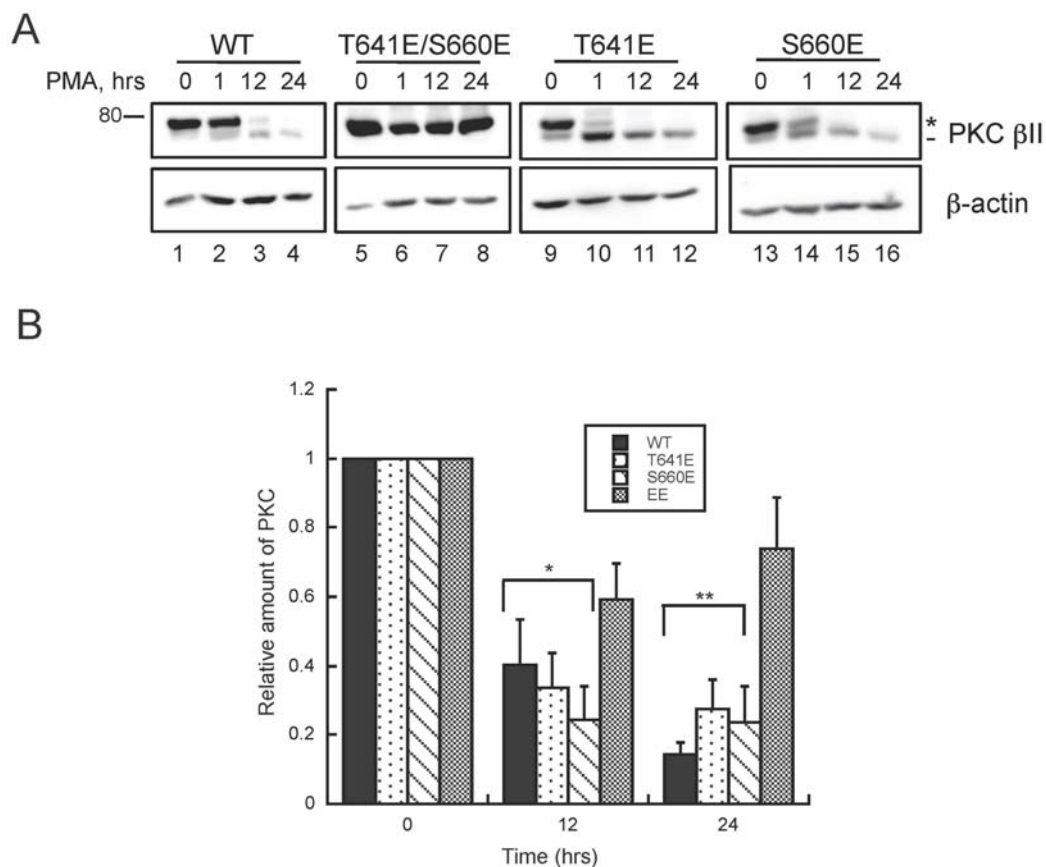


**Figure 3.4:** Dephosphorylation of the priming sites in PKC is required for phorbol ester-mediated down-regulation. *A*, COS7 cells were transiently transfected with WT PKC  $\beta$ II (lanes 1-4), PKC  $\beta$ II-T641E/S660E (lanes 5-8), PKC  $\beta$ II-T641E (lanes 9-12), or PKC  $\beta$ II-S660E (lanes 13-16) and treated with 200 nM PMA for the indicated times. Whole cell lysates were analyzed by SDS-PAGE and Western blotting for total PKC (PKC  $\beta$ II) and total protein ( $\beta$ -actin). The asterisk denotes the position of fully phosphorylated PKC, and the dash denotes the position of unphosphorylated PKC. *B*, Graph representing densitometric analysis of the data quantified in *A*. The total amount of PKC  $\beta$ II was normalized using  $\beta$ -actin as a loading control. The initial time point was set to 1, and the relative amount of PKC was obtained by normalizing to time zero (no PMA treatment). Data represent the mean  $\pm$  S.E. of three independent experiments. \*,  $p < 0.01$  versus time zero by Student's *t*-test. \*\*,  $p < 0.005$  versus time zero by Student's *t*-test.

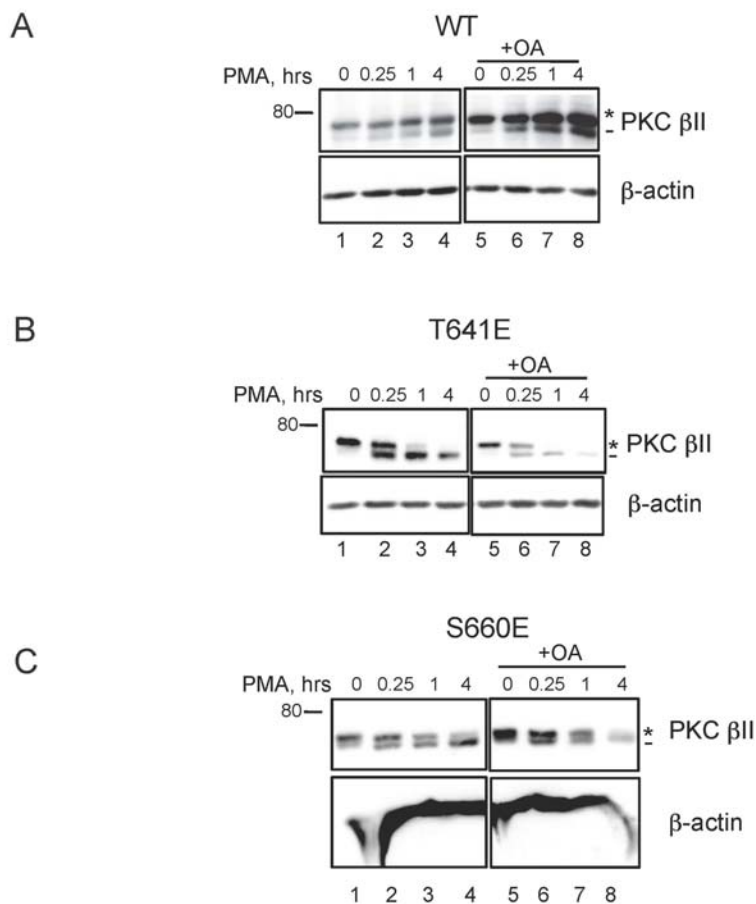


**Figure 3.5:** The phorbol ester-mediated down-regulation of PKC is insensitive to the phosphatase inhibitor, okadaic acid. *A*, COS7 cells were transiently transfected with WT PKC  $\beta$ II and treated with 200 nM PMA alone (*lanes 1-4*) or after pretreatment with 50 nM okadaic acid (*lanes 5-8*) for the indicated times. Whole cell lysates were analyzed by SDS-PAGE and Western blotting for total PKC (PKC  $\beta$ II) or total protein ( $\beta$ -actin). The *asterisk* denotes the position of fully phosphorylated PKC, and the *dash* denotes the position of unphosphorylated PKC. *B*, COS7 cells were transiently transfected with PKC  $\beta$ II-T641E and analyzed as described in *A*. *C*, COS7 cells were transiently transfected with PKC  $\beta$ II-S660E and analyzed as described in *A*.

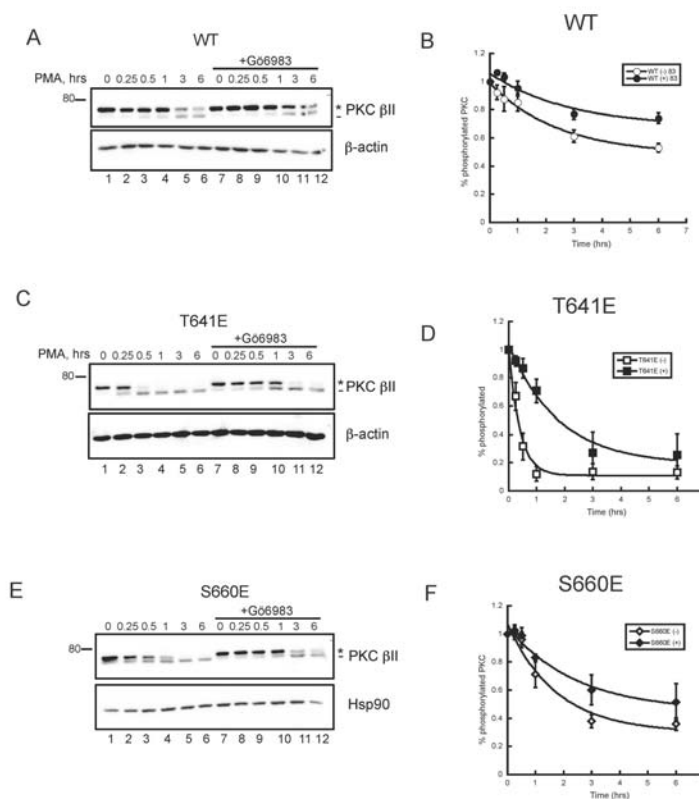


**Figure 3.6:** Inhibition of PKC slows the phorbol ester-mediated dephosphorylation of PKC. *A*, COS7 cells were transiently transfected with WT PKC  $\beta$ II and treated with 200 nM PMA in the absence (*lanes 1-6*) and presence (*lanes 7-12*) of 1  $\mu$ M Gö6983 for the indicated times. Whole cell lysates were analyzed by SDS-PAGE and Western blotting for total PKC (PKC  $\beta$ II) and total protein ( $\beta$ -actin). The *asterisk* denotes the position of fully phosphorylated PKC, and the *dash* denotes the position of unphosphorylated PKC. *B*, Graph representing densitometric analysis the rate of dephosphorylation of WT PKC  $\beta$ II in the absence (*white circles*) and presence (*black circles*) of 1  $\mu$ M Gö6983 as shown in *A*. The amount of the upper band (*asterisk*) was normalized to the total amount of PKC detected by the PKC  $\beta$ II antibody. The initial time point was set to 1, and the relative amount of phosphorylation (% of total) was obtained by normalizing to time zero (no PMA treatment). Data represent the mean  $\pm$  S.E. of three independent experiments. *C*, COS7 cells were transiently transfected with PKC  $\beta$ II-T641E and analyzed as described in *A*. *D*, Graph representing densitometric analysis of the rate of dephosphorylation of PKC  $\beta$ II-T641E in the absence (*white squares*) and presence (*black squares*) of 1  $\mu$ M Gö6983 as shown in *C*. Data represent the mean  $\pm$  S.E. of three independent experiments. *E*, COS7 cells were transiently transfected with PKC  $\beta$ II-S660E and analyzed as described in *A*. Total protein was detected with an anti-Hsp90 antibody. *F*, Graph representing densitometric analysis of the rate of dephosphorylation of PKC  $\beta$ II-S660E in the absence (*white diamonds*) and presence (*black diamonds*) of 1  $\mu$ M Gö6983 as shown in *C*. Data represent the mean  $\pm$  S.E. of three independent experiments.

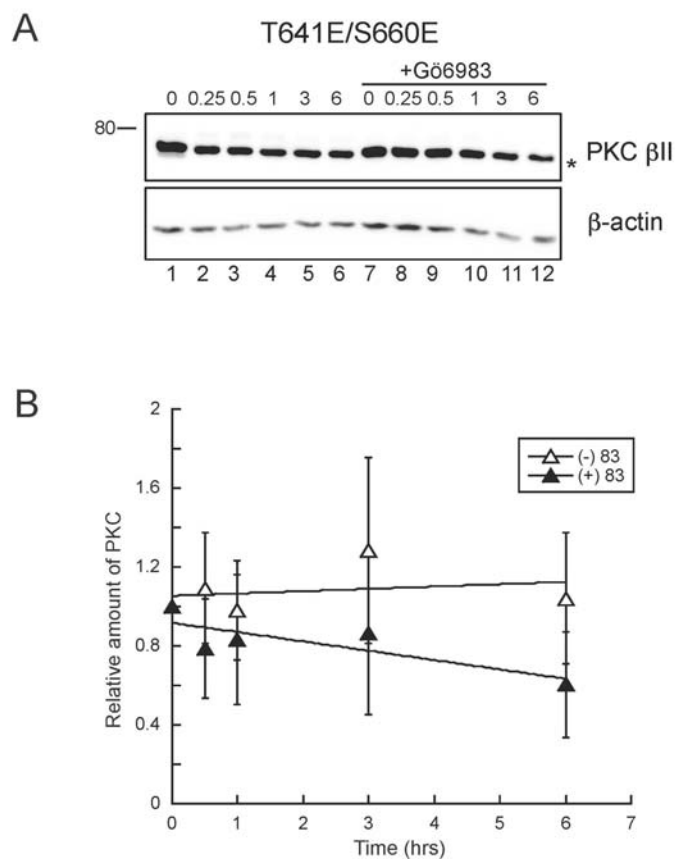


**Figure 3.7:** Inhibition of PKC activity does not affect protein levels of PKC  $\beta$ II-T641E/S660E, which cannot be dephosphorylated, after phorbol ester stimulation. *A*, COS7 cells were transiently transfected with PKC  $\beta$ II-T641E/S660E and treated with 200 nM PMA in the absence (*lanes 1-6*) and presence (*lanes 7-12*) of 1  $\mu$ M Gö6983 for the indicated times. Whole cell lysates were analyzed by SDS-PAGE and Western blotting for total PKC (PKC  $\beta$ II) and total protein ( $\beta$ -actin). The *asterisk* denotes the position of fully phosphorylated PKC. *B*, Graph representing densitometric analysis the rate of down-regulation of PKC  $\beta$ II-T641E/S660E levels in the absence (*white triangles*) and presence (*black triangles*) of 1  $\mu$ M Gö6983 as shown in *A*. The amount of the total PKC (*asterisk*) was normalized to the total amount of protein detected by the  $\beta$ -actin antibody. The initial time point was set to 1, and the relative amount of PKC was obtained by normalizing to time zero (no PMA treatment). Data represent the mean  $\pm$  S.E. of three independent experiments.

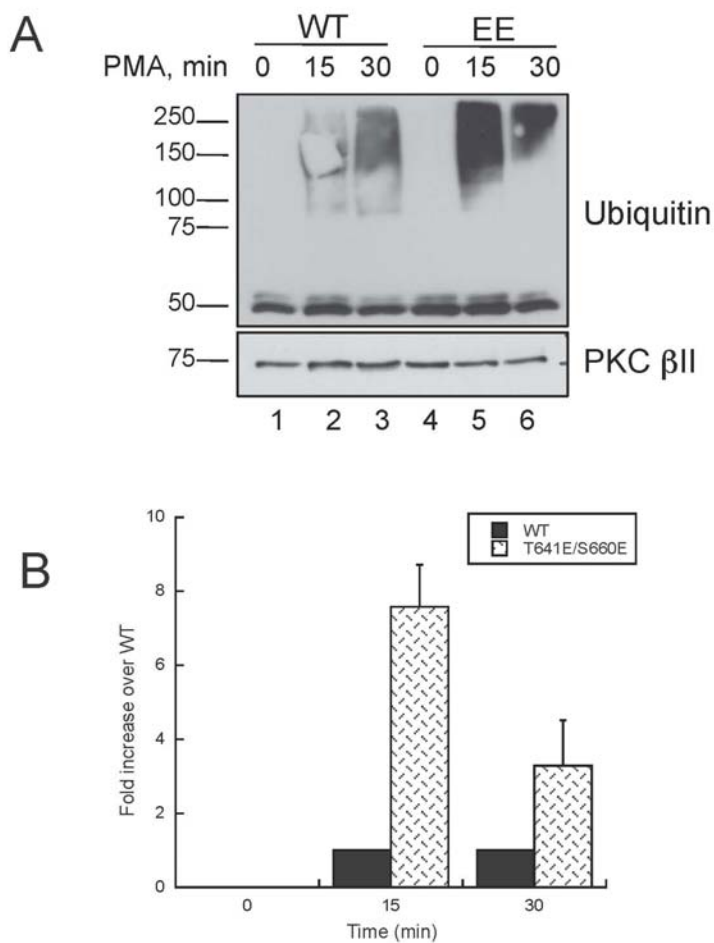


**Figure 3.8:** Dephosphorylation is not a prerequisite for ubiquitination when PKC is down-regulated by phorbol esters. *A*, tsA201 cells were transiently transfected with WT PKC  $\beta$ II (*lanes 1-3*) or PKC  $\beta$ II-T641E/S660E (*lanes 4-6*) and treated with 200 nM PMA for the indicated times. PKC was immunoprecipitated from detergent-solubilized lysates and analyzed by Western blotting for ubiquitin and PKC  $\beta$ II. *B*, Graph representing densitometric analysis of the data shown in *A*. The amount of ubiquitination in the IP was normalized to the amount of PKC in the IP as detected by the PKC  $\beta$ II antibody. Data represent the fold increase in ubiquitination over WT from three independent experiments.

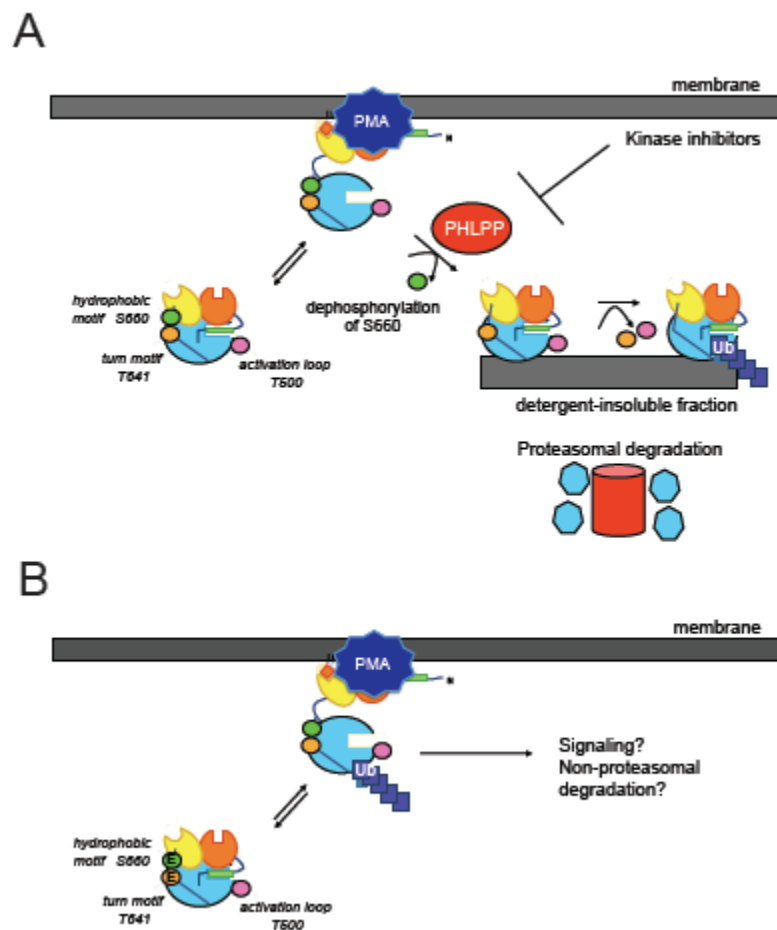


**Figure 3.9:** Model showing the proposed requirement of PKC activity-dependent dephosphorylation to promote the phorbol ester-mediated down-regulation of PKC. *A*, Mature PKC is phosphorylated at the three priming sites: activation loop (Thr-500, *pink circle*), turn motif (Thr-641, *orange circle*), and hydrophobic motif (Ser-660, *green circle*). PKC remains inactive in the cytosol with the autoinhibitory pseudosubstrate (*green rectangle*) occupying the active site. Upon addition of phorbol esters that bind with high affinity to the C1 domain in the absence of  $\text{Ca}^{2+}$ , PKC translocates to the membrane and undergoes a dramatic conformational change to allow phosphorylation of downstream substrates. This chronic activation of PKC maintains PKC in an open conformation where it can be dephosphorylated at the hydrophobic motif by the PHLPP phosphatase (*red oval*). This dephosphorylation is dependent upon the activity of PKC. Once PKC has been dephosphorylated at the hydrophobic motif, the other phosphorylation sites are rapidly dephosphorylated, and PKC is ubiquitinated and degraded by the proteasome. *B*, A phospho-mimetic mutant that cannot be dephosphorylated, PKC  $\beta\text{II-T641E/S660E}$  (note E at those C-terminal positions), is unable to be down-regulated by phorbol esters. Although this fully phosphorylated mimic is robustly ubiquitinated after phorbol ester stimulation, the role of this ubiquitination remains unclear.

## References

1. Newton, A. C. (2003) *Biochem J* **370**, 361-371
2. Gould, C. M., and Newton, A. C. (2008) *Curr Drug Targets* **9**, 614-625
3. Castagna, M., Takai, Y., Kaibuchi, K., Sano, K., Kikkawa, U., and Nishizuka, Y. (1982) *J Biol Chem* **257**, 7847-7851
4. Blumberg, P. M., Sharkey, N. A., Konig, B., Jaken, S., Leach, K. L., and Jeng, A. Y. (1983) *Princess Takamatsu Symp* **14**, 75-87
5. Newton, A. C. (2004) *Trends Pharmacol Sci* **25**, 175-177
6. Hansra, G., Bornancin, F., Whelan, R., Hemmings, B. A., and Parker, P. J. (1996) *J Biol Chem* **271**, 32785-32788
7. Ohno, S., Konno, Y., Akita, Y., Yano, A., and Suzuki, K. (1990) *J Biol Chem* **265**, 6296-6300
8. Hansra, G., Garcia-Paramio, P., Prevostel, C., Whelan, R. D., Bornancin, F., and Parker, P. J. (1999) *Biochem J* **342** ( Pt 2), 337-344
9. Becker, K. P., and Hannun, Y. A. (2004) *J Biol Chem* **279**, 28251-28256
10. Idkowiak-Baldys, J., Becker, K. P., Kitatani, K., and Hannun, Y. A. (2006) *J Biol Chem* **281**, 22321-22331
11. Prevostel, C., Alice, V., Joubert, D., and Parker, P. J. (2000) *J Cell Sci* **113** ( Pt 14), 2575-2584
12. Gao, T., Brognard, J., and Newton, A. C. (2008) *J Biol Chem* **283**, 6300-6311
13. Gao, T., and Newton, A. C. (2002) *J Biol Chem* **277**, 31585-31592
14. Gao, T., and Newton, A. C. (2006) *J Biol Chem* **281**, 32461-32468
15. Leontieva, O. V., and Black, J. D. (2004) *J Biol Chem* **279**, 5788-5801
16. Herrmann, J., Lerman, L. O., and Lerman, A. (2007) *Circ Res* **100**, 1276-1291
17. Adhikari, A., and Chen, Z. J. (2009) *Dev Cell* **16**, 485-486
18. Poulin, B., Maccario, H., Thirion, S., Junoy, B., Boyer, B., Enjalbert, A., and Drouva, S. V. (2009) *Neuroendocrinology* **89**, 252-266

19. Lee, H. W., Smith, L., Pettit, G. R., and Smith, J. B. (1997) *Mol Pharmacol* **51**, 439-447
20. Sonnenburg, E. D., Gao, T., and Newton, A. C. (2001) *J Biol Chem* **276**, 45289-45297
21. Lee, H. W., Smith, L., Pettit, G. R., and Bingham Smith, J. (1996) *Am J Physiol* **271**, C304-311
22. Knighton, D. R., Zheng, J. H., Ten Eyck, L. F., Xuong, N. H., Taylor, S. S., and Sowadski, J. M. (1991) *Science* **253**, 414-420
23. Keranen, L. M., Dutil, E. M., and Newton, A. C. (1995) *Curr Biol* **5**, 1394-1403
24. Behn-Krappa, A., and Newton, A. C. (1999) *Curr Biol* **9**, 728-737
25. Gould, C. M., Kannan, N., Taylor, S. S., and Newton, A. C. (2009) *J Biol Chem* **284**, 4921-4935
26. Chen, D., Gould, C., Garza, R., Gao, T., Hampton, R. Y., and Newton, A. C. (2007) *J Biol Chem*
27. Lee, H. W., Smith, L., Pettit, G. R., Vinitsky, A., and Smith, J. B. (1996) *J Biol Chem* **271**, 20973-20976
28. Oliveria, S. F., Gomez, L. L., and Dell'Acqua, M. L. (2003) *J Cell Biol* **160**, 101-112
29. Gallegos, L. L., Kunkel, M. T., and Newton, A. C. (2006) *J Biol Chem* **281**, 30947-30956
30. Faux, M. C., Rollins, E. N., Edwards, A. S., Langeberg, L. K., Newton, A. C., and Scott, J. D. (1999) *Biochem J* **343 Pt 2**, 443-452
31. Edwards, A. S., and Newton, A. C. (1997) *J Biol Chem* **272**, 18382-18390
32. Edwards, A. S., Faux, M. C., Scott, J. D., and Newton, A. C. (1999) *J Biol Chem* **274**, 6461-6468
33. Bornancin, F., and Parker, P. J. (1996) *Curr Biol* **6**, 1114-1123
34. Hauge, C., Antal, T. L., Hirschberg, D., Doehn, U., Thorup, K., Idrissova, L., Hansen, K., Jensen, O. N., Jorgensen, T. J., Biondi, R. M., and Frodin, M. (2007) *Embo J* **26**, 2251-2261

35. Frodin, M., Antal, T. L., Dummler, B. A., Jensen, C. J., Deak, M., Gammeltoft, S., and Biondi, R. M. (2002) *Embo J* **21**, 5396-5407

## Chapter 4

### Characterization of an *In Vitro* Autophosphorylation Site in PKC $\beta$ II

**Abstract**

Phosphorylation is a primary mechanism that regulates protein function. Indeed, PKC is highly controlled by phosphorylation by other kinases as well as itself; the phosphorylation state dictates the catalytic competence of the enzyme. This chapter focuses on the role of previously identified but poorly uncharacterized *in vitro* autophosphorylation sites in PKC  $\beta$ II. Specifically, this research addresses the function of autophosphorylation at Ser-16 and Thr-17 in N-terminus of PKC  $\beta$ II. By generating a phospho-specific antibody to Thr-17 in PKC  $\beta$ II, we show that PKC autophosphorylates at this site in cells under various agonist conditions. Additionally, we show that phospho-Thr17-PKC  $\beta$ II is localized at the membrane upon treatment with phorbol esters. However, double mutation of these sites to either nonphosphorylatable or phospho-mimetic residues, PKC  $\beta$ II-S16A/T17A or PKC  $\beta$ II-S16E/T17D, respectively, shows no significant difference in activity, maturation, or phorbol ester-mediated down-regulation. The only functional consequence of autophosphorylation at these sites that we have unveiled so far is a reduced translocation of the phospho-mimetic mutant, PKC  $\beta$ II-S16E/T17D, to the membrane under natural agonist stimulation. These data reveal that autophosphorylation at Thr-17 in PKC  $\beta$ II could serve as a potential marker for activation; however, the direct functional consequence of this modification still remains unknown.

## Introduction

Phosphorylation is one of the key regulatory mechanisms that controls the ability of PKC to transduce extracellular signals (1). Three well-characterized phosphorylation sites in PKC are the priming steps to PKC maturation: the activation loop, the turn motif, and the hydrophobic motif (2). Each of these sites has a defined function for PKC. The upstream kinase PDK-1 catalyzes the activation loop phosphorylation, which is required for the two C-terminal processing sites. Turn motif phosphorylation has recently been shown to be regulated by the mTORC2 complex and is absolutely essential for catalytic function (3,4). Finally, hydrophobic motif phosphorylation is an intramolecular reaction that promotes the stability and phosphatase-resistance of the enzyme. When PKC is fully phosphorylated at these sites, it is catalytically-competent and capable of responding to lipid second messengers. Conversely, dephosphorylation of PKC at these sites leads to the degradation and ‘down-regulation’ of PKC in the cell (5).

As a kinase, PKC not only phosphorylates downstream substrates but can also phosphorylate itself, thus adding an additional layer of complexity to regulation of PKC function. Recent studies have characterized isozyme-specific autophosphorylation sites in PKC  $\alpha$ ,  $\delta$ ,  $\eta$ , and  $\theta$  (6-9). All of these autophosphorylations serve as a marker for activated PKC. However, each of them has different functional outcomes depending on the isozyme- and cell-type context.

Purified PKC  $\beta$ II autophosphorylates *in vitro* at four sites: Ser-16 and Thr-17 in the N-terminus preceding the pseudosubstrate peptide sequence and Thr-314 and Thr-324 in the hinge between the regulatory moiety and catalytic domain (10). The locations of these sites are interesting in that they are located in poorly conserved regions of PKC,

thus implying that these phosphorylations would have specific functions for PKC  $\beta$ II – even independent of its conventional counterparts PKC  $\alpha$  and PKC  $\gamma$ . An early study characterizing alanine mutants at these sites *in vivo* did not find differences in activity, solubility, or phorbol ester-responsiveness (11). However, this study was by no means complete, and more recent studies of autophosphorylation sites in other PKC isozymes have uncovered specific functions for this type of modification.

Here, we developed a phospho-specific antibody to phospho-Thr-17 to monitor autophosphorylation in cells under various agonist conditions. Our data reveal that this site could serve as a potential marker for PKC  $\beta$ II activation in cells.

Autophosphorylation at Thr-17 in PKC  $\beta$ II may also fine-tune PKC's ability to translocate to membranes in cells and subsequently alter its localization for a specific signaling purpose.

## Material and Methods

*Materials* - Unphosphorylated and phosphorylated T17 peptides (Ac-CSEGEEST(PO<sub>3</sub>H<sub>2</sub>)VRFARKGA-NH<sub>2</sub>) and PKC substrate peptide (Ac-FKKSFKL-NH<sub>2</sub>) were obtained from Anaspec, Inc. Oligonucleotides were purchased from Integrated DNA Technologies. Easy Tag [<sup>35</sup>S]Met/Cys (1175 Ci mmol<sup>-1</sup>) and [<sup>32</sup>P]ATP (3000 Ci mmol<sup>-1</sup>) were purchased from PerkinElmer Life Sciences. Met/Cys-deficient DMEM was purchased from Invitrogen. Phorbol 12-myristate 13-acetate (PMA), phorbol-12,13-dibutyrate (PDBu), Calyculin A, Gö6983, and uridine-5'-triphosphate (UTP) were purchased from Calbiochem. Lysophosphatidic acid (LPA) was purchased from Cayman Chemical. 1,2-dioctanoyl-*sn*-glycerol (diC8) was purchased from Sigma Aldrich. 1-palmitoyl-2-oleoyl-*sn*-glycero-3-phosphoserine and 1,2-*sn*-dioleoylglycerol in chloroform were from Avanti Polar Lipids, Inc. A phospho-specific, polyclonal PKC antibody that specifically recognizes phosphorylated Thr17 (pT17) was generated from a KLH-conjugated, phosphorylated peptide (Ac-CSEGEEST(PO<sub>3</sub>H<sub>2</sub>)VRFARKGA-NH<sub>2</sub>) by NeoMPS, Inc. Polyclonal antibodies to PKC βII and PKC α were purchased from Santa Cruz Biotechnology. Monoclonal antibodies to PKC α and PKC β were purchased from B.D. Transduction Laboratories. A polyclonal antibody to the turn motif phosphorylation site (PKC α/βII Thr-638/641) was purchased from Cell Signaling Technology. Monoclonal antibodies to γ-tubulin and β-actin antibody were purchased from Sigma Aldrich. Ultra-Link protein A/G beads were purchased from Thermo Scientific. Electrophoresis reagents were obtained from Biorad. All other chemicals and materials were reagent-grade.

*Plasmids* – A baculovirus PKC βII expression construct was generated by PCR

amplification and subsequent cloning into the pFastBac HTB vector (Invitrogen) using BamHI (5') and XhoI (3') (Jaime Marach, Ph.D. thesis, 2006). PKC  $\beta$ II-YFP was cloned as previously described (12). The PKC mutants, PKC  $\beta$ II-S16A/T17A and PKC  $\beta$ II-S16E/T17D (and subsequent YFP mutants), were generated using the QuikChange site-directed mutagenesis kit (Stratagene). A myristoylated/palmitoylated CFP (PM-CFP) to target to the plasma membrane was cloned as previously described (13).

*Cell culture and transfection* - tsA201, HeLa, and COS7 cells were maintained in DMEM (Cellgro) containing 10% fetal bovine serum (Hyclone) and 1% penicillin/streptomycin at 37°C in 5% CO<sub>2</sub>. K562 cells were maintained in DMEM containing 10% heat-inactivated fetal bovine serum and 1% penicillin/streptomycin at 37°C in 5% CO<sub>2</sub>. Transient transfection of tsA201 cells was carried out using Effectene transfection reagent (Qiagen), and transient transfections of COS7 and HeLa cells were carried out using FuGENE transfection reagent (Roche Applied Science).

*Dot blot assay* - Unphosphorylated and phosphorylated peptides were spotted at the indicated concentrations onto nitrocellulose in a Schleicher and Schuell vacuum manifold (Keene). The individual wells were blocked with 5% (w/v) non-fat dried milk and incubated overnight with affinity-purified antibody at 1:10000 dilution in 1% (w/v) BSA in PBS-T [PBS with 0.5% (w/v) Tween 20 and 0.1% (w/v) thimersol] solution. The following day, the membrane was analyzed by chemiluminescence.

*Insect cell culture and PKC purification* - Sf-21 cells were maintained in serum-free Sf-900 II SFM media (Gibco) in T75 flasks at 26°C. His-PKC  $\beta$ II virus was prepared according to the manufacturer's protocol. Prior to infection,  $5 \times 10^6$  cells were seeded in T75 flasks and then incubated with His-PKC  $\beta$ II virus for 40 min. The virus was then

removed and replaced with fresh media. Forty-eight h post-infection, the insect cells were harvested and centrifuged at 1000 x g. The cell pellet was lysed in Buffer A (50 mM NaH<sub>2</sub>PO<sub>4</sub>, 300 mM NaCl, 10 mM imidazole, 1% Triton X-100, 0.5% β-mercaptoethanol, and protease inhibitors (1 mM benzamidine, 1 mM PMSF, 1 μg/μL aprotinin, 5 μg/μL leupeptin, 1 μg/μL pepstatin, 0.3 μg/μL bestatin)). The resulting lysate was precleared by centrifugation for 10 min at 7000 x g at 4°C and then added to prewashed Ni-NTA beads (Qiagen) for 2 h at 4°C. Beads were washed three times in Buffer A and two times in Buffer B (50 mM NaH<sub>2</sub>PO<sub>4</sub>, 300 mM NaCl, 20 mM imidazole, 0.5% β-mercaptoethanol and protease inhibitors). His-PKC βII was eluted with Buffer C (50 mM NaH<sub>2</sub>PO<sub>4</sub>, 300 mM NaCl, 250 mM imidazole, 1.5% β-mercaptoethanol, and protease inhibitors). After elution, His-PKC βII was dialyzed into 20 mM HEPES, 1 mM dithiothreitol (DTT), 20 mM NaCl. For long-term storage and stability, glycerol was added to 10% final concentration.

*In vitro autophosphorylation assay* - His-PKC βII (30 nM) was incubated with 20 mM HEPES, 2 mM DTT, 500 μM Ca<sup>2+</sup>, 140 μM phosphatidylserine/38 μM diacylglycerol membranes, and 5 mM MgCl<sub>2</sub> in the absence and presence of 100 μM ATP for 30 min at 30°C. For experiments with inhibitor, 1 μM Gö6983 was added to the reaction. The reaction was stopped with the addition of Laemmli sample buffer. The samples were separated by SDS-PAGE, transferred to polyvinylidene difluoride membrane, and analyzed by Western blotting.

*PMA time courses* - K562 cells were treated with 200 nM PMA for 0, 0.25, 1 or 4 h in the absence or presence of either 50 nM Calyculin A or 1 μM Gö6983. Cells were lysed in Buffer D (50 mM Tris, 50 mM NaF, 10 mM Na<sub>4</sub>P<sub>2</sub>O<sub>7</sub>, 100 mM NaCl, 5 mM EDTA, 1%

Triton X-100, 1 mM Na<sub>3</sub>VO<sub>4</sub>, and 1 mM PMSF). Whole cell lysates were analyzed by SDS-PAGE and Western blotting. For the PKC mutant experiments, COS7 cells were transiently transfected with WT PKC  $\beta$ II, PKC  $\beta$ II-S16A/T17A, or PKC  $\beta$ II-S16E/T17D, and then treated with 200 nM PMA for 0, 2, 4, or 8 h. Cells were lysed in Buffer D, and whole cell lysates were analyzed by SDS-PAGE and Western blotting. Densitometric analysis was performed using NIH Image J analysis software (version 1.40).

*Immunoprecipitation time courses* – COS7 cells were transiently transfected with PKC  $\beta$ II-YFP. Approximately 24 h post-transfection, cells were treated with 50 nM Calyculin A and either 200 nM PMA or 100  $\mu$ M diC8 for the indicated times. Cells were harvested, lysed in Buffer D, and lysates were centrifuged at 16,000 x g for 5 min at 22°C. The detergent-solubilized supernatants were incubated with an anti-monoclonal PKC  $\alpha$  antibody (cross-reactive with PKC  $\beta$ II) overnight at 4°C. The immune complexes were collected with Ultra-Link protein A/G beads and washed with Buffer D, and bound proteins were analyzed by SDS-PAGE and Western blotting. For the LPA/Gö6983 experiments, cells were starved for 6 h and pretreated for 30 min with 1  $\mu$ M Gö6983 prior to stimulation with either 200 nM PMA or 10  $\mu$ M LPA for 15 min.

Chemiluminescent images were obtained using the FluorChem Q (Alpha Innotech), and densitometric analysis was performed using the AlphaView Q software.

*Confocal imaging* - COS7 or HeLa cells were plated on glass coverslips prior to transient transfection with cDNA for PKC  $\beta$ II-YFP. COS7 cells were treated with 200 nM PMA for 15 min, and HeLa cells were either pretreated or not with 1  $\mu$ M Gö6983 prior to PMA treatment. After stimulation with PMA, cells were washed with PBS and then fixed for 15 min with 3% PFA, 2% sucrose in PBS (pH 8.0). Cells were then washed with PBS,

quenched with 50 mM NH<sub>4</sub>Cl in CB (2x CB = 20 mM Pipes pH 6.8, 300 mM NaCl, 10 mM EGTA, 10 mM glucose, and 10 mM MgCl<sub>2</sub>). After quenching, cells were permeabilized with 0.5% Triton X-100 in PBS for 15 min and then blocked with 1% BSA in PBS/5% goat serum for 15 min. Cells were incubated in blocking buffer containing phospho-Thr17 antibody overnight at 4°C. Following overnight incubation with the primary antibody, cells were washed in 0.1% Triton X-100 in PBS prior to incubation with rabbit-Alexa594 secondary antibody (Molecular Probes) for 1 hr at room temperature. Cells were then washed in 0.1% Triton X-100 in PBS and quenching buffer prior to mounting in vectorshield. Images were required on Radiance 2000 confocal microscope. Analysis was performed using NIH Image J software (version 1.40).

*Kinase assay* - Detergent-solubilized lysates (20 mM HEPES, pH 7.5, 0.1% Triton X-100, 2 mM DTT, 1 mM phenylmethylsulfonyl fluoride) from untransfected tsA201 cells or tsA201 cells transfected with empty vector, WT PKC βII, PKC βII-S16A/T17A, or PKC βII-S16E/T17D were assayed for PKC activity for 8 min by monitoring <sup>32</sup>P incorporation from [γ-<sup>32</sup>P]ATP into a synthetic PKC-selective peptide (Ac-FKKSFKL-NH<sub>2</sub>) using a paper assay as described previously (14). The standard reaction mix contained 20 mM HEPES, pH 7.5, 2 mM DTT, 5 mM MgCl<sub>2</sub>, 100 μM ATP, 50 μM peptide substrate, and 100 μCi of [γ-<sup>32</sup>P]ATP. Non-activating conditions included 2 mM EGTA. Activating conditions included 140 μM phosphatidylserine/3.8 μM diacylglycerol dispersions and 500 μM CaCl<sub>2</sub>. The activity of the transfected kinase was determined by first subtracting <sup>32</sup>P incorporation in control (vector-transfected) lysate samples and then normalizing the Ca<sup>2+</sup>/lipid-stimulated peptide phosphorylation to PKC expression (determined by Western blot analysis); activity is expressed in relative units.

*Pulse-chase analysis* – COS7 cells were transfected with WT PKC  $\beta$ II, PKC  $\beta$ II-S16A/T17A, or PKC  $\beta$ II-S16E/T17D. 24–30 h post-transfection, cells were incubated with Met/Cys-deficient DMEM for 30 min at 37 °C. The cells were then pulse-labeled with 0.5 mCi ml<sup>-1</sup> [<sup>35</sup>S]Met/Cys in Met/Cys-deficient DMEM for 7 min at 37 °C, media were removed, and cells were chased with DMEM containing 5 mM unlabeled methionine and 5 mM unlabeled cysteine (15). At the indicated times, cells were lysed in Buffer A and centrifuged at 16,000 x g for 5 min at 22 °C, and PKC  $\beta$ II in the supernatant was immunoprecipitated with an anti-PKC  $\alpha$  monoclonal antibody (cross-reactive with PKC  $\beta$ II) overnight at 4 °C. The immune complexes were collected with Ultra-Link protein A/G beads and washed with Buffer D, and bound proteins were analyzed by SDS-PAGE and autoradiography.

*Translocation assay* – COS7 cells were transiently co-transfected with WT PKC  $\beta$ II-YFP, PKC  $\beta$ II-S16A/T17A-YFP, or PKC  $\beta$ II-S16E/T17D-YFP and PM-CFP. At 24 h post-transfection cells were imaged as described previously (13). Briefly, cells were first treated with 100  $\mu$ M UTP prior to treatment with 200 nM PDBu (to induce maximal membrane binding). The data were analyzed as previously described (12).

## Results

*PKC autophosphorylates at its N-terminus and hinge in vitro* – PKC  $\beta$ II has been shown to autophosphorylate at Ser-16 and Thr-17, which precede the autoinhibitory pseudosubstrate, and Thr-314 and Thr-324 in the hinge region between the N-terminal regulatory moiety and catalytic domain by an intramolecular mechanism (10, Figure 4.1). These autophosphorylation sites are not conserved within the other PKC family members and are thus specific to PKC  $\beta$ II; however, their role has not been extensively characterized *in vivo*. Therefore, we sought to address the role of these sites in cells by generating phospho-specific antibodies to each of the autophosphorylation sites. To determine whether these antibodies were phospho-specific, we performed a dot blot assay using unphosphorylated and phosphorylated peptides to each of the sites. Only one of the four antibodies, pT17, showed phospho-specificity in the dot blot assay (Figure 4.2 A (*compare phos to dephos*) and data not shown). Immunoreactivity of the pT17 antibody increased with increasing concentration of phospho-peptide, although some basal signal was observed with the unphosphorylated peptide. The fold selectivity for phospho over dephospho peptide was  $\sim 10$ ; pT17 detected signal of the phospho peptide at 1 ng *versus* 10 ng for the dephospho peptide (*compare lanes 1 and 2*). From this point on, we chose only to focus on the Thr-17 autophosphorylation site since the other three antibodies were not phospho-specific by the dot blot assay.

To test whether PKC  $\beta$ II autophosphorylated at this site *in vitro*, as been previously described, we performed an *in vitro* autophosphorylation assay using purified His-PKC  $\beta$ II in the absence or presence of ATP. Figure 4.2 B shows that in the absence of ATP, PKC  $\beta$ II is phosphorylated at one of the processing phosphorylation sites (*lane*

1, *pT641 panel*) but not at Thr-17 (*pT17 panel*). However, when ATP is added to the reaction, PKC  $\beta$ II shows a robust increase in pT17 (*lane 2*). Interestingly, a very slight mobility shift can be observed for this autophosphorylated PKC (*lane 2, pT641 panel*). This result indicates quantitative autophosphorylation of the *in vitro* phosphorylation site of PKC. To see if we could block this increase in Thr-17 phosphorylation pharmacologically, we performed another *in vitro* autophosphorylation assay in the absence or presence of the PKC inhibitor, Gö6983 (Figure 4.2 C). As shown previously, in the absence of ATP, PKC  $\beta$ II is not phosphorylated at Thr-17 (*lanes 1-2*) but robustly phosphorylated when ATP is added (*lane 3*). However, when the inhibitor Gö6983 is included in the reaction, phosphorylation at Thr-17 is blocked (*lane 4*). These data reveal that PKC  $\beta$ II autophosphorylates at Thr-17 *in vitro*.

*PKC  $\beta$ II autophosphorylates at Thr-17 in cells under phorbol ester stimulation and that autophosphorylation is enhanced with phosphatase inhibition* - Since we have the capability to assay Thr-17 phosphorylation with a phospho-specific antibody, we explored if PKC  $\beta$ II autophosphorylated at this site in cells. To determine if this phosphorylation was specific for Thr-17 in cells, we transfected tsA201 cells with WT PKC  $\beta$ II, PKC  $\beta$ II-S16A/T71A, or PKC  $\beta$ II-S16E/T17D and treated with the phorbol ester, PMA. (We mutated both autophosphorylation sites to prevent compensatory autophosphorylation at the adjacent serine). PKC was immunoprecipitated from detergent-solubilized lysates, and phosphorylation at Thr-17 was assessed by Western blot (Figure 4.3 A). WT PKC  $\beta$ II robustly autophosphorylated in the presence of PMA (*lane 2*). Importantly, immunoreactivity was absent when the sites were mutated to either non-phosphorylatable or phospho-mimetic residues (*lanes 4 and 6*). These data show that

the phospho-antibody specifically recognizes phosphorylated at Thr-17 in cells.

To assess the background of the phospho-Thr17 antibody in cells, we compared untreated and PMA-treated lysates for Thr17 phosphorylation from untransfected or COS7 cells transfected with WT PKC  $\beta$ II (Figure 4.3 B, lanes 1-4, *pT17 panel*). However, we were only able to detect Thr17 phosphorylation, albeit faintly, when we immunoprecipitated PKC  $\beta$ II from COS7 cells (*lane 6*). We hypothesized that this phosphorylation site may be highly sensitive to phosphatases. Therefore, we repeated the experiment in the presence of the phosphatase inhibitor, Calyculin A (*lanes 7-12*). In the presence of Calyculin A, some background signal that migrated at the same mobility as PKC was detected in the untransfected as well as the untreated PKC  $\beta$ II samples (*lanes 7-9, 11*). However, in the presence of PMA and Calyculin A, a robust signal was detected for PKC  $\beta$ II transfected lysates as well as immunoprecipitated PKC  $\beta$ II samples (*lanes 10 and 12*) in comparison to PMA-treated samples alone. These data indicate that Thr17 phosphorylation is sensitive to phosphatases; therefore, in future assays, we included Calyculin A in our samples in order to enhance Thr17 phosphorylation in cells.

To address whether endogenous PKC is phosphorylated at Thr17 in cells, we utilized the K562 lymphoma cell line that expresses high levels of endogenous PKC  $\beta$ II. K562 cells were treated with the phorbol ester PMA, and whole cell lysates were assayed for Thr-17 phosphorylation by Western blot (Figure 4.3 C, lanes 1-4). In the absence of PMA, some basal phosphorylation at Thr-17 is observed (*lane 1, pT17 (dark)*); however, upon treatment with PMA, phosphorylation at Thr-17 increased in a time-dependent manner, with maximal phosphorylation occurring between 0.25 and 1 h (*lanes 2 and 3*). At 4 h after PMA treatment, pT17 levels were reduced to near basal levels (*compare 1*

and 4). This decrease in phosphorylation observed at 4 h reflects the down-regulation of PKC protein that occurs upon treatment with phorbol esters (*note the decrease in total PKC  $\alpha$  and PKC  $\beta$ II levels, lane 4, PKC  $\alpha$  and PKC  $\beta$ II panels*). Upon reprobe of the pT17 blot, we noticed that this phosphorylation tracks with the slower mobility, fully phosphorylated species of PKC  $\beta$ II (*reprobe PKC  $\beta$ II panel, asterisk*). These data indicate that PKC  $\beta$ II autophosphorylates in cells at Thr-17 under both constitutive (basal) and induced (PMA) signals in K562 cells, suggesting that several factors contribute to PKC activation.

We noticed in our PMA time course in the K562 cells that the pT17 signal was not very robust, and it was only observed upon a very long exposure of the blot. We hypothesized that this phosphorylation may be readily susceptible to phosphatases; therefore, we wanted to test if global inhibition of bulk phosphatases in the cell with Calyculin A would boost the pT17 signal. K562 cells were treated with PMA in the presence of Calyculin A (Figure 4.3 C, *lanes 5-8*). Similar to the time course performed in the absence of Calyculin A, phosphorylation at Thr-17 is increased upon PMA stimulation with maximal phosphorylation occurring near 1 h (*lane 7*). However, the pT17 signal was greatly enhanced in the presence of Calyculin A (*compare lanes 5-8 to lanes 1-4 of both pT17 and pT17 (dark) panels; also note that a contaminating band is detected by the antibody that migrates near the mobility of PKC (arrow)*). This result is consistent with our over-expression studies in COS7 cells (Figure 4.3 B). Again, phosphorylation at Thr-17 was decreased as PKC levels were down-regulated with PMA treatment. Indeed, Calyculin A trapped the faster mobility, unphosphorylated species of PKC that is generated upon phorbol ester treatment (*lane 8, reprobe PKC  $\beta$ II panel,*

*dash*). These data suggest that phosphorylation at Thr-17 is highly labile and sensitive to bulk phosphatases in the cell.

As a control, we tested whether this autophosphorylation event in cells was sensitive to the PKC inhibitor, Gö6983. K562 cells were treated with PMA (and Calyculin A) in the absence or presence of Gö6983, and whole cell lysates were analyzed for pT17 by Western blot (Figure 4.3 D). Phosphorylation at Thr-17 increased upon PMA stimulation in a time-dependent manner (*lanes 2-3, asterisk*) that diminished as PKC  $\beta$ II levels were down-regulated (*lane 4, asterisk*). This increase in Thr-17 phosphorylation is abolished with Gö6983 (*lanes 5-8, arrow is contaminating band*); additionally, down-regulation of PKC is also inhibited because PKC activity is required for this process (*compare lanes 4 and 8, see Chapter 3*). Thus, these data show that PKC  $\beta$ II autophosphorylates at Thr-17 in cells when it is activated by phorbol esters.

*Autophosphorylation at Thr-17 in PKC  $\beta$ II is dependent upon the strength of the stimulus* - Phorbol esters are functional diacylglycerol analogues that bind PKC with a 200-fold higher affinity than diacylglycerol; these compounds potently and chronically activate PKC, ultimately resulting in its down-regulation (5). This strong stimulus of PKC induces autophosphorylation of PKC  $\beta$ II at Thr-17 (Figure 4.3). However, we were curious if other agonists, potentially natural agonists such as growth factors, could induce autophosphorylation at this site. To this end, we transfected COS7 cells with PKC  $\beta$ II-YFP (to induce a mobility shift from contaminating bands near the molecular weight of PKC – see Figure 4.3) and treated with either PMA or exogenous diacylglycerol (diC8) for the indicated times. PKC was immunoprecipitated from detergent-solubilized lysates, and pT17 was assessed by Western blot (Figure 4.4 A). Both agonists induced Thr-17

phosphorylation in a time-dependent manner that peaked between 0.5 and 1 h (*lanes 3-4* and *9-10*) and then declined as PKC levels began to down-regulate at longer time points (*lanes 5-6* and *lane 11-12*). Thus, exogenous diacylglycerol can stimulate autophosphorylation at Thr-17 similarly to PMA.

Next we tested if a natural agonist, which would generate physiological levels of diacylglycerol through activation of G<sub>q</sub>-coupled receptors, could promote autophosphorylation of PKC  $\beta$ II at Thr-17. COS7 cells were transfected with PKC  $\beta$ II-YFP, and cells were either treated with PMA or starved prior to treatment with LPA. In addition, these stimulations were performed in the absence or presence of the PKC inhibitor, Gö6983. PKC was immunoprecipitated from detergent-solubilized lysates, and pT17 was assessed by Western blotting (Figure 4.4 B). As shown previously, PMA promoted autophosphorylation at Thr-17 (*lane 2*) that was reduced to basal levels in the presence of the inhibitor (*compare lane 3 to lane 1*). LPA stimulation also promoted autophosphorylation, albeit to a much lower extent than PMA (*lane 5*), which was also reduced with the inhibitor (*lane 6*). Quantitative analysis of these data revealed a 10-fold increase in pT17 immunoreactivity with PMA (Figure 4.4 C, *grey columns*), but only a 30% increase in pT17 immunoreactivity with LPA (Figure 4.4 C, *black columns*). These data demonstrate that the amount of Thr-17 autophosphorylation tracks with the strength of the stimulus; PMA is a stronger agonist of PKC than the mitogen LPA.

*Autophosphorylated PKC  $\beta$ II localizes to membranes* – Because autophosphorylation at Thr-17 reflected an activation of PKC  $\beta$ II, we next asked where this activated species of PKC was localized in the cell. To this end, immunofluorescence was performed to determine the cellular localization of Thr-17-phosphorylated PKC  $\beta$ II.

COS7 cells were transfected with PKC  $\beta$ II-YFP and treated with PMA for 30 min, the approximate time where optimal phosphorylation occurs (Figure 4.4 A). In unstimulated cells, PKC  $\beta$ II-YFP was localized uniformly throughout the cytosol (Figure 4.5, *top row, YFP panel*). However, upon PMA treatment, COS7 cells underwent a dramatic morphological change as PKC  $\beta$ II-YFP translocated to the plasma membrane (*bottom row, YFP panel*). The phospho-Thr-17 signal only increased with PMA treatment in cells that were transfected with PKC  $\beta$ II-YFP (*bottom row, pT17 panel*). This Thr17-phosphorylated PKC species was concentrated at the plasma membrane (*bottom row, merge*), indicating that it is this translocated and activated species that autophosphorylates. These data reveal that Thr-17-phosphorylated PKC  $\beta$ II localizes to membranes.

*Mutation of the in vitro autophosphorylation sites in PKC  $\beta$ II does not alter intrinsic catalytic activity, maturation, or down-regulation.* – Phosphorylation at Thr-17 occurs when PKC is activated, and this phospho-species of PKC is localized at the membrane. However, the exact function of this phosphorylation still remains unknown. In order to delineate the function of this autophosphorylation, we utilized PKC mutants, PKC  $\beta$ II-S16A/T17A and PKC  $\beta$ II-S16E/T17D, a nonphosphorylatable and phospho-mimetic mutant, respectively, and assessed activity in an *in vitro* kinase assay (Figure 4.6 A). Lysates from tsA201 cells expressing WT PKC  $\beta$ II, PKC  $\beta$ II-S16A/T17A, or PKC  $\beta$ II-S16E/T17D were assayed for activity toward a PKC peptide substrate in the presence or absence of activating cofactors; activity attributed to the transfected PKC was obtained by subtracting the endogenous activity determined from control lysates. Mutation of the autophosphorylation sites to either nonphosphorylatable or phospho-mimetic mutants did

not significantly alter PKC activity relative to WT. Western blot analysis of the lysates revealed that both mutants expressed and migrated at a similar mobility as WT PKC  $\beta$ II (Figure 4.6 B, lanes 3 and 4). Thus, autophosphorylation at Thr-17 does not alter the intrinsic catalytic activity of PKC  $\beta$ II.

As a control, we next confirmed whether the mutation of Ser-16 and Thr-17 altered the processing of PKC into a mature, fully phosphorylated enzyme. The maturation of PKC can be monitored by a pulse-chase analysis. COS7 cells transfected with WT PKC  $\beta$ II, PKC  $\beta$ II-S16A/T17A, or PKC  $\beta$ II-S16E/T17D were pulse-labeled with [ $^{35}$ S]Met/Cys and chased for up to 90 min with unlabeled media. Immunoprecipitated PKC was analyzed by autoradiography, and the processing of the pulsed pool was determined by the mobility of the radiolabeled band on SDS-PAGE. The autoradiogram in Figure 4.6 C shows that newly synthesized PKC  $\beta$ II appeared as a faster migrating species (*lane 1, dash*) that shifted to a slower mobility species over the course of the chase (*lanes 2–4, asterisk*). The mobility shift reflects the two tightly coupled processing phosphorylations at the C terminus, the turn motif (Thr-641), and the hydrophobic motif (Ser-660) (Figure 4.1). Importantly, mutation of Ser-16 and Thr-17 to either Ala or Glu/Asp did not alter the rate of PKC processing; both mutants processed with half-time of approximately 15 min, similar to WT (*compare lanes 6-8 and 10-12 with 2-4*).

Chronic activation of PKC that occurs with phorbol esters results in the dephosphorylation, degradation, and depletion of PKC protein levels, a process termed ‘down-regulation’ (5). This process is activity-dependent; a catalytically-inactive PKC is unable to down-regulate (5). However, not much is really known about the molecular

mechanism of this process. One group has postulated that PEST sequences (Pro/Glu/Ser/Thr) in PKC may target PKC for degradation; indeed, phosphorylation in PEST sequences has been shown to target other signaling molecules for degradation (16,17). The autophosphorylation sites, Ser-16 and Thr-17, lie in a putative PEST sequence in PKC  $\beta$ II (16). We, therefore, hypothesized that autophosphorylation at Thr-17 could facilitate the phorbol ester-mediated down-regulation of PKC. COS7 cells were transiently transfected with WT PKC  $\beta$ II, PKC  $\beta$ II-S16A/T17A, or PKC  $\beta$ II-S16E/T17D and treated with PMA for the times indicated (Figure 4.6 D). For WT PKC  $\beta$ II, PMA treatment caused a characteristic increase in the amount of unphosphorylated PKC (*lanes 2-4, dash*), consistent with the ability of phorbol esters to promote the dephosphorylation and degradation of the enzyme (see Chapter 3). Similarly, both mutants, PKC  $\beta$ II-S16A/T17A and PKC  $\beta$ II-S16E/T17D, also showed a similar increase in unphosphorylated PKC with PMA treatment (*lanes 6-8 and lanes 10-12, dash*). Quantitative analysis of these data indicates that all three constructs showed a similar decrease in PKC levels at 8 h PMA treatment (Figure 4.6 E). Therefore, mutation of the Ser-16 and Thr-17 autophosphorylation sites does not alter the ability of PKC to be down-regulated by phorbol esters.

*Autophosphorylation at Ser-16 and Thr-17 in PKC  $\beta$ II delays translocation to membranes* – Membrane translocation of PKC, which occurs upon binding to lipid second messengers, is the ‘hallmark’ of PKC activation and can be monitored in real-time in live cells. Once PKC binds the second messengers,  $\text{Ca}^{2+}$  and diacylglycerol, the autoinhibitory pseudosubstrate is expelled from the active site, resulting in an activated kinase capable of phosphorylating downstream substrates (18). The *in vitro*

autophosphorylation sites Ser-16 and Thr-17 are located a few residues before the pseudosubstrate; this peptide region is rich in basic residues that favorably interact with acidic phospholipids in the membrane (19). Therefore, we were curious if autophosphorylation or having negative charge locked at these sites (phospho-mimetic) would hinder translocation and interaction with the membrane or serve as a possible mechanism for release from the membrane. COS7 cells were co-transfected with a plasma membrane-targeted CFP (PM-CFP) and WT PKC  $\beta$ II-YFP, PKC  $\beta$ II-S16A/T17A, or PKC  $\beta$ II-S16E/T17D, and translocation to the plasma membrane was monitored as an increase in the ratio of FRET-based YFP emission:CFP emission (FRET ratio) (13). To stimulate the production of diacylglycerol at the plasma membrane, COS7 cells were treated with UTP, which acts through endogenous P2Y receptors (20). Figure 4.7 shows that stimulation of COS7 cells with UTP resulted in an increase in FRET ratio for all three constructs. Interestingly, the nonphosphorylatable mutant, PKC  $\beta$ II-S16A/T17A-YFP (*open squares*) responded first while WT PKC  $\beta$ II-YFP (*open circles*) and PKC  $\beta$ II-S16E/T17D-YFP (*open diamonds*) lagged behind. In fact, PKC  $\beta$ II-S16E/T17D-YFP responded weakly compared to the other two constructs, suggesting that the negative charge may be hindering translocation to the membrane. These data demonstrate that negative charge at the *in vitro* autophosphorylation sites, Ser-16 and Thr-17, delay translocation to the plasma membrane upon agonist stimulation.

## Discussion

In this study, we generated a phospho-specific antibody to Thr-17 in PKC  $\beta$ II, a previously identified *in vitro* autophosphorylation site, in order to investigate its biological function. We found that PKC  $\beta$ II autophosphorylates at this site both *in vitro* and in cells under stimulation by various agonists. This phosphorylated species of PKC  $\beta$ II is localized to the plasma membrane upon phorbol ester stimulation; however, a phospho-mimetic at this position hinders translocation under UTP stimulation. Interestingly, we found no difference in kinase activity, maturation, or phorbol ester-mediated down-regulation of either a nonphosphorylatable or phospho-mimetic mutant. These data confirm that PKC  $\beta$ II does autophosphorylate at Thr-17 in cells, although the functional consequence still remains unknown.

We generated phospho-specific antibodies to both the Ser-16 and Thr-17 autophosphorylation sites in PKC  $\beta$ II. However, by dot blot assay, only the Thr-17 site is phospho-specific. PKC  $\beta$ II robustly autophosphorylates at Thr-17 *in vitro*, which is blocked by a PKC inhibitor. Interestingly, a slight mobility shift was observed with the autophosphorylated PKC species; this shift may be indicative of phosphorylation at not only Thr-17 but possibly other sites, such as the other *in vitro* autophosphorylation sites.

Using this phospho-specific antibody, we demonstrated that exogenous PKC  $\beta$ II autophosphorylates in cells at Thr-17 upon PMA, exogenous diacylglycerol, and LPA stimulation. We utilized COS7 cells as our model system because they lack endogenous PKC  $\beta$ II and would provide a clean background for studying autophosphorylation at this site. Both PMA and diC8 induced Thr-17 phosphorylation in a time-dependent manner,

which decreased as PKC was down-regulated by these stimuli. Interestingly, we also observed Thr-17 phosphorylation upon stimulation of endogenous LPA receptors. However, the increase observed with LPA was ~30-fold less than that of the PMA. This difference could be attributed to the rapid removal of the second messenger diacylglycerol that occurs under physiological conditions (due to the metabolizing activities of diacylglycerol kinases) versus the prolonged presence of the high-affinity phorbol esters in the membrane (5). However, these data show our phospho-antibody can serve as readout for PKC activation in response to natural stimuli.

Thr-17-phosphorylated PKC  $\beta$ II was localized to the plasma membrane upon activation with phorbol esters. However, mutation of the autophosphorylation site to alanine did not prevent translocation from occurring with UTP stimulation, indicating that autophosphorylation is not driving this process. In fact, autophosphorylation has been shown to be a mechanism of 'reverse translocation,' relocalization back to the cytosol. This mechanism of 'reverse translocation' directly opposes the action of the membrane-targeting modules, the C1 and C2 domains, which drive PKC to the membrane (21). Interestingly, the phospho-mimetic mutant showed a delayed translocation to membranes in response to UTP, supporting this model. Acute activation of PKC that occurs through activation of  $G_q$ -coupled receptors results in a transient translocation unlike phorbol esters, which chronically activate PKC and prolong membrane interaction. Further studies are needed to investigate whether Thr-17-phosphorylated PKC  $\beta$ II can be detected with natural agonist stimulation as well as whether this phospho-specific antibody can be used as marker for activated PKC in tissue samples from pathological states.

PKC  $\beta$ II autophosphorylates at Thr-17 in cells in response to PMA, an event that is significantly enhanced by inhibition of cellular phosphatases. Thr-17 lies N-terminal to the autoinhibitory pseudosubstrate, which rests in the active site until PKC is activated by second messengers. A space-filling model of PKC  $\beta$ II with this sequence docked into the active site reveals that the negative charge from phosphate at Thr-17 would be repelled by the surrounding acidic residues, thus potentially kicking it out of the active site into a more exposed conformation (Figure 4.8, A, *red*). This conformational change would make phosphorylation at Thr-17 more phosphatase labile. Indeed, we found that inclusion of Calyculin A in our time courses enhanced Thr-17 phosphorylation compared with PMA-treated samples that lacked it.

Using a pharmacological inhibitor, we have shown that PKC activity is required for PMA-induced phosphorylation of endogenous PKC  $\beta$ II in K562 cells. This result is consistent with the *in vitro* data. In cells, it is possible that other PKC isozymes could phosphorylate these sites. Although we only tested Gö6983, which inhibits all PKC isozymes, a predictive database that looks at putative PKC  $\delta$  and PKC  $\zeta$  phosphorylation sites did not favor either Ser-16 or Thr-17 as favorable phosphorylation sites for these isozymes, suggesting that these sites are highly likely to be specific for PKC  $\beta$ II (22). However, further studies are needed to address whether other conventional PKC isozymes, such as PKC  $\alpha$ , can phosphorylate them.

Functionally, we have been unable to identify a clear role for these autophosphorylation sites using the assays tested in this study. Both mutants, PKC  $\beta$ II-S16A/T17A and PKC  $\beta$ II-S16E/T17D, did not show any difference in activity, maturation, or phorbol ester-mediated down-regulation. An early study also failed to find

any significant difference of these mutants with WT PKC  $\beta$ II (11). However, sequence alignment indicates that these sites are highly conserved among different organisms, suggesting a functional significance (Figure 4.8 B). This sequence is unique to PKC  $\beta$ II, indicating an isozyme-specific purpose. Further analysis is required to delineate the purpose of this specific modification to PKC  $\beta$ II.

In summary, we have shown that PKC  $\beta$ II autophosphorylates *in vitro* and in cells at Thr-17 in its N-terminus immediately preceding the pseudosubstrate. This phosphorylation can occur under strong, chronic stimuli (phorbol esters) or weak, acute stimuli (LPA), and this phosphorylated species of PKC  $\beta$ II localizes to the membrane when activated. Although its direct functional consequence remains unknown, the Thr-17 phospho-specific antibody could serve as a potential marker for activated PKC in the cell as been shown for other PKC isozymes (6-9).

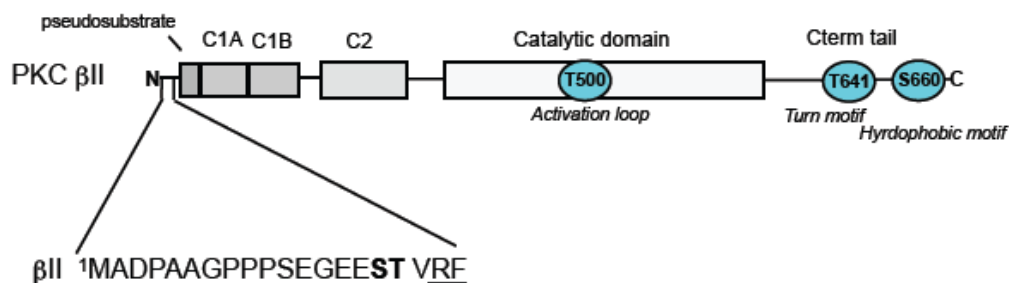


**Figure 4.1:** Location of the *in vitro* autophosphorylation sites in PKC  $\beta$ II. Schematic representation of the domain composition of PKC  $\beta$ II showing the pseudosubstrate, C1A and C1B domains, and C2 domain in the N-terminal regulatory moiety followed by the catalytic domain and C-terminal tail in the kinase moiety. The three processing phosphorylation sites, activation loop (T500), turn motif (T641), and hydrophobic motif (S600), in PKC  $\beta$ II are indicated by cyan circles. The two autophosphorylation sites preceding the pseudosubstrate (*underlined* in sequence) (Ser-16 and Thr-17) are indicated in *bold* in the sequence below.

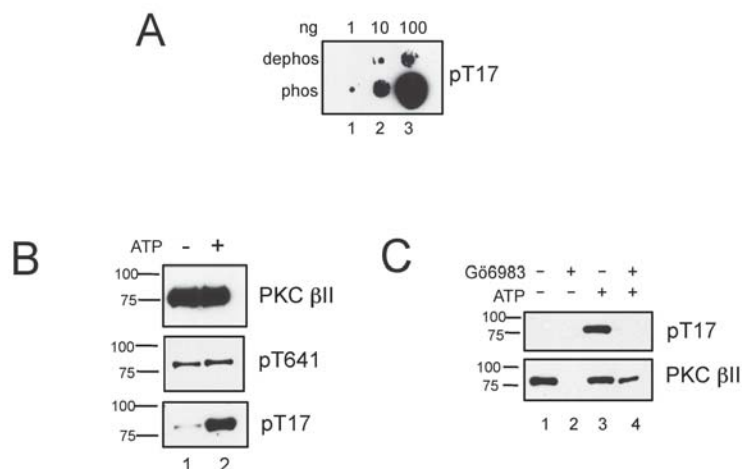


**Figure 4.2:** PKC  $\beta$ II autophosphorylates at Thr-17 *in vitro*. *A*, Dot blot showing reactivity of affinity-purified, phospho-specific pT17 antibody with 1 ng (*lane 1*), 10 ng (*lane 2*), or 100 ng (*lane 3*) of the unphosphorylated and phosphorylated, immunizing peptide. The dephospho peptide sequence is Ac-CSEGEESTVRFARKGA-NH<sub>2</sub>, and the phospho peptide sequence is Ac-CSEGEEST(PO<sub>3</sub>H<sub>2</sub>)VRFARKGA-NH<sub>2</sub>. *B*, *In vitro* autophosphorylation assay of purified, His-PKC  $\beta$ II in the absence (*lane 1*) or presence (*lane 2*) of 100  $\mu$ M ATP. Phosphorylation at the turn motif phosphorylation site (pT641) and the autophosphorylation site (pT17) as well as total PKC (PKC  $\beta$ II) were assessed by Western blotting. *C*, *In vitro* autophosphorylation assay of purified, His-PKC  $\beta$ II in the absence (*lanes 1 and 2*) and presence (*lanes 3 and 4*) of 100  $\mu$ M ATP and in the absence (*lanes 1 and 3*) and presence (*lanes 2 and 4*) of 1  $\mu$ M G66983. Phosphorylation at the autophosphorylation site (pT17) and total PKC (PKC  $\beta$ II) were assessed by Western blotting.

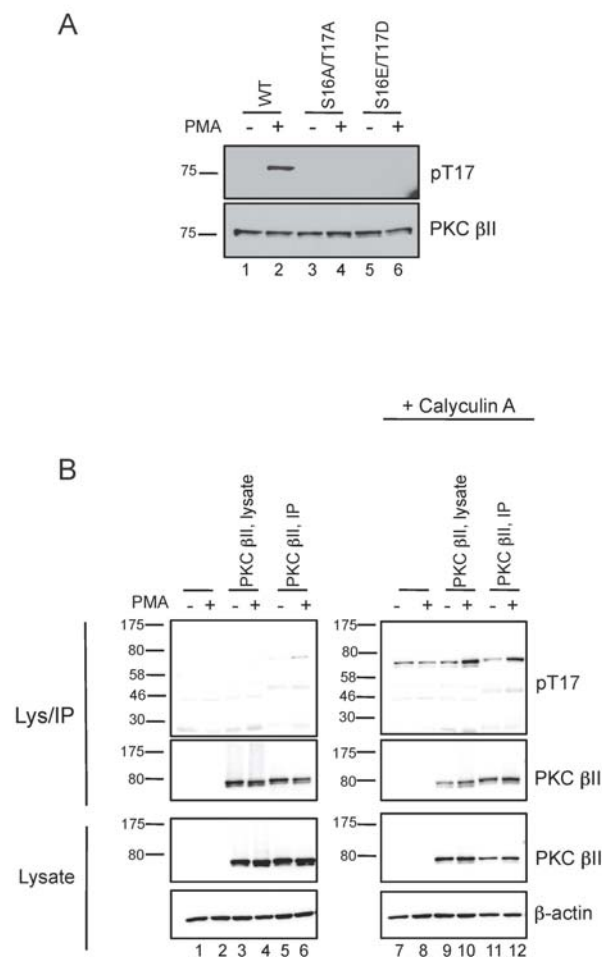


**Figure 4.3:** Endogenous PKC  $\beta$ II autophosphorylates at Thr-17 in cells under phorbol ester stimulation, which is enhanced with inhibition of phosphatases and diminished by inhibition of PKC. *A*, tsA201 cells were transiently transfected with WT PKC  $\beta$ II (*lanes 1-2*), PKC  $\beta$ II-S16A/T17A (*lanes 3-4*), or PKC  $\beta$ II-S16E/T17D (*lanes 5-6*) and treated with 200 nM PMA for 15 min. PKC was immunoprecipitated from detergent-solubilized lysates, separated by SDS-PAGE, and analyzed by Western blotting for phosphorylation at Thr-17 (pT17) and total PKC (PKC  $\beta$ II). *B*, Untransfected COS7 cells (*lanes 1-2, 7-8*) or COS7 cells that were transiently transfected with WT PKC  $\beta$ II (*lanes 3-6, 9-12*) and treated with 200 nM PMA for 15 min in the absence (*lanes 1-6*) or presence (*lanes 7-12*) of 50 nM Calyculin A. PKC was either immunoprecipitated (*lanes 5-6, 11-12*) or whole cell lysates (*lanes 1-4, 7-10*) were analyzed by SDS-PAGE for Thr17 phosphorylation (pT17). The amount of PKC in the immunoprecipitates was detected by the PKC  $\beta$  antibody (*IP*). The amount of PKC in whole cell lysates (*lanes 1-4, 7-10*) as well as the input for the immunoprecipitations (*lanes 5-6, 11-12*) were also detected by the PKC  $\beta$  antibody.

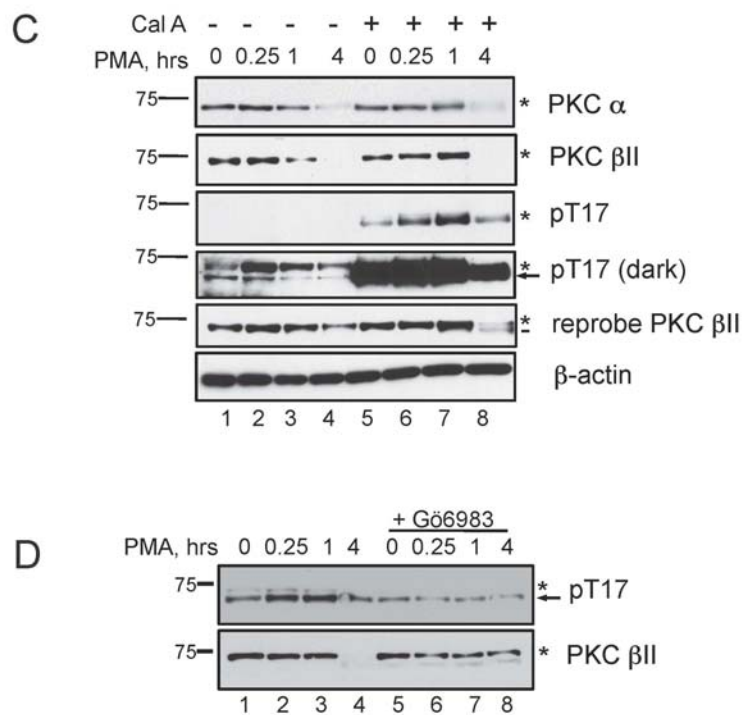


**Figure 4.3:** (continued) *C*, K562 cells were treated with 200 nM PMA for the indicated times in the absence (*lanes 1-4*) or presence (*lanes 5-8*) of 50 nM Calyculin A. Whole cell lysates were separated by SDS-PAGE and analyzed by Western blotting for total PKC (PKC  $\alpha$  and PKC  $\beta$ II), phosphorylation at Thr-17 (pT17) and total protein content ( $\beta$ -actin). *D*, K562 cells were treated with 200 nM PMA for the indicated times in the absence (*lanes 1-4*) or presence (*lanes 5-8*) of 1  $\mu$ M Gö6983. Whole cell lysates were separated by SDS-PAGE and analyzed by Western blotting for phosphorylation at Thr-17 (pT17) and total PKC (PKC  $\beta$ II).

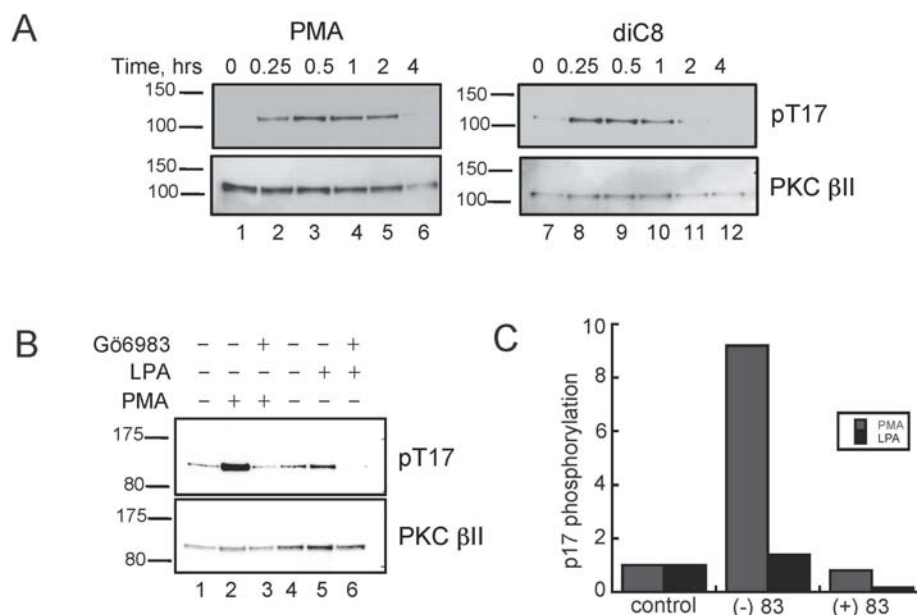


**Figure 4.4:** PKC  $\beta$ II robustly autophosphorylates at Thr-17 in the presence of phorbol esters and exogenous diacylglycerol but only weakly under natural agonist conditions. *A*, COS7 cells were transiently transfected with PKC  $\beta$ II-YFP and stimulated with 200 nM PMA (*lanes 1-6*) or 100  $\mu$ M diC8 (*lanes 7-12*) for the indicated times. PKC was immunoprecipitated from detergent-solubilized lysates and assessed for pT17 phosphorylation and total PKC by Western blotting. *B*, COS7 cells were transiently transfected with PKC  $\beta$ II-YFP and stimulated with 200 nM PMA (*lanes 2-3*) for 15 min in the absence (*lane 2*) or presence (*lane 3*) of 1  $\mu$ M Gö6983 or starved for 6 h prior to stimulation with 10  $\mu$ M LPA (*lanes 5-6*) for 15 min in the absence (*lane 5*) or presence (*lane 6*) of 1  $\mu$ M Gö6983. PKC was immunoprecipitated from detergent-solubilized lysates and assessed for Thr-17 phosphorylation (pT17) and total PKC by Western blotting. *C*, a graph showing densitometric analysis of Western blots in *B*.

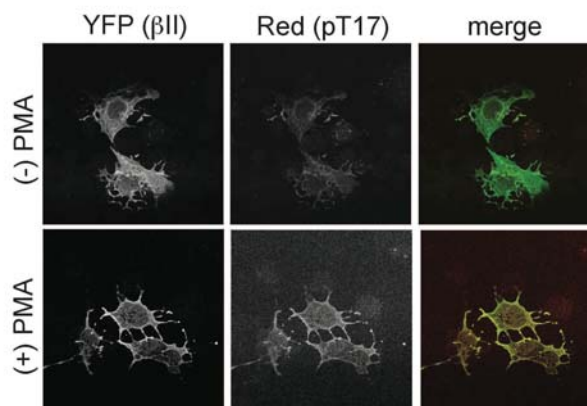


**Figure 4.5:** PKC  $\beta$ II that is phosphorylated at Thr-17 is localized at the membrane upon phorbol ester stimulation. Representative images of COS7 cells transiently transfected with PKC  $\beta$ II-YFP and immunostained for Thr-17 phosphorylation (*middle panels*) in the absence (*top panels*) or presence (*bottom panels*) of 200 nM PMA for 15 min.

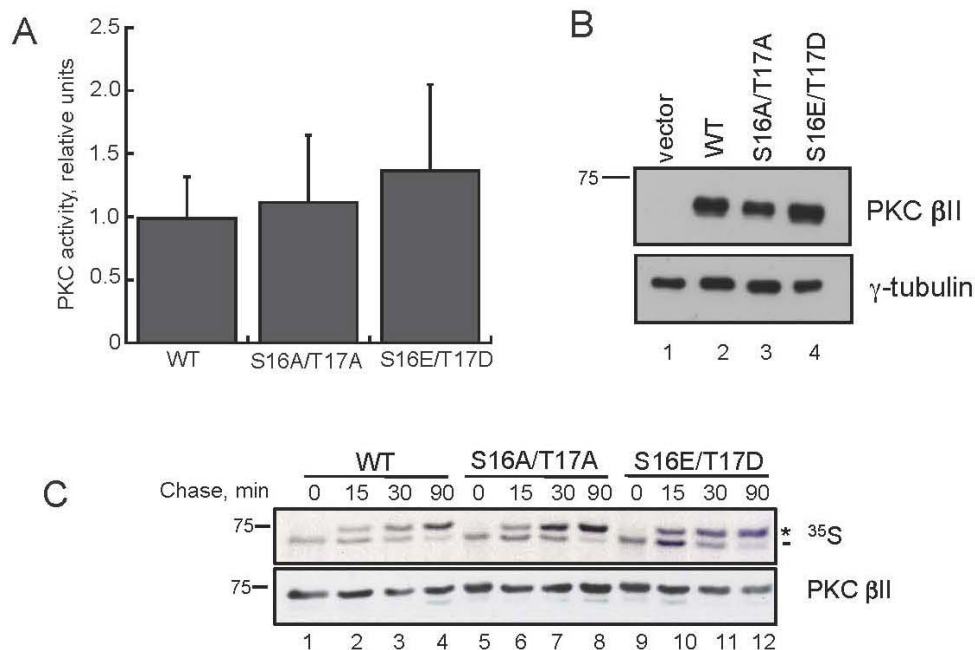


**Figure 4.6:** Mutation in the *in vitro* autophosphorylation sites, Ser-16 and Thr-17, in PKC  $\beta$ II to either nonphosphorylatable or phospho-mimetic residues does not alter its catalytic activity, its ability to be processed, or its down-regulation by phorbol esters. *A*, lysates from tsA201 cells expressing WT PKC  $\beta$ II, PKC  $\beta$ II-S16A/T17A or PKC  $\beta$ II-S16E/T17D were assayed for PKC activity in the absence or presence of lipid and  $\text{Ca}^{2+}$ . Cofactor-dependent activity attributed to transfected PKC  $\beta$ II (*i.e.* after subtraction of endogenous activity obtained from control lysates) was normalized to PKC  $\beta$ II expression in the lysate determined by Western blot. Data represent the mean  $\pm$  S.E. from six independent experiments. *B*, Western blot showing the expression of WT  $\beta$ II (*lane 2*), PKC  $\beta$ II-S16A/T17A (*lane 3*), and PKC  $\beta$ II-S16E/T17D (*lane 4*) used in the kinase assay with the indicated antibody. Lysates were probed with  $\gamma$ -tubulin as a loading control (*lower panel*). *C*, autoradiogram from a pulse-chase analysis of COS7 cells transfected with WT PKC  $\beta$ II (*lanes 1-4*), PKC  $\beta$ II-S16A/T17A (*lanes 5-8*), or PKC  $\beta$ II-S16E/T17D (*lanes 9-12*). Transfected cells were labeled with [ $^{35}$ S]Met/Cys and then chased for the indicated times. PKC was immunoprecipitated from detergent-solubilized lysates and analyzed by autoradiography. The *asterisk* denotes the position of mature, fully phosphorylated PKC, and the *dash* denotes the position of newly synthesized, unphosphorylated PKC. An anti-PKC  $\beta$ II antibody indicates the amount of PKC in the immunoprecipitates.

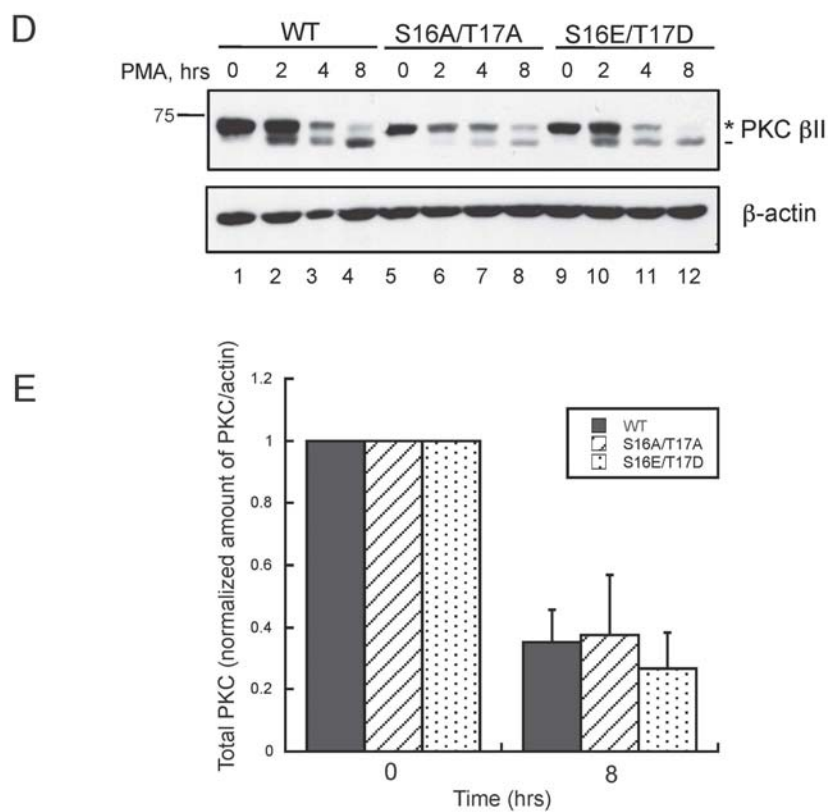


**Figure 4.6:** (continued) *D*, COS7 cells were transiently transfected with WT PKC  $\beta$ II (lanes 1-4), PKC  $\beta$ II-S16A/T17A (lanes 5-8), or PKC  $\beta$ II-S16E/T17D (lanes 9-12) and stimulated with 200 nM PMA for the indicated times. Whole cell lysates were separated by SDS-PAGE and analyzed by Western blotting for total PKC (PKC  $\beta$ II) or total protein content ( $\beta$ -actin). The *asterisk* denotes the position of fully phosphorylated PKC, and the *dash* denotes the position of unphosphorylated PKC. *E*, a graph representing densitometric analysis of the Western blot shown in *D*. Data represent the mean  $\pm$  S.E. of four independent experiments.

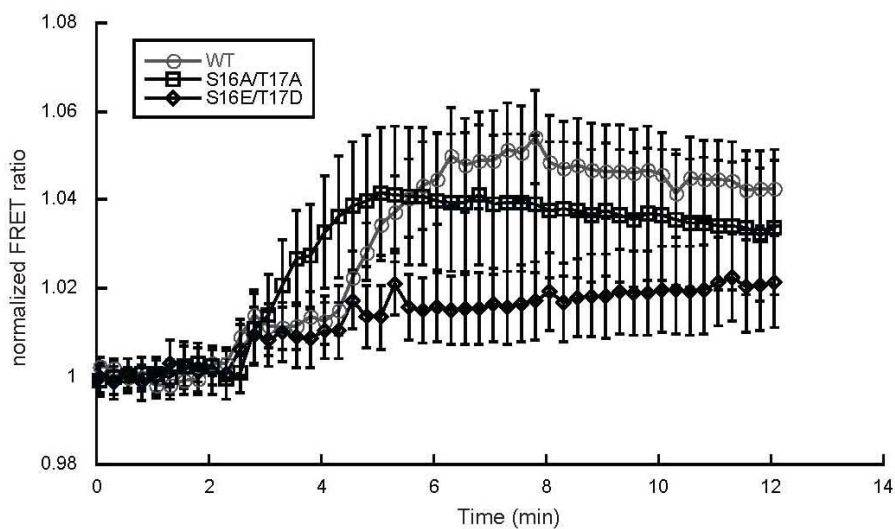


**Figure 4.7:** The phospho-mimetic, PKC  $\beta$ II-S16E/T17D, shows a reduced translocation to membranes upon agonist stimulation. COS7 cells were co-transfected with WT PKC  $\beta$ II-YFP (*open circles*), PKC  $\beta$ II-S16A/T17A-YFP (*open squares*), or PKC  $\beta$ II-S16E/T17D-YFP (*open diamonds*) with PM-CFP. The relative translocation in response to UTP (100  $\mu$ M) and PDBu (200 nM) treatment was calculated and plotted as a function of time. Data represent the mean  $\pm$  S.E. of 15-20 cells from three independent experiments.

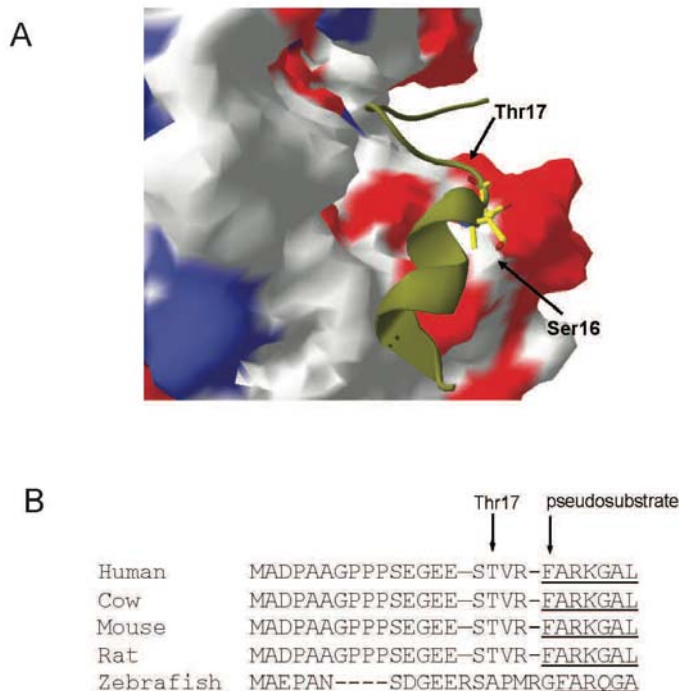


**Figure 4.8:** Sequence conservation of Thr-17 in PKC  $\beta$ II and a model of how Thr-17 may be sensitive to phosphatases. *A*, space filling model of the catalytic domain of PKC  $\beta$ II with N-terminal 18 residues indicated in *yellow* and the autophosphorylation sites indicated as *sticks* representation. *Blue* denotes basic, *grey* denotes nonpolar, and *red* denotes acidic regions in the protein. *B*, sequence alignment of the first 26 residues in PKC  $\beta$ II from human (NP\_002729.2), cow (NP\_777012.1), mouse (NP\_023881.1), rat (NP\_036845.2), and zebrafish (NP\_957272.1). The pseudosubstrate peptide sequence is *underlined*.

## References

1. Newton, A. C. (2003) *Biochem J* **370**, 361-371
2. Keranen, L. M., Dutil, E. M., and Newton, A. C. (1995) *Curr Biol* **5**, 1394-1403
3. Facchinetti, V., Ouyang, W., Wei, H., Soto, N., Lazorchak, A., Gould, C., Lowry, C., Newton, A. C., Mao, Y., Miao, R. Q., Sessa, W. C., Qin, J., Zhang, P., Su, B., and Jacinto, E. (2008) *EMBO J* **27**, 1932-1943
4. Ikenoue, T., Inoki, K., Yang, Q., Zhou, X., and Guan, K. L. (2008) *EMBO J* **27**, 1919-1931
5. Gould, C. M., and Newton, A. C. (2008) *Curr Drug Targets* **9**, 614-625
6. Thuille, N., Heit, I., Fresser, F., Krumbock, N., Bauer, B., Leuthaeusser, S., Dammeier, S., Graham, C., Copeland, T. D., Shaw, S., and Baier, G. (2005) *Embo J* **24**, 3869-3880
7. Ng, T., Squire, A., Hansra, G., Bornancin, F., Prevostel, C., Hanby, A., Harris, W., Barnes, D., Schmidt, S., Mellor, H., Bastiaens, P. I., and Parker, P. J. (1999) *Science* **283**, 2085-2089
8. Durgan, J., Michael, N., Totty, N., and Parker, P. J. (2007) *FEBS Lett* **581**, 3377-3381
9. Littler, D. R., Walker, J. R., She, Y. M., Finerty, P. J., Jr., Newman, E. M., and Dhe-Paganon, S. (2006) *Biochem Biophys Res Commun* **349**, 1182-1189
10. Flint, A. J., Paladini, R. D., and Koshland, D. E., Jr. (1990) *Science* **249**, 408-411
11. Tsutakawa, S. E., Medzihradszky, K. F., Flint, A. J., Burlingame, A. L., and Koshland, D. E., Jr. (1995) *J Biol Chem* **270**, 26807-26812
12. Dries, D. R., Gallegos, L. L., and Newton, A. C. (2007) *J Biol Chem* **282**, 826-830
13. Gallegos, L. L., Kunkel, M. T., and Newton, A. C. (2006) *J Biol Chem* **281**, 30947-30956
14. Edwards, A. S., Faux, M. C., Scott, J. D., and Newton, A. C. (1999) *J Biol Chem* **274**, 6461-6468
15. Sonnenburg, E. D., Gao, T., and Newton, A. C. (2001) *J Biol Chem* **276**, 45289-45297

16. Lee, H. W., Smith, L., Pettit, G. R., and Smith, J. B. (1997) *Mol Pharmacol* **51**, 439-447
17. Rechsteiner, M., and Rogers, S. W. (1996) *Trends Biochem Sci* **21**, 267-271
18. Dutil, E. M., and Newton, A. C. (2000) *J Biol Chem* **275**, 10697-10701
19. Mosior, M., and McLaughlin, S. (1991) *Biophys J* **60**, 149-159
20. Balboa, M. A., Firestein, B. L., Godson, C., Bell, K. S., and Insel, P. A. (1994) *J Biol Chem* **269**, 10511-10516
21. Feng, X., and Hannun, Y. A. (1998) *J Biol Chem* **273**, 26870-26874
22. Fujii, K., Zhu, G., Liu, Y., Hallam, J., Chen, L., Herrero, J., and Shaw, S. (2004) *Proc Natl Acad Sci U S A* **101**, 13744-13749

## Chapter 5

# Determining the Contribution of mTOR Kinase Activity to the Maturation of PKC

**Abstract**

Studies over the last several years have shown that the maturation of PKC into a fully phosphorylated enzyme is not as simple as phosphorylation by the upstream kinase PDK-1 and subsequent autophosphorylation at the C-terminus. Recent evidence now indicates that the mTORC2 complex, consisting of the kinase mTOR, Rictor, mLST8, and Sin1, can regulate this process. However, whether this regulation occurs through direct phosphorylation of PKC or through an indirect mechanism remains unclear. This chapter focuses on the role of mTOR kinase activity in the processing of PKC. By utilizing an ATP-competitive inhibitor to mTOR, we show that mTOR's activity facilitates the processing of PKC at the C-terminal phosphorylation sites, the turn motif and the hydrophobic motif. However, endogenous PKC or a membrane-tethered PKC construct is insensitive to the inhibitor. Using the FRET-based CKAR reporter in mTORC2 functional and deficient cells, we find that over-expressed PKC is processed and active in cells lacking a functional mTORC2 complex. Our studies confirm that mTOR kinase activity is required for the proper maturation of PKC. However, this requirement can be bypassed and is not essential. Future work is still required in order to clearly define the role of mTORC2 in the processing of PKC.

## Introduction

The mammalian target of rapamycin (mTOR) is a conserved serine/threonine kinase of the phosphatidylinositol-3-kinase-related kinases (PIKK) family that is a critical regulator of cell growth and a recently favored target in cancer therapeutics (1,2). As the name implies, mTOR is a target of the drug rapamycin, a macrolide antibiotic from *Streptomyces hygroscopicus*, which exerts its effects by binding a small protein receptor FK506-binding protein 12 kDa (FKBP12); this complex binds mTOR and inhibits phosphorylation of some downstream substrates. mTOR forms two functionally distinct complexes in the cell, mTOR complex 1 (mTORC1) and mTOR complex 2 (mTORC2). A primary, distinguishing difference between these two complexes is that mTORC1 is sensitive to rapamycin while mTORC2 is not (3-5). The mTORC1 complex consists of mTOR, regulatory associated protein of mTOR (Raptor), mammalian lethal with Sec13 protein 8 (mLST8); recent work has identified additional constituents such as Proline-rich Akt substrate 40 kDa (PRAS40) and DEPTOR (6-8). Raptor is a key scaffolding protein of the mTORC1 complex; rapamycin inhibits mTORC1 by disrupting this critical interaction (9-11). The mTORC2 complex consists of mTOR, rapamycin-insensitive companion of mTOR (Rictor), mLST8, Sin1, and protein associated with Rictor (Protor) (3,12-15). Both of these complexes mediate cellular processes responsible for the increase in cell size such as translation, ribosome biogenesis, nutrient transport, autophagy, and more recently, AGC kinase activation.

The factors that control the regulation of the mTORC1 complex are more widely understood. mTORC1 responds to four inputs: nutrients (amino acids), growth factors (insulin), cellular energy levels (AMP:ATP ratio), and stress (hypoxia). The major

upstream regulators of mTORC1 are the tuberous sclerosis complex 1/2 (TSC1/TSC2) and the Rheb GTPase (4). In its GTP-bound, active form, Rheb stimulates mTORC1 activity; however, TSC2 acts as a GTPase activating protein (GAP) to convert Rheb to its GDP-bound form, thus inhibiting mTORC1 (16). Upon stimulation with growth factors, phosphorylation of PRAS40 and TSC1/TSC2 by Akt results in activation of the Rheb (and thus mTORC1) by relieving the inhibition of TSC1/TSC2 (17-19). Through these two regulators, mTORC1 integrates signals from growth factors and energy levels to regulate protein translation by phosphorylation of two primary targets, p70 ribosomal S6 kinase (S6K) and eukaryotic initiation translation factor 4EB binding protein 1 (4EBP1) (4,20). mTORC1 phosphorylates S6K, an AGC kinase family member, at the conserved hydrophobic motif (11,21). These two proteins serve as markers of mTORC1 activity. In contrast, the upstream factors that regulate the function of mTORC2 are still unknown.

Recent studies have identified a specific function of the mTORC2 complex: regulation of AGC kinase phosphorylation (13,22). mTORC2 phosphorylates S6K1 at the conserved hydrophobic motif, which consists of Phe-X-X-Phe-Ser/Thr-Tyr (where X is any amino acid). Phosphorylation at the hydrophobic motif has been extensively studied in AGC kinases. Structurally, this phosphorylation stabilizes the closed, active conformation and allows proper positioning of the residues necessary for catalysis (23). Studies have shown that PKC autophosphorylates at this site by an intramolecular mechanism to promote its stability and increase phosphatase resistance (24-27). For another AGC kinase family member, Akt, studies have debated over the existence of a phosphoinositide-dependent kinase 2 (PDK-2), which would phosphorylate Akt at the hydrophobic motif (Ser473 in Akt1), or whether this phosphorylation also occurs through

intramolecular autophosphorylation like PKC. mTORC2 was initially characterized as this putative PDK-2; studies in which mTORC2 was genetically ablated by RNAi showed a decreased phosphorylation of the hydrophobic motif of Akt (13,28-30). In addition, purified mTORC2 can phosphorylate recombinant Akt *in vitro*, suggesting that this complex directly regulates this site (28). In Rictor<sup>-/-</sup> MEFs, which lack functional mTORC2, Ser473 phosphorylation is diminished, indicating that this phosphorylation could serve as a marker for mTORC2 activity *in vivo* (13,14,31,32). Interestingly, in these cells, there is decreased hydrophobic motif phosphorylation of PKC as well as decreased protein levels; this result is consistent with the role of hydrophobic motif phosphorylation in promoting the stability of PKC (13). While mTORC2 control of the hydrophobic motif phosphorylation of Akt is growth factor-dependent, mTORC2 control of PKC is not.

Interestingly, in another *in vivo* model of dysfunctional mTORC2, the Sin1<sup>-/-</sup> MEFs, Akt and PKC lack phosphorylation not only at the hydrophobic motif but also at the turn motif, another highly conserved C-terminal phosphorylation site in AGC kinases (32,33). This sequence, which exists primarily as a Ser/Thr-Pro in most AGC kinases, was initially characterized in PKC as the rate-limiting step in the maturation of the catalytically-competent species; mutation of the turn motif in PKC abrogates catalytic activity and prevents hydrophobic motif phosphorylation (34). Structurally, the turn motif phosphorylation also serves a stabilizing role for the active conformation and may also protect the hydrophobic motif from dephosphorylation (35). For Akt, the turn motif is constitutively phosphorylated shortly after synthesis, but this phosphorylation is not required for hydrophobic motif phosphorylation as is the case for PKC (36,37). In

mTORC2-deficient cells, Akt and PKC lack phosphorylation at the turn motif, which leads to their increased ubiquitination and decreased stability (33). For PKC, this lack of turn motif phosphorylation in mTORC2-deficient cells provides one explanation why earlier studies showed a lack of hydrophobic motif phosphorylation in similar conditions: phosphorylation of the hydrophobic motif depends on the turn motif. Although these studies have shown that turn motif phosphorylation is mTORC2-dependent, the mechanism by which mTORC2 controls these phosphorylation sites remain unclear. Direct phosphorylation of PKC by mTORC2 has not been shown; however, inhibition of mTOR kinase activity decreases phosphorylation of these sites (22,32,38).

Here, we utilize an ATP-competitive inhibitor of mTOR, PI-103, to dissect the role of mTOR kinase activity in the maturation of PKC. By pulse-chase analysis, we find that mTOR activity is necessary for both turn motif and hydrophobic motif phosphorylation. However, the processing of endogenous PKC and membrane-tethered PKC is insensitive to mTOR inhibition. In cells that lack functional mTORC2, over-expressed PKC is mature and active, thus bypassing the requirement of mTORC2 for maturation. These studies confirm the role of mTOR kinase activity in the maturation of PKC; however, the mechanism by which mTORC2 controls these phosphorylations still remains unclear.

## Materials and Methods

*Materials* - Sin1<sup>+/+</sup> MEFs and Sin1<sup>-/-</sup> MEFs were a kind gift from Estela Jacinto (UMDNJ). Easy Tag [<sup>35</sup>S]Met/Cys (1175 Ci mmol<sup>-1</sup>) was purchased from PerkinElmer Life Sciences. Met/Cys-deficient DMEM was purchased from Invitrogen. Phorbol-12,13-dibutyrate (PDBu), KT5720, and Gö6983 were purchased from Calbiochem. PI-103 and OSU03012 were purchased from Cayman Chemical. Polyclonal antibodies to PKC  $\beta$ II and PKC  $\alpha$  were purchased from Santa Cruz Biotechnology. Monoclonal antibodies to PKC  $\alpha$  and PKC  $\beta$  were purchased from B.D. Transduction Laboratories. Polyclonal antibodies to the turn motif phosphorylation site (PKC  $\alpha$ / $\beta$ II-Thr638/641) of PKC, the hydrophobic motif phosphorylation site (PKC  $\beta$ II Ser-660) of PKC, the activation loop phosphorylation site of Akt (Thr-308), total S6K, and the hydrophobic motif of S6K (Thr-389) were purchased from Cell Signaling Technology. Monoclonal antibodies to  $\beta$ -actin and the Flag epitope were purchased from Sigma Aldrich. A monoclonal antibody to the HA epitope was purchased from Roche Applied Sciences. A polyclonal antibody to dsRed (to detect RFP) was purchased from Clontech. Ultra-Link protein A/G beads were purchased from Thermo Scientific. Electrophoresis reagents were obtained from Biorad. All other chemicals and materials were reagent-grade.

*Plasmids* - The PKC  $\beta$ II mutants, PKC  $\beta$ II-T641E, PKC  $\beta$ II-S660E, and PKC  $\beta$ II-T641E/S660E, were all generated using the QuikChange site-directed mutagenesis (Stratagene). An NH<sub>2</sub>-terminal HA tagged PKC  $\alpha$  was generated by PCR amplification and subsequent cloning into EcoRI (5') and XbaI (3') sites in pCDNA3. Flag-PKC  $\epsilon$  was a generous gift of Dr. Alex Toker (Harvard). A myristoylated/palmitoylated PKC  $\alpha$ ,

Myr-PKC  $\alpha$ -Flag, was obtained from Addgene. The C kinase activity reporter (CKAR) was constructed as previously described (39). PKC  $\beta$ II-RFP was cloned as previously described, and PKC  $\beta$ II-T641E/S660E-RFP was generated by QuikChange site-directed mutagenesis (40).

*Cell culture and transfection* - COS7 cells and the Sin1 MEFs were maintained in DMEM (Cellgro) containing 10% fetal bovine serum (Hyclone) and 1% penicillin/streptomycin at 37°C in 5% CO<sub>2</sub>. Transient transfections of both cell lines were carried out using FuGENE transfection reagent (Roche Applied Science).

*Pulse-chase analysis* - COS7 cells were transfected with WT PKC  $\beta$ II, PKC  $\beta$ II-T641E, PKC  $\beta$ II-S660E, HA-PKC  $\alpha$ , Flag-PKC  $\epsilon$ , or Myr-PKC  $\alpha$ -Flag. At 24–30 h after transfection, cells were incubated with Met/Cys-deficient DMEM for 30 min at 37 °C. The cells were then pulse-labeled with 0.5 mCi ml<sup>-1</sup> [<sup>35</sup>S]Met/Cys in Met/Cys-deficient DMEM for 7 min at 37 °C, media were removed, and cells were chased with DMEM containing 5 mM unlabeled methionine and 5 mM unlabeled cysteine (41). At the indicated times, cells were lysed in Buffer A (50 mM Tris, 50 mM NaF, 10 mM Na<sub>4</sub>P<sub>2</sub>O<sub>7</sub>, 100 mM NaCl, 5 mM EDTA, 1% Triton X-100, 1 mM Na<sub>3</sub>VO<sub>4</sub>, and 1 mM phenylmethylsulfonyl fluoride) and centrifuged at 16,000 x g for 5 min at 22°C. PKC in the supernatant was immunoprecipitated with the appropriate antibody (monoclonal PKC  $\alpha$  (cross-reactive with PKC  $\beta$ II) for PKC  $\beta$ , monoclonal HA for PKC  $\alpha$ , and monoclonal Flag for PKC  $\epsilon$  and Myr-PKC  $\alpha$ ) overnight at 4 °C. The immune complexes were collected with Ultra-Link protein A/G beads, washed with Buffer A, separated by SDS-PAGE, transferred to polyvinylidene difluoride (PVDF) membrane, and analyzed by autoradiography. For inhibitor experiments, cells were pretreated for 3 h with 10  $\mu$ M

OSU03012, 1  $\mu$ M KT5720, or 10  $\mu$ M PI-103. Pulse-chase experiments of endogenous PKC  $\alpha$  followed the same protocol. Densitometric analysis of scanned autoradiograms was performed using NIH Image J analysis software, and the kinetic analysis was performed using Kaleidograph software (version 4.0).

*Cell imaging* – Sin1<sup>+/+</sup> and Sin1<sup>-/-</sup> MEFs transfected with CKAR alone or cotransfected with RFP-PKC  $\beta$ II or RFP-PKC  $\beta$ II-T641E/S660E were imaged and analyzed for changes in fluorescence resonance energy transfer (FRET) according to the methods detailed in (42).

## Results

*Inhibition of the upstream kinase, PDK-1, or the intrinsic catalytic activity of PKC does not alter the rate of processing by phosphorylation* – Studies performed in our lab as well as our colleagues' have demonstrated that PDK-1 is the upstream kinase for PKC; PDK-1 phosphorylates PKC, as well as other AGC kinase family members, at a conserved Thr in the activation loop sequence (41,43-45). This phosphorylation is the first step in the processing of PKC by phosphorylation. Mutation of this site to an Ala or Val prevents PKC maturation; in addition, cells that are deficient in PDK-1 lack significant levels of PKC isozymes (46,47). We were curious if inhibition of PDK-1 kinase activity would ablate the processing of PKC into a mature, fully phosphorylated species. To monitor the rate of PKC processing, we transfected COS7 cells with WT PKC  $\beta$ II and performed a pulse-chase analysis in the absence or presence an ATP-competitive, PDK-1 inhibitor, OSU03012 (Figure 5.1 A, lanes 1-8). The autoradiogram in Figure 5.1 A shows that newly-synthesized PKC migrated as a single, faster mobility band (*lane 1, dash*), which shifted to a slower mobility band (*asterisk*) over the course of the chase. This mobility shift reflects the two tightly coupled C-terminal phosphorylations, the turn motif (Thr-641 in PKC  $\beta$ II) and the hydrophobic motif (Ser-660 in PKC  $\beta$ II). Note that phosphorylation at the activation loop site by PDK-1 does not cause a visible mobility shift (48). In the absence of inhibitor, PKC processed with half-time of ~30 min (*lane 3*). Interestingly, in the presence of the PDK-1 inhibitor, PKC also processed at a similar rate with a half-time of ~ 30 min (*compare lanes 3 and 7*). These data suggest that inhibition of PDK-1 under these conditions does not affect the rate of PKC processing into the mature, fully phosphorylated species.

To control for activity of the PDK-1 inhibitor, we analyzed detergent-solubilized lysates from the pulse-chase analysis by Western blotting for phosphorylation at the activation loop site of Akt, Thr-308 (Figure 5.1 B). PDK-1 regulation of Akt phosphorylation is dependent upon engagement of the PH domain of Akt with phosphoinositol-3,4-trisphosphate (PIP<sub>3</sub>) in the membrane to unmask the activation loop site (37). Similarly, PDK-1 requires an open conformation in PKC to allow access to the activation loop phosphorylation sequence, but this regulation is constitutive and occurs independently of signaling events in the cell (49). The Western blot in Figure 5.2 B shows that Akt is robustly phosphorylated at Thr-308 in the absence of the inhibitor (*lanes 1-4*), with a modest increase after the chase begins (*lanes 2-4; note that lane 1 represents growth factor-starved conditions prior to the chase in normal, growth factor-rich media (lanes 2-4)*). In the presence of the inhibitor, Akt is weakly phosphorylated in starved conditions (*lane 5*) but is phosphorylated during the chase in normal media (*lanes 6-8*). Although this Thr-308 phosphorylation appears to be weaker, an ~ 80% reduction, in the presence of the PDK-1 inhibitor, the data indicate that PDK-1 still retains activity.

To determine if another commercial PDK-1 inhibitor would have greater efficacy, we performed another pulse-chase analysis of WT PKC  $\beta$ II transfected into COS7 cells in the absence or presence of another ATP-competitive inhibitor, KT5720 (Figure 5.1 C). This inhibitor has been characterized as a PKA inhibitor, but it has demonstrated a lower IC<sub>50</sub> for PDK1 compared to PKA (50). Similarly to OSU03012, PKC  $\beta$ II processed from the newly-synthesized, faster mobility band (*lane 1, dash*) to the fully phosphorylated, slower mobility band (*asterisk*) with a half-time of ~30 min in the absence or presence of KT5720 (*compare lanes 3 and 7*). Western blot analysis of detergent-solubilized lysates

from the pulse-chase showed that the inhibitor reduced by ~ 80%, but not abolished, Thr-308 phosphorylation on Akt, similar to the effects of OSU03012 (Figure 5.1 *D*, compare lanes 2-4 to 6-8). These data reveal that reducing PDK-1 activity by ~80% is not enough to prevent the processing of PKC.

Previous work in our lab has shown that PKC  $\beta$ II autophosphorylates at the hydrophobic motif by an intramolecular mechanism; this phosphorylation is the final step in the maturation of PKC and accounts for the ~4 kDa mobility shift observed in PKC (24,27). Therefore, we were interested to see if inhibition of PKC would hinder PKC processing, particularly the hydrophobic motif step. COS7 cells were transfected with WT PKC  $\beta$ II and analyzed by pulse-chase analysis in the absence or presence of the specific PKC inhibitor Gö6983 (Figure 5.1, lanes 9-12). Interestingly, PKC processed with a half-time of ~30 min in the absence and presence of Gö6983 (compare lane 3 and lane 11). These data reveal that the PKC inhibitor, like the PDK-1 inhibitor, was not sufficient to inhibit PKC processing by phosphorylation.

*Inhibition of mTOR slows the processing of PKC  $\beta$ II* – Recent studies have shown that the integrity and catalytic activity of the mTORC2 complex is required for the maturation and stability of PKC by regulating phosphorylation at the turn motif (32,33). We took advantage of an ATP-competitive, mTOR kinase inhibitor described in one of these studies, PI-103, and used our pulse-chase assay to determine the contribution of mTOR catalytic activity to the processing of PKC. This compound inhibits both mTOR complexes, mTORC1 and mTORC2, with IC<sub>50</sub> values of 20 nM and 83 nM *in vitro*, respectively (51). COS7 cells were transfected with WT PKC  $\beta$ II and analyzed by pulse-chase in the absence or presence of PI-103 (Figure 5.2 *A top panel*). As shown

previously, WT PKC  $\beta$ II processes from the newly-synthesized, faster mobility band (*lane 1, dash*) to the fully phosphorylated, slower mobility band over the course of the chase (*lane 2-4, asterisk*). The addition of PI-103 slowed the maturation of PKC (*compare lane 3 and lane 8*). Quantitative analysis of the ratio of the upper mobility species to the total PKC for WT PKC  $\beta$ II revealed that in the absence of the inhibitor, PKC was processed with a half-time of  $21.4 \pm 0.4$  min (Figure 5.2 B, *white circles*); this rate is consistent with previous studies (40). However, in the presence of PI-103, the rate of processing of PKC was slowed ~3-fold with a half-time of  $71 \pm 8$  min (*black circles*). These data reveal that inhibition of mTOR kinase activity decreases the rate of processing of WT PKC  $\beta$ II.

Debate exists in the field over whether the mTORC2 complex directly regulates the turn motif phosphorylation site alone, the hydrophobic motif phosphorylation site alone, or both sites. To explore which of the two C-terminal processing sites mTORC2 regulates, we investigated the rate of processing of phosphorylation site constructs of PKC  $\beta$ II in which the C-terminal phosphorylation site residues were individually replaced with Glu, the phospho-mimetics PKC  $\beta$ II-T641E (turn motif mutant) and PKC  $\beta$ II-S660E (hydrophobic motif mutant), as executed in a similar manner with Hsp90 (see Chapter 2, Figure 5.2 *middle and bottom panels*). As reported previously, both mutants were processed by phosphorylation with half-times slightly slower than WT PKC  $\beta$ II (40). Note that the mobility shift for PKC  $\beta$ II-T641E reflects phosphorylation of Ser-660, which causes a readily detectable mobility shift, and that the mobility shift for PKC  $\beta$ II-S660E reflects phosphorylation of Thr-641, which causes a smaller mobility shift. Importantly, for both mutants, PI-103 treatment slowed the processing ~2-fold, similarly

to WT PKC  $\beta$ II (compare the ratios of upper and lower mobility species at the 30-min time point, *lane 3* and *lane 8*). Quantitative analysis of the ratio of the upper mobility species to the total PKC for turn motif mutant, PKC  $\beta$ II-T641E, revealed that PKC processed with a half-time of  $35 \pm 4$  min in the absence of the inhibitor (Figure 5.2 C, *white squares*). Similarly to WT PKC  $\beta$ II, this rate was slowed  $\sim 3$ -fold in the presence of PI-103 with a half-time of  $88 \pm 4$  min (*black squares*). Quantitative analysis was not performed for the hydrophobic motif mutant, PKC  $\beta$ II-S660E, because the faint mobility shifts were difficult to analyze accurately. However, visual inspection suggests that PKC  $\beta$ II-S660E was  $\sim 50\%$  processed at 90 min in the absence of the inhibitor (*lane 4*) but  $\sim 25\%$  at 90 min in the presence of the inhibitor (*lane 8*). These data reveal that mTOR kinase activity is necessary for phosphorylation at both sites; however, whether this mechanism is direct remains unclear.

To ensure that PI-103 was effective at inhibiting mTOR activity, we checked a well-characterized downstream target of the mTORC1 complex, S6K. mTORC1 phosphorylates the hydrophobic motif of S6K, Thr-389, and this phosphorylation is blocked by inhibitors of this complex, such as rapamycin, as well as inhibitors of the mTOR kinase, resulting in a detectable mobility shift. Whole cell lysates from cells treated with PI-103 for 1 and 3 h (the pretreatment time of the pulse-chase) were analyzed by SDS-PAGE and Western blotting for total S6K and phospho-Thr-389 (Figure 5.2 D). In the absence of PI-103, S6K migrates as a slower mobility species that is phosphorylated at Thr-389 (*lane 1, asterisk*). However, at 1 h and 3 h treatment with PI-103, S6K migrates as a faster mobility species that is not phosphorylated at Thr-389

(lanes 2-3, *dash*). These data indicate that mTORC1 is inhibited under the conditions of our pulse-chase analysis.

*Inhibition of mTOR slows the processing of PKC  $\alpha$ , another conventional PKC isozyme, and PKC  $\epsilon$ , a novel PKC isozyme* – Given the conservation of the C-terminal processing phosphorylation sites among PKC isozymes, we next addressed whether other PKC isozymes were controlled by mTOR in a similar manner. We chose another conventional PKC isozyme, PKC  $\alpha$ , and a novel PKC isozyme, PKC  $\epsilon$ , which are both regulated by mTORC2 (32,33). Additionally, both isozymes show distinct mobility shifts during processing in a pulse-chase analysis. COS7 cells were transfected with HA-PKC  $\alpha$  or Flag-PKC  $\epsilon$ , and a pulse-chase analysis was performed in the absence or presence of PI-103 (Figure 5.3). Both isozymes were processed from a newly-synthesized, faster mobility band (*lane 1, dash*) to a fully phosphorylated, slower mobility species (*lanes 2-4, asterisk*) over the course of a 90 min chase in the absence of the mTOR inhibitor. However, in the presence of PI-103, the half-times for both maturation of PKC  $\alpha$  and PKC  $\epsilon$  were similar to control at ~90 min (*compare lane 4 and lane 8*), but the rate to that point was slowed (*compare lane 3 and lane 7, note the ratio of the upper mobility species to the total PKC*). These data suggest that mTOR activity is also required for the processing of these PKC isozymes.

*Inhibition of mTOR does not affect the processing of endogenous PKC  $\alpha$  or a membrane-targeted PKC  $\alpha$  in COS7 cells* – For exogenous PKC, inhibition of the mTORC2 complex with PI-103 slowed the maturation of PKC. However, to determine if the inhibitor had a similar effect on endogenous PKC, we performed a pulse-chase analysis of endogenous PKC  $\alpha$  in COS7 cells in the absence or presence of PI-103

(Figure 5.4 A). In the absence of inhibitor, PKC processed from the newly-synthesized, faster mobility band (*lane 1, dash*) to the fully phosphorylated, slower mobility band (*asterisk*) over the course of a 60 min chase with a half-time of ~10 min (*lane 3*), consistent with previous reports (40). Interestingly, treatment with PI-103 had no effect on the half-time of PKC processing (*compare lane 3 and lane 8*). These data indicate that the mTOR inhibitor does not affect the processing of endogenous PKC in COS7 cells under the conditions where it inhibits the processing of over-expressed PKC  $\alpha$  and PKC  $\beta$ II.

Endogenous PKC is processed at the membrane of cells, whereas exogenous PKC is processed in both the cytosol and membrane compartments (41). We were curious if the difference in the effect of the inhibitor could be explained by the location of PKC during its maturation. To this end, we utilized a myristoylated/palmitoylated PKC  $\alpha$  construct (Myr-PKC  $\alpha$ ) that would target PKC to the plasma membrane, where endogenous processing of PKC would be occurring. Again, we performed a pulse-chase analysis in the absence or presence of PI-103 (Figure 5.4 B). Myr-PKC  $\alpha$  processed with a half-time of ~90 min in the absence of the inhibitor (*lane 4*); no difference in the rate of processing was observed in the presence of the inhibitor (*compare lane 4 and lane 8*). Thus, a processing of an over-expressed, membrane-targeted PKC becomes insensitive to the mTOR inhibitor.

*Exogenous PKC can signal in mTORC2-deficient cells* – Ongoing studies currently debate the phosphorylation target of the mTORC2 complex in PKC, either the turn motif phosphorylation or the hydrophobic motif phosphorylation site. Our data with the phospho-mimetic mutants, PKC  $\beta$ II-T641E and PKC  $\beta$ II-S660E, are consistent with

mTORC2 working on BOTH sites. However, the possibility exists that the catalytic activity of mTOR is required for some other function related to the processing of PKC that is independent of direct phosphorylation of either C-terminal sites. To test this hypothesis, we utilized a cell system that is deficient in mTORC2 signaling, *Sin1*<sup>-/-</sup> MEFs, and a double phospho-mimetic mutant, PKC  $\beta$ II-T641E/S660E. We were curious if by adding exogenous PKC with constant negative charge at both C-terminal sites, we could bypass the mTORC2 requirement. By transfecting PKC  $\beta$ II-T641E/S660E in an mTORC2-null background (*Sin1*<sup>-/-</sup> MEFs) and then assaying activity with the FRET-based CKAR reporter, we could then determine if mTORC2's target involved another phosphorylation site or possibly regulated a scaffolding function. To this end, we transfected *Sin1*<sup>+/+</sup> MEFs (functional mTORC2) and *Sin1*<sup>-/-</sup> MEFs (nonfunctional mTORC2) with CKAR alone (*squares*), CKAR and PKC  $\beta$ II-RFP (*triangles*), or CKAR and PKC  $\beta$ II-T641E/S660E-RFP (*diamonds*) (Figure 5.5). We utilized an RFP-tagged PKC to monitor expression in cells. In the *Sin1*<sup>+/+</sup> MEFs, stimulation with the phorbol ester, PDBu, induced a mild response for endogenous PKC (CKAR alone) and a robust response for the over-expressed PKC constructs that were all reversed upon addition of the PKC inhibitor, Gö6983 (Figure 5.5 A). Both WT PKC  $\beta$ II-RFP and PKC  $\beta$ II-T641E/S660E-RFP had a similar response profile in the *Sin1*<sup>+/+</sup> MEFs. In the *Sin1*<sup>-/-</sup> MEFs, stimulation with PDBu did not induce a response for CKAR alone (*squares*), consistent with reports of the lack of functional PKC in these cells (33). However, PDBu induced a robust CKAR response for both WT PKC  $\beta$ II-RFP and PKC  $\beta$ II-T641E/S660E-RFP in the *Sin1*<sup>-/-</sup> MEFs that was reversed with the PKC inhibitor Gö6983 (*triangles and diamonds, respectively*). Unexpectedly, over-expressed WT and the

phospho-mimetic PKC exerted a similar response profile in both cell types. Thus, exogenous PKC is capable of bypassing the requirement of mTORC2 for PKC activity and therefore not allowing us to determine if locking negative charge at both C-terminal processing sites bypasses mTORC2.

*Over-expressed PKC is processed in mTORC2-deficient cells* – Our discovery that over-expressed PKC could signal in the Sin<sup>-/-</sup> MEFs to the same capabilities as PKC in the Sin<sup>+/+</sup> MEFs was surprising and puzzling because endogenous PKC did not signal in the Sin<sup>-/-</sup> MEFs. Therefore, we wanted to check if the over-expressed PKC in these cells was phosphorylated at the C-terminal processing sites. Figure 5.6 shows a Western blot of lysates obtained from the cell imaging studies that were analyzed by SDS-PAGE and Western blotting for total and phosphorylated RFP-PKC. In the Sin<sup>+/+</sup> MEFs, endogenous PKC  $\alpha$  is phosphorylated at both C-terminal sites; in contrast, no endogenous PKC  $\alpha$  can be detected in the Sin<sup>-/-</sup> MEFs, attesting to the instability of the unphosphorylated form of PKC (*PKC  $\alpha$  panel*). Using the dsRED antibody to detect RFP, fully processed, WT PKC  $\beta$ II was observed in both cell types (*dsRED panel, asterisk*); however, the expression in the Sin<sup>-/-</sup> MEFs was greatly reduced, ~10-fold, compared to the Sin<sup>+/+</sup> MEFs. Due to these expression differences and the poor transfection efficiency of these cells, phosphorylation of the exogenous PKC could only be detected in the Sin<sup>+/+</sup> MEFs (*pS660 panel, asterisk*). These data reveal that exogenous PKC can bypass the requirement of mTORC2 for processing.

## Discussion

Until recently, the classic model of PKC maturation by phosphorylation described a constitutive process initiated by phosphorylation at the activation loop site by the upstream kinase, PDK-1, followed by autophosphorylation at the two C-terminal tail sites, the turn motif and the hydrophobic motif. This maturation results in the generation of a catalytically-competent species, capable of responding to the production of second messengers upon receptor-mediated lipid hydrolysis. However, current evidence indicates that the mTORC2 complex regulates these sites, adding another layer of complexity to the life cycle of PKC. HOW mTORC2 controls phosphorylation at the turn and hydrophobic motifs of PKC remains unclear in the literature as direct phosphorylation at these sites has not been clearly demonstrated with the use of kinase-inactive PKC controls to rule out autophosphorylation (13,32,33). However, in cells deficient for mTORC2, PKC is unphosphorylated and unstable, indicating that the complex is necessary to facilitate the proper maturation of PKC. Our studies confirm that the kinase activity of mTOR is, indeed, involved in the maturation process of PKC. We propose two models: 1) mTORC2 activity is required for proper membrane localization of PKC where it can be processed by phosphorylation (indirect) or 2) mTORC2 activity directly regulates phosphorylation of both the turn and hydrophobic motif sites (Figure 5.7).

*mTORC2 activity facilitates proper subcellular localization of PKC where it can be processed by phosphorylation by an indirect mechanism - Inhibition of mTOR slows the rate of processing of exogenous PKC  $\beta$ II by affecting both the turn and hydrophobic motif phosphorylation sites as demonstrated by the use of the single phospho-mimetics,*

PKC  $\beta$ II-T641E and PKC  $\beta$ II-S660E. This effect was also observed with exogenous PKC  $\alpha$  and PKC  $\epsilon$ . These data are consistent with previous results demonstrating the necessity of mTOR activity for the phosphorylation of PKC (32,33). One explanation for this result is that mTOR activity is required for a step that PRECEDES phosphorylation at both sites (Figure 5.7 A).

Our lab has previously shown by subcellular fractionation experiments that endogenous PKC matures in a membrane compartment, while exogenous PKC matures both at the membrane and in the cytosol (41). Interestingly, treatment with the mTOR inhibitor did NOT affect the rate of processing of endogenous PKC  $\alpha$  in COS7 cells. To determine if endogenous PKC  $\alpha$ , which matures in a membrane compartment, is insensitive to the mTOR inhibitor due to its localization, we tested if a myristoylated/palmitoylated PKC  $\alpha$  construct that would target to the plasma membrane would also be insensitive to the mTOR inhibitor. Indeed, this mutant was insensitive to the mTOR inhibitor, indicating that membrane-bound PKC is able to process in an mTORC2-independent manner. Unpublished results from our lab have shown that the isolated catalytic domain of PKC  $\beta$ II is unable to mature by phosphorylation; however, when the regulatory C1 and C2 domains were added (which will target PKC to the membrane), the isolated catalytic domain was processed. These studies emphasize the necessity of membrane localization for the proper maturation of PKC. Therefore, we propose that mTOR activity is required to target PKC to this membrane compartment where it can be processed by phosphorylation. mTOR itself is localized to membrane compartments such as the Golgi and endoplasmic reticulum (52). In yeast, TOR2 localizes to discrete regions in the plasma membrane (53). Thus, mTOR is potentially

poised at the proper subcellular location to facilitate PKC processing. The insensitivity of endogenous PKC, which is pretargeted to the membrane, and the membrane-targeted PKC indicates that forcing this localization bypasses the mTORC2 requirement.

However, we expected to see an effect of the inhibitor on the endogenous PKC. One possibility is that mTORC2 is in excess in the cell, and even though we see inhibition of mTOR by PI-103 (as measured by a decrease in phospho-S6K), most likely we are unable to significantly affect the majority of mTORC2 complexes in the cell. However, exogenous PKC will outnumber the amount of endogenous mTORC2 complexes such that it becomes rate-limiting; therefore, PKC processing is slowed in the presence of the inhibitor.

Membrane localization preceding phosphorylation events is a mechanism utilized by another AGC kinase family member, Akt. Unlike PKC, phosphorylation at the turn motif of Akt (Thr-450 in Akt1) is constitutive and does not affect activation-induced phosphorylation of the activation loop and hydrophobic motif; however, phosphorylation of Akt's turn motif is dependent upon an intact PH domain, the membrane-targeting module, as well as the integrity and activity of mTORC2 (37). Mutations in the PH domain that abrogate responsiveness to growth factors prevent constitutive phosphorylation at the turn motif (37). Additionally, cells that lack functional mTORC2 are deficient in turn motif phosphorylation on Akt (32,33). One hypothesis is that PH domain, in a phospholipid-independent manner, facilitates the activatable conformation of Akt through recruitment of chaperones and the possible turn motif kinase (mTORC2?) (37). Therefore, phosphorylation at the turn motif of Akt merely serves as a marker to indicate that Akt completed this pre-activation process. When the turn motif of Akt is

mutated to an Ala, Akt-T450A still responds to growth factors and is phosphorylated at the hydrophobic motif; interestingly, PKC  $\beta$ II-T641A is also phosphorylated at the hydrophobic motif (33,34). However, compensatory phosphorylation at nearby threonines and serines accounts for this result; a triple alanine mutant, PKC  $\beta$ II T634A/T641A/S654A is not processed by phosphorylation. Whether mutation of similar residues in Akt would have a similar effect has not been examined. It is plausible that turn motif phosphorylation on PKC may also serve as a similar 'marker' to indicate that it has gone through a pre-activation process mediated by mTORC2 and the inability of PKC  $\beta$ II T634A/T641A/S654A to process results from impairing the mTORC2 step. Whether this process involves the recruitment of chaperones or even other kinases (the REAL turn motif kinase) remains to be determined.

*mTORC2 activity directly regulates phosphorylation at the turn and hydrophobic motif sites in PKC* - Our pulse-chase data with the single phospho-mimetic mutants, PKC  $\beta$ II-T641E and PKC  $\beta$ II-S660E, reveal that inhibition of mTOR slows the processing of PKC by affecting BOTH phosphorylation sites. Recent studies in the literature currently debate which phosphorylation site is the primary target of mTORC2. Work from our lab has shown that the turn motif phosphorylation step is rate-limiting in the processing of PKC  $\beta$ II; mutation of this site and the nearby compensating residues prevents hydrophobic motif phosphorylation (34).

In order to determine whether mTORC2 works directly on these sites or whether its activity is required for an upstream event (as described in the first model), we transfected a double phospho-mimetic, PKC  $\beta$ II-T641E/S660E, into Sin1<sup>-/-</sup> MEFs, which lack a functional mTORC2 complex, and measured activity with the FRET-based CKAR

reporter. In the *Sin1*<sup>-/-</sup> MEFs, PKC migrates primarily as a faster mobility species that is unphosphorylated and readily degraded by the proteasome and, as expected, does not phosphorylate CKAR. Surprisingly, both transfected WT PKC  $\beta$ II and PKC  $\beta$ II-T641E/S660E phosphorylated CKAR in the *Sin1*<sup>-/-</sup> MEFs at a comparable level as the *Sin1*<sup>+/+</sup> MEFs. These results have several implications: 1) exogenous PKC can bypass the requirement of mTORC2 for proper processing and activity and 2) other mTORC2 complexes may exist in the cell to facilitate proper maturation of PKC. Perhaps these other mTORC2 complexes (generated with other *Sin1* isoforms? (29)) are unable to work on the membrane-localized endogenous PKC but can affect the over-expressed, cytosolic PKC. In order to confirm that exogenous PKC can bypass the requirement of mTORC2, this experiment should be repeated in the *Rictor*<sup>-/-</sup> MEFs, which also demonstrate similar defects in PKC processing (32).

No group has been able to show direct phosphorylation of mTORC2 on PKC although genetic depletion of mTORC2 components abolishes phosphorylation of PKC. Why is the activity of mTORC2 required for the processing of PKC? Does it work in conjunction with Hsp90 chaperones? Does it inhibit a turn motif phosphatase? The role of mTORC2 in PKC maturation, in light of our recent data, remains elusive. However, sequence differences within PKC family members may shed some light on the mechanism of mTORC2 regulation of PKC. These recent PKC/mTORC2 studies have shown that the novel isozymes, PKC  $\delta$  and PKC  $\theta$ , are insensitive to the inhibition of mTORC2 and retain turn motif phosphorylation (32,33). Interestingly, these isozymes lack the TP-motif at the turn motif site (which also makes them insensitive to Pin1 inhibition, submitted results), which is a favored phosphorylation site for mTOR, as well

as the upstream FTN-motif, which contains another possible autophosphorylation site as demonstrated *in vitro* but not in cells (Figure 5.8 A, 54). Additionally, PKC  $\delta$  can be fully processed in bacteria whereas PKC  $\beta$ II cannot (55). These apparent sequence differences beg the question if they have a role in the mTORC2-regulation of PKC. Unpublished results from our lab show that substitution of ten amino acids preceding and including the turn motif of PKC  $\delta$  into PKC  $\beta$ II allows PKC  $\beta$ II to be processed in bacteria. This result implies that something about that ten residue cassette facilitates PKC processing in a system that lacks mTORC2, thus indicating why PKC  $\delta$  may be insensitive to mTORC2. Several mutations have been made in this cassette in PKC  $\beta$ II (Thr-634, Leu-640, Thr-641, Pro-642), but none have dramatically altered the maturation of PKC, suggesting that mTORC2 may not be directly acting on PKC through those residues (56). Another possibility is that mTORC2 regulates those PKC isozymes that require autophosphorylation at the hydrophobic motif. Indeed, the novel PKC isozymes, PKC  $\delta$  and PKC  $\theta$ , can be phosphorylated at the hydrophobic motif by alternative mechanisms than autophosphorylation (57-59). In contrast, conventional PKC isozymes and the novel PKC  $\epsilon$ , which do autophosphorylate, are sensitive to regulation by mTORC2. Interestingly, the atypical PKC isozyme, PKC  $\zeta$ , is also insensitive to mTORC2; this isozyme has a Glu at the hydrophobic motif position (32). Interestingly, these isozymes appear to cluster together in the AGC branch of the human kinome (Figure 5.8 B). However, future work is required to thoroughly test this hypothesis.

*The effects of other inhibitors on the maturation of PKC.* Interestingly, PDK-1 and PKC inhibitors did not have an effect on the rate of processing of PKC. Inhibition of activity *in vitro* does not always translate to strong inhibition in cells. In the case of

PDK-1, a decrease in T308 phosphorylation was observed compared to control; however, activity still remained. Most likely PDK-1 and PKC are in such a tight complex (and there is so much endogenous PDK-1 in the cell) that a slight inhibition is not enough to affect the maturation of PKC. Inhibition of autophosphorylation in cells poses an even harder challenge because the selected concentration of inhibitor is competing with the high cellular concentrations of ATP. Autophosphorylation of PKC at the hydrophobic motif is not the rate-limiting step in its maturation process; therefore, even a 10-fold decrease in activity would still not prevent the fast autophosphorylation reactions from occurring (49). Perhaps higher concentrations of these inhibitors could be utilized to test the contribution of PDK-1 and PKC activity to its maturation process.

*The contribution of mTORC2 to the maturation of PKC* – In summary, our work does reveal that mTOR activity is necessary for the maturation of over-expressed PKC. The insensitivity of the endogenous PKC implies that differences in localization could affect mTOR's ability to regulate this process. However, better inhibitors have been developed and should be tested under these same conditions. What remains puzzling is why over-expressed PKC can bypass the requirement of mTORC2 for processing and activity. Future work with other systems (Rictor<sup>-/-</sup> MEFS?) is required in order to determine the exact mechanism of mTORC2 regulation of PKC maturation.

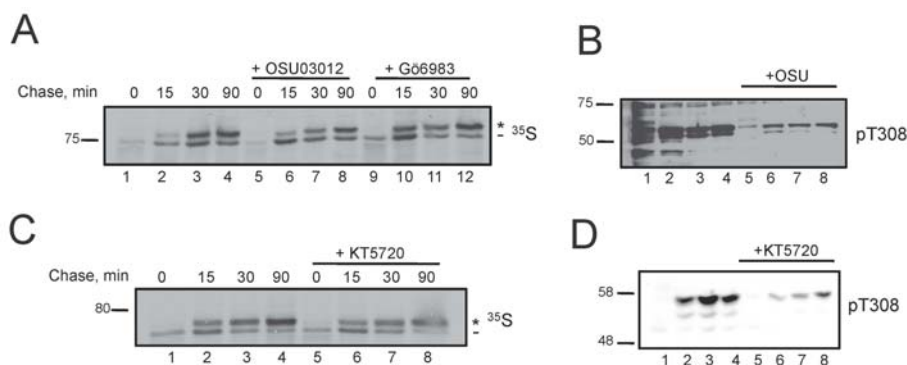


**Figure 5.1:** Inhibition of PDK-1 or PKC activity does not block the processing of PKC. *A*, Autoradiogram from a pulse-chase analysis of COS7 cells transfected with WT PKC  $\beta$ II. Transfected cells were labeled with [ $^{35}$ S]Met/Cys and chased for the indicated times in the absence (*lanes 1-4*) or presence (*lanes 5-8*) of OSU-03012 (10  $\mu$ M) or Gö6983 (1  $\mu$ M, *lanes 9-12*). PKC was immunoprecipitated from detergent-solubilized lysates and analyzed by autoradiography. The *asterisk* denotes the position of the mature, fully phosphorylated PKC, and the *dash* denotes the position of then newly-synthesized, unphosphorylated PKC. *B*, Western blot of detergent-solubilized lysates in *A* analyzed for phospho-Akt (pT308). *C*, Autoradiogram from a pulse-chase analysis of COS7 cells transfected with WT PKC  $\beta$ II. Transfected cells were labeled with [ $^{35}$ S]Met/Cys and chased for the indicated times in the absence (*lanes 1-4*) or presence (*lanes 5-8*) of KT5720 (1  $\mu$ M). PKC was immunoprecipitated from detergent-solubilized lysates and analyzed by autoradiography. The *asterisk* denotes the position of mature, fully phosphorylated PKC, and the *dash* denotes the position of newly-synthesized, unphosphorylated PKC. *D*, Western blot of detergent-solubilized lysates in *C* analyzed for phospho-Akt (pT308).

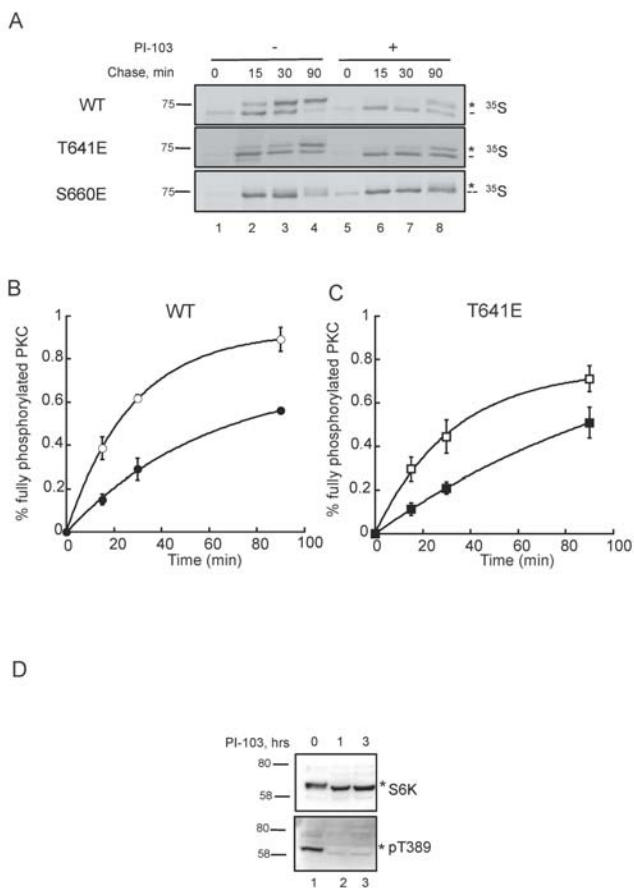


**Figure 5.2:** Inhibition of mTOR slows the processing by affecting phosphorylation at both the turn motif (Thr-641) and the hydrophobic motif (Ser-660) of the conventional isozyme, PKC  $\beta$ II. *A*, Autoradiogram from a pulse-chase analysis of COS7 cells transfected with WT PKC  $\beta$ II, PKC  $\beta$ II-T641, or PKC  $\beta$ II-S660E. Transfected cells were labeled with [ $^{35}$ S]Met/Cys for the indicated times in the absence (*lanes 1-4*) or presence (*lanes 5-8*) of PI-103 (10  $\mu$ M). PKC was immunoprecipitated from detergent-solubilized lysates and analyzed by autoradiography. The *asterisk* denotes the position of mature, fully phosphorylated PKC, the *double dash* denotes the position of phosphorylation at Thr-641, and the *dash* denotes the position of newly-synthesized, unphosphorylated PKC. *B*, Graph representing the data shown in the autoradiogram in *A* for WT PKC  $\beta$ II. The graph shows the relative amount of fully phosphorylated PKC (*asterisk*) as a percentage of the total protein in the absence (*white circles*) and presence (*black circles*) of PI-103 (10  $\mu$ M). Data are representative of the mean  $\pm$  S.E. of three independent experiments. *C*, Quantitative analysis of the data shown in the autoradiogram in *A* for PKC  $\beta$ II-T641E. The graph shows the relative amount of fully phosphorylated PKC (*asterisk*) as a percentage of the total protein in the absence (*white squares*) and presence (*black squares*) of PI-103 (10  $\mu$ M). Data are representative of the mean  $\pm$  S.E. of three independent experiments. *D*, Lysates from *A* analyzed by SDS-PAGE and Western blotting for total and phospho-S6K after 1 and 3 h treatment with 1  $\mu$ M PI-103.

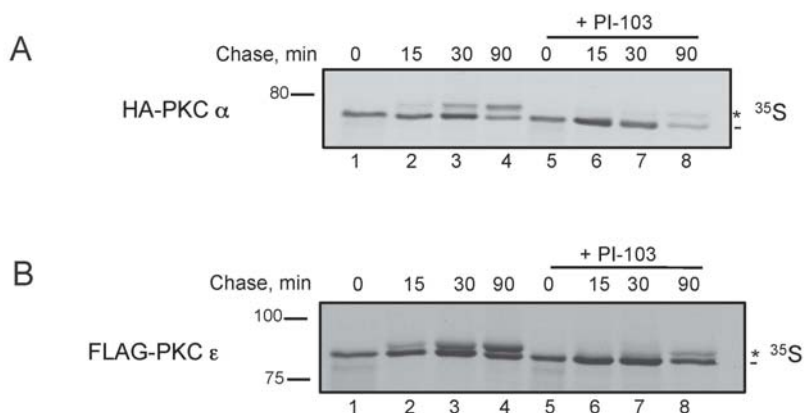


**Figure 5.3:** Inhibition of mTOR slows the processing of exogenous PKC  $\alpha$ , a conventional PKC isozyme, and exogenous PKC  $\epsilon$ , a novel PKC isozyme. *A*, Autoradiogram from a pulse-chase analysis of COS7 cells transfected with WT HA-PKC  $\alpha$ . Transfected cells were labeled with [ $^{35}$ S]Met/Cys and chased for the indicated times in the absence (*lanes 1-4*) and presence (*lanes 5-8*) of PI-103 (10  $\mu$ M). PKC was immunoprecipitated from detergent-solubilized lysates and analyzed by autoradiography. The *asterisk* denotes the position of mature, fully-phosphorylated PKC, and the *dash* denotes the position of newly-synthesized, unphosphorylated PKC. *B*, Autoradiogram from a pulse-chase analysis of COS7 cells transfected with WT Flag-PKC  $\epsilon$ . Transfected cells were treated and analyzed as described in *A*. Data are representative of two independent experiments.

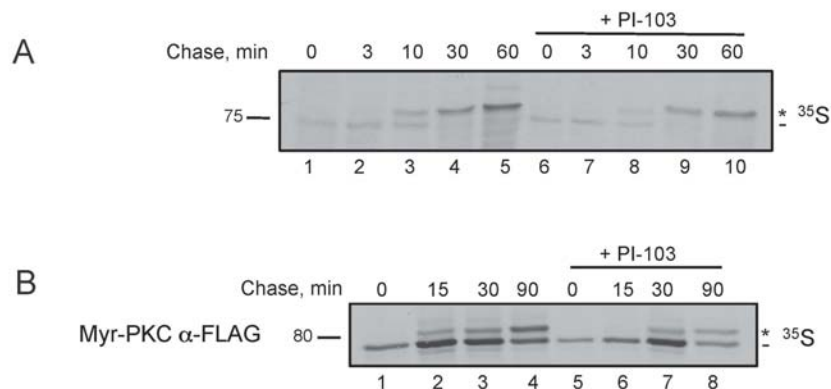


**Figure 5.4:** The processing of endogenous PKC  $\alpha$  is insensitive to the mTOR inhibitor and cannot be rescued by membrane-targeting. *A*, Autoradiogram from a pulse-chase analysis of endogenous PKC  $\alpha$  in COS7 cells in the absence (*lanes 1-5*) and presence (*lanes 6-10*) of PI-103 (10  $\mu$ M). Cells were labeled with [ $^{35}$ S]Met/Cys and chased for the indicated times. PKC was immunoprecipitated from detergent-solubilized lysates and analyzed by autoradiography. The *asterisk* denotes the position of mature, fully-phosphorylated PKC, and the *dash* denotes the position of newly-synthesized, unphosphorylated PKC. *B*, Autoradiogram from a pulse-chase analysis of COS7 cells transfected with plasma membrane-targeted PKC  $\alpha$ , Myr-PKC  $\alpha$ -Flag. Transfected cells were treated and analyzed as described in *A*. Data are representative of two independent experiments.

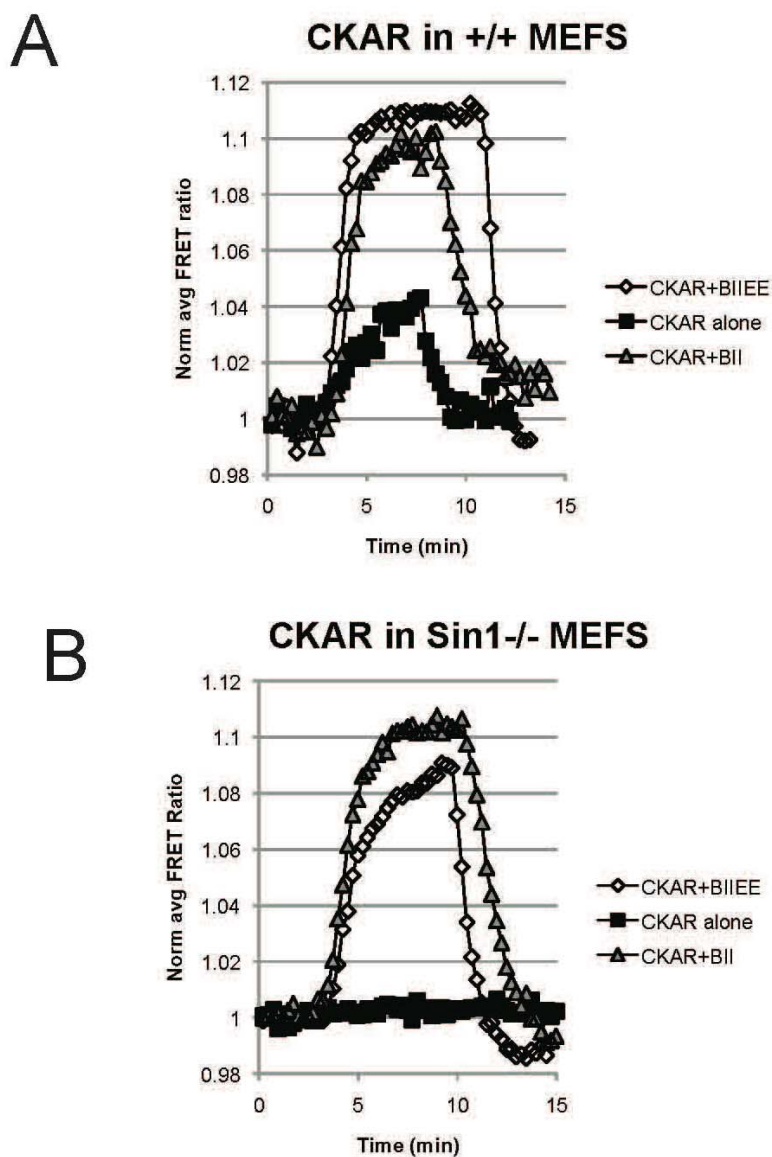


**Figure 5.5:** Exogenous PKC signals in mTORC2-deficient MEFs. *A*, Sin1<sup>+/+</sup> MEFs were transfected with CKAR alone (*squares*), CKAR and WT RFP-PKC  $\beta$ II (*triangles*), or CKAR and RFP-PKC  $\beta$ II-T641E/S660E (EE, *diamonds*), and the FRET ratio was quantified following addition of PDBu (200 nM) and then the specific PKC inhibitor Gö6983 (250 nM). *B*, Sin1<sup>-/-</sup> MEFs were transfected and analyzed in the same manner as *A*. Imaging data courtesy of Lisa L. Gallegos.

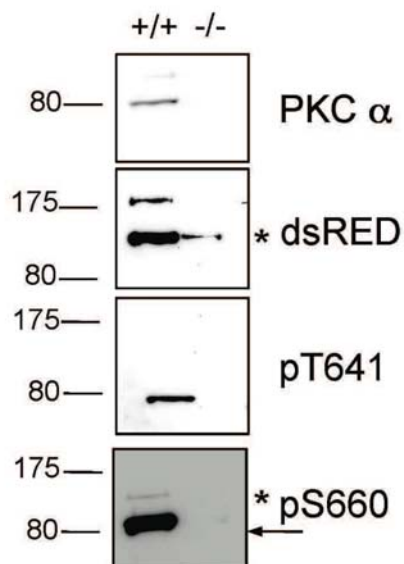


**Figure 5.6:** Exogenous PKC  $\beta$ II is processed in mTORC2-deficient MEFs.  $\text{Sin}^{+/+}$  and  $\text{Sin}^{-/-}$  MEFs were transfected with WT RFP-PKC  $\beta$ II. Whole cell lysates were analyzed by SDS-PAGE and Western blotting for PKC  $\alpha$ , dsRED (for RFP), and phospho-specific antibodies to Thr-641 and Ser-660. The *asterisk* denotes the position of processed RFP-PKC  $\beta$ II, and the *arrow* denotes the position of endogenous PKC  $\alpha$ .

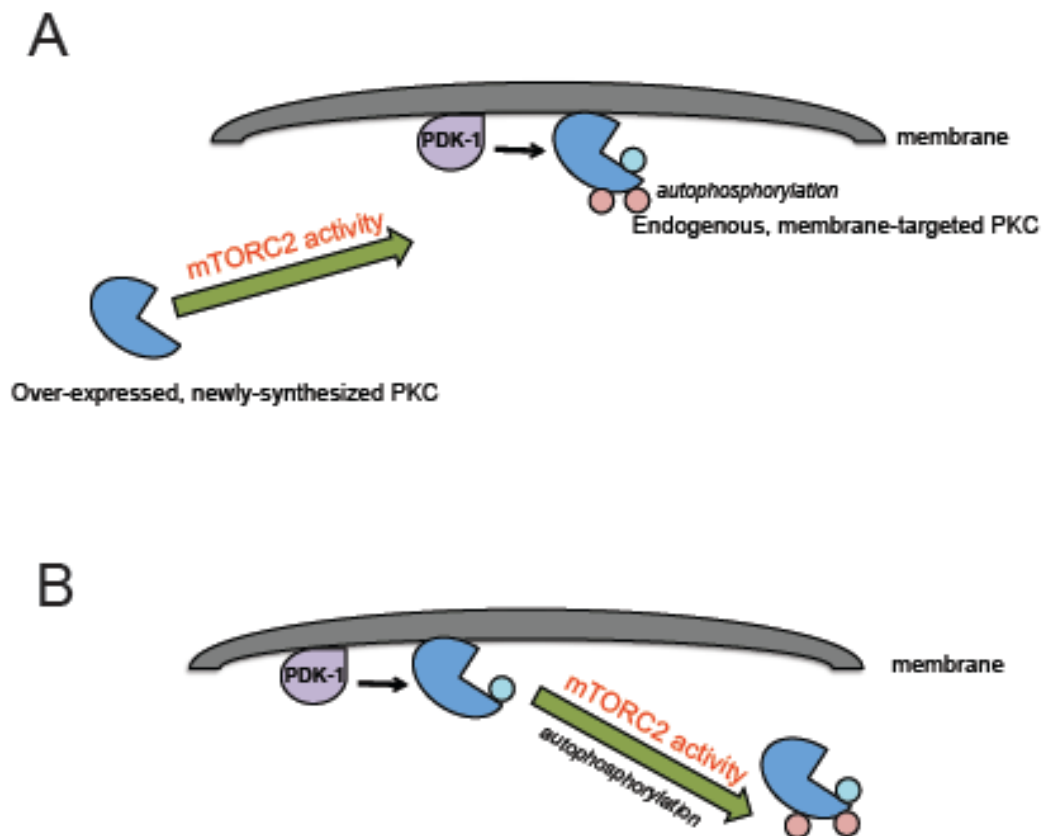


**Figure 5.7:** Proposed models for the role of mTORC2 in the maturation of PKC. *A*, The activity of mTORC2 is required for events that precede the processing phosphorylations (shown in *pink*). When mTORC2 is rate-limiting (in the case for over-expressed PKC), inhibition of mTORC2 prevents processing by phosphorylation. However, endogenous PKC, which localizes to the membrane after synthesis, or a membrane-targeted PKC is insensitive to the mTOR inhibitor, implying that mTOR activity is required for events upstream of this localization (perhaps at the ribosome?). *B*, mTORC2 acts directly on the processing phosphorylations (shown in *pink*) through an unknown mechanism.

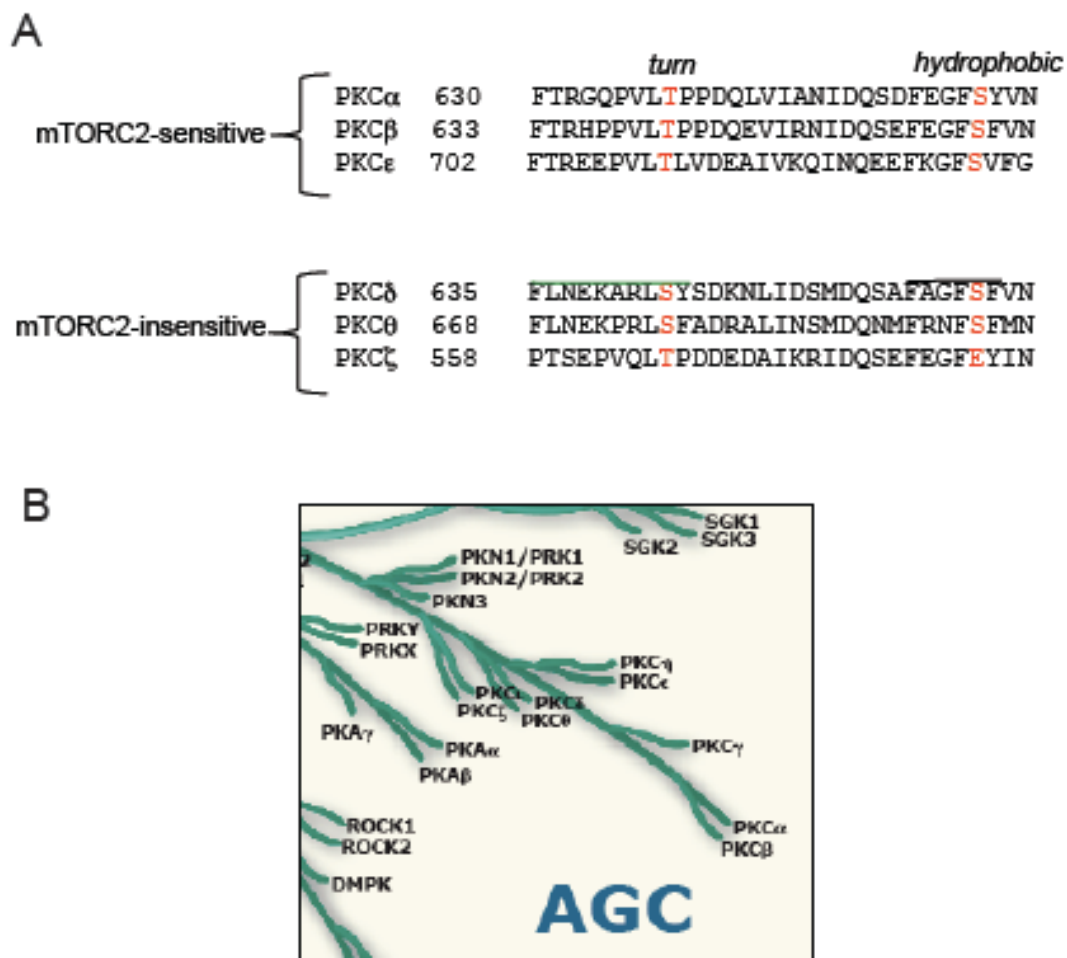


**Figure 5.8:** Identification of mTORC2-sensitive and mTORC2-insensitive PKC isozymes. *A*, Partial sequence alignment of the C-terminal phosphorylation sites in mTORC2-sensitive (PKC  $\alpha$ , PKC  $\beta$ , and PKC  $\epsilon$ ) and mTORC2-insensitive (PKC  $\delta$ , PKC  $\theta$ , and PKC  $\zeta$ ) human PKC isozymes. The turn motif and hydrophobic motif phosphorylation sites are indicated in *red*. The hydrophobic motif is underlined in *black*, and the putative ‘mTORC2 cassette’ is underlined in *green*. *B*, Segment of the AGC kinase branch of the human kinome indicating the position of the various PKC isozymes (adapted from 60).

## References

1. Ikenoue, T., Hong, S., and Inoki, K. (2009) *Methods Enzymol* **452**, 165-180
2. Guertin, D. A., and Sabatini, D. M. (2007) *Cancer Cell* **12**, 9-22
3. Sarbassov, D. D., Ali, S. M., Kim, D. H., Guertin, D. A., Latek, R. R., Erdjument-Bromage, H., Tempst, P., and Sabatini, D. M. (2004) *Curr Biol* **14**, 1296-1302
4. Yang, Q., and Guan, K. L. (2007) *Cell Res* **17**, 666-681
5. Jacinto, E., Loewith, R., Schmidt, A., Lin, S., Ruegg, M. A., Hall, A., and Hall, M. N. (2004) *Nat Cell Biol* **6**, 1122-1128
6. Thedieck, K., Polak, P., Kim, M. L., Molle, K. D., Cohen, A., Jenö, P., Arriemerlou, C., and Hall, M. N. (2007) *PLoS ONE* **2**, e1217
7. Wang, L., Harris, T. E., Roth, R. A., and Lawrence, J. C., Jr. (2007) *J Biol Chem* **282**, 20036-20044
8. Peterson, T. R., Laplante, M., Thoreen, C. C., Sancak, Y., Kang, S. A., Kuehl, W. M., Gray, N. S., and Sabatini, D. M. (2009) *Cell*
9. Oshiro, N., Yoshino, K., Hidayat, S., Tokunaga, C., Hara, K., Eguchi, S., Avruch, J., and Yonezawa, K. (2004) *Genes Cells* **9**, 359-366
10. Yonezawa, K., Tokunaga, C., Oshiro, N., and Yoshino, K. (2004) *Biochem Biophys Res Commun* **313**, 437-441
11. Kim, D. H., Sarbassov, D. D., Ali, S. M., King, J. E., Latek, R. R., Erdjument-Bromage, H., Tempst, P., and Sabatini, D. M. (2002) *Cell* **110**, 163-175
12. Yang, Q., Inoki, K., Ikenoue, T., and Guan, K. L. (2006) *Genes Dev* **20**, 2820-2832
13. Guertin, D. A., Stevens, D. M., Thoreen, C. C., Burds, A. A., Kalaany, N. Y., Moffat, J., Brown, M., Fitzgerald, K. J., and Sabatini, D. M. (2006) *Dev Cell* **11**, 859-871
14. Jacinto, E., Facchinetti, V., Liu, D., Soto, N., Wei, S., Jung, S. Y., Huang, Q., Qin, J., and Su, B. (2006) *Cell* **127**, 125-137
15. Pearce, L. R., Huang, X., Boudeau, J., Pawlowski, R., Wullschleger, S., Deak, M., Ibrahim, A. F., Gourlay, R., Magnuson, M. A., and Alessi, D. R. (2007) *Biochem J* **405**, 513-522

16. Tee, A. R., Manning, B. D., Roux, P. P., Cantley, L. C., and Blenis, J. (2003) *Curr Biol* **13**, 1259-1268
17. Sancak, Y., Thoreen, C. C., Peterson, T. R., Lindquist, R. A., Kang, S. A., Spooner, E., Carr, S. A., and Sabatini, D. M. (2007) *Mol Cell* **25**, 903-915
18. Huang, J., and Manning, B. D. (2009) *Biochem Soc Trans* **37**, 217-222
19. Inoki, K., Li, Y., Zhu, T., Wu, J., and Guan, K. L. (2002) *Nat Cell Biol* **4**, 648-657
20. Holz, M. K., and Blenis, J. (2005) *J Biol Chem* **280**, 26089-26093
21. Schalm, S. S., and Blenis, J. (2002) *Curr Biol* **12**, 632-639
22. Alessi, D. R., Pearce, L. R., and Garcia-Martinez, J. M. (2009) *Sci Signal* **2**, pe27
23. Frodin, M., Antal, T. L., Dummler, B. A., Jensen, C. J., Deak, M., Gammeltoft, S., and Biondi, R. M. (2002) *Embo J* **21**, 5396-5407
24. Newton, A. C., and Koshland, D. E., Jr. (1987) *J Biol Chem* **262**, 10185-10188
25. Edwards, A. S., and Newton, A. C. (1997) *J Biol Chem* **272**, 18382-18390
26. Gysin, S., and Imber, R. (1997) *Eur J Biochem* **249**, 156-160
27. Behn-Krappa, A., and Newton, A. C. (1999) *Curr Biol* **9**, 728-737
28. Sarbassov, D. D., Guertin, D. A., Ali, S. M., and Sabatini, D. M. (2005) *Science* **307**, 1098-1101
29. Frias, M. A., Thoreen, C. C., Jaffe, J. D., Schroder, W., Sculley, T., Carr, S. A., and Sabatini, D. M. (2006) *Curr Biol* **16**, 1865-1870
30. Bayascas, J. R., and Alessi, D. R. (2005) *Mol Cell* **18**, 143-145
31. Shiota, C., Woo, J. T., Lindner, J., Shelton, K. D., and Magnuson, M. A. (2006) *Dev Cell* **11**, 583-589
32. Ikenoue, T., Inoki, K., Yang, Q., Zhou, X., and Guan, K. L. (2008) *EMBO J* **27**, 1919-1931
33. Facchinetti, V., Ouyang, W., Wei, H., Soto, N., Lazorchak, A., Gould, C., Lowry, C., Newton, A. C., Mao, Y., Miao, R. Q., Sessa, W. C., Qin, J., Zhang, P., Su, B., and Jacinto, E. (2008) *EMBO J* **27**, 1932-1943

34. Edwards, A. S., Faux, M. C., Scott, J. D., and Newton, A. C. (1999) *J Biol Chem* **274**, 6461-6468
35. Hauge, C., Antal, T. L., Hirschberg, D., Doehn, U., Thorup, K., Idrissova, L., Hansen, K., Jensen, O. N., Jorgensen, T. J., Biondi, R. M., and Frodin, M. (2007) *Embo J* **26**, 2251-2261
36. Alessi, D. R., Andjelkovic, M., Caudwell, B., Cron, P., Morrice, N., Cohen, P., and Hemmings, B. A. (1996) *EMBO J* **15**, 6541-6551
37. Bellacosa, A., Chan, T. O., Ahmed, N. N., Datta, K., Malstrom, S., Stokoe, D., McCormick, F., Feng, J., and Tsichlis, P. (1998) *Oncogene* **17**, 313-325
38. Thoreen, C. C., Kang, S. A., Chang, J. W., Liu, Q., Zhang, J., Gao, Y., Reichling, L. J., Sim, T., Sabatini, D. M., and Gray, N. S. (2009) *J Biol Chem* **284**, 8023-8032
39. Violin, J. D., Zhang, J., Tsien, R. Y., and Newton, A. C. (2003) *J Cell Biol* **161**, 899-909
40. Gould, C. M., Kannan, N., Taylor, S. S., and Newton, A. C. (2009) *J Biol Chem* **284**, 4921-4935
41. Sonnenburg, E. D., Gao, T., and Newton, A. C. (2001) *J Biol Chem* **276**, 45289-45297
42. Gallegos, L. L., Kunkel, M. T., and Newton, A. C. (2006) *J Biol Chem* **281**, 30947-30956
43. Dutil, E. M., Toker, A., and Newton, A. C. (1998) *Curr Biol* **8**, 1366-1375
44. Le Good, J. A., Ziegler, W. H., Parekh, D. B., Alessi, D. R., Cohen, P., and Parker, P. J. (1998) *Science* **281**, 2042-2045
45. Chou, M. M., Hou, W., Johnson, J., Graham, L. K., Lee, M. H., Chen, C. S., Newton, A. C., Schaffhausen, B. S., and Toker, A. (1998) *Curr Biol* **8**, 1069-1077
46. Orr, J. W., and Newton, A. C. (1994) *J Biol Chem* **269**, 27715-27718
47. Balendran, A., Hare, G. R., Kieloch, A., Williams, M. R., and Alessi, D. R. (2000) *FEBS Lett* **484**, 217-223
48. Keranen, L. M., Dutil, E. M., and Newton, A. C. (1995) *Curr Biol* **5**, 1394-1403
49. Newton, A. C. (2003) *Biochem J* **370**, 361-371

50. Davies, S. P., Reddy, H., Caivano, M., and Cohen, P. (2000) *Biochem J* **351**, 95-105
51. Guertin, D. A., and Sabatini, D. M. (2009) *Sci Signal* **2**, pe24
52. Liu, X., and Zheng, X. F. (2007) *Mol Biol Cell* **18**, 1073-1082
53. Sturgill, T. W., Cohen, A., Diefenbacher, M., Trautwein, M., Martin, D. E., and Hall, M. N. (2008) *Eukaryot Cell* **7**, 1819-1830
54. Flint, A. J., Paladini, R. D., and Koshland, D. E., Jr. (1990) *Science* **249**, 408-411
55. Stempka, L., Girod, A., Muller, H. J., Rincke, G., Marks, F., Gschwendt, M., and Bossemeyer, D. (1997) *J Biol Chem* **272**, 6805-6811
56. Gao, T., and Newton, A. C. (2006) *J Biol Chem* **281**, 32461-32468
57. Freeley, M., Volkov, Y., Kelleher, D., and Long, A. (2005) *Biochem Biophys Res Commun* **334**, 619-630
58. Parekh, D., Ziegler, W., Yonezawa, K., Hara, K., and Parker, P. J. (1999) *J Biol Chem* **274**, 34758-34764
59. Ziegler, W. H., Parekh, D. B., Le Good, J. A., Whelan, R. D., Kelly, J. J., Frech, M., Hemmings, B. A., and Parker, P. J. (1999) *Curr Biol* **9**, 522-529
60. Manning, G., Whyte, D. B., Martinez, R., Hunter, T., and Sudarsanam, S. (2002) *Science* **298**, 1912-1934

## Chapter 6

### Summary and Conclusions

The primary goal of this dissertation was to identify and to describe additional mechanisms that contribute to our knowledge of the regulation of the life cycle of PKC. Through the use of standard biochemical techniques, we characterized key structure-function relationships and signaling pathways that control the maturation and down-regulation of PKC. From this work, we can conclude that PKC's maturation is more tightly regulated than previously thought with the discovery of previously undescribed regulators, and that the phosphorylation status and catalytic activity dictate the down-regulation of PKC. Although our understanding of how PKC is regulated has increased in complexity, the identification of new regulatory mechanisms provides novel therapeutic targets. Thus, understanding these finer details in the life cycle of PKC opens new avenues to therapeutically target this family of enzymes.

### **A model for the life cycle of PKC**

Phosphorylation, second messengers, subcellular localization, and binding partners are key regulators of the life cycle of PKC (Figure 6.1). When PKC is newly synthesized, it loosely engages the membrane with its regulatory modules (the C1 and C2 domains), and the autoinhibitory pseudosubstrate does not occupy the active site. This species of PKC is inactive but in an open conformation, allowing the upstream kinase PDK-1 to dock onto its C-terminal tail and phosphorylate the conserved activation loop. Upon phosphorylation of the activation loop, PKC undergoes two conserved, sequential phosphorylations in the C-terminal tail, the turn motif and the hydrophobic motif. The activity of the mTORC2 complex is required for these two phosphorylations, as described in Chapter 5. Additionally, the molecular chaperones, Hsp90 and Cdc37, bind PKC through an interaction mediated by a conserved PXXP motif in the C-terminal tail to

facilitate autophosphorylation at the hydrophobic motif and modulate PKC stability, as described in Chapter 2. Once PKC has become fully phosphorylated, it is released into the cytosol where it adopts a closed conformation; the autoinhibitory pseudosubstrate now occupies the active site. This species of PKC is catalytically-competent but inactive. Upon signals that promote lipid hydrolysis and the generation of the second messengers,  $\text{Ca}^{2+}$  and diacylglycerol, or by chronic activation with the diacylglycerol analogues, phorbol esters, PKC translocates to the plasma membrane. The binding of  $\text{Ca}^{2+}$  to the C2 domain and diacylglycerol/phorbol esters to the C1 domain provides the energy to release the autoinhibitory pseudosubstrate from the active site to allow for substrate phosphorylation as well as autophosphorylation. Indeed, this activation-induced autophosphorylation serves as a marker for activated PKC, as described in Chapter 4. In this activated, open conformation, PKC is susceptible to the action of phosphatases, such as PHLPP. This dephosphorylation causes PKC to redistribute to the insoluble fraction of cells, where it is ubiquitinated and degraded by the proteasome; this is the driving mechanism of the down-regulation of PKC, as described in Chapter 3. However, dephosphorylated PKC can bind heat shock proteins, such as Hsp70, which rescues it from the down-regulation pathway. This down-regulation is dependent upon the intrinsic catalytic activity of PKC. This model is far from complete as we continue to identify and characterize additional regulators (Hsp90, mTORC2) of PKC.

### **How PKC structure dictates function**

‘Structure determines function’ is an important paradigm in biology. A simple PubMed search of ‘structure function kinase’ generates over 40,000 hits. Certainly PKC is no exception to this concept. To date, attempts to crystallize the entire PKC enzyme

have been unsuccessful; however, individual components (the C1 and C2 domains, the catalytic domain) have been solved (1-7). The solved structures of the C1 and C2 regulatory domains have provided useful information on how PKC binds its activating cofactors. Interestingly, analysis of the crystal structure of the C2 domain of the novel PKC, PKC  $\delta$ , indicated that it was a phosphotyrosine binding domain; this finding was the first discovery of this type of module in a Ser/Thr kinase (8). Only within the last few years has the crystal structure of the catalytic domain of PKC been determined; the first solved catalytic domain was PKC  $\theta$  in 2004, followed by PKC  $\iota$  in 2005 and PKC  $\beta$ II in 2006 (5-7). Previously, the catalytic domain of PKC had been modeled on the structure of its AGC kinase relative, PKA. Like PKA, the structure of PKC's catalytic domain follows the classic bilobal fold, and its activity is regulated by key movements of the C-helix, the N and C lobes upon ATP binding, and the activation loop (7,9). The determination of PKC structure allowed us to see how the three conserved phosphorylations, the activation loop, turn motif and hydrophobic motif, dictate the functioning of the kinase and how it differs from other AGC kinase members.

*The C-terminal tail as a link between structure and function/disease* - The AGC kinase family, as a whole, has evolved a unique mode of regulation, different from other eukaryotic protein kinases, that cleverly exemplifies how structure regulates function. In AGC kinases, the C-terminal tail mediates movement of the C-helix, which forms a key salt bridge interaction to facilitate coordination of ATP, and two lobes of the kinase domain (9). In fact, the interactions that the C-terminal tail forms with the catalytic domain of AGC kinases make this kinase family unique (9). Kannan *et al.* identified key features in the C-terminal tail of AGC kinases that were important for kinase function by

a systematic, structural analysis. One of these features, the hydrophobic motif, has been studied extensively, particularly in Akt and PKC. In collaboration, we addressed the role of another feature identified in this study, the PXXP motif, in regulating the function of PKC.

Described in Chapter 2, our work demonstrated that the PXXP motif forms an intramolecular clamp with conserved residues in the catalytic domain to facilitate interaction with the molecular chaperones, Hsp90 and Cdc37 (10). Disruption of this clamp ablated the maturation of PKC, thus inactivating the enzyme. This study is a classic example of how structure dictates function. Another key interaction occurs between a conserved basic residue in the C-terminal tail (K611 in PKC  $\beta$ II) and a conserved Phe in the  $\alpha$ C- $\beta$ 4 loop of the catalytic domain (F402 in PKC  $\beta$ II). Mutation of either of these residues severely hinders the processing of PKC. The  $\alpha$ C- $\beta$ 4 loop is one of the critical regions identified that mediates the interaction with the Hsp90/Cdc37 chaperones (11). Analysis of these conserved interactions between the C-terminal tail and the catalytic domain reveal how structure regulates PKC function.

One interesting finding is that mutation of the individual Pro of the PXXP motif had different degrees of severity in the processing of PKC. Whereas mutation of the first Pro, Pro-616 in PKC  $\beta$ II, completely abolished PKC maturation, mutation of the second Pro, Pro-619 in PKC  $\beta$ II, only partially abrogated processing. This Pro in PKC  $\beta$ II aligns with the same Pro in the PXXP motif of its conventional counterpart, PKC  $\alpha$  (P613S), which has recently been shown to be a potential cancer-driving mutation in glioblastoma multiforme (12). How does this mutation promote cancer? A recent study linked PKC  $\alpha$  downstream of the epidermal growth factor (EGF) receptor, a gene that is amplified in

this cancer, and suggested that use of PKC inhibitors could be effective in the treatment of glioblastoma (13,14). Indeed, several other studies have proposed the use of PKC inhibitors for the treatment of glioblastoma due to the up-regulation in PKC expression and activity (15-18). However, mutation of P613S in PKC  $\alpha$  is an inactivating mutation, suggesting that PKC  $\alpha$  activity may be not necessary for PKC's role in glioblastoma. In fact, a recent study reports that PKC  $\alpha$  protein, but not activity, is required for cell survival and proliferation in glioma (19). Using a malignant glioma cell line, U87MG, Cameron *et al.* found that depletion of PKC  $\alpha$  increased sensitivity to apoptosis (19). In addition, re-expression of PKC  $\alpha$  into PKC  $\alpha^{-/-}$  MEFS conferred protection from apoptosis; however, treatment with PKC inhibitors had no effect on proliferation and cell survival (19). Interestingly, expression of a kinase-dead PKC  $\alpha$ , which lacks PKC processing similar to the PXXP mutants, resulted in apoptosis (19). This study suggests that different forms of PKC (active *versus* inactive) may be scaffolded differently, thus exerting different cellular effects; indeed, unphosphorylated PKCs tend to localize in the insoluble fraction of cells. In a B-cell leukemia model, kinase-dead PKC  $\alpha$  induced transformation, indicating that PKC  $\alpha$  is capable of transducing pro-oncogenic signals in the absence of kinase activity; this mechanism could account for the potential cancer-driving properties of the PKC  $\alpha$  PXXP mutant (20). Conversely, since mutation of the PXXP motif renders PKC catalytically-inactive, PKC  $\alpha$ -P613S's cancer-driving properties may arise from the inability to transduce *anti*-tumorigenic signals. In an endocrine tumor model, a mutation in the hinge region of PKC  $\alpha$  rendered it unable to signal effectively, thus promoting an invasive phenotype (21). Importantly, our study

links PKC to Hsp90, an important regulator of kinases, such as Akt, Src, B-Raf, and ErbB-2, that are often mutated or dysregulated in pathological states (22). Inhibitors of Hsp90 are also being used as treatment for glioblastoma (23). Mutation of the PXXP motif would therefore subvert the regulation by Hsp90, which would potentially increase the pro-oncogenic potential of the PKC PXXP mutant.

In summary, our study of the PXXP motif of PKC demonstrates how structure is intimately associated with function. Future work is required to discern its exact role in cancer, but additional analysis of the conserved interactions between the C-terminal tail and the catalytic domain may lend further insight into the regulation and function of PKC.

### **Autophosphorylation, a marker of PKC activation**

The classical marker for PKC activation in the cell, specifically conventional and novel isozymes, is translocation to the membrane, where it engages its membrane-bound ligand, diacylglycerol. This event can be readily visualized in real time using fluorescence techniques. However, this method does not readily apply to analysis of pathological samples, such as tumor tissues, and PKC can associate with membranes independent of cell stimulation, making it inadequate as a marker for PKC activity. In addition, PKC isozymes do not vary significantly in substrate specificity (i.e. the peptide sequence of the CKAR reporter can be phosphorylated by all of the PKC isozymes) so finding a readout of activation for specific PKC isozymes in the cell poses a challenge.

However, not only does PKC phosphorylate other proteins in the cell, but it can also phosphorylate itself. One of these autophosphorylation sites that has been

extensively characterized is the hydrophobic motif. For most PKC isozymes, though, this phosphorylation occurs in a constitutive manner and does not serve as a marker for induced PKC activity. Instead, dephosphorylation of this site is used to indicate a loss in activity; PKC that is not phosphorylated at the hydrophobic motif is markedly destabilized in the cell.

Studies have shown that PKC can autophosphorylate in the regulatory domains (C1, C2), the hinge between the regulatory and catalytic domains, and the catalytic domain itself (24-27). Most of these sites that have been identified are specific to the particular PKC isozyme, with the exception of the site in PKC  $\alpha$  that is conserved in the conventional family of PKC isozymes. The functions of these autophosphorylation sites have not all been characterized, but most of them occur upon activation of PKC. The autophosphorylation site identified in PKC  $\theta$  is important for proper cellular targeting and has a critical role in the signaling of the enzyme (27). The autophosphorylation site identified in PKC  $\alpha$  has been used to stain tumor samples and has shown promise as a marker for PKC activity (25). As described in Chapter 4, the autophosphorylation sites that we have identified in PKC  $\beta$ II are specific for that isozyme and occur upon activation with either phorbol esters or physiological agonists. Although future work is required to determine the specific role for these phosphorylations (i.e., localization, recruitment of protein regulators), the potential to use as a marker for PKC  $\beta$ II activity in the cell is high.

As more structural details about the different PKC isozymes become available, the specific role of these autophosphorylation sites may become clearer. In the meantime, the development of phospho-specific antibodies to these different sites will

serve as a useful tool to monitor the activity of several PKC isozymes in a cell, both under normal and pathological conditions.

### **PKC down-regulation: the ‘black box’ in PKC regulation**

Upon chronic activation of PKC that occurs with treatment of phorbol esters, the protein levels of PKC are depleted in the cell; this process is the ‘down-regulation’ of PKC. Extensive studies have characterized the molecular mechanisms that govern the maturation and activation of PKC. However, much less information is available about the mechanisms that dictate the down-regulation of PKC. In order for PKC to be efficiently down-regulated, it must have its intrinsic catalytic activity. A kinase-inactive construct of PKC is not down-regulated with phorbol esters, and PKC inhibitors slow this process. Essentially, PKC initiates its own suicide mechanism.

Debate has existed in the field as to what form of PKC is down-regulated (phosphorylated versus unphosphorylated). Several studies have shown that dephosphorylation of the priming, C-terminal phosphorylation sites (the turn and hydrophobic motif) precedes the degradation of the enzyme (28-30). Other studies have indicated that the fully phosphorylated enzyme is degraded in the cell (31). In order to address this question, we utilized a phospho-mimetic construct, PKC  $\beta$ II-T641E/S660E, which cannot be dephosphorylated (as described in Chapter 3). Interestingly, we found that PKC  $\beta$ II-T641E/S660E is NOT down-regulated upon phorbol ester treatment but CAN be readily ubiquitinated. These data indicate that dephosphorylation and ubiquitination can be uncoupled, but dephosphorylation is a prerequisite for degradation.

With the use of pharmacological inhibitors, we uncoupled the down-regulation of the unphosphorylated and phosphorylated forms of PKC. Down-regulation of unphosphorylated PKC was sensitive to the proteasome inhibitor while down-regulation of fully phosphorylated PKC was sensitive to the PKC inhibitor. What remains to be determined is if the PKC activity is required for dephosphorylation prior to degradation or the degradation of the fully phosphorylated form. Preliminary results suggest that PKC activity is necessary for its dephosphorylation after phorbol ester stimulation; whether this activity controls the activity of a phosphatase still remains to be elucidated. However, our work has helped to dissect the molecular mechanism involved in this process.

The down-regulation of PKC primarily occurs through a proteasome-dependent process. What form of PKC is ubiquitinated? Our work has indicated that both the unphosphorylated and fully phosphorylated forms can be ubiquitinated. Indeed, the E3 ligase RINCK regulates the levels of both forms of PKC. The E3 ligases that ubiquitinate PKC in response to phorbol esters are currently unknown; the identification of these regulators will provide a possible avenue for designing novel therapeutics to target PKC.

Several questions remain regarding the down-regulation of PKC. Can PKC still signal as it goes through this process? What are the E3 ligases and other protein regulators involved? Where does this process occur in the cell? Are there isozyme-specific mechanisms? Answers to these questions will further our knowledge of PKC regulation and provide insight into how PKC can be targeted therapeutically in diseases where PKC activity is up-regulated, such as cancer.

## Summary

This dissertation used biochemical methods to dissect mechanisms that regulated the maturation (Chapters 2 and 5), activity (Chapter 4), and down-regulation (Chapter 3) of PKC. We identified a novel regulator of PKC maturation (Hsp90/Cdc37), characterized a marker of PKC activation (autophosphorylation at Thr-17 in PKC  $\beta$ II), and elucidated the mechanisms involved in the phorbol ester-mediated down-regulation of PKC. The information obtained from these studies will be useful in monitoring and targeting activated PKC therapeutically in pathological conditions.

*The future of PKC* – With a family of 10 isozymes that overlap in substrate specificity as well as activating conditions, the ability to monitor and target specific PKC isozymes in the cell poses a significant challenge. The prevalence of dysregulated PKCs in specific disease conditions lends some insight as to how particular isozymes may be alternatively regulated. By increasing our understanding of the spatio-temporal dynamics of how these different isozymes are regulated, the ability to design novel therapeutics to target specific isozymes will be greatly enhanced.



## References

1. Verdaguer, N., Corbalan-Garcia, S., Ochoa, W. F., Fita, I., and Gomez-Fernandez, J. C. (1999) *EMBO J* **18**, 6329-6338
2. Xu, R. X., Pawelczyk, T., Xia, T. H., and Brown, S. C. (1997) *Biochemistry* **36**, 10709-10717
3. Zhang, G., Kazanietz, M. G., Blumberg, P. M., and Hurley, J. H. (1995) *Cell* **81**, 917-924
4. Ochoa, W. F., Garcia-Garcia, J., Fita, I., Corbalan-Garcia, S., Verdaguer, N., and Gomez-Fernandez, J. C. (2001) *J Mol Biol* **311**, 837-849
5. Messerschmidt, A., Macieira, S., Velarde, M., Badeker, M., Benda, C., Jestel, A., Brandstetter, H., Neufeind, T., and Blaesse, M. (2005) *J Mol Biol* **352**, 918-931
6. Xu, Z. B., Chaudhary, D., Olland, S., Wolfrom, S., Czerwinski, R., Malakian, K., Lin, L., Stahl, M. L., Joseph-McCarthy, D., Benander, C., Fitz, L., Greco, R., Somers, W. S., and Mosyak, L. (2004) *J Biol Chem* **279**, 50401-50409
7. Grodsky, N., Li, Y., Bouzida, D., Love, R., Jensen, J., Nodes, B., Nonomiya, J., and Grant, S. (2006) *Biochemistry* **45**, 13970-13981
8. Benes, C. H., Wu, N., Elia, A. E., Dharia, T., Cantley, L. C., and Soltoff, S. P. (2005) *Cell* **121**, 271-280
9. Kannan, N., Haste, N., Taylor, S. S., and Neuwald, A. F. (2007) *Proc Natl Acad Sci U S A* **104**, 1272-1277
10. Gould, C. M., Kannan, N., Taylor, S. S., and Newton, A. C. (2009) *J Biol Chem* **284**, 4921-4935
11. Citri, A., Harari, D., Shohat, G., Ramakrishnan, P., Gan, J., Lavi, S., Eisenstein, M., Kimchi, A., Wallach, D., Pietrokovski, S., and Yarden, Y. (2006) *J Biol Chem* **281**, 14361-14369
12. McLendon, R., Friedman, A., Bigner, D., Van Meir, E. G., Brat, D. J., Mastrogiannis, M., Olson, J. J., Mikkelsen, T., Lehman, N., Aldape, K., Alfred Yung, W. K., Bogler, O., Vandenberg, S., Berger, M., Prados, M., Muzny, D., Morgan, M., Scherer, S., Sabo, A., Nazareth, L., Lewis, L., Hall, O., Zhu, Y., Ren, Y., Alvi, O., Yao, J., Hawes, A., Jhangiani, S., Fowler, G., San Lucas, A., Kovar, C., Cree, A., Dinh, H., Santibanez, J., Joshi, V., Gonzalez-Garay, M. L., Miller, C. A., Milosavljevic, A., Donehower, L., Wheeler, D. A., Gibbs, R. A., Cibulskis, K., Sougnez, C., Fennell, T., Mahan, S., Wilkinson, J., Ziaugra, L.,

- Onofrio, R., Bloom, T., Nicol, R., Ardlie, K., Baldwin, J., Gabriel, S., Lander, E. S., Ding, L., Fulton, R. S., McLellan, M. D., Wallis, J., Larson, D. E., Shi, X., Abbott, R., Fulton, L., Chen, K., Koboldt, D. C., Wendl, M. C., Meyer, R., Tang, Y., Lin, L., Osborne, J. R., Dunford-Shore, B. H., Miner, T. L., Delehaunty, K., Markovic, C., Swift, G., Courtney, W., Pohl, C., Abbott, S., Hawkins, A., Leong, S., Haipek, C., Schmidt, H., Wiechert, M., Vickery, T., Scott, S., Dooling, D. J., Chinwalla, A., Weinstock, G. M., Mardis, E. R., Wilson, R. K., Getz, G., Winckler, W., Verhaak, R. G., Lawrence, M. S., O'Kelly, M., Robinson, J., Alexe, G., Beroukhi, R., Carter, S., Chiang, D., Gould, J., Gupta, S., Korn, J., Mermel, C., Mesirov, J., Monti, S., Nguyen, H., Parkin, M., Reich, M., Stransky, N., Weir, B. A., Garraway, L., Golub, T., Meyerson, M., Chin, L., Protopopov, A., Zhang, J., Perna, I., Aronson, S., Sathiamoorthy, N., Ren, G., Wiedemeyer, W. R., Kim, H., Won Kong, S., Xiao, Y., Kohane, I. S., Seidman, J., Park, P. J., Kucherlapati, R., Laird, P. W., Cope, L., Herman, J. G., Weisenberger, D. J., Pan, F., Van Den Berg, D., Van Neste, L., Mi Yi, J., Schuebel, K. E., Baylin, S. B., Absher, D. M., Li, J. Z., Southwick, A., Brady, S., Aggarwal, A., Chung, T., Sherlock, G., Brooks, J. D., Myers, R. M., Spellman, P. T., Purdom, E., Jakkula, L. R., Lapuk, A. V., Marr, H., Dorton, S., Gi Choi, Y., Han, J., Ray, A., Wang, V., Durinck, S., Robinson, M., Wang, N. J., Vranizan, K., Peng, V., Van Name, E., Fontenay, G. V., Ngai, J., Conboy, J. G., Parvin, B., Feiler, H. S., Speed, T. P., Gray, J. W., Brennan, C., Socci, N. D., Olshen, A., Taylor, B. S., Lash, A., Schultz, N., Reva, B., Antipin, Y., Stukalov, A., Gross, B., Cerami, E., Qing Wang, W., Qin, L. X., Seshan, V. E., Villafania, L., Cavatore, M., Borsu, L., Viale, A., Gerald, W., Sander, C., Ladanyi, M., Perou, C. M., Neil Hayes, D., Topal, M. D., Hoadley, K. A., Qi, Y., Balu, S., Shi, Y., Wu, J., Penny, R., Bittner, M., Shelton, T., Lenkiewicz, E., Morris, S., Beasley, D., Sanders, S., Kahn, A., Sfeir, R., Chen, J., Nassau, D., Feng, L., Hickey, E., Weinstein, J. N., Barker, A., Gerhard, D. S., Vockley, J., Compton, C., Vaught, J., Fielding, P., Ferguson, M. L., Schaefer, C., Madhavan, S., Buetow, K. H., Collins, F., Good, P., Guyer, M., Ozenberger, B., Peterson, J., and Thomson, E. (2008) *Nature*
13. Vogt, P. K., and Hart, J. R. (2009) *Sci Signal* **2**, pe26
  14. Fan, Q. W., Cheng, C., Knight, Z. A., Haas-Kogan, D., Stokoe, D., James, C. D., McCormick, F., Shokat, K. M., and Weiss, W. A. (2009) *Sci Signal* **2**, ra4
  15. Begemann, M., Kashimawo, S. A., Lunn, R. M., Delohery, T., Choi, Y. J., Kim, S., Heitjan, D. F., Santella, R. M., Schiff, P. B., Bruce, J. N., and Weinstein, I. B. (1998) *Anticancer Res* **18**, 3139-3152
  16. Lahn, M. M., Sundell, K. L., and Paterson, B. M. (2004) *Oncol Rep* **11**, 515-522
  17. Mandil, R., Ashkenazi, E., Blass, M., Kronfeld, I., Kazimirsky, G., Rosenthal, G., Umansky, F., Lorenzo, P. S., Blumberg, P. M., and Brodie, C. (2001) *Cancer Res* **61**, 4612-4619

18. Zellner, A., Fetell, M. R., Bruce, J. N., De Vivo, D. C., and O'Driscoll, K. R. (1998) *Clin Cancer Res* **4**, 1797-1802
19. Cameron, A. J., Procyk, K. J., Leitges, M., and Parker, P. J. (2008) *Int J Cancer* **123**, 769-779
20. Nakagawa, R., Soh, J. W., and Michie, A. M. (2006) *Cancer Res* **66**, 527-534
21. Zhu, Y., Dong, Q., Tan, B. J., Lim, W. G., Zhou, S., and Duan, W. (2005) *Cancer Res* **65**, 4520-4524
22. Pearl, L. H. (2005) *Curr Opin Genet Dev* **15**, 55-61
23. Sauvageot, C. M., Weatherbee, J. L., Kesari, S., Winters, S. E., Barnes, J., Dellagatta, J., Ramakrishna, N. R., Stiles, C. D., Kung, A. L., Kieran, M. W., and Wen, P. Y. (2009) *Neuro Oncol* **11**, 109-121
24. Durgan, J., Michael, N., Totty, N., and Parker, P. J. (2007) *FEBS Lett* **581**, 3377-3381
25. Ng, T., Squire, A., Hansra, G., Bornancin, F., Prevostel, C., Hanby, A., Harris, W., Barnes, D., Schmidt, S., Mellor, H., Bastiaens, P. I., and Parker, P. J. (1999) *Science* **283**, 2085-2089
26. Flint, A. J., Paladini, R. D., and Koshland, D. E., Jr. (1990) *Science* **249**, 408-411
27. Thuille, N., Heit, I., Fresser, F., Krumbock, N., Bauer, B., Leuthaeusser, S., Dammeier, S., Graham, C., Copeland, T. D., Shaw, S., and Baier, G. (2005) *Embo J* **24**, 3869-3880
28. Hansra, G., Garcia-Paramio, P., Prevostel, C., Whelan, R. D., Bornancin, F., and Parker, P. J. (1999) *Biochem J* **342** ( Pt 2), 337-344
29. Gould, C. M., and Newton, A. C. (2008) *Curr Drug Targets* **9**, 614-625
30. Lee, H. W., Smith, L., Pettit, G. R., and Bingham Smith, J. (1996) *Am J Physiol* **271**, C304-311
31. Leontieva, O. V., and Black, J. D. (2004) *J Biol Chem* **279**, 5788-5801